TEXAS HIPLEX SUMMARY REPORT

1975-1980
Increasing Rainfall through
Research in Weather Modification

LP-184

TEXAS DEPARTMENT OF WATER RESOURCES

1983

TEXAS HIPLEX SUMMARY REPORT, 1975-1980

By

Robert F. Riggio
William O. Alexander
Thomas J. Larkin
George W. Bomar
Texas Department of Water Resources

TEXAS DEPARTMENT OF WATER RESOURCES

Charles E. Nemir, Executive Director

TEXAS WATER DEVELOPMENT BOARD

TEXAS WATER COMMISSION

TABLE OF CONTENTS

TABLE OF CONTENTS—Continued

TABLE OF CONTENTS—Continued

TABLES

FIGURES

TABLE OF CONTENTS—Continued

FOREWORD

The Texas HIPLEX Program was planned to be a long term multi-phase research effort to develop a technology to augment West Texas summer rainfall in an acceptable socioeconomic manner. The initial phase of the Program included collecting, processing, and analyzing meteorological data to better understand the characteristics and rainmaking processes important to shower-producing West Texas clouds. In turn, that information was to be used to develop a statistical design for a rainfall augmentation experiment which is the next phase of the Program.

Due to Federal funding cutbacks, the timely progress of the Texas HIPLEX Program was severely hampered, leaving much analyses to be completed before an experimental design could be finalized. Therefore, this report should be considered a progress report of research completed through 1980. The design document will be completed at a later time subject to availability of funding.

This report presents a summary of the Texas HIPLEX research during the period 1975 through 1980. Its purpose is to synthesize the important findings of the many individual studies which comprised the Texas HIPLEX Program and offer recommendations concerning the experimental design. The reader is referred to the technical reports for details of a particular research study summarized in this report.

ABSTRACT

The goal of the Texas HIPLEX Program for its initial period, 1976 through 1980, was to collect meteorological information on cloud characteristics and precipitation processes associated with summertime clouds which develop over the High Plains of Texas. Mesoscale and microscale environmental and convective cloud data were collected and partially analyzed. Six summer field projects were organized and conducted during which mesoscale surface and upper-air data, and cloud physics, radar, satellite, and raingage data were collected and processed for analysis.

Mesoscale analyses based on field data have identified relationships between development and organization of convective clouds, low level moisture, convective instability, and the magnitude of the 850-500 mb wind shear vector. Based on analyses of numerical models and radar information, interactions between individual cumulonimbus clouds were observed.

Microscale analyses have indicated that the ice process is associated with significant precipitation. Mathematical models suggest that seeding for dynamic effects may have a positive impact on West Texas clouds.

Recommendations for an experimental unit, seeding hypotheses and response variables are offered for consideration for the experimental phase of the Texas HIPLEX Program.

1. Introduction

1.1 Need for Research

The Texas economy is diverse, viable, and growing. The State has a total land area of 693,233 km² (267,339 mi²) with a 1980 population of about 14.228 million people. The State's population is projected to grow to 17.8 million by 1990 and 20.9 million by the year 2000.

Approximately 2.37×10^{10} m³ (19.2 million acre-feet) of Texas water (one acre-foot is 1,235 m³, or 325,851 gallons) are used each year to meet the needs of households, industry, irrigation, steam-electric power generation, mining and livestock. Nearly 75 percent of the total water available each year, or 1.62×10^{10} m³ (13.1 million acre-feet), is consumed by farmers and ranchers for irrigation to produce food and fiber to meet the demands of both the State and the Nation. By the year 2000, it is projected that 2.75×10^{10} m³ (22.3 million acre-feet) of water will be needed to meet the demands of the State, assuming that agricultural water use is held at 1.62×10^{10} m³ (13.1 million acre-feet).

Though the State's supply of fresh water is sufficient to meet current needs, the areal distribution of much of it does not coincide with the locations of Texas cities, industries, and agricultural land. In some regions of the State, if additional water sources are not found, regional water shortages will seriously affect the economy which is dependent upon adequate water. This scenario is clearly evident in the fertile but semiarid Texas High Plains area where the Ogallala aquifer, the major source of municipal and irrigation water, is being exhausted. Currently, the Ogallala supplies irrigation water for 23,900 km² (5.9 million acres). However, at present annual use trends, by the year 2000 the Ogallala is estimated to be able to supply irrigation water for only 9,000 km² (2.2 million acres). Aside from the fact that ground water is becoming more scarce, it is also becoming more expensive to obtain as the water table declines and energy costs to pump the water continue to rise.

In order to meet the water needs of the State, and specifically in the Texas High Plains, additional and cost effective fresh water supplies must be developed. One relatively new technique of providing additional fresh water is to tap the moisture available in the atmosphere which does not fall as rain naturally. The value of this additional water has been demonstrated by recent exploratory studies of the Texas Department of Water Resources (Allaway *et al.*, 1975; Lippke, 1976; and Kengla *et al.*, 1979) which reveal that the net economic effects of weather modification activities in a 33,000 km² (8.1 million-acre) project area of the southern High Plains, yielding 10 percent additional rainfall during the growing season, would result in an overall expansion in regional output of approximately $3.68 million and a similar expansion in regional income of $2.30 million.

1.2 History of Weather Modification in Texas

Deliberate attempts by man to change or control the weather in Texas generally were unregulated and undocumented prior to 1967. Literature contains records of only a few "rainmaking" experiments, the earliest of which describes an experiment carried out on the Texas High Plains during the early 1890's. This particular endeavor consisted of war-time simulations of heavy artillery bombardment of surrounding hills in an attempt to determine if significant correlations existed between the artillery explosions and occurrences of rainfall.

This experiment was based on observations made by Edward Powers, during the Civil War, that rain would develop after most major battles. He later published a book (Powers, 1890), documenting his observations. To test Power's hypothesis, Congress appropriated $10,000, while an additional $2,000 were allocated by the Department of Agriculture, to support an experiment in the Texas High Plains. The experiment, conducted by General R. G. Dyrenforth and a party of scientists and technicians armed with cannons and explosives, ended inconclusively after one season of testing.

Mr. Charles William Post, founder of Post cereals, was also active in weather modification experiments in Texas during the period between 1911 and 1914 (Eaves, 1952). Because of ill health, Mr. Post moved from Battle Creek, Michigan, to Texas in 1906, and purchased a quarter-million-acre ranch in Garza and Lynn Counties on the Texas High Plains. His penchant for experimentation, coupled with his desire to grow grain in the semiarid West Texas climate, led to the most spectacular of his experiments. Based on the Power's hypotheses, Post attempted to cause rain by dynamite blasts. Fifteen firing stations were established along the edge of the Cap Rock above Post, Texas, and from each station four pounds of dynamite were exploded every four minutes over a period of several hours or until rain occurred. Altogether he spent over $50,000 on rainmaking experiments, the results of his experimentation, which spanned four years, were inconclusive.

For several decades subsequent to the Post experiment, no other weather modification projects in Texas were documented in the literature. However, in the mid-1940's, shortly after Vincent Schaefer demonstrated the effect dry ice had on super-cooled water droplets and, subsequently, on clouds, weather modification operations in Texas resumed (Hearings before the Committee on Commerce, U.S. Senate, 89th Congress, 1966). Since the number of commercial weather modification projects in Texas increased markedly beginning in the 1950's, it soon became necessary for the State of Texas to adopt a weather modification statute, not only to properly administer commercial cloud-seeding projects but also to encourage research and development. Consequently, in 1967, the Texas Weather Modification Act was adopted, which charged the Texas Water Development Board (currently a part of the Texas Department of Water Resources)* to license and permit weather modification activities and to promote research and development in weather modification technology.

---

*To avoid confusion, the Texas Water Development Board will be referred to as the Texas Department of Water Resources throughout this report. The Texas Department of Water Resources was created in 1977, by Act of the Texas Legislature (H.B. 1139, 65th Legislature). The Texas Water Quality Board and the Texas Water Rights Commission were placed in one agency—The Texas Department of Water Resources by this Act.

1.3 Recent Cloud Seeding Research in Texas

In the decade of the 1970's, four significant cloud seeding research operations were initiated in the State of Texas. Three of these programs were completed during the decade, while the fourth weather modification program continued in 1980. The three completed research operations were known as: (1) the San Angelo Cumulus Project; (2) the Colorado River Municipal Water District Rain Augmentation Program; and (3) Hail Suppression Activities in the Texas High Plains.

1.3.1 San Angelo Cumulus Project

The first documented weather modification experiment in Texas, performed under the 1967 Weather Modification Act, was conducted in the northern reaches of the Edwards Plateau region around San Angelo during the summers of 1971, 1972 and 1973 (Smith *et al.*, 1974). The experiment was funded by the Bureau of Reclamation and the Texas Department of Water Resources.

The primary objective of the experiment was to determine the feasibility of treating summertime cumulus clouds for increasing rainfall. The approach was to treat half of the sample cloud population with cloud seeding material, leaving the other half untreated as the control sample cloud population for comparison. Clouds to be treated were selected at random. Equipment used in the project included an M-33 radar system, a seeding aircraft, and a cloud sampling aircraft. Additional measurements were made with balloon-borne instruments (rawinsondes) measuring temperature, dewpoint, pressure, and wind direction and speed as a function of height above the ground. Rainfall reaching the ground was measured with wedge-type raingages.

Initially, the San Angelo Cumulus Project was designed to evaluate the potential of two methods for seeding clouds. One method was to seed summertime cumulus-type clouds with a material which tends to absorb moisture by accelerating the condensation of water vapor; this process is known as hygroscopic seeding. The hygroscopic seeding was carried out either with dry salt particles or urea. The second method introduced surrogate ice crystals to absorb moisture by accelerating the diffusion of water vapor on them; this process is called ice-phase seeding. The ice-phase seeding was carried out with silver iodide dispersed from an airborne platform. Since only a small number of test cases were obtained during the first year of the experiment, it was decided that only hygroscopic seeding would be tested further, using only dry salt particles as the seeding material during the remaining two years of the experiment.

The findings of the experiment were based on a total of 83 events. Analyses of the data suggested that precipitation processes within those clouds examined were initiated by the coalescence process, i.e., water drops growing by condensation and subsequent collisions with one another. Subsequent to the coalescence process, the large drops would apparently freeze in the edges or tops of the clouds. The freezing of the large drops was not considered an important contributor to the observed initial precipitation processes. However, the experiment concluded that

light ice-phase seeding may play an important role in the rainmaking process, inasmuch as natural ice crystals were observed infrequently in the active portion of the clouds measured.

The San Angelo Cumulus Project also examined the usefulness of a number of mathematical cloud models. Three cloud models were used during the experiment as both operational tools and as a guide for data analysis. Although the models were utilized during the project, the potential and/or shortcomings inherent in each were not fully evaluated. However, in spite of the models' limitations, it was concluded that they can provide a broad understanding of cloud behavior, though their usefulness as a tool for data analysis is subject to individual interpretation.

1.3.2 Colorado River Municipal Water District—Rain Augmentation Program

The Colorado River Municipal Water District, hereinafter termed the District, located in Big Spring, Texas, has sponsored a cloud seeding program to increase rainfall—and particularly runoff—into Lakes J. B. Thomas and E. V. Spence since 1971. The target area is located in the upper reaches of the Colorado River Basin. The District's weather modification effort was conceived initially as an operational project based upon the assumption that ice-phase cloud seeding, using silver iodide (AgI) dispersed by aircraft at cloud base to increase rainfall, could be productive and beneficial. Two independent evaluations of the effectiveness of the District's project were performed, one by the District and the other by the Texas Department of Water Resources.

1.3.2.1 District Evaluation

The District published a series of five annual reports describing their weather modification activities conducted during each operational rain-enhancement season. The reports describe operational procedures, including flight operations and the use of equipment during seeding operations. The latest two reports (Girdzus, 1979; 1980) investigate the programs' seeding effectiveness by a basic statistical examination of both rainfall amounts and crop-yield responses.

Rainfall comparisons were made between the unseeded period 1951-1970 and the seeded period 1971-1979, utilizing eighteen National Weather Service precipitation reporting stations. Crop yield responses to rainfall were also studied by examining departures from normal, based on 28 years of cotton-yield data from 12 to 14 counties contained within the District's operational area. Because cotton is the primary agricultural crop of the area and is highly dependent on spring rains, it was used as the primary response variable of rainfall for the crop yield portion of the study.

While definitive conclusions about the achievements of the weather modification program were not reached because of the relatively small sample size, when compared with the high variability of natural rainfall

amounts, qualitative analyses based on percent of average precipitation revealed a positive anomaly in those areas thought to be affected by cloud seeding. A corresponding increase was also noted in the production of cotton for those counties within which seeding occurred, as well as those counties downwind of the seeded area, when compared to upwind counties.

1.3.2.2 Texas Department of Water Resources—Sponsored Evaluation

In 1973 the Texas Legislature appropriated funds to be administered through the Texas Department of Water Resources, hereinafter termed Department, for an evaluation of the District's cloud seeding program. In 1975, additional funds were provided by the Department and the Bureau of Reclamation, hereinafter termed Bureau, to extend the evaluation study to include a portion of the 1975 operational season. Administration of the evaluative effort, however, remained with the Department.

The evaluation (Smith *et al.*, 1977) examined seeded and nonseeded summertime shower-producing clouds during the years 1973, 1974, and 1975. A total of 66 individual events were examined. As a result of improved measurement capabilities, the 30 events studied in 1975 provided a more extensive set of observational data than those of the two preceding years.

Observational data were obtained from quantitative radar measurements made by an M-33 radar in Snyder, Texas, operated in conjunction with an extensive raingage network which was made available through the Texas HIPLEX Program.

A case-study examination of the individual events indicated that most of the events studied were parts of larger, organized cloud systems that had a lifetime at least several times greater than that of individual cells making up the system.

The seeding technique used by the District in 1973-1975 was largely based on treatment of new cells which developed around the periphery of an existing organized system for the purpose of extending the dimensions and lifetime of the system. An examination of pilot reports in conjunction with the M-33 radar data revealed that, in many cases, the cloud growth areas were seeded after the organized system had begun a general decay cycle that usually led to eventual dissipation. Under these conditions, it was believed that the new growth areas existed in an environment relatively unfavorable for the accomplishment of the program objectives, and that little positive effect from the seeding could be realized.

Time-history plots of precipitation totals and sizes of rain areas were made to compare seeded and nonseeded cases. No appreciable difference was found. The study suggested that possible factors contributing to these

results were the lack of adequate amounts of AgI material in the cloud, insufficient time for precipitation growth in the cloud, and unfavorable environmental conditions for new cell growth.

This study provided the first opportunity for a detailed physical examination of seeding results in the Big Spring area of Texas. Valuable insight into cloud organization and consequent implications for proper seeding techniques and the importance of understanding the ambient air characteristics were gained as a result of this work.

The study recommended certain improvements in the District's seeding operations. These included the following: earlier recognition of organized cloud systems and their life cycles; more timely seeding to coincide with the developing stages of the organized system; possible increase in AgI burn rate, or longer burn time of flares in the cloud updraft; and consideration of some exploratory seeding tests with AgI releases at cloud top.

1.3.3   Hail Suppression Activities in the Texas High Plains

The most recent cloud seeding program for hail suppression in Texas began in 1970 when a group of businessmen, ranchers, farmers, and citizens from the Plainview area organized themselves to sponsor a program to prevent or reduce the occurrence of hail by airborne treatment of clouds having hail potential. Over the five subsequent years, the program grew from a 2-county target area in 1970 to all or portions of eight counties in 1974. The cloud seeding activities for suppressing hail were operated during the months of May through October.

The results of this commercial hail suppression program were evaluated by Henderson and Changnon (1972) and by Schickedanz (1974; 1975). The results of the evaluations, based on hailfall data and/or insurance loss costs, indicated evidence of hail suppression. No alterations to rainfall in and around the target area were observed.

In 1974, Texas A&M University evaluated the effects of the commercial cloud seeding program in the Texas High Plains over the 4-year period, 1970-1973 (Scoggins *et al.,* 1975).

The primary objectives of the study were to evaluate the effectiveness of cloud seeding activities in the Texas High Plains in terms of the prevention or reduction of hail damage on the ground, and the influence of commercial seeding for hail suppression upon rainfall. The study concluded, after rigorous statistical analyses of all available rainfall data, that cloud seeding for hail suppression purposes had no discernible effect on the area's rainfall. Also, the statistical analyses of the hailfall and cotton loss did not indicate any significant reduction in hail damage at the ground due to cloud seeding. The authors of the study's final report stressed that this did not prove that there was no effect from the seeding program, but based on the available data, no effect from seeding could be discerned.

Evaluating a commercial hail-suppression project is particularly difficult because certain statistical controls are compromised. For example, the seed-no-seed randomization is not performed because it would negate the intended purpose of the commercial project. Consequently, the evaluator has to settle on a data set which introduces additional variables to the analyses. In the Texas study, for example, it was proposed that the effects of seeding on hailfall could be determined from cotton-loss data. However, this data set introduced additional variables to the analyses, such as stage of growth, and wind and water damage to the cotton crop.

1.4 High Plains Cooperative Program

1.4.1 General

During the decade of the 1970's, a new, concerted effort was undertaken by the Federal government, in cooperation with various states—including Texas—and local entities, to gain a better understanding of the behavior of clouds following the application of various cloud-seeding techniques on convective cloud types common to the High Plains. This ambitious program of research and development, including physical and statistical experimentation in weather modification, is known as the "High Plains Cooperative Program," or "HIPLEX." Field research sites were located in eastern Montana, western Kansas and western Texas in order to lessen bias in the results observed at one particular region of the High Plains. This three site concept also provides a means for technology transfer from one region to another.

1.4.2 Goals and Objectives

The HIPLEX Program is part of the U.S. Department of the Interior's "Project Skywater," which is designed to develop an effective technology for precipitation management to help supplement the nation's fresh-water supply needs. The program is intended to be a coordinated series of studies, investigations, and experiments leading to a viable water resource technology.

The objectives of the HIPLEX Program are:

(a) to increase the understanding of natural cloud and precipitation processes in convective cloud entities in the High Plains, and of the alterations in cloud structure and resultant precipitation that occur when these processes are modified in a prescribed manner;

(b) to establish a data bank of microscale and mesoscale cloud information upon which to base an experiment for the purpose of identifying possible seeding hypotheses;

(c)   to determine, through physical and statistical evaluations, the level of certainty with which these modifications will result in the predicted alterations, using a randomized experiment of simple cloud systems; and

(d)   to develop the physical and socioeconomic baseline information needed for designing and conducting an area-wide experiment.

1.4.3   HIPLEX Design

The design of the first five years of HIPLEX (1975-1980) was developed by the Illinois State Water Survey (ISWS) (Ackerman *et al.*, 1971). The ISWS design addresses two broad areas of study: (1) atmospheric, and (2) socioeconomic and environmental. The avenue of completion of these areas of study consists of four phases, beginning with exploratory studies, and followed by single cloud experimentation studies, area rain experiments, and technology transfer. Strong overlap exists between the first phase—which is exploratory, and the second phase— which is experimentation, implying that exploratory studies are on-going into the experimentation phase.

Though the concept of HIPLEX called for three research sites to be located in the northern, central and southern regions of the nation's High Plains, financial and manpower efforts were concentrated mostly in the northern region. Here, Bureau of Reclamation personnel were stationed year-round to design a randomized rain augmentation experiment for the Montana High Plains summer shower-producing clouds, based on the recommendations of the ISWS document. After four years of meteorological fact finding, a detailed design plan for the first HIPLEX experiment in Montana was completed in early 1979 (Bureau of Reclamation, 1979). The design document presents the experimental unit, the seeding hypotheses, response variables, and experimental procedures for a Montana cloud seeding experiment.

The Texas HIPLEX Program progressed along with the Montana program, but at a relatively reduced scale due to less funding. The goal of the Texas program was to accomplish HIPLEX objectives (a) and (b) by the end of FY 1980. The following sections describe the Texas HIPLEX Program and its accomplishments relative to HIPLEX objectives (a) and (b).

2. TEXAS HIPLEX

2.1 Statutory Responsibility

The Texas Department of Water Resources is charged by Chapter 18 of the Texas Water Code (formerly the Texas Weather Modification Act of 1967) to regulate weather modification activities in Texas. Chapter 18 also provides that the Department promote research and development in the field of weather modification. To this end, the Department entered into a 1976 Master Agreement (Contract No. 14-06-D-7587) with the Bureau to conduct the Texas portion of the HIPLEX Program.

In March 1973, the Bureau initiated the HIPLEX Program as a joint effort, involving both Federal, State and local participation. In November 1973, the Department along with the cities of San Angelo and Lubbock, the Colorado River Municipal Water District, the Upper Colorado River Authority, Texas Tech University, and Texas A&M University all gave their official endorsement to the concept of the HIPLEX Program. In 1974, the Bureau entered into negotiations with several interested High Plains states where three experimental sites, representative of the climates and economies of the northern, central, and southern sectors of the Great Plains, were to be selected. The Governor of Texas recommended that four Texas cities be designated as potential southern region sites for consideration by the Bureau. The sites recommended were: (1) San Angelo, Texas, where the San Angelo Cumulus Project—also sponsored by the Bureau, was carried out in the early 1970's cooperatively with the Department; (2) Lubbock, Texas, the home of Texas Tech University and a cultural and population center located in the Texas High Plains; (3) Big Spring, Texas, located on the western edge of a 3,700 square-mile area in which a commercial cloud seeding project by the District had been underway since 1971; and (4) Amarillo, Texas, a cultural and population center located in the northern reaches of the Texas High Plains where the Bureau maintained one of its Regional offices.

In March 1974, the Department recommended that the Big Spring-Snyder area serve as the site in Texas for conducting a part of the High Plains Cooperative Experiment. Soon thereafter the Secretary of the Interior announced that Miles City (Montana), Colby (Kansas), and Big Spring (Texas) had been selected as the three research sites for the HIPLEX Program.

The Bureau then entered into an agreement with the Department in 1974, whereby the HIPLEX Program in Texas would be a cooperative effort, with State and local groups sharing in planning, operating, and supporting the program. The agreement stipulated that the Bureau would provide financial and technical support to the Texas HIPLEX Program, as well as the overall program design, so that the results obtained could be integrated into the overall HIPLEX Program in an optimum manner. Some equipment, including a weather radar and rawinsonde system, recording raingages, automated weather stations, a cloud physics airborne package, a satellite photo facsimile receiver, computer terminals, and a ground-based precipitation probe, were furnished by the Bureau.

2.2 Administration

Under the terms of the Agreement with the Bureau, the Department was responsible for administration of the Texas HIPLEX Program, including handling the financing, drafting and management of contracts, and coordination of various elements of the Texas program's research efforts. Other responsibilities of the Department included weather forecasting services for Texas HIPLEX field operations, developing a forecasting technique for summertime rainshower development, and examining the economic effects of weather modification.

The Department negotiated, executed, and administered over 35 contracts for work and services in support of the Texas HIPLEX Program during the 6-year period of Federal FY 1975 through FY 1980. Contracts were executed by the Department in cooperation with the District; Texas A&M University; Texas Tech University; Meteorology Research, Incorporated; Big Spring Aircraft, Incorporated; and North American Weather Consultants.

As part of these contract negotiations, budgets and work plans submitted by the performing agencies were reviewed by the Department staff in coordination with the Bureau. A comprehensive operations plan for each Texas HIPLEX field program was developed and adopted each year. All reports, including monthly, interim, annual, biennial, final, and technical, were reviewed, reproduced and distributed by the Department staff.

2.3 Texas HIPLEX Design

The design of the Texas HIPLEX Program follows the recommendation of the ISWS's HIPLEX design document. The first phase of the Texas HIPLEX Program, covering the initial six years and, as reported in this Summary Report, was totally an exploratory program. Much of the work and financial resources during the initial phase were directed at planning, equipping, and operating annual field projects of two to three months duration for the purpose of collecting and processing a large enough meteorological data base with which to adequately document the variability of natural convective rainfall development. The second phase of the Texas HIPLEX Program, i.e., the single cloud experimentation studies, would not begin until the data were analyzed and integrated and the statistical design of the Texas HIPLEX experiment was completed.

It was recognized at the beginning that the exploratory phase of the Texas HIPLEX Program would require many years to complete for two reasons. First, a large data base of reliable meteorological information had to be collected, processed and analyzed, and second, the majority of exploratory efforts would be performed on a mostly part-time basis by University faculty and graduate students. (This does not imply that working through the Universities is a bad approach. On the contrary, it is an excellent approach, because the cost of manpower is significantly less when compared to private contractor's costs, and new atmospheric scientists can obtain valuable knowledge and experience from which the meteorological community can benefit at a later time.) It was not possible to predict at the outset when the experimental phase would begin because of a number of unknowns inherent in the HIPLEX Program. Two outstanding unknowns were weather conditions and annual budget uncertainties.

2.4   Objectives

The Texas HIPLEX objectives evolved from HIPLEX objectives (a) and (b) (Section 1.4.2), with emphasis placed on collecting a large base of quality data. As information was obtained and the data base grew during the latter years of the program, the central theme of the program focused more on gaining a better understanding of how the meteorological mesoscale processes work to develop rain that eventually reaches the ground, with specific attention on establishing ambient air, rainfall, and cloud characteristics common to the Texas HIPLEX region. The approach taken to examine these natural processes was to study initially the mesoscale environment and converge on the microphysical processes.

2.4.1   Technical

The Texas HIPLEX technical objectives included the following:

(a)   to collect and analyze mesoscale data, both surface and upper air, on a scale approaching storm size, thereby permitting more accurate and deterministic studies of the interactions between convective clouds and their environment;

(b)   to collect and analyze satellite, radar, rainfall, and airborne (cloud physics) data to be used with the mesoscale data in order to establish a detailed description of environmental conditions and processes associated with natural as well as seeded clouds;

(c)   to identify the dominant precipitation mechanism(s) in the Texas HIPLEX region;

(d)   to develop and evaluate objective-type, operational forecast procedures for the Texas HIPLEX Program;

(e)   to refine procedures for using real-time satellite data to locate regions of initial convective activity, and to determine the movement of lines of convective activity into and within the target area;

(f)   to refine procedures and analysis of rawinsonde and surface mesoscale data to forecast the onset, location, and intensity of convective activity; and

(g)   to perform economic and social impact studies.

2.4.2   Delivery Techniques

The Texas HIPLEX Program also focused on techniques for seeding and making cloud and environmental measurements. These objectives included the following:

(a)   to gain limited and preliminary experience in the seeding of turrets in the -4°C to -10°C region of growing cumuli;

(b)   to evaluate the practicability of on-top seeding; and

(c)   to evaluate the behavior of cloud systems in the project area, using measurement systems now available.

2.5   Project Area

The project area for the Texas HIPLEX field project is located in the upper reaches of the Colorado River Basin, in the southern High Plains area of Texas. The project area, too, evolved with the requirements and objectives of the Texas HIPLEX Program. Figure 2.1 shows the 1980 project area which is very similar to the project area of previous years. The project area includes all or portions of a 14-county region of the Texas High Plains, lying generally in the area bounded by Abilene, Lubbock, Midland and San Angelo. The counties or portions of counties included in the project area are Andrews, Borden, Dawson, Gaines, Garza, Glasscock, Howard, Lynn, Martin, Midland, Mitchell, Scurry, Sterling and Terry.

2.5.1   Terrain

The terrain is characterized by broad, level plains in the west, sloping downward to rolling hills in the east. The Caprock Escarpment divides the two types of terrain. Soils in the area are generally red or brown sandy loams of several feet thickness. When sufficient water is available, this type of soil easily supports extensive crop production.

2.5.2   Climate

The climate in the area is subtropical steppe, characterized by rapid changes in both temperature and precipitation. The precipitation in the area varies from an annual mean of about 356 mm (14 in) in the southwest, to about 559 mm (22 in) in the east. Approximately two-thirds of the area's total annual rainfall occurs during the latter spring and summer months. During this period one- to two-day rainfall periods usually occur no more than four times per month. Rainfall amounts per contiguous occurrence are normally less than 25 mm (1 in). The most frequently occurring precipitation event produces 6 mm (0.24 in) or less.

Daytime temperatures are hot in the summer, with a daily maximum temperature normally reaching 35°C (95°F), while cooling to a comfortable 21 °C (70°F) at night. Winters are mild during the day, with a temperature range from near 16°C (60°F) to a nighttime low of 0°C (32°F), and are characterized by frequent cold periods that are followed by rapid warming. Prevailing wind direction is from the south to southeast throughout the year, although northerly winds are frequent during the winter.
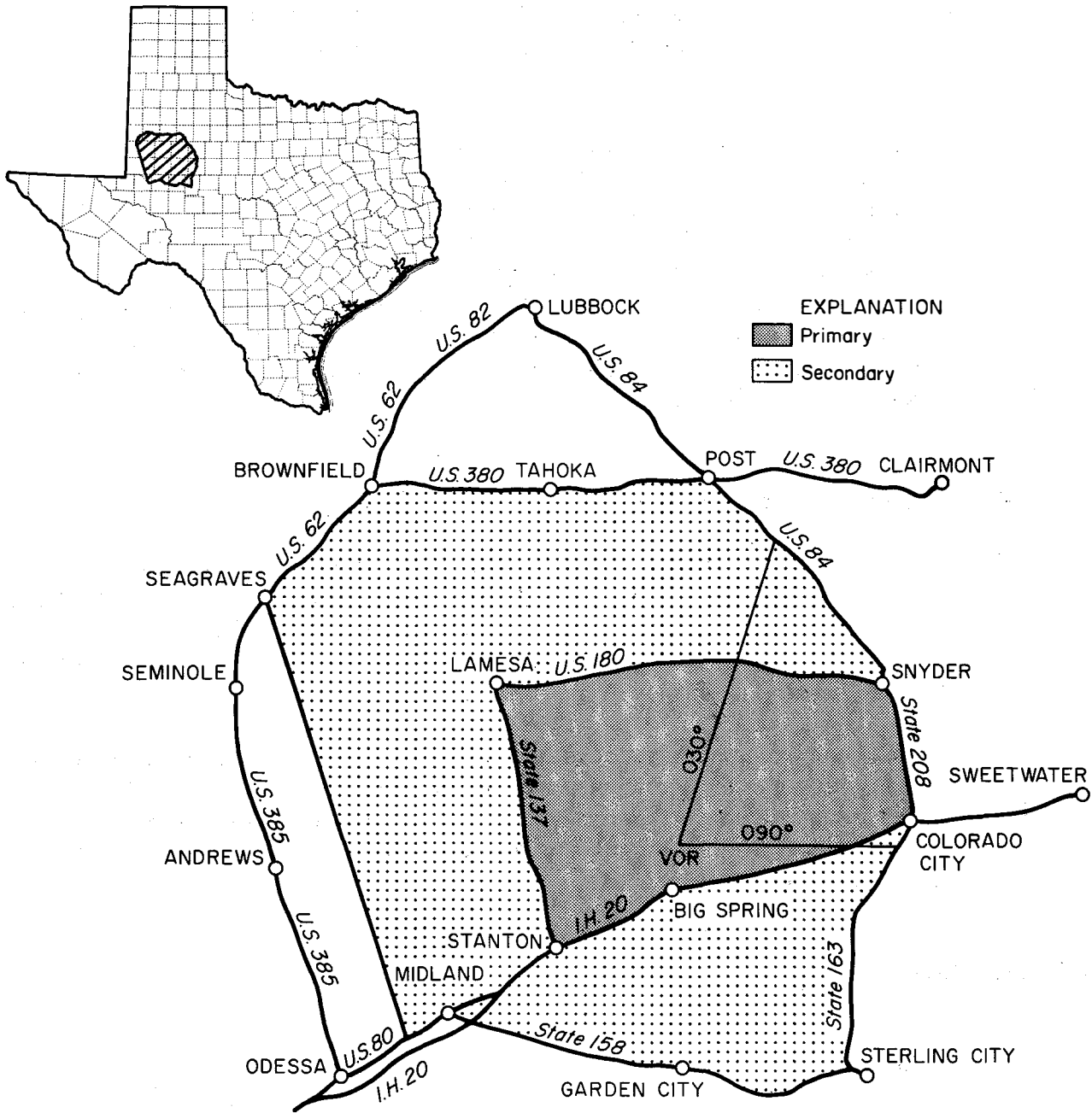
Figure 2.1. Texas HIPLEX project area.

2.5.3 Economy

The population of the project area* declined from 128,587 in 1970 to 126,191 in 1980; though declining over the decade, this population change represents a leveling off of the more rapid decline from 194,056 persons in 1960. Approximately 50 percent of the region's population is concentrated in the cities of Big Spring, Snyder, Lamesa and Sweetwater. Population in the project area is projected to increase to 133,135 and 137,284 in the years 1990 and 2000, respectively.

The region's total amount of farmland (cropland, pasture, rangeland) is about 31,600 km² (7.8 million acres). Between 1969 and 1978, average farm size increased from 4.3 to 5.3 km² (1,050 acres to 1,300 acres), while the total number of farms in the area decreased from 6,950 to 6,025. The harvested area for the region exceeded 6,880 km² (1.7 million acres) in 1979, with about 9 percent of this area irrigated with water from the Ogallala Aquifer, an exhaustible underground water supply. The average annual market value of all agricultural commodities produced in the study area during the period 1970 through 1979 is $257.7 million. Almost 17 percent of the labor and proprietor's income in the study area is produced by the farm sector.

2.5.4 Water Resources and Needs

Five surface water facilities on the Colorado River and its tributaries are located in or near the Texas HIPLEX project area: Lake J. B. Thomas, Lake Colorado City, and E. V. Spence Reservoir on the Colorado River, and Champion Creek and Oak Creek Reservoirs on the tributaries. These surface facilities provide water to major cities and industries in the region.

Ground water is the major source of irrigation water in the study area. Some of the ground water is high in salts and can only be used for irrigating salt-tolerant crops. Wells are characteristically shallow and weak throughout the area. These conditions substantiate the need to increase rainfall, thereby saving ground water of useable quality for later use.

2.6 Field Operations

2.6.1 General

In order to achieve the objectives of the Texas HIPLEX Program, six summer-time field projects were conducted during the 6-year period ending in 1980. The purpose of the field projects was to gather data to provide sufficient details on environmental, cloud and precipitation characteristics in the Texas High Plains

---

*When the economic studies were performed, the project area did not include Andrews, Gaines and Midland counties, but did include Fisher, Nolan and Coke counties.

area, and to lay the foundation for a suitable experimental program design. The field projects were conducted consecutively each summer season, beginning in 1975.

The field projects expanded from a relatively simple data-gathering effort in 1975, to a more exhaustive and quite sophisticated field project in 1980. The marked contrast between the first year's project to that of 1980 may be directly attributed to the cooperation among the Bureau, the Department and other participants in the Texas HIPLEX Program.

The 1978, 1979, and 1980 Texas HIPLEX field project daily operations were documented by Department staff (Riggio and Alexander, 1978; Alexander and Riggio, 1980; and Alexander and Riggio, 1981). The reports include equipment summaries, surface analyses, daily weather and operations summaries, surface weather observations, and aircraft flight records and debriefing notes.

2.6.2 Participants

For the 1975 through 1980 period, the Texas HIPLEX field participants included the following:

— Texas Department of Water Resources, which provided the overall field project management;

— Colorado River Municipal Water District, which supplied the services of a cloud physics and seeding aircraft, a meteorologist, monitoring radar systems, and installed, maintained and operated the surface raingage network;

— Texas A&M University, which installed, maintained and operated the surface weather stations and rawinsonde network, performed analyses and gave interpretations of mesoscale data and cloud physics data;

— Texas Tech University, which operated and maintained the Skywater radar, performed analyses of aircraft, rainfall and radar data, collected and interpreted visible and infrared satellite imagery in real-time support of the field operations as well as for satellite analysis;

— Meteorology Research, Incorporated, which operated and maintained the M-33 radar system through the 1978 field season, and provided an instrumented cloud physics aircraft during the 1978 and 1979 field seasons;

— Colorado International Corporation, which provided a cloud seeding/physics aircraft during the 1978 field season, and technical assistance in operating and maintaining the airborne cloud physics system during the 1979 and 1980 field seasons;

—   Big Spring Aircraft, which furnished an aircraft for cloudbase sampling during the 1975, 1976 and 1977 field seasons; and

—   North American Weather Consultants, which analyzed M-33 radar data collected during the 1976-1978 period.

2.6.3   Instrumentation

2.6.3.1   Radar

Radar data were collected during each of the six field seasons, with the M-33 radar used as the primary radar data-collection system from 1975 through 1978, and the Bureau's Skywater radar, used as the primary radar data-collection system during 1979 and 1980. The District also operated a 3-cm radar unit and a 5-cm FPS-77 radar unit in a monitoring mode as support to project aircraft operations. Radar data were also made available from the National Weather Service WSR-57 radar.

The M-33 radar is a dual wavelength system capable of operating as a 3-cm radar and/or a 10-cm radar. The M-33 radar was developed and used for military purposes, but was freed from military use and modified (Carbone et al., 1976) to fit the needs of the Texas HIPLEX Program. The radar was used for data collection purposes during the 1975-1978 field projects. It was operated in a 360-degree volume scan sequence which typically began at an elevation angle of 1.5 degrees, with subsequent scans increased in increments of 1.5 degrees to a maximum angle generally ranging from 9 to 18 degrees. A volume scan would normally take five minutes to complete, after which the cycle would be repeated. Radar data were recorded over a radius of 136.5 km (84.6 mi). The radar was located at Winston Field Airport in Snyder, Texas, during the four years of its use in the Texas HIPLEX Program.

During the 1979 and 1980 field projects, the Texas HIPLEX Program operated the Skywater radar that had been developed principally by the Bureau for the HIPLEX Program. The Skywater radar has a 5.4-cm wavelength and a 1-degree beam width. The radar scanned in volume modes of 360 degrees in the azimuth at elevations ranging from 1 degree to 12 degrees in 1-degree step increments. Each volume scan took approximately 5 minutes to complete. The Skywater radar was capable of operating in one of four scanning modes. The MON (monitoring) mode was used when aircraft were not flying a HIPLEX mission. The Z-R (reflectivity-rainfall) mode was used in conjunction with aircraft flying near cloud base to collect data and compare observed reflectivity values with rainfall rates. The ACC (Aircraft Close In) mode was used when Texas HIPLEX aircraft conducted a mission within 50 km (31 mi) of the radar. The ACF (Aircraft Far Out) mode was used when Texas HIPLEX aircraft conducted a mission greater than 50 km (31 mi) from the radar.

The data collected by the Skywater radar was digitized and recorded in a computer-compatible format, as described by Schroeder and Klazura (1978). Data output included composite maximum reflectivity and echo top displays, an equivalent reflectivity file, and a case study summary file which contained location, area, volume, rain, and motion information for radar echoes that were identified and tracked.

Radar echo data were also collected by using the National Weather Service WSR-57 radar. The radar was operated according to standard procedures, outlined in the Weather Surveillance Radar Manual. The radar operated in the S-band, i.e., a 10.3-cm wavelength. The antenna could rotate at a rate of 3 to 5 rpm, normally at a 1-degree elevation. The beam width, both vertical and horizontal, was 2 degrees.

2.6.3.2 Rawinsonde

Rawinsonde data were collected during all six Texas HIPLEX field seasons. The number of rawinsonde release sites increased from one in 1975, to four sites in 1976-1978, thence to seven sites in 1979-1980. During 1975, one rawinsonde site was located at Big Spring when, during each operational day, sondes were launched at 3-hour intervals as long as operational conditions existed. From 1976 through 1978, rawinsonde sites were located at Midland, Big Spring, Robert Lee and Post, Texas. Then, during 1979 and 1980, in order to achieve better spatial resolution for mesoscale analyses, seven rawinsonde sites were used. They were located at Midland, Big Spring, Sterling City, Post, Lamesa, Snyder and Seagraves, Texas (Figure 2.2). During 1976-1980 the rawinsondes were normally launched at 3-hour intervals, beginning at 1000 CDT (1500 GMT) on each operational day, and were usually terminated no later than 2200 CDT (0300 GMT).

2.6.3.3 Surface Weather Stations

In 1976 a network of manually read surface weather stations was installed for the Texas HIPLEX Program in support of the mesoscale analyses (Figure 2.2). The parameters measured at each surface station were temperature, relative humidity, atmospheric pressure, and wind speed and wind direction. Temperature and relative humidity were obtained from hygrothermographs, atmospheric pressure from microbarographs, and wind speed and direction from an automatic wind recording instrument. Ten of these surface stations were located in the field during the 1976 and 1977 field seasons. This number was increased to 16 during 1978. During 1979 the Bureau set up a network of twenty-five (25) special automatic surface weather stations with five co-located manual stations (Figure 2.2). The data collected at each automatic station consisted of 5-minute averages of temperature, relative humidity, pressure, wind speed, wind direc-
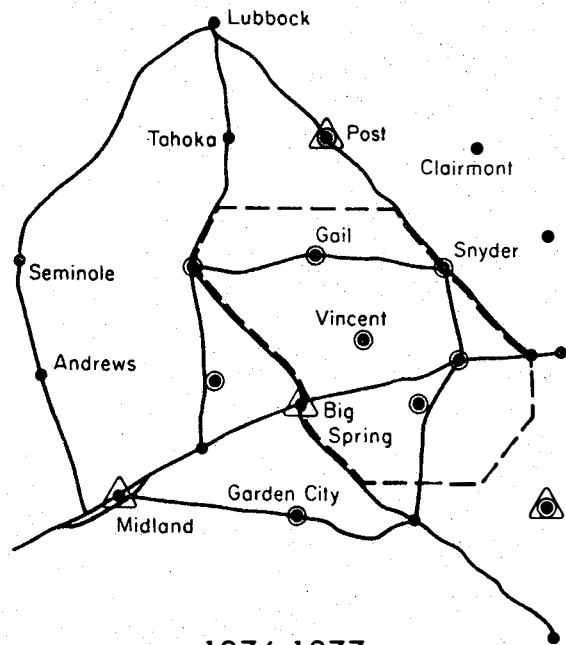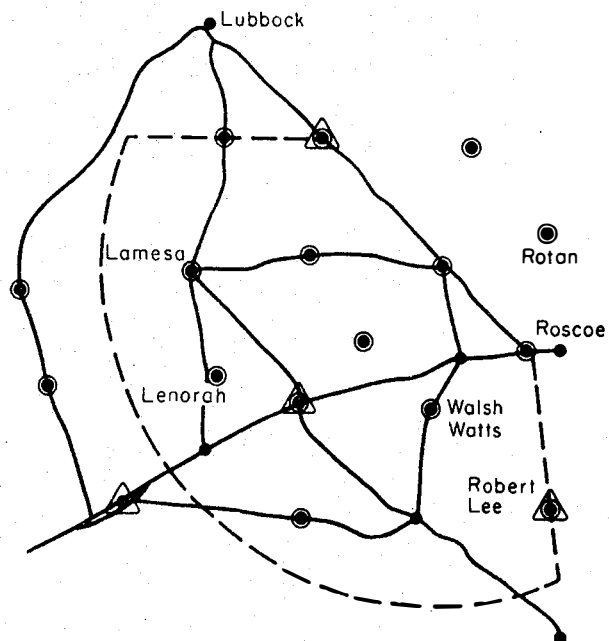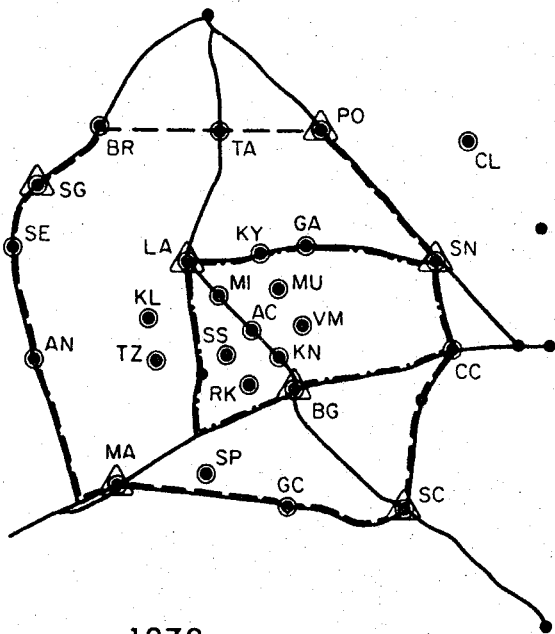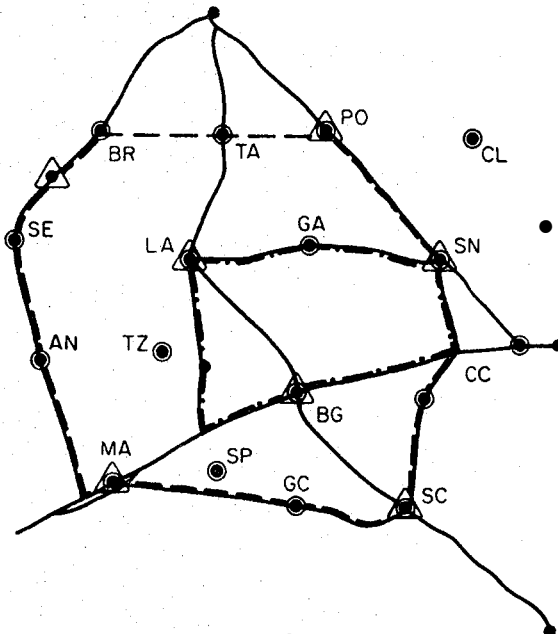
Figure 2.2. Texas HIPLEX rawinsonde and surface weather station networks.

tion, precipitation and battery voltage. The data were stored in a micro-processor as they were collected during the hour for each 5-minute period, and transmitted to a ground receiving station via satellite once each hour on a predetermined schedule. The automatic weather stations were deployed in the field for the first time in Texas in 1979, after they were manufactured. Therefore, the 1979 season's data served as an initial field test and systems shakedown, resulting in some unreliable data. Because the automatic stations were needed to support the Montana HIPLEX project in 1980, the automatic stations were not available to the Texas HIPLEX project. The network of 16 manually-read surface stations, used in 1978, was reinstated and used in 1980 (Figure 2.2).

2.6.3.4 Aircraft

2.6.3.4.1 Colorado River Municipal Water District

Under contract to the Department, the District supplied the Texas HIPLEX Program with two aircraft. For the first three years, the District operated one aircraft—a Piper Aztec—as a cloud base seeding and cloud physics aircraft. The Aztec had an average rate of climb of 2.5 to 4.1 m s^{-1} (500 to 800 ft min^{-1}) for altitudes up to 3,660 m (12,000 ft) above mean sea level. During the 1975, 1976, and 1977 field seasons the aircraft was used to seed clouds at cloud base. Information collected by this aircraft on each mission consisted of cloud-base height, updraft diameter, and an estimation of maximum updraft velocity. During the 1978 field season, a cloud-base measurement package was installed on the aircraft. The cloud physics package consisted of instrumentation for measuring and recording temperature, humidity, vertical velocity and rain drop spectra (300 to 4,500 μm). Other parameters measured and recorded included time, pressure altitude, air pressure, and true air speed. An observer accompanied the pilot on board the Aztec to record any visual cloud characteristics pertinent to the mission.

Beginning in 1978, the District also provided the Program with a PA31-P pressurized Navajo as an on-top cloud-seeding aircraft, and subsequently in 1979 and 1980 as a cloud physics aircraft. The aircraft was powered by two turbocharged engines, rated at 425 hp each. The aircraft was equipped with a fuselage-mounted AgI dispenser capable of dropping a total of 96, 30-gram AgI cartridges at various rates. Cloud seeding performed by this aircraft was generally accomplished by dispensing AgI ejectable pyrotechnics (or flares) at the -10°C level into growing turrets. The District p-Navajo was equipped with cloud physics measurement instruments during the 1979 and 1980 field seasons. Tables 2.1 and 2.2 list the meteorological variables measured by the aircraft for the respective seasons.

Table 2.1   Variables Measured and Recorded by the District's P-Navajo in 1979 Texas HIPLEX Field Program

Cloud liquid water content (Johnson-Williams hot wire)

Total liquid water content

Ice particle concentration (CIC/Lawson laser device)

Air temperature (Rosemount total temperature probe and NCAR-type reverse flow probe)

Dewpoint (E.G. & G. hygrometer)

Absolute pressure (Cognition absolute pressure transducer)

True airspeed (Cognition differential pressure transducer)

Location (HT Instruments VOR; aircraft avionics DME)

Table 2.2   Variables Measured and Recorded by the District's P-Navajo in 1980 Texas HIPLEX Field Program

Meteorological Sensors

Air Temperature probes; Rosemount Model 101E, Reverse Flow Housing with Platinum Element
Dew Point Temperature: EG&G Model 137
Johnson-Williams, Liquid Water Content
CIC/Lawson, Cross-Polarized Ice Crystal Counter
Total Water Content Device (NOAA version)
PMS 2-D particle probe (25 to 800 μ m)
PMS Forwarding Scattering Spectrometer Probe (FSSP) (2 to 3 μ m or 3 to 45 μ m)
Accelerometer (Sunstrand)

Aircraft Sensors

Aircraft Position:
    Air Speed: Rosemount 506
Altitude: "Pick-Off" from Aircraft Altimeter
VOR/DME; "Pick-Off" from Aircraft Avionics

Microprocessor/Display/Recorder

Microprocessor/16K core: Z-80 with S-100 boards
Sony 7-inch Cathode Ray Tube (CRT)
Sony Audio Cassette Recorder
Axiom Digital Printer
9-Track Incremental Recorder

The crew on board the Aztec and p-Navajo during each Texas HIPLEX flight consisted of a pilot and an observer who documented cloud features and who made written records of other meteorological data pertinent to the mission.

2.6.3.4.2 Meteorology Research, Incorporated

Meteorology Research, Incorporated (MRI), operated a cloud-physics aircraft during the 1978 and 1979 field seasons. The MRI Piper Navajo was an unpressurized, de-iced aircraft, powered by two 300-hp turbocharged engines. It had the capability of operating at altitudes up to 7,600 m (25,000 ft), with air speeds between 150 and 400 km h^{-1} (80 and 220 Kts). The range of the aircraft extended to about 2,400 km (1,500 mi). The crew on board the aircraft consisted of a pilot, a scientist, and an equipment technician.

The instrument package was designed to take measurements of cloud physics, environmental, and aircraft state parameters. The measurements made by the respective sensors are listed in Table 2.3.

In addition to the sensors, the scientist used two 35-mm cameras to take cloud and on-board radar screen photographs. An event box was located in the cockpit for marking the important events on the data tape.

2.6.3.4.3 Colorado International Corporation

Colorado International Corporation (CIC) operated a Learjet (Model 23) during the 1978 Texas HIPLEX Program. The aircraft was equipped with a cloud physics data acquisition system and ejectable AgI pyrotechnic flares. The cloud physics parameters measured by the aircraft are listed in Table 2.4.

The Learjet was used during the 1978 field project to (1) help select suitable clouds for seeding, (2) conduct cloud-seeding operations near the -10°C level, and (3) make repeated penetrations of the treated cloud(s) at altitudes around the -10°C level, while another cloud physics aircraft penetrated the cloud at lower altitudes. If the cloud top did not extend above the -10°C level, the Learjet would obtain data on the cloud environment around cloud top, take photographs and record verbal comment, and penetrate untreated clouds for comparative data. During a few missions when the Learjet was the only aircraft used, it treated a target cloud and then rapidly descended or ascended, as deemed appropriate, up to 60 m s^{-1} (12,000 ft min^{-1}) descent and 25 m s^{-1} (5,000 ft min^{-1}) ascent, to collect cloud physics data. On one occasion (June 28, 1979), the Learjet conducted a low-level (300 m [1,000 ft]), above ground, high-speed (460 km h^{-1} [285 mi h^{-1}]) mapping mission over the surface recording and rawinsonde network.

Table 2.3   Variables Measured by MRI Cloud Physics Package During the 1978-1979 Texas HIPLEX Field Program

Cloud Physics

Particle size and distribution
   PMS Axially Scattering Spectrometer Probe (3 to 45 μ m)
   PMS Cloud Particle Spectrometer Probe (20 to 300 μ m)
   PMS Precipitation Particle Spectrometer (300 to 4,500 μ m)

Ice particle concentration
   Continuous Ice Crystal Counter (Turner-Radke type)
   (100 to 600 μ m); 0 to 5,000 particles s^{-1}

Nuclei concentrations
   Millipore Filters
   CCN Bag Samples

Particle Replicators and Imaging
   MRI Foil Impactor
   2-D Cloud Particle Imaging Probe (25 to 800 μ m)

Liquid Water Content
   Johnson-Williams Liquid Water Content Indicator
   Bulk Water Sampler

Photos and Film
   Recording Bendix RDR-130, X-Band Weather Radar
   Super 8-mm Time Lapse Movie Camera
   35-mm Cloud Photos

Environmental

Air temperature
   Rosemount 102 Total Temperature Probe (+50°C)
   MRI Axial Flow Vortex Thermometer (-30 to +50 °C)

Dewpoint
   EG&G Model 137-C1 Hygrometer (-57 to +71°C)
   MRI Lyman-Alpha Hygrometer (-35 to +30°C)

Turbulence
   MRI Universal indicating turbulence system (0 to 10 R units)

Aircraft State

Altitude
   Validyne Absolute Pressure Transducer 0 to 101 × 10^3 Pa (0 to 14.7 lb in^{-2})

Airspeed
   Validyne Differential Pressure Transducer 0.0 to 4.8 × 10^3 Pa (0.0 to 0.7 lb in^{-2})

Rate of climb
   Ball Brothers Variometer +7.6 m s^{-1} (+1,500 ft min^{-1})

Navigation
   Dual Digital VOR/DME 0 to 359° and 0 to 185 km (0 to 100 nmi); Scanning DME

Compass Heading
   Humphrey's DG04 North-Seeking Gryo Compass (0 to 359°)

Table 2.4 Variables Measured by the CIC Learjet During the 1979 Texas HIPLEX Field Season

Parameter	Manufacturer	Sample Rate
Static pressure	Rosemount	10 s^{-1}
Dynamic pressure	Rosemount	10 s^{-1}
Total pressure	Rosemount	10 s^{-1}
Dew Point	EG&G	1 s^{-1}
Heading	Lear Sigler	1 s^{-1}
Pitch	Lear Sigler	10 s^{-1}
Roll	Lear Sigler	10 s^{-1}
Angle of attack	Rosemount	10 s^{-1}
Vertical acceleration	Sundstrand	10 s^{-1}
DME range	King Radio	1 s^{-1}
VOR azimuth	Wilcox Radio	1 s^{-1}
Liquid water content	Johnson-Williams	1 s^{-1}
Cloud particle size and concentration	PMS-2-D	Continuous
Ice crystal concentration	CIC	Continuous
CO_2 seeding rate	CIC	1 s^{-1}
Agl flare number	CIC	Continuous
Discrete events	CIC	Continuous
Time	PMS	Continuous

35-mm hand-held photos

2.6.3.4.4 Big Spring Aircraft

A Big Spring-based company, Big Spring Aircraft (BSA), operated a cloud base monitoring aircraft during the field programs of 1975-1977. During 1975 and 1976, BSA used a Cessna 206 for collecting and manually recording data on cloud base height, temperature, dew point, updraft speed and diameter, and making an estimate of maximum updraft velocity. During the 1977 field season, BSA operated a Cherokee PA-32-300, which was equipped with a data recording system whereby dew-point temperature, temperature, pressure and rate of climb were automatically recorded.

2.6.3.5 Raingages

The Texas HIPLEX Program operated a concentrated raingage network throughout the 6-year duration of its first phase. The raingage network consisted of two different types of raingages: a fence-post wedge raingage, and a weighing-bucket recording raingage. The number of recording raingages located in the field increased from a total of 26 raingages used during the 1975 field season to 106 raingages used during the 1980 season.

During the 1975 field season, 12 of the 26 recording raingages were clustered together in groups of three, in triangles, separated by 1 km on a side. The purpose of clustering the raingages was to provide a spatial rainfall measurement average, as opposed to a point source measurement. However, as more raingages were added to the network and the raingage density increased, this type of grouping became unnecessary.

Forty-nine recording raingages were used to obtain rainfall data in 1976; of this total, 41 were installed within an area roughly 24 km × 28 km square (14.9 mi × 17.4 mi square), and centered near Vincent, Texas. Also, 94 nonrecording wedge-type fence post raingages were installed by the District throughout the study area. These raingages furnished data of daily rainfall accumulations. The nonrecording raingages were read by District staff after each rainfall event.

A network of 68 recording raingages was operated in the Texas HIPLEX region during the 1977 field season. The density of this network was approximately one raingage per 104 km^2 (40 mi^2). All 68 raingages had a daily chart rotation. Wedge-type, fence-post raingages were also collocated by the District with the recording raingages, and an additional 81 wedge-type raingages were placed at new locations within the project area.

The 1978 Texas HIPLEX Program utilized an even larger recording raingage network. The density of the network remained the same as the previous year, but the coverage area was increased. Each of the 81 recording raingages used had a daily chart rotation. Data were also collected from 81 wedge-type fence-post raingages that were spaced approximately 5 km (3 mi) apart along various highways that traversed the project area.

The recording raingage network for the 1979 and 1980 Texas HIPLEX seasons was increased to 106 raingages, capable of measuring up to 305 mm (12 in) of rainfall on a 7-day chart. Figure 2.3 shows the 1980 Texas HIPLEX recording raingage network. As in 1978, the recording raingage network was augmented by an 81 wedge-type raingage network. The wedge-type raingages were read after each rain event. Near the center of the Texas HIPLEX project area, around Lake J. B. Thomas, the density of the recording raingage network was increased from one raingage per 104 km^2 (40 mi^2) to one raingage per 25 km^2 (9 mi^2) during the 1979 and 1980 field seasons. Approximately 39 recording raingages were located in this center grid primarily for the purpose of better documenting ground-truth rainfall rates for comparison with radar-reported rainfall rates.
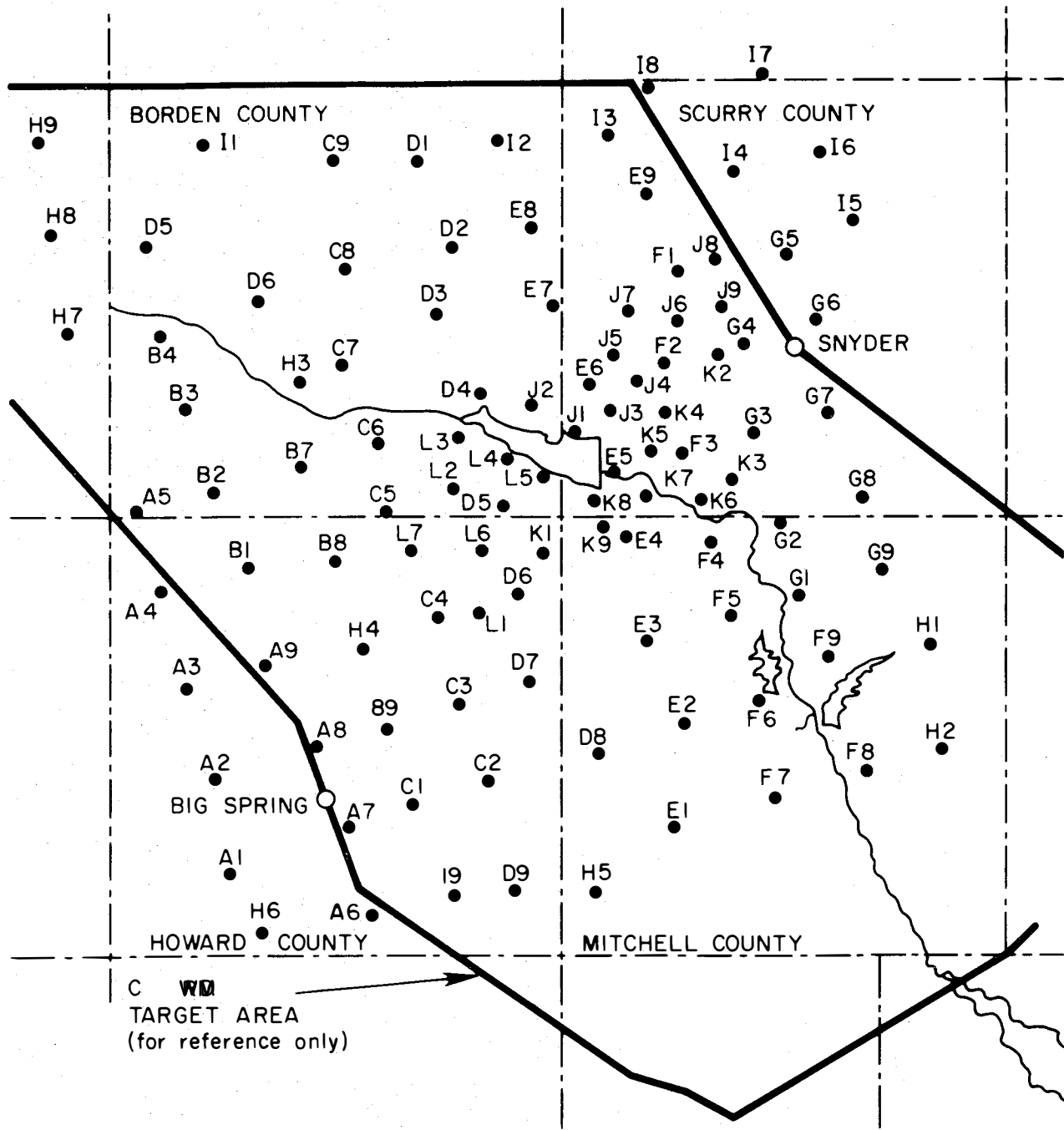
Figure 2.3. 1980 Texas HIPLEX recording raingage network with approximately 10 km (some closer) spacing between raingages.

Before and after each season, each recording raingage was calibrated at 1-inch intervals by Department and District technicians. All raingage data were processed and archived with the Bureau.

2.6.3.6 Satellite Laserfax

Laserfax satellite imagery was collected during the 1979 and 1980 Texas HIPLEX field program. These data were provided by Geostationary Operational Environmental Satellites (GOES) at 30-minute intervals each day; the types of imagery received alternated between visible and infrared data during the daylight hours, while at night infrared data were collected. These data were used in near real time in support of forecasting and aircraft operations.

2.6.4 Data Inventory

All data collected during the Texas HIPLEX field seasons were forwarded to the Bureau and incorporated into the HIPLEX Data Bank. These data can be requested from the Bureau by writing to:

Bureau of Reclamation
Attn: Data Manager, Code D-1220
P. O. Box 25007, Denver Federal Center
Denver, Colorado 80225

Inventory documents of data collected during the 1975, 1976, 1977, 1978, 1979, and 1980 HIPLEX field seasons are also available through the Bureau. These documents are intended to acquaint the researcher with the type, format and period of record of the data available.

2.6.5 Reports

Throughout the Texas HIPLEX Program, the Department submitted numerous reports to the Bureau for the purposes of keeping the Bureau informed about Texas HIPLEX activities, coordinating Texas HIPLEX work with other HIPLEX studies, and documenting achievements, techniques and conclusions of Texas HIPLEX research. These reports include monthly progress reports describing work performed, travel, and personnel changes during each month; interim progress reports, prepared every six months, containing all work, data, and results obtained during the reporting period; and final reports, documenting specific areas of Texas HIPLEX research, including all technical data relevant to the particular area of research, the techniques developed, analyses performed, and the conclusions and recommendations derived.

Heretofore, all Departmental reports submitted to the Bureau were either individual reports that focused on one element of the Texas HIPLEX Program, or

were collections of reports submitted to the Department by individual subcontractors. These reporting procedures were followed because the major thrust of the Texas HIPLEX Program has been the collecting and processing of data, and subsequently reporting these data to the Bureau. Only during the last few years when the data base was relatively large, exploratory studies were begun for the purpose of analyzing the data. These exploratory studies included analyses of thermodynamic and kinematic properties of the environment of convective activity, radar echo and rainfall characteristics needed to define seeding hypotheses and response variables, and the development of measuring and seeding techniques.

2.6.6 Summary

A comprehensive table (Table 2.5) of all Texas HIPLEX operations from 1975 through 1980 follows. It provides documentation of all operational days during the years reported on and summarized in this report.

Table 2.5
Summary of Texas Hiplex Field Operations, 1975-1980
[Non-operational days not included in table]

(√ Denotes data collected)

1975

Date	Rawinsonde*	Aircraft	Radar
6-09			√
12	√		
16			√
17	√		
20	√	Seed	√
21			√
22			√
6-03			
04	√		
05	√		√
09			√
29	√	Seed	√
30			√
7-01	√		√
02	√	Seed	√
03	√		√
04			√
09		Samp[1]	√
11		S/S[2]	√
12		S/S	√
17			√
18	√		√
19	√	Seed	√
20	√	Seed	√
24	√	Seed	√
25	√	S/S	√
26	√		
28	√	Seed	√
29	√		
31	√	Samp	√
8-01	√	Seed	√
02	√	Seed	√
04	√		√
05	√		√
06	√		√
07	√		√
08	√		√
12	√		√
13	√	S/S	√
14	√	S/S	√
15	√	S/S	√

1976

Date	Mesoscale	Aircraft	Radar
5-10		Samp	
20		Samp	√
21		Samp	√
22		Samp	√
25		Samp	√
6-03		Samp	√
04		Samp	√
05		Samp	√
08	√	Samp	
09	√		√
11	√		√
12			√
15	√	Samp	√
17		Samp	√
21		Samp	√
22	√	Samp	√
23	√	Samp	√
25	√	Samp	√
27		Samp	√
28	√	Samp	√
30			√
7-01	√	Samp	√
02		Samp	√
03	√	Samp	√
04		Samp	√
05		Samp	√
08	√		√
10	√	Samp	√
11	√	Samp	√
12	√	Samp	√
14		Samp	√
15		Samp	√
16		Samp	√
17		Samp	√
18			√
21		Samp	√
22		Samp	√
23		Samp	√
26			√
27		Samp	√
28			√
29			√
30			√

1977

Date	Mesoscale	Aircraft	Radar
6-01	√		√
07	√		
08			√
09	√		√
11	√	Seed	√
12		Seed	
13		Recn	√
14	√	Seed	
20			
21	√		√
22	√	Recn[3]	√
23	√	Seed	√
24	√		√
25	√		√
26		Seed	√
27	√	Seed	√
28			√
30			√
7-07	√		√
08	√		√
10	√		√

1978

Date	Mesoscale	Aircraft	Radar
6-01	√	Recn	√
02	√(4)	Samp	
04	√	Recn	√
05	√	Seed	√
06	√	Seed	√
07	√	Seed	√
13	√	Seed	√
14	√(5)		
27	√(4)		√
28	√(4)	Samp	√
29	√	Samp	√
30	√	Seed	√
7-01		Seed	√
02		Samp	√
03		Seed	√
15		Samp	√
17	√	Recn	√
20		Seed	√
21	√		√
22	√	Samp	√
23	√	Seed	√
24	√	Samp	√
25	√(4)		
26		Seed	√
30			√

1979

Date	Mesoscale	Aircraft	Radar
5-20			√
21	√		
26	√		√
27	√?		√
28	√	Recn	√
31		Samp	√
6-01	√		√
02			√
04	√	S/S	√
05	√	Samp	√
07	√	Tfb[6]	√
08	√		√
09	√(4)		√
21	√(4)	Recn	√
24	√	S/S	√
25		Recn	√
7-02	√(4)	Samp	√
03	√		√
04	√(4)	S/S	√
05	√(4)	S/S/ZR[7]	√
06	√		√
07	√(4)	ZR	√
08		S/S	√
09		Recn	√
12		Tfb	√
14	√(4)		√
15		Samp	√
16	√	Recn	√
17	√(5)	MM[8]	√
18	√(5)		√
19			√
20			√

1980

Date	Mesoscale	Aircraft	Radar
5-15	√		√
18		Samp	√
19	√(4)		√
20		Samp	√
21	√(4)	Recn	√
23	√(4,5)	Samp	√
26	√	Samp	√
27	√	Recn	√
28	√(4)		√
29	√(4)		√
6-01	√	Recn	√
02		Samp	√
03	√(4)		√
04		CC[9]	√
05		Tfb	√
08	√		√
09	√(5)	Recn	√
10	√(4)		√
13		Tfb/CC	√
14	√(4)	MM	√
15		Iac[10]	√
17	√		√
18	√(4)	Samp	√
19	√(4)	Samp	√
20		S/S	√
21	√(4)	Samp	√
22			√
25			√
27			√

* Big Spring launch only
[1] Samp—Sampling mission
[2] S/S—Seeding and sampling mission
[3] Recn—Reconnaissance mission
[4] Partial mesoscale day
[5] Research Rapid Scan Satellite Day (RRSD)
[6] Tower fly-by
[7] Sampling, seeding, and radar reflectivity-precipitation calibration
[8] Mesoscale mapping
[9] Cross-country cloud sampling
[10] Interaircraft comparison

3. TEXAS HIPLEX STUDIES

3.1 General

At the beginning of the Texas HIPLEX Program it was decided that to fully understand the meteorological processes involved in cloud and subsequent rain development, it would be necessary to collect observational data at the mesoscale and at the microscale. It was recognized that the mesoscale environment has a substantial effect on the convective cloud and microphysical properties within the cloud. A total integration of the effects of these processes at the two scales is important to understand better the variability of natural cloud development. The effects of the mesoscale environment on the variability of natural development have been reported by Chen et al. (1978), Matthews and Silverman (1980), Tripoli and Cotton (1980), Chen and Orville (1980), and others.

Therefore, the Texas HIPLEX Program established a measurement network to examine the mesoscale physical properties of the environment within which clouds develop. Primary emphasis of Texas HIPLEX was directed at understanding the relationships between the dynamic environmental properties and convective development. As the mesoscale program evolved over the initial years, secondary emphasis was placed on understanding the cloud microphysical processes.

The definition of mesoscale and microscale used throughout this report follows Orlanski (1975). The mesoscale ranges in horizontal scale from 2,000 km to 2 km. To further refine the mesoscale, it was subdivided into three divisions: the meso α-scale, ranging from 2,000 km to 200 km; the meso β-scale, ranging from 200 km to 20 km; and the meso γ-scale, ranging from 20 km to 2 km. The microscale falls into a range less than 2 km. Table 3.1 details the dimensions of each scale.

Satellite, radar and networks of ground-based and upper-air recording devices (rawinsondes) are the principal Texas HIPLEX tools for acquiring mesoscale data. The microscale, which encompasses meteorological events that transpire within convective elements, requires radar and internal cloud sensing instrumentation to acquire data.

Acquiring basic knowledge of the events characteristic of each scale is fundamental to interpreting their interrelationships, and hence is the key to developing the science of precipitation augmentation and management. The background observations collected during the exploratory phase of the Texas HIPLEX Program consisted of data with which to measure and study the mesoscale cloud environment (Scoggins et al., 1978, Chen et al., 1979; Scoggins et al., 1979; Williams and Scoggins, 1980; and Sienkiewicz et al., 1980). Concurrent observations have been made in cloud (Long, 1980; Takeuchi, 1980), by radar (Smith et al., 1977; Driscoll 1978; Humbert et al., 1978; Driscoll 1980; and Haragan et al., 1980), at ground level (Haragan, 1978), and by satellite (Jurica, 1979).

Table 3.1 Texas HIPLEX Scale Definitions

Scale	Time (h)	Horizontal (km)	Precipitation Area (km²)	Phenomena
Microscale	<1	<2	<30	Cloud properties updraft/downdraft, turbulence, thermal, cloud tower
Meso γ -scale	1-6	2-20	$30\text{-}10^2$	Raincell, small convective complex, cloud cluster, congestus, thunderstorm, gust front
Meso β -scale	6-12	20-200	$10^3\text{-}10^4$	Cloud ensemble, convergence line, squall line, mountain/valley circulation, low-level jet, vorticity sheet, inertial wave, jet streak, dryline
Meso α -scale	>12	200-2,000	$>10^4$	Large cloud clusters, front, hurricane, baroclinic wave, mid-tropospheric wave, low easterly wave

Note: A certain amount of flexibility must be accepted when categorizing real atmospheric events. A given cloud grouping may have the time characteristics of one scale but the horizontal extent of another scale. For example, a grouping may be classified as a cloud ensemble even though it exists for less than 6 hours.

In summary, the first six years of the Texas HIPLEX Program consisted mostly of exploratory research, i.e. data collection and some initial exploratory analyses. During the last year of the Texas HIPLEX Program increased analysis efforts were directed at understanding the mesoscale controls of convective cloud development and the microscale properties of the cloud and precipitation processes. No attempt has been made to offer a statistical design for the Texas HIPLEX experiment because the degree of analytic effort has not reached that level. The analyses presented in this Summary Report only represent the findings derived from the initial exploratory studies. The future work of the Texas HIPLEX Program will focus on the statistical design of the cloud experiment through a greater analysis effort of data collected.

The various initial exploratory studies reported are categorized according to meteorological scale. The meteorological scales within which the studies reported in this Summary Report are presented include the meso α-scale, meso β-scale, meso γ-scale, and microscale. The reader is encouraged to review any of the many referenced reports for a more comprehensive and complete presentation of any of the individual studies which comprise the Summary Report.

Meso α-scale systems are responsible for transporting moisture into the Texas HIPLEX area, and for establishing the average wind field and stability conditions over the area; meso β- and meso γ-scale systems are responsible for initiating convective activity and for modifying the environment near (within a few cloud diameters) the convective activity; and microscale systems and processes within the clouds are responsible for droplet formation, the formation of rain, and the exchange of mass at the cloud boundary between the cloud and its environment. While it appears that mesoscale systems control the development of convective cloud systems, it is the integrated effect of systems at all scales and their interactions which ultimately affect precipitation mechanisms and lead to

rain on the ground. The high variability of rainfall, both amount and areal coverage, attests to the complexity of the integrated effects.

Based on results of the initial exploratory studies and other weather modification research, some highly tentative ideas of the statistical experimental design have evolved and are presented in the Summary Report. Section 3 of the Report summarizes the initial exploratory studies. Section 4 attempts to bring together the salient findings in terms of convective development and subsequent precipitation. Section 5 offers tentative experimental units, seeding hypotheses and response variables.

/

3.2   Meso α-scale Observations

3.2.1   Satellite

Among the many contemporary tools used by the Texas HIPLEX Program, the weather satellite has proven to be a valuable source of information to project scientists. Data provided by these orbiting systems offer researchers a unique view of the behavior of interacting cloud systems over the Texas High Plains. Measurements made routinely by these satellites quantify elements of the atmosphere, such as profiles of vertical temperature and water vapor, liquid water content, land/water surface temperature, cloud height and movement, and total outgoing longwave radiation flux.

During the 1975-1980 six-year period, the Texas HIPLEX Program has utilized two different types of data from GOES: visible and infrared photographic imagery, and visible and infrared radiance data. Using these sets of data, project scientists have been able to determine the amount, distribution, temperature, height, and movement of various kinds of clouds that enter the Texas HIPLEX project site. Preparation of the data for analysis was conducted with the ADVISAR (All Digital Video Imaging System for Atmospheric Research), developed at Colorado State University and described by Reynolds and Smith (1979). Results are presented in a Texas HIPLEX study by Jurica and Chi (1979), entitled *Determination of Cloud Properties from Bispectral Satellite Measurements.*

Bispectral radiance data from the weather satellites were analyzed in relation to meso α-scale weather features as a case study for June 22, 1976. A critical visible (VIS) radiance value was derived for distinguishing clouds from the underlying noncloud surface. Then the infrared and visible data were examined thoroughly to ascertain cloud properties, such as cloud populations, percent cloud cover, cloud albedo, cloud height, and cloud movement. Since the resolution of the satellite data is well within the meso β-scale, the results of the analyses are given in Section 3.3.1.

Matthews (1980) made comparisons of the 1976-1977 geosynchronous satellite imagery among the three HIPLEX sites. He analyzed the daily frequency of occurrence of various cloud types and mesoscale triggering mechanisms of convective development at each of the HIPLEX sites.

From this limited 2-year data base it was surmised that certain similarities and differences were evident among the HIPLEX sites. All the sites exhibited a large number of days when convective clouds were observed by satellite. Also the most intense convective clouds occurred with mesoscale forcing. Each site did show some differences in cloud organization. The Montana site was characterized mainly by orographic clouds and cloud lines. Cloud lines and cloud clusters were predominate at the Kansas site, while the satellite imagery revealed mesoscale lines, clusters and airmass-isolated convection at the Texas site, with airmass-type convection being the most common.

3.2.2 Radar Echo Characteristics

3.2.2.1 Radar Echo Climatology

Analyses of weather data, collected by the M-33 radar system during the 1976, 1977, and 1978 Texas HIPLEX field seasons, examined the relationship between meso α-scale atmospheric patterns and radar echo characteristics. These analyses are reported in two Texas HIPLEX publications. One study was by Sutherland et al. (1980), entitled *Analysis of Digitized M-33 Radar Data From Texas HIPLEX, 1976-1978,* and the other study was by Humbert et al. (1978), entitled *Development and Interpretation of a M-33 Radar Climatology for the HIPLEX Region.*

The source of the synoptic information used in both studies was primarily from NWS surface charts and upper air 500 mb charts. Days were subjectively categorized in terms of meso α-scale features, i.e. the presence of fronts, troughs, inverted troughs, and ridges. The meso α-scale properties had a spatial dimension of about 700 km (430 mi), and a temporal dimension of about 15 hours. Radar data used in the analyses were taken from Plan Position Indicator display.

The general results from both studies were similar. The most frequent weather pattern observed during the period was a day that had no fronts in the target area with a 500 mb ridge overhead. Only 15 percent of the days with this synoptic feature had radar echoes. The most favorable meso α-scale patterns for radar echo occurrence were prefrontal or frontal days under the influence of a trough at 500 mb. All of the days with this pattern had echoes. A categorical breakdown of radar echo occurrence by surface features only revealed that the percentage frequencies of frontal days, post-frontal days and no-front days with echoes were 79 percent, 44 percent and 27 percent, respectively. For upper-air features only, echo frequencies of trough, ridge, and inverted trough days with echoes were 80 percent, 20 percent, and 33 percent, respectively.

3.2.2.2 Radar Echo Organization

Radar-echo organization with respect to mesoscale motion was examined by using M-33 radar data with echo intensity contours, NWS surface charts, NWS hourly radar summaries, data from a network of mechanical surface weather stations, and a rawinsonde array. These data were collected during the 1976 and 1977 Texas HIPLEX field seasons. A report describing this examination was prepared by Chen et al. (1979), entitled *Radar Echo Organization and Development in the Mesoscale Environment, A Case Study Approach.*

Two scales of atmospheric motion were defined and addressed. First, the meso α-scale included the evolution of echo systems in relation to synoptic features, such as fronts, troughs (at surface and upper-air), large-scale convergence zones, and moisture advection. Second, the meso β-scale addressed cloud and wave dynamics.

The primary objective of this study was to examine the effects of atmospheric parameters on the organization and development of radar echoes. Only the meso α-scale environmental effects upon the radar echo organization will be discussed in this Section. The reader is referred to Section 3.3.2 for additional discussions of the effects of the meso β-scale parameters on radar echo organization.

The radar echo organization used in this study was categorized as isolated cells, clusters and squall lines. The meso α-scale environmental effects, or the evolution and organization of three types of convection, were examined by using a case study approach. Six case studies were presented by Chen (1979), and are discussed below.

The Chen report examined only one case study when isolated cells were observed. Isolated cells were recorded by radar during the late afternoon on June 9, 1977, in association with the passage of a surface trough through the Texas HIPLEX area. The atmosphere was convectively unstable during the late afternoon and early evening, becoming near-neutral by 2100 CDT (0200 GMT). At 500 mb, a north-south zone of confluence was evident in western Texas, accompanied by a pocket of cold air (-10°C) approaching from the west. Low level winds were southerly with south-westerly flow in the mid and upper levels. The upper air sounding analysis indicated that tropical maritime air was overrun by tropical continental air. An upper level trough was west of the target area, and a surface trough was in the project area. The triggering mechanism appeared to be local convergence.

The second type of convective entity, a convective complex of cells, was studied by means of data based on three case study days. The three days were July 10, 1976, June 23, 1977, and July 8, 1977. Among the three case studies no single common meso α-scale environmental characteristic was noted, except that the atmosphere was convectively unstable in all

cases. Surface and upper air troughs were observed either in the Texas HIPLEX project area or in the vicinity of the project area to the west for all three cases. The triggering mechanism for each of the three case study days was different and was the result of either mesoscale dynamics, large-scale convergence or surface heating.

Two squall line case-study days were analyzed. The days were characterized by a convectively unstable atmosphere, but not of sufficient magnitude to support large-scale convection without additional dynamic support. It appeared that the development and maintenance of the squall line was aided by the 850-500 mb wind shear vector. The magnitude of the shear vector was greater on the convectively active days when squall lines developed than on days when complexes or isolated cells were observed. Also, the orientation of the lines was sensitive to the vertical shear of the horizontal winds.

Only during one case-study day was convection triggered by intense surface heating. As described by Chen *et al.* (1978) in the case study for July 10-11, 1976, surface features indicated the presence of a general confluence pattern in West Texas, with surface flow directed (around the western side of a high-pressure cell) into the Texas HIPLEX area from the east and east-southeast; no predominant frontal system or other meso α-scale organization was evident. At the 500 mb level, a low-pressure area existed above the Texas HIPLEX area. Upper-air soundings at Big Spring indicated that convective instability was present to some exent during the late afternoon, but then greatly increased through deep moist layers after the peak heating period. Accordingly, convective activity was triggered by surface heating which resulted in the formation of a convective complex that remained active for a three-hour period.

A summary of meso α-scale environmental parameters influencing radar echo organization is presented in Table 3.2 (reproduced directly from Chen *et al.* [1978]), and is in agreement with the results of Sutherland *et al.* (1980), and Humbert *et al.* (1980). At the meso α-scale, the majority of radar-echo formations were associated with the presence of a surface front or an upper-air trough located to the west of the Texas HIPLEX area. The case studies revealed that low-level convergence of moist air was important to the initiation and development of all three types of radar echoes, and that the magnitude of the 850-500 mb wind shear was directly related to echo organization. Only the July 10, 1976, case study was initiated by surface heating.

Table 3.2 Summary of Case Study Events During 1976-1977 Texas HIPLEX Field Seasons

	Time[1]	Troughs[2] sfc	Troughs[2] Upper air	Feature[3]	θe-Sounding[4]	LOC[5]	Windshear[6] (°)	Windshear[6] (m sec⁻¹)	T.M.[7]
1976									
June 22-23	N	W	I	SQ-LN	U-N	P	113	13.2	MESO-DYN
July 10-11	D	W	I	CMPX	U	BS	98	4.2	SFC-HT
1977									
June 9-10	N	I	W	IC, (LN)	U	P	121	9.1	CONV
June 11-12	N	W	W	SQ-LN	U	MAF	160	11.0	MESO-DYN
June 23-24	D	W	W	CMPX(SQ-LN)	U	BS	98	10.0	MESO-DYN
July 8-9	D	I	I	CMPX	U	RL	215	5.4	L.S. CONV

Key: [1]N-Night, D-Day
[2]I-In-site, W-West
[3]Sq-LN-Squall-Line, CMPX-Complex, IC-Isolated cells
[4]U-Unstable, N-Neutral
[5]LOC-Location of storm: P-Post, BS-Big Spring, RL-Robert Lee, MAF-Midland Air Force Base
[6]Shear is calculated at the observation station closest to echo activities (expressed in vector direction and magnitude, 500-850 mb)
[7]T.M.-Triggering mechanism of cloud formation; MESO-DYN - Mesoscale dynamics
SFC-HT - Surface heating
CONV - Local convergence
L.S. CONV - Large scale convergence

3.2.3 Precipitation

3.2.3.1 General

Of crucial significance in designing and ultimately evaluating a cloud seeding program for rainfall augmentation in the Texas HIPLEX project area is a sufficient understanding of the natural variability of precipitation that characterizes the area. Prior to 1978, a climatography of the Texas HIPLEX area which describes as completely and concisely as possible the pattern of rainfall occurrences that typify the region, did not exist. In April 1978, however, Haragan (1978) of Texas Tech University published a cloud and precipitation climatology of the HIPLEX region, entitled *Precipitation Climatology for the HIPLEX Southern Region.*

In providing an adequate statistical base for ascertaining "natural variability" of rain-producing clouds in the Texas HIPLEX area, the study enhances the capability of scientists to judge the effects of cloud-seeding activities on rainclouds. It serves as one of the tools for properly and accurately responding to the question, "Are the rainfall patterns observed when cloud seeding is performed due to the effects of the seeding, or are they merely a part of the natural variability of rainfall occurrence in the region?"

3.2.3.2 Rainfall Distribution

As is well known to climatologists and to residents of the southern High Plains region of Texas, the weather in the Texas HIPLEX area is character-ized by rapid changes and marked extremes, as well as large ranges in temperature from day-to-day and month-to-month. Approximately two-thirds of Big Spring's mean annual rainfall of 441.7 mm (17.4 in) is observed during the six warmest months of the year, or typically from April through September. The spring and summer rainfall common to the area results from several relatively large storm systems that migrate across the region, while often in September substantial rains in the area reflect the flow of moist, tropical air into the region from the Gulf of Mexico. Daily precipitation data for the months of April through September, collected over a 55-year period at Big Spring and Snyder, Texas, were examined first, using a statistical procedure that calculated "7-day running means" (Fig-ures 3.1 and 3.2). It was learned that from a minimum in late June, rainfall characteristically increases to a maximum in early July. Then from a low in early August it again increases to a broad period of maximum rainfall in late August and early September.

The study by the Texas Tech University group also showed the spatial distribution of rainfall changes during each of the five months of May-September (Figures 3.3 through 3.7). For example, for rainfall distribution in May shows a rather uniform decrease in precipitation amounts from east to
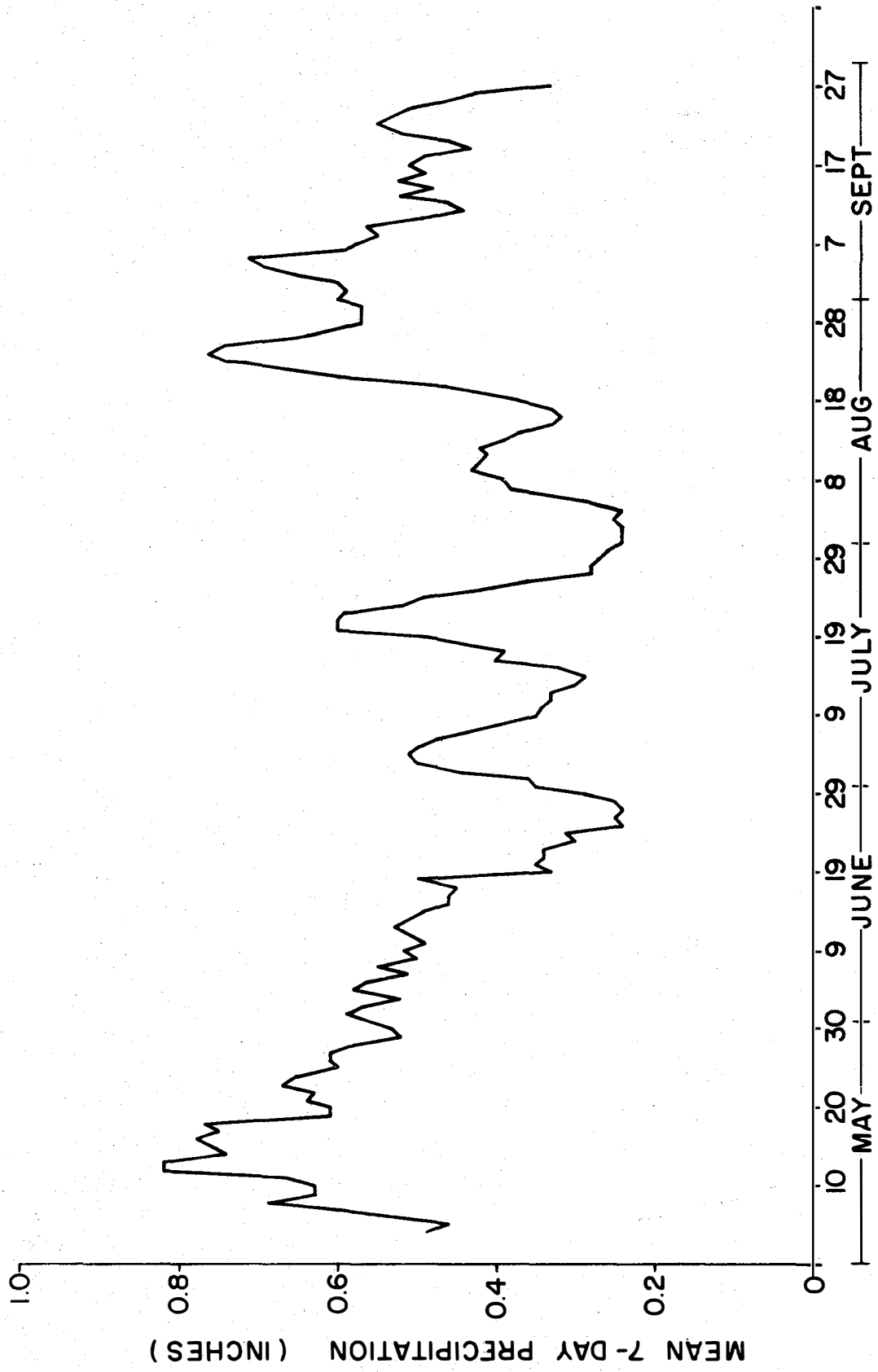
Figure 3.1. Daily precipitation 7-day running means—Big Spring.
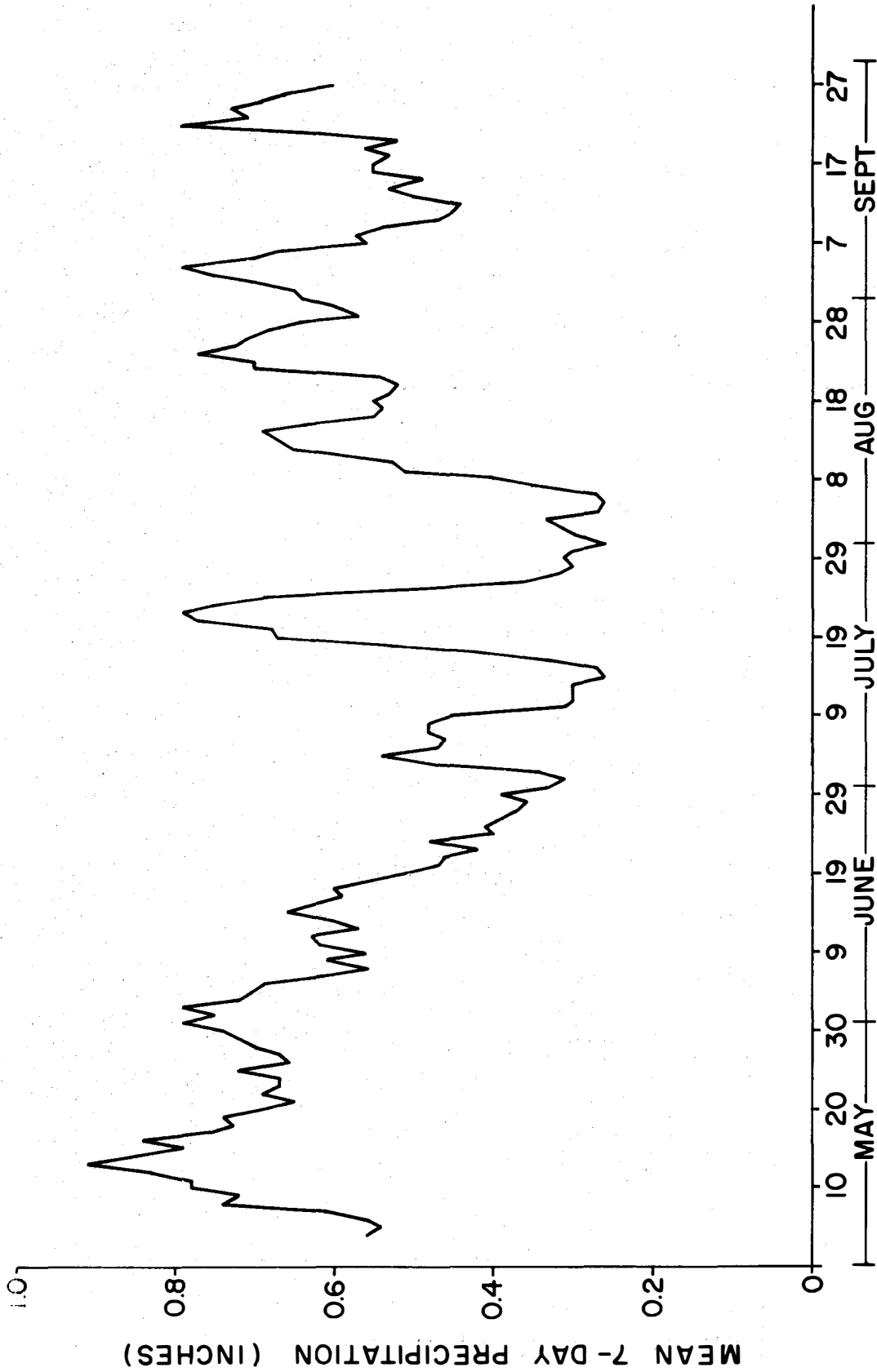
Figure 3.2. Daily precipitation 7-day running means—Snyder.

MEAN 7-DAY PRECIPITATION (INCHES)

west across the Texas HIPLEX area. In June, total amounts of precipitation area-wide are less, but the variation across the HIPLEX region is about the same as in May, except for a shift to a more northeast-southwest orientation. The July pattern is much less organized, reflecting the scattered nature of precipitation characterizing the summer. August is a bit more organized, with a broad maximum running from Muleshoe to Seymour and generally lesser amounts of rainfall than in July. Precipitation amounts increase in September, and once again exhibit a definite east-west gradient.

Space-autocorrelation analyses were used to gain further insight to the nature of the spatial change in distribution of rainfall over the Texas HIPLEX area (Longley, 1974). The results point to a track-oriented southwest to northeast along which many of the rain producing storm systems move during May (Figure 3.8), while in June the track becomes oriented more in a northwest-southeast direction (Figure 3.9). They also substantiate the observation that rainfall in June is more spotty, with a preponderance of localized showers often the rule.

3.2.3.3   Rainstorm Characteristics

Investigators at Texas Tech University (Jurica *et al.*, 1981) performed a series of analyses of rainfall data to describe the natural variability of certain rainstorm characteristics in the southern High Plains region of Texas. The examined data consisted of rainfall totals at 15-minute intervals, collected during four summer field programs (1977-1980), using a network of weighing-bucket recording raingages. While the density of the raingage network was altered from season to season, continuous data were obtained for the period April through September of each of the four years. A rainstorm was defined as a "rain period of at least 0.5-hour duration, separated from preceding and succeeding rain periods by at least one hour." In all, 120 rainstorms were identified for further study.

Initially, subjective isohyetal analyses were performed, using rainfall data for the 1979 and 1980 field seasons. From the spatial patterns that were generated, it was possible to estimate relationships among such parameters as storm depth, storm area, and storm duration. The maximum intensity of each rainstorm event was computed as a function of time and storm velocity. Furthermore, volumetric analyses were performed to compute storm area, integrated storm rainfall, and mean rainfall depth for each rain event. From this exercise, it was demonstrated that the calculation of rain volumes delivered acceptable results when a dense network with regular spacing was used.

The types of rainstorms observed in the southern High Plains of Texas were found to have a great degree of variability in intensity; rain volumes ranged from as much as 5.17×10^8 m^3 (419 thousand acre-feet) to as little
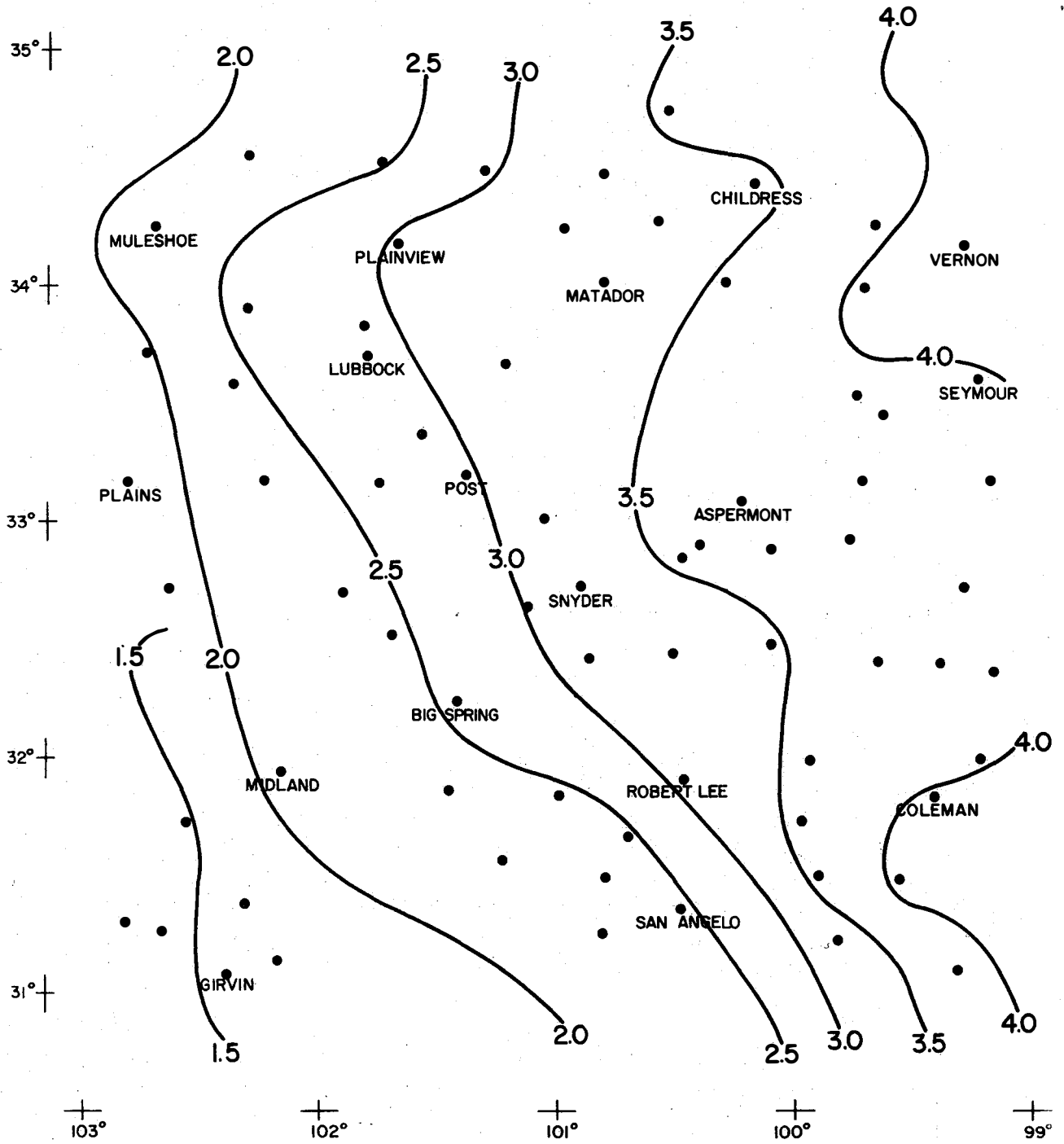
Figure 3.3.   Mean monthly precipitation (inches)—May.
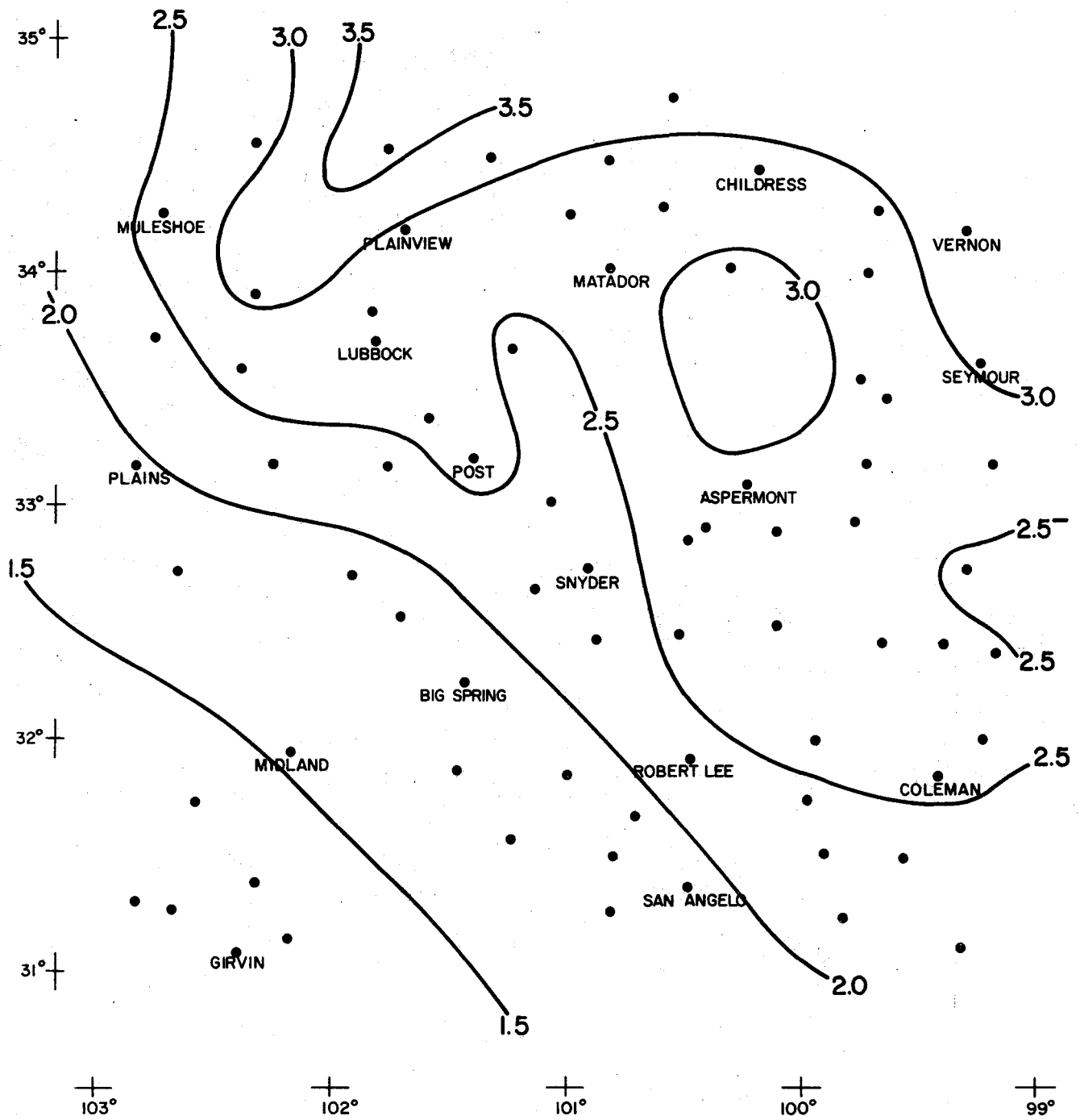
Figure 3.4 Mean monthly precipitation (inches)—June.

- 41 -
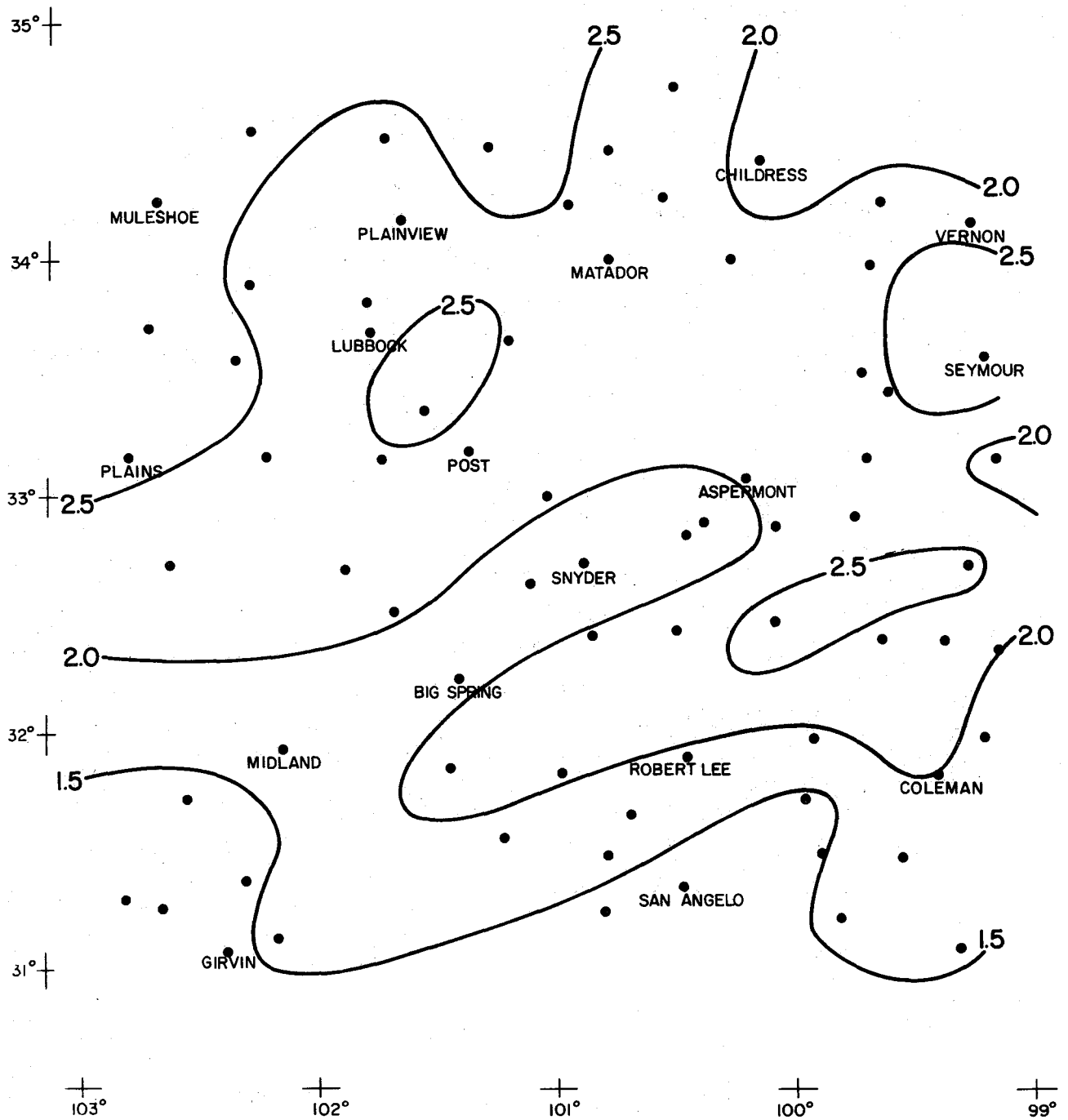
Figure 3.5. Mean monthly precipitation (inches)—July.
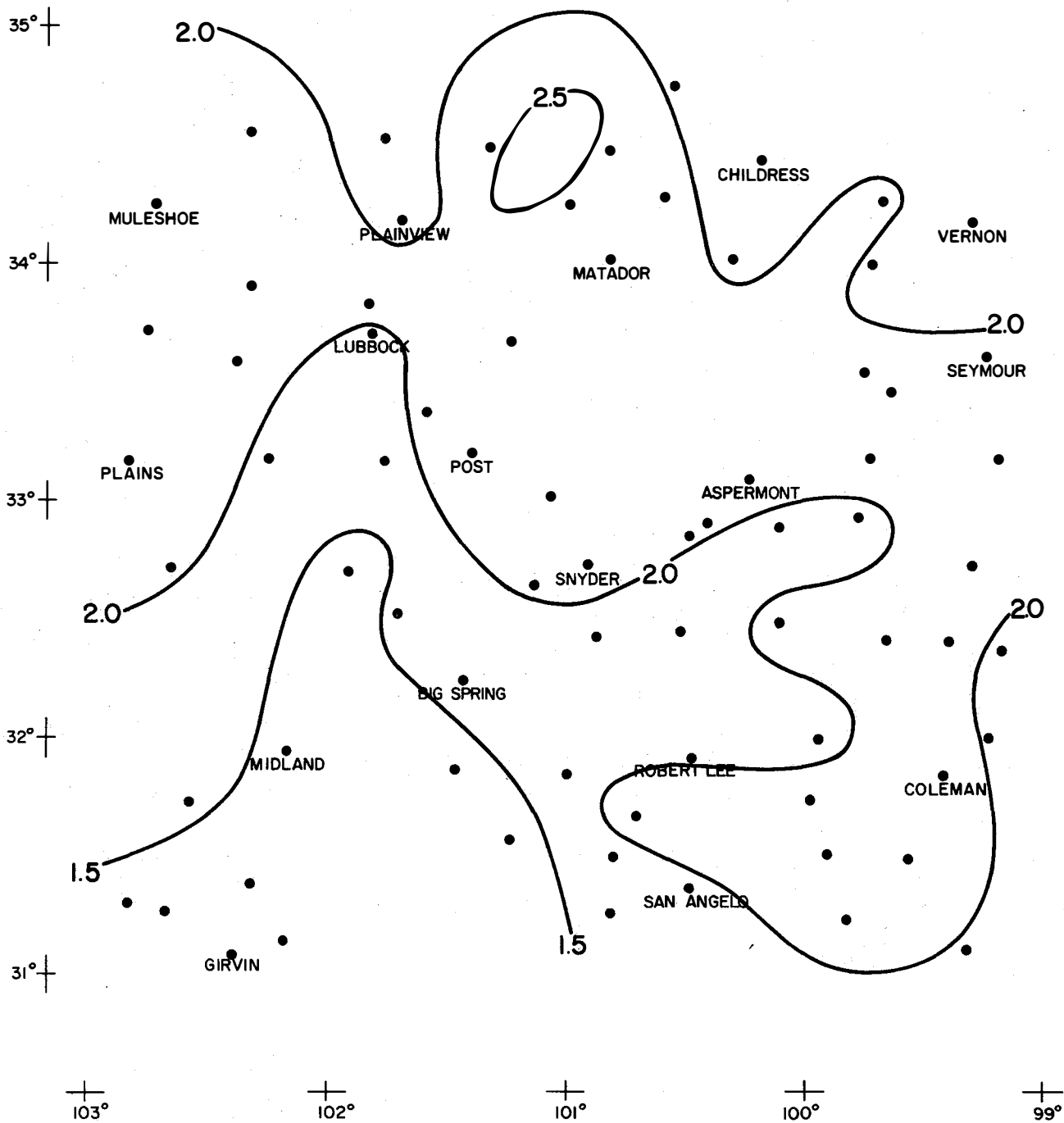
Figure 3.6. Mean monthly precipitation (inches)—August.
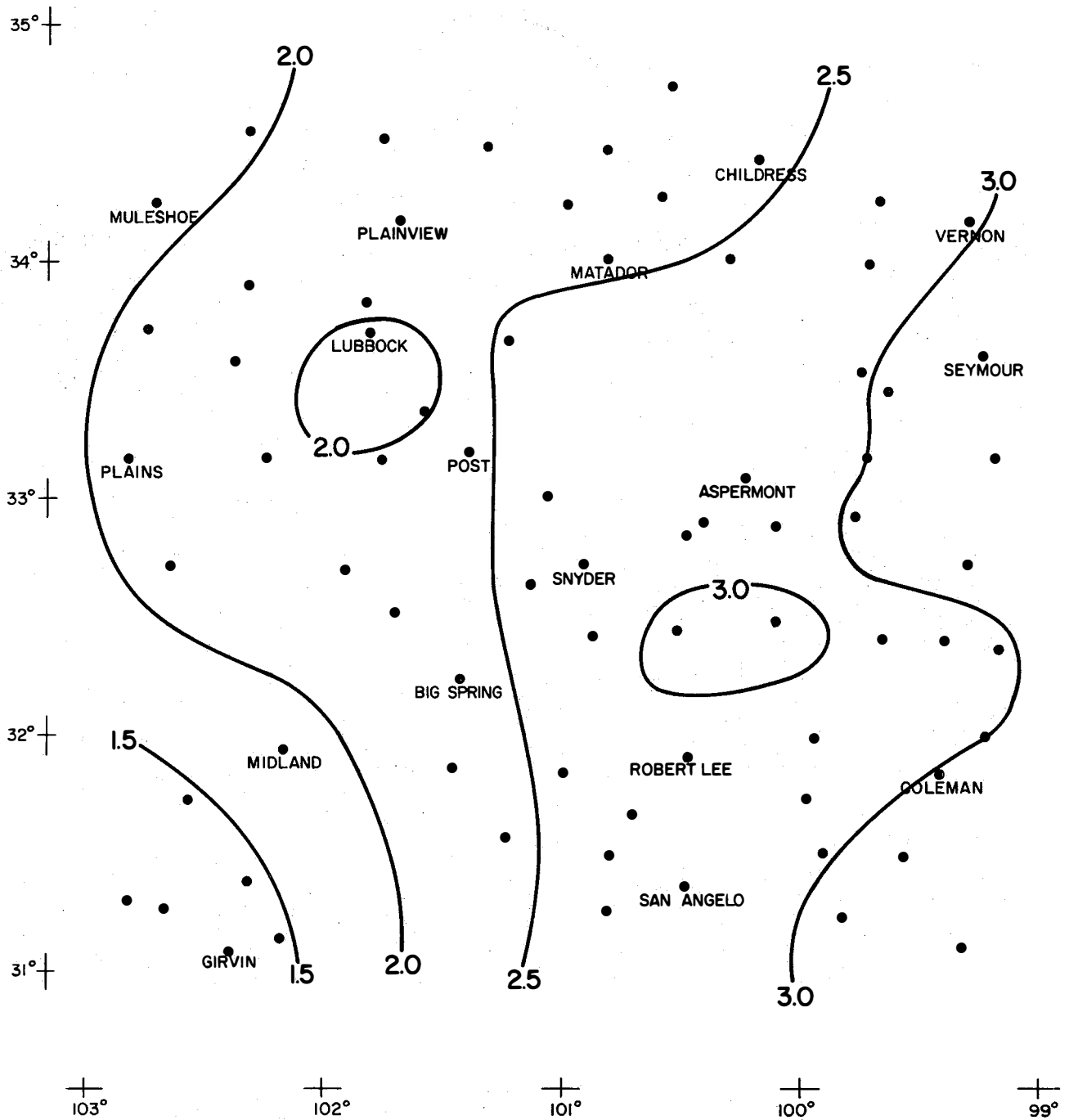
Figure 3.7. Mean monthly precipitation (inches)—September.
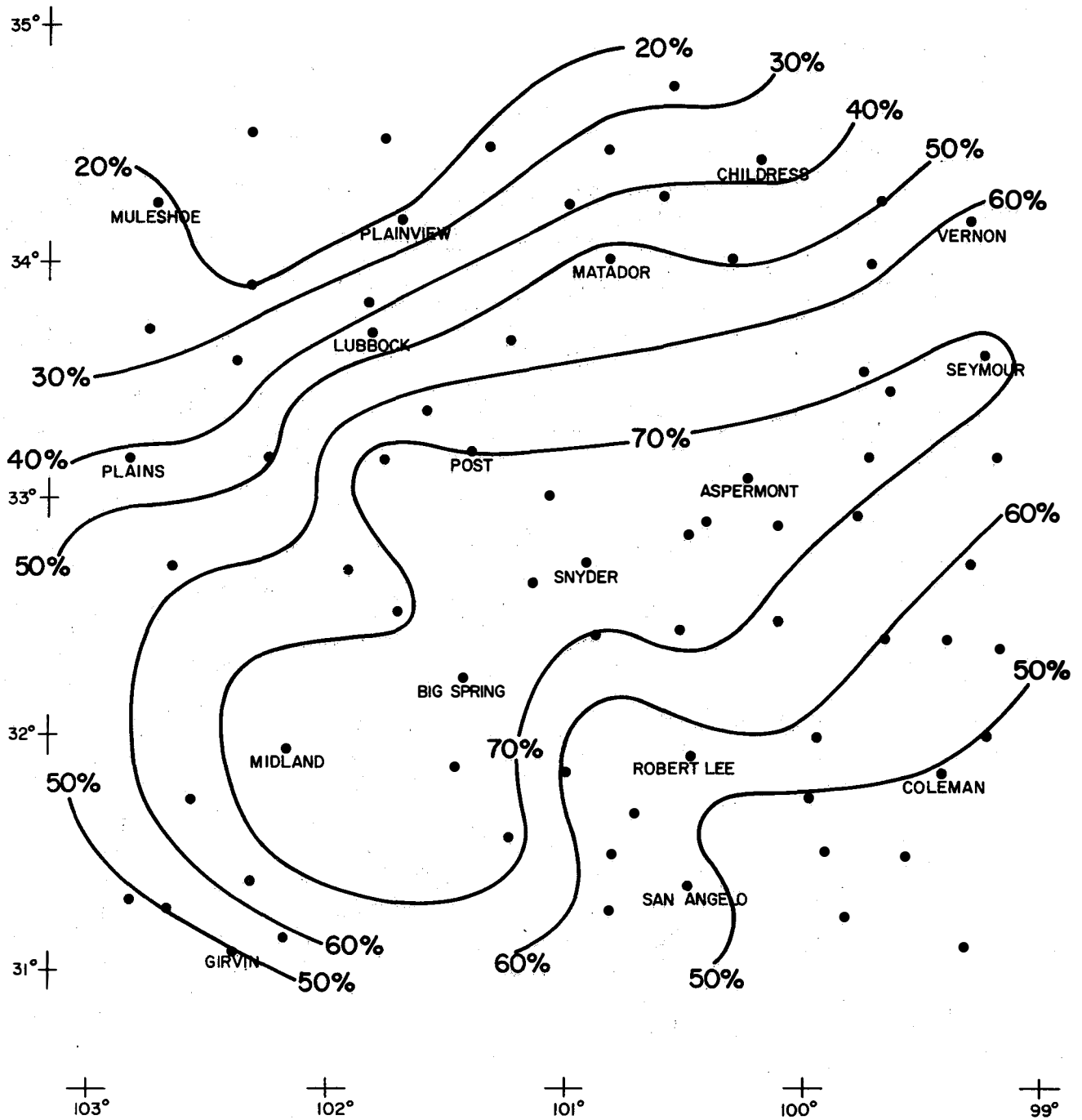
Figure 3.8.   Precipitation correlation with Big Spring—May.
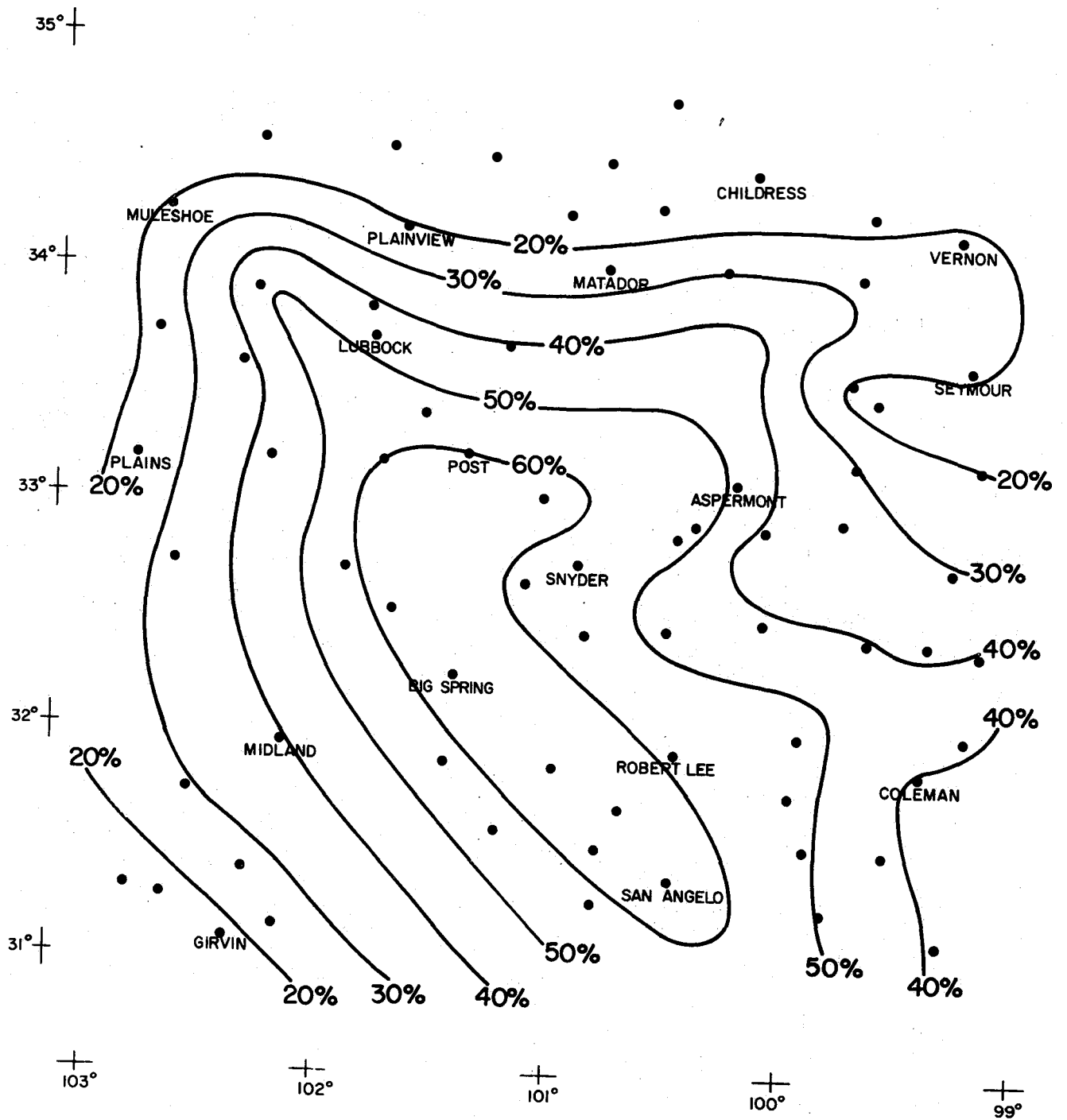
Figure 3.9. Precipitation correlation with Big Spring—June.

as 1.07×10^5 m^3 (87 acre-feet). This variation warrants the need for a systematic stratification of rainfall events. So, using Skywater radar (5.4 cm) data, the researchers then established four categories of convective elements, based upon the stage of growth and scale of organization: (1) convective cells, (2) small convective clusters, (3) large convective clusters, and (4) nested convective clusters. A boundary between small and large convective clusters was established near 100 km (62 mi). Examples of these classifications are shown in Section 5.2.

The following characteristics were assigned to each of the categories:

cell — contains a single reflectivity maximum.

small cluster — contains two or more maxima, generally within a common echo boundary, but having no horizontal dimension greater than 100 km (62 mi).

large cluster — has two or more maxima, generally within a common echo boundary, but having at least one horizontal dimension greater than 100 km (62 mi).

nested cluster— an organization too large to be fully depicted by radar.

A comparison was made, using these statistics and those generated by a study performed in 1980 by North American Weather Consultants, Inc. (NAWC).* Some differences between the two distributions were observed, but they were not substantial enough to warrant concern.

The TTU rainfall analyses found that a few rainstorm events were responsible for producing a large percentage of the Texas HIPLEX area's total rainfall. Using raingage data for the period 1978-1980, the following percentages of total rainfall were attributable to the four radar echo categories defined earlier:

cells — 0.1 percent

clusters
    small — 4.3 percent
    large — 27.5 percent

nested clusters — 67.9 percent

Since small clusters generated only 4.3 percent of the total HIPLEX rainfall in 1978-1980, a 20-percent increase in rainfall effected by cloud seeding would yield an additional 0.18 inch, which is an apparent small percentage increase in the total rainfall. However, since large clusters are responsible for giving 27.5 percent of the total 3-year rainfall, it was

---

*The reader is reminded that TTU rainfall amount was based on raingage data, whereas NAWC rainfall amount was based on Z-R relationships. Also, TTU used 5.4 cm radar data, and NAWC used 10 cm radar data.

concluded that if small clusters could be induced to develop into large clusters the increase in rainfall through cloud seeding would be substantial. Consequently, it was suggested that further investigations should be directed toward discerning the feasibility of inducing small clusters to intensify into large clusters.

Following the technique used by Huff (1967) to study Illinois convective storms for the period when the storm passed over the raingage network, temporal rainfall characteristics were calculated to determine if redistribution of the time element of rainfall occurrence would result in a significant increase in rain volume over the HIPLEX site. This procedure indicated "a greater tendency for the heaviest rain to occur near the midpoint of the storm's lifetime in the network in Texas." However, the study emphasized the fact that, when small-scale precipitation networks like that of Texas HIPLEX are used, the total storm duration is not always measured. This is because many rain events are present over the raingage network only for short segments of their lifetimes. Hence, the rate of advection of the storm system is a major determinant in the temporal distribution of rainfall occurrence. The TTU rainfall study could not substantiate the possibility that rainstorms in Texas HIPLEX yielded more rainfall in the second and third quartiles of their existence than in the first or fourth.

Comparisons of the temporal distributions of Texas and Illinois rainstorm events were performed (Figure 3.10 and 3.11). Interpretation of Figure 3.10 is as follows: for third quartile storms there is a 0.10 probability that 70 percent or more of the rainfall occurs during the first 60 percent of the storm's *network* lifetime. The greatest differences in the 10-percent probability curves between the two classes of rainstorms were observed in third quartile storms (Figure 3.10). With Illinois storms, a rapid rise in cumulative rainfall occurs fairly early in their life cycle, followed by leveling off, and then a second rapid rise. Texas storms displayed a smoother transition throughout their life cycles. The percent frequency of occurrence of second and third quartile storm events in Texas (Table 3.3) demonstrated clearly the variability of precipitation in the southern High Plains region. Composite distributions, using all second and third quartile storms in Texas (Figure 3.11), also show the high degree of variability that typifies precipitation occurrences in Texas, though a tendency for large clusters to occur most frequently was observed. When conditions are unfavorable for strong convection, little rain is generated.

Finally, the TTU rainfall study described storm properties of each convective category to show the value of convective stratification as a powerful evaluative tool. Table 3.4 lists the first four statistical moments for each Texas HIPLEX convective category for rainstorm durations and volumes. The Student's t-test showed statistically significant differences at the one-percent level between small clusters and large clusters, and large clusters and nested clusters in both rainstorm durations and volumes. Between cells and small clusters the rainstorm durations and volumes did not prove to be significantly different through the 10-percent significance level. How-
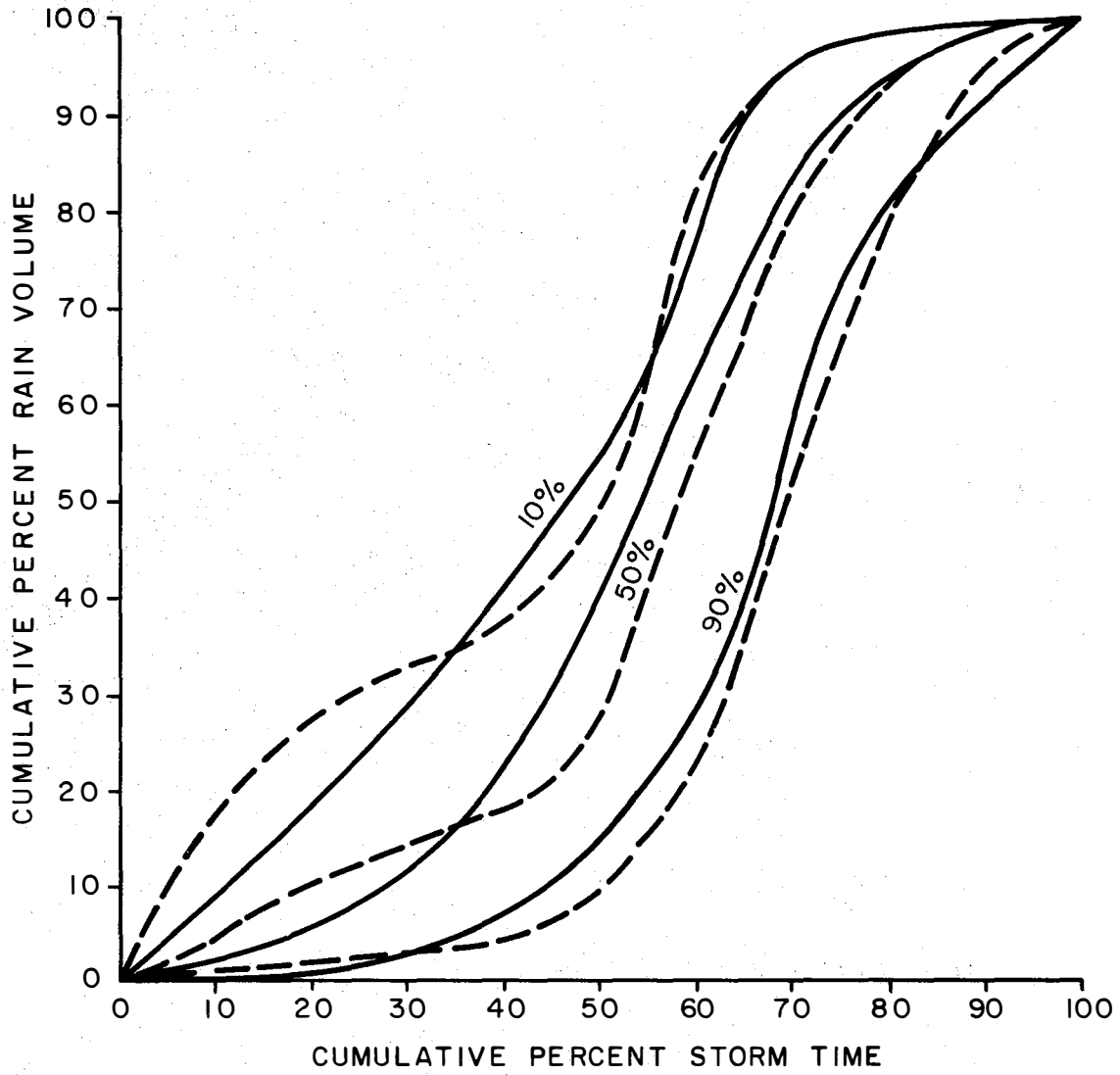
Figure 3.10. Third quartile storm distributions for Texas (solid) and Illinois (dashed).
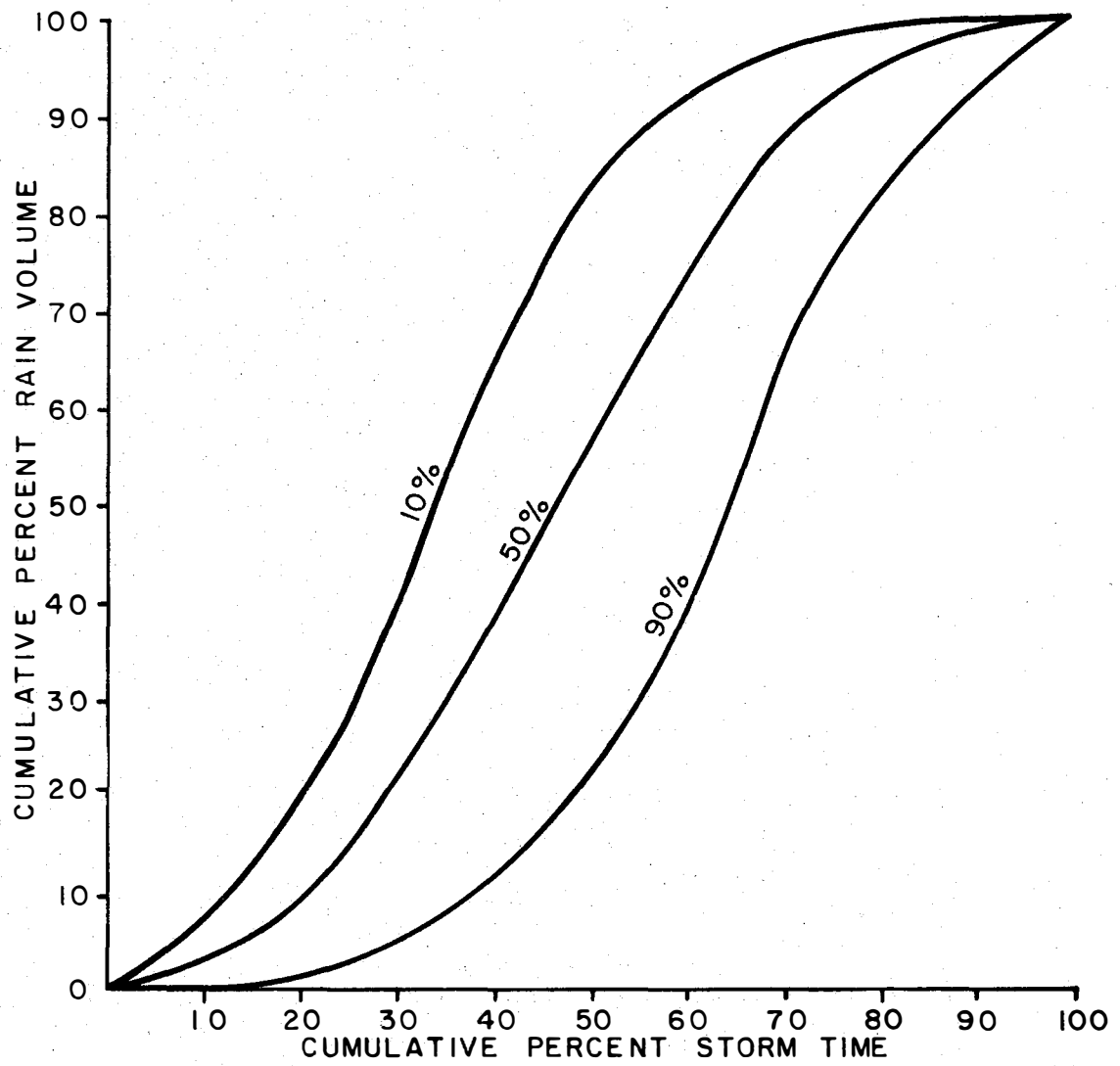
Figure 3.11. Composite storm distributions for Texas using all second and third quartile storms.

ever, this may be a result of the cells' small sample size. Indeed, examination of Table 3.4 shows storm volumes to differ by a factor of approximately five between categories. Storm durations do not appear to show as clear a separation. However, the fact that only four cells were found to be raining suggests that there are some differences between the two categories. Again, this indicates that when unfavorable conditions exist which limit development of cells, little rain is produced.

Table 3.3 Frequency of Occurrence of Convective Categories for Texas Storms

Category	2nd Quartile		3rd Quartile		Composite	
	Number	Percent	Number	Percent	Number	Percent
Cell	0	0	2	5	2	3
Small Cluster	12	25	14	37	26	30
Large Cluster	22	46	14	37	36	42
Nested Cluster	12	25	8	21	20	23
Unclassified	2	4	0	0	2	2
	48	100	38	100	86	100

3.2.3.4 Results

An examination of precipitation data collected on the meso α-scale revealed that during the period mid-May to mid-June the efficiency of natural rain is quite high. This deduction was based on the observation that the peak of rainfall occurrence is associated with relatively large storm systems (clusters) that migrate across the region most frequently in mid-May. Rainstorms that occur later in the April to September warm season generally are more scattered and cell-type, and stem from showers that result from daytime heating of a moist layer of air near the surface. The study revealed that upper-atmospheric weather systems migrating into the HIPLEX region from the west and from the east are responsible for about three-fourths of all precipitation that occurs during the warm season.

The TTU study was not able to determine when, during its lifetime, the rainstorm yielded maximum rainfall amounts. The study did suggest, however, that the greatest rainfall amount recorded appeared to occur near the mid-point of the rainstorm's life span. Yet due to the size of the raingage network, the entire life span of the rainfall event was not always recorded by the raingages. It was learned that a few large convective storms produced most of the summer rainfall. Also, significant differences were noted among cells, clusters and nested clusters relative to rain volume produced and storm lifetime, as measured by the Texas HIPLEX raingage network.

Table 3.4   Statistical Moments of Texas HIPLEX
Convective Category Rainstorm Durations and Volumes

Convective category	Duration				Number of cases	Volume			
	Mean (hours)	Standard deviation	Skewness	Kurtosis		Mean (km^3)	Standard Deviation	Skewness	Kurtosis
Cells	1.88	1.2	0.38	1.06	4	0.0941	0.1047	0.25	0.84
Small Clusters	2.67	1.88	2.06	8.53	40	.4413	1.0859	3.21	12.37
Large Clusters	4.54	3.47	1.19	4.84	49	2.1459	3.1442	1.54	4.54
Nested Clusters	9.72	9.51	1.86	6.38	23	12.1724	15.4397	1.74	5.13

3.3   Meso β-scale Observations

3.3.1   Satellite

The resolution of data provided by the Geostationary Operational Environmental Satellite (GOES) is of such quality as to allow Texas HIPLEX researchers to focus on the nature and behavior of individual cloud masses whose dimensions lie well within the mesoscale range. Consequently, it has been possible, using photographic imagery with both visible and infrared radiance data from the satellite, to compute an assortment of values of various cloud systems in the Texas HIPLEX region that allow researchers to gage the development and growth of rain-producing clouds potentially treatable by cloud seeding techniques. This was done as part of a study performed by Jurica and Chi (1979) at Texas Tech University, and documented in a report entitled *Determination of Cloud Properties from Bispectral Satellite Measurements*. The following describes some of the cloud properties derived through extensive analyses of the two different kinds of weather satellite data.

3.3.1.1   Albedo

The "albedo" of a particular cloud is defined as "the ratio of the radiation reflected by a surface to the amount incident upon it." It is usually expressed in the form of a fraction, with 0 representing a perfect absorber of radiation; and, at the other extreme, 1 indicating a perfect reflector of radiation. For example, the "albedo" of water bodies (rivers and oceans) ranges from 0.03 to 0.10, while dry land surfaces usually are in the category of 0.07 to 0.20. For clouds the range is typically 0.05 to 0.84.

It was observed that, late in the afternoon as the zenith angle of the sun grew so that greater shadowing effects occurred in the nonuniform cloud-top surfaces, these shadows reduced the overall brightness of the clouds, with the result that a low albedo value was obtained. By matching the satellite data with concurrent radar data, strong convection late in the day, associated with shadowing of adjacent lower clouds, was readily discernible. Strong convection produces cirrus outflow in the upper atmosphere which blankets lower cloud forms. Subsequently, a minimum mean cloud albedo was observed at the time of strongest shadow effect, or at about 0115 GMT (2015 CDT) in the evening. Since very low temperatures and low albedo values are associated with cirrus clouds, the determination of albedo values is important when addressing the distribution of those high-level clouds composed of ice.

3.3.1.2   Brightness Analysis

The data from the GOES were also used to determine the values of brightness of individual clouds and their noncloud backgrounds. One find-

ing of the research confirmed that it is difficult to distinguish cloud from noncloud background late in the day (or at low sun angles). Cloud brightness was found to vary widely with cloud size; the correlation between the two characteristics was not high.

3.3.1.3 Populations and Cloud Cover

After separating various types of clouds into several categories according to their size, the use of both visible and infrared satellite radiance data showed that, at most times of the typical HIPLEX day, a number of medium isolated convective clouds (those with a diameter between 4.7 km [2.9 mi] and 10 km [6.2 mi] known mostly as cumulus congestus), dominated the total number of clouds. Exceptions to this rule were at 1945 CDT (0045 GMT) and 2015 CDT (0115 GMT) in the evening when the small isolated clouds (those with a diameter of less than 4.7 km [2.9 mi] and known as fair weather cumulus clouds) were most numerous. Although "widespread area clouds" (those with a diameter of more than 20 km [12.4 mi] and known as deep convective clouds) represented only about 10 percent of the total number of clouds, those "few" clouds were responsible for 80 to 90 percent of the cloud cover in the study region.

While the vast majority of the clouds in the HIPLEX area are isolated convective clouds, their size is such that they constitute only a small percentage of the total cloud cover. A relatively small number of much larger, widespread convective clouds accounts for up to 96 percent of the cloud cover just before dusk on a typical summer HIPLEX day. While counts of cloud populations made from both imagery and radiance data were nearly the same, the study found that the radiance data gave more reliable counts "because of the ability to use a time-dependent cloud/noncloud critical brightness value." These results confirm the reliability of cloud climatologies derived for HIPLEX sites, utilizing the objective techniques of the ADVISAR at Colorado State University (Reynolds and Vonder Haar, 1979).

3.3.1.4 Satellite-Tracked Cloud Movement

One other product of the analyses of satellite radiance data is an estimate of the movement of cloud masses through the Texas HIPLEX area. The study found that by comparing the estimate of cloud movement derived from the satellite data with the estimate using rawinsonde and radar data, the precision of measuring the direction of cloud motion was within ± 5 degrees. The precision for measuring speed of cloud movement was estimated at 5.8 km hr^{-1} (3.6 mi hr^{-1}); the speed obtained from the satellite radiance data was larger than that measured with the radar, satellite-visible imagery or rawinsonde. Little success was made in estimating accurately cloud movement by using visible imagery.

One important factor that influenced the reliability of the measurements of cloud motion was the change in cloud patterns that typically occurred between times of measurement. This may be due to variations in speed of movement at different levels of the atmosphere; for instance, the presence of cirrus clouds located above the convective cloud of interest to the observer frequently posed problems. Too, further development or even dissipation of clouds from one time period to the next altered noticeably the shapes of the cloud masses being studied.

The study recommended the use of short time interval (or "rapid scan") satellite radiance data to help overcome the problems cited above.

3.3.1.5   Satellite-Derived Cloud Top Heights

Radiance data obtained from weather satellites allowed Texas HIPLEX researchers to estimate the temperature of tops of clouds in the HIPLEX area and, by relating the temperature to measurements made by rawinsondes, to estimate the heights of the tops of the same clouds. By comparing these estimates of cloud top heights with those obtained by radar, agreement between the two was found to be quite satisfactory, although in all cases the satellite estimate understandably was greater than that derived from radar (since radar detects precipitation-sized particles, whereas the satellite detects cloud droplets which extend higher into the cloud turret). As in previous studies of cloud top temperatures and heights using satellite data, the presence of cirrus clouds presented special problems. In more than one instance, cirrus clouds detected at ground level by weather observers early in the day went undetected by the weather satellite.

3.3.1.6   Satellite Analyses Compared with Radar and Raingage Data

An extension of the satellite-derived determination of cloud properties involved intercomparison of the satellite results with both radar and raingage data. The study focused on four days in the 1977 Texas HIPLEX field program (June 22, 24 and 27, and July 8); the complete results are available in a report by Jurica and Chao, entitled *A Study of Clouds Using Satellite Radiance Data in Comparison with Raingage Network and Radar Observations.* A brief summary of the results follows.

The latitude and longitude coordinates of each raingage station have been located in the satellite radiance data arrays. After plotting the raingage data, isohyetal patterns were constructed in the transformed coordinate system for comparison with the satellite radiance data. Note that the reference coordinate system was selected to be the rectangular array of visible satellite radiance data. Figure 3.12 shows the relative location of cloud albedo, cloud top temperature and the rain area. Note that only the coldest isotherm is shown.
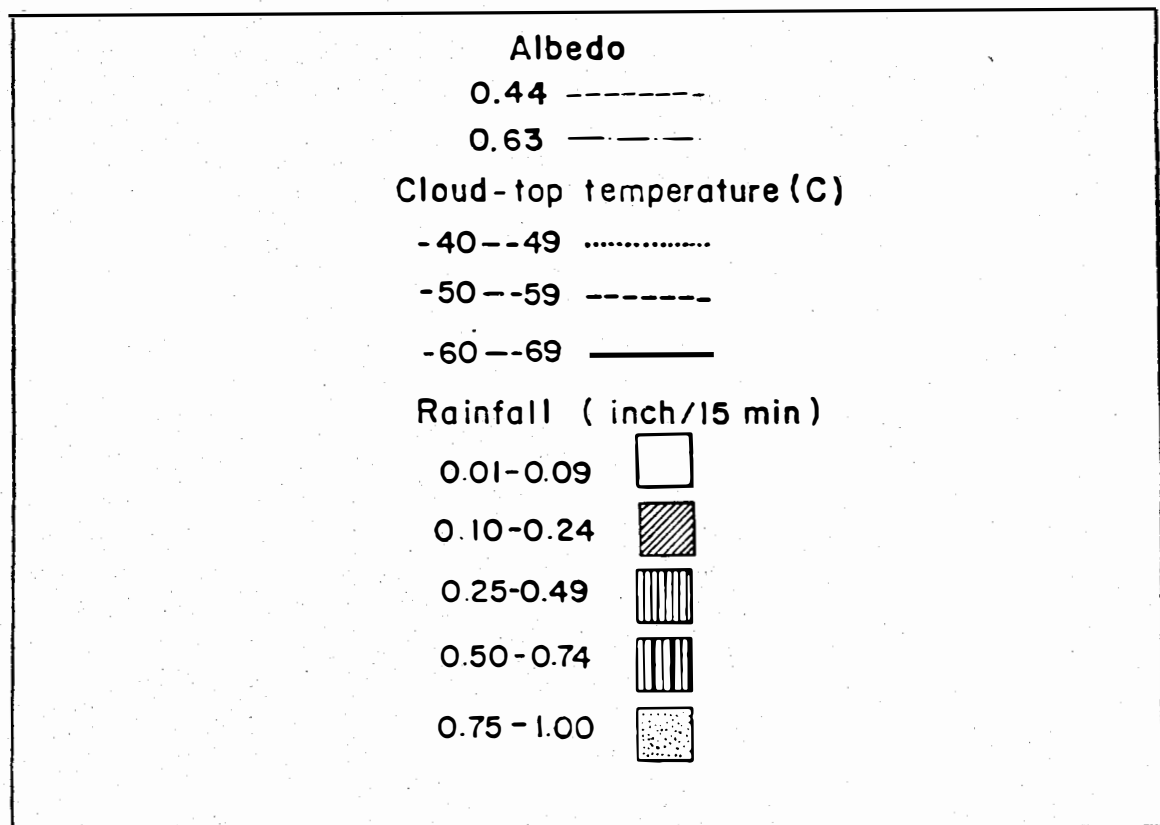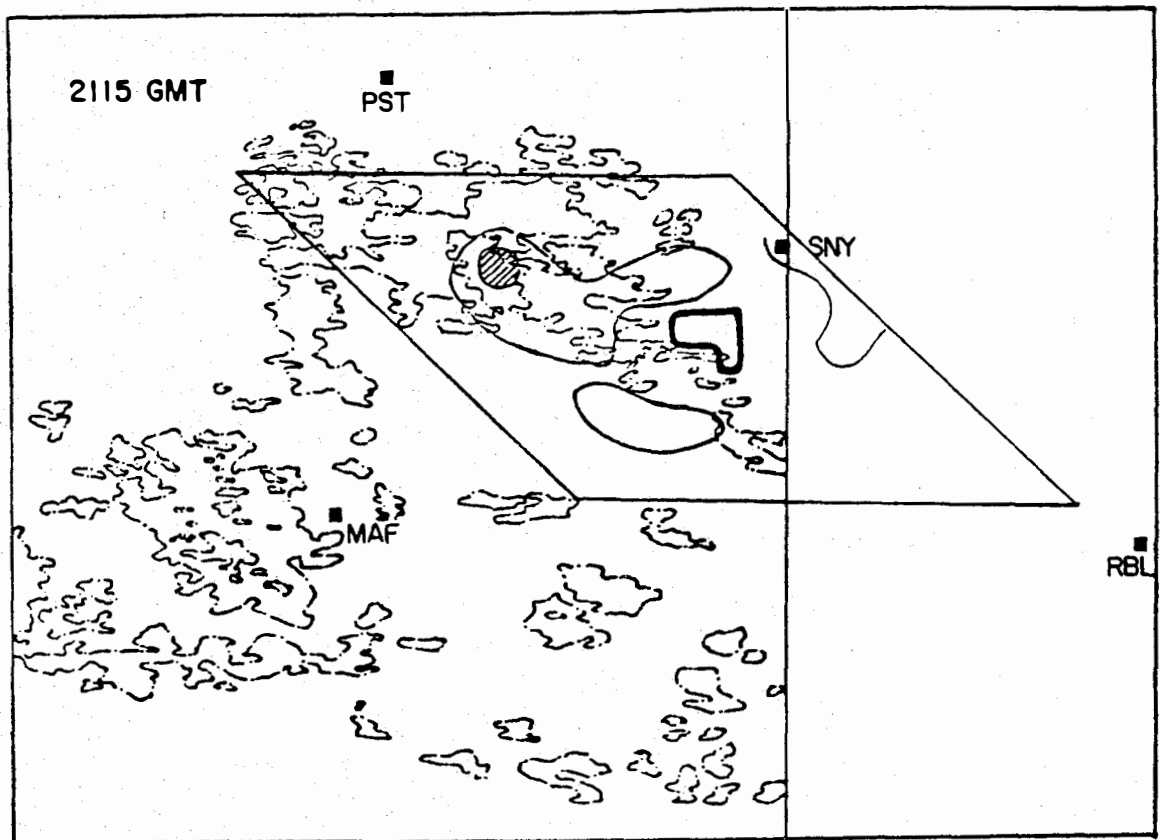
Figure 3.12. Cloud albedo, cloud top temperature and rainfall intensity at 2015 GMT on 8 July 1977. The parallelogram delineates the extent of the raingage network.

At 1515 CDT (2015 GMT) the raingage network was totally covered by bright and high-topped clouds with albedos over 0.63 and top heights above 15 km. The PPI digital radar analysis also indicated that the reflectivity gradients within the rain band became quite sharp. The rainfall intensity decreased rapidly after the precipitation peak, and little precipitation was recorded after 1700 CDT (2200 GMT). In addition, the bright cloud area decreased and the cloud tops became lower, as seen in the sequence of satellite visible and infrared data following 1615 CDT (2115 GMT). Finally, the PPI digital plots indicated that the rain band structure broke up, and reflectivities weakened after 1614 CDT (2114 GMT).

The isohyetal pattern for the period 1515-1530 CDT (2015-2030 GMT) on July 8, 1977, is shown in Figure 3.13. Four RHI cross sections at 1518 CDT (2018 GMT) along azimuth angles 211 degrees, 223 degrees, 253 degrees, and 259 degrees were studied because each of them passed through an intense storm (Figure 3.13).

The radar cross section at an azimuth angle of 253 degrees, shown by line FF' in Figure 3.13, is presented in Figure 3.14. This line passed through the most intense rainfall area at this time. The total precipitation measured in the center of this cell over 15 minutes was 22.6 mm (0.89 in), while the reflectivity there was close to 60 dBz. The satellite-derived cloud heights were quite uniform over the intense reflectivity area, but decreased rapidly beyond the storm. The satellite cloud heights and radar echo tops over-lapped within the intense radar reflectivity cells. However, the overlap was within the uncertainty of the satellite-derived cloud top heights. The gradient of precipitation intensity under the strong storm cell was sharp, with the heaviest rain occurring immediately under the intense reflectivity core. The radar reflectivity under that strong storm cell was about 55 dBz, inferring 24.9 mm (0.98 in) of rain within 15 minutes from the assumed Z-R relation.

One case of special interest is the cross section along the line GG', for an azimuth angle of 259 degrees (Figure 3.15). This case is discussed because the most intense radar reflectivity at 1518 CDT (2018 GMT) occurred along this line. The structure was similar to the previous case along the FF'. A strong storm cell with large reflectivity gradients was located 35 km (21.7 mi) from the radar site. This cross section was along the edge of a strong rain band which passed through the area. The cloud top heights from the infrared radiances varied from 11 to 12.5 km (6.8 to 7.4 mi) over two intense storm cells, but decreased rapidly beyond the third storm cell which was located about 80 km (49.6 mi) from the radar. The agreement between the satellite cloud top heights and radar reflectivity was good along this cross section. A strong reflectivity maximum of more than 60 dBz was located 35 km (21.7 mi) from the radar site. It is probable that heavy rain fell under this intense echo which occurred within the raingage network, but there was no raingage located exactly along this direction. This example
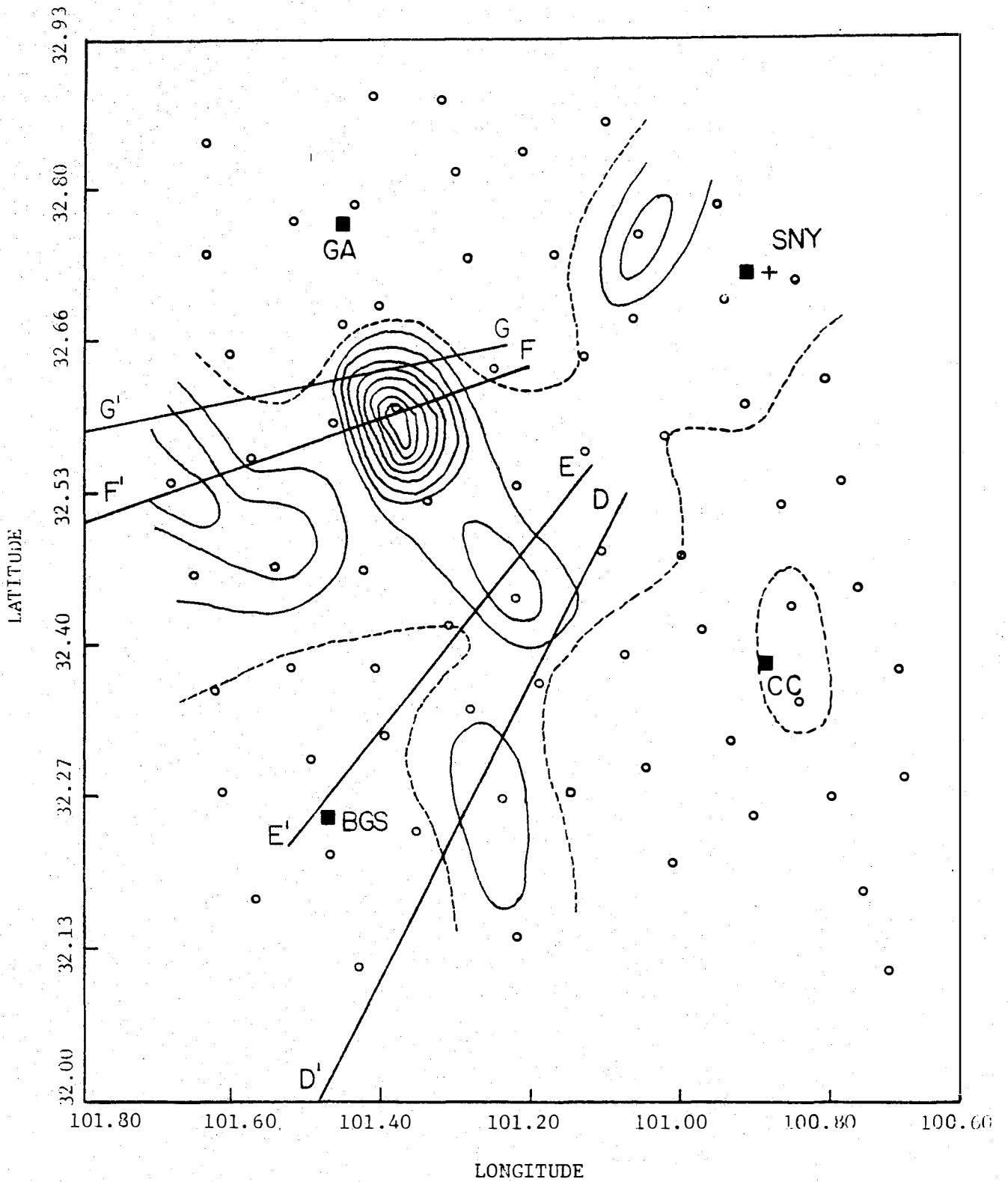
Figure 3.13. Isohyet pattern for the period 2015-2030 GMT on 8 July 1977. The dashed line is the isohyet for 0.01 inch, and the solid lines are contoured with a threshold of 0.1 inch and given in 0.1 inch increments. Raingage locations are shown as open circles.
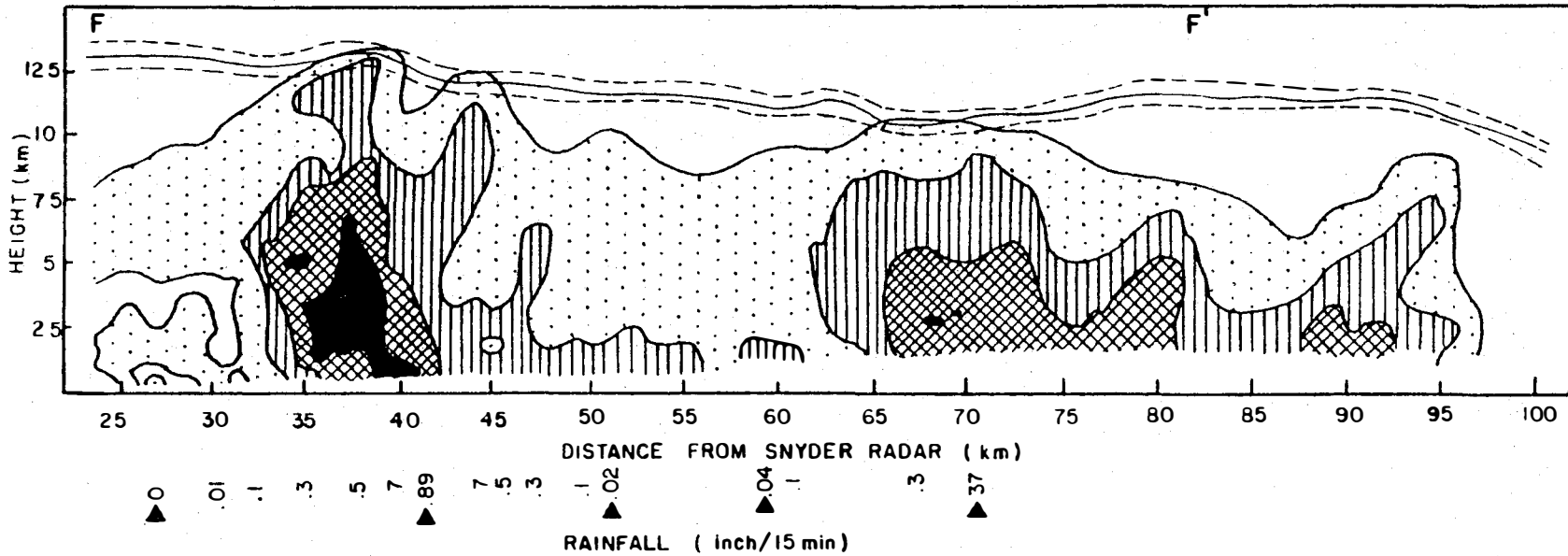
Figure 3.14. RHI display derived from M-33 radar data for the azimuth angle 253° at 2018 GMT 8 July 1977. The data threshold is 20 dBz and is contoured in 10 dBz increments. The upper solid line is the cloud top height derived from satellite infrared data and the dashed lines correspond to a temperature uncertainty of ± 3 C. Also shown are rainfall analysis results with actual raingage measurements marked by ▲.
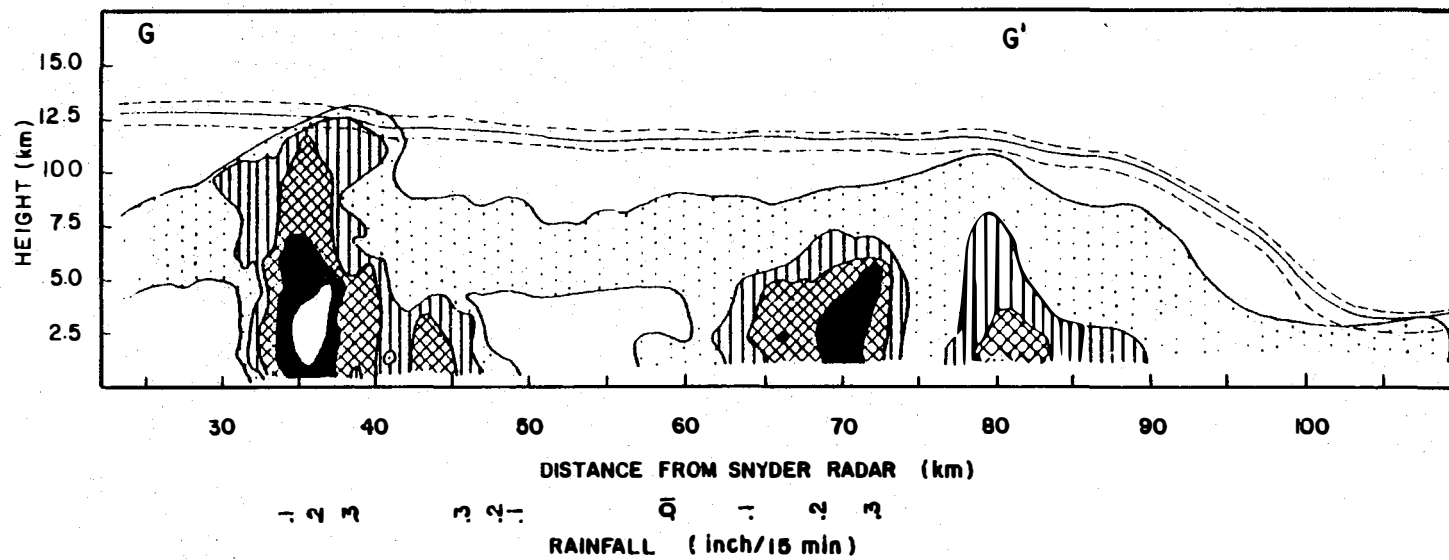
Figure 3.15. Same as Figure 3.14 for azimuth angle 259°.

illustrates the restrictions associated with interpreting rainfall measurements even from a raingage network with rather dense spacing, and points to the desirability of higher resolution data sources, such as radar or satellite measurements.

Meso α-, meso β-, and meso γ-features were utilized to follow the development of thunderstorm activity, as well as to offer evidence regarding the mechanisms of precipitation formation during the several case study days. Convective clouds caused by the cold front on July 8, 1977, and by the passage of a squall line on June 22, 1977, produced the observed precipitation. There were no significant features to cause rainfall inside the raingage network on June 24 and 27, 1977, although thunderstorms did migrate into the study area in the late afternoon on both days.

Two sources of verification for the satellite-derived results were raingage and radar measurements. The heavy rainfalls observed on June 22, 1977, and July 8, 1977, occurred under those high albedo and cold cloud top temperature areas of the cloud systems present. The cloud top heights, derived from infrared satellite radiance data and radar echo tops, showed realistic correlations, except for those narrow high cells which were averaged out by the large spatial resolution of the infrared sensors. The comparisons made in this study demonstrate the consistency of results derived from satellite radiance measurements with analyses of radar and raingage data, thereby establishing the usefulness of satellite data in the absence of radar or raingage measurements.

3.3.1.7 Results

Using visible and infrared radiance data from the GOES, a number of characteristics were identified, such as cloud amount and brightness, albedo and height as well as movement of convective clouds that typically form in the Texas HIPLEX area. Using data from the orbiting weather satellites, it was found that the satellite could resolve a small isolated cloud with a diameter of as small as 4.6 km (2.9 mi). While the number of clouds and percent cloud cover gaged by the radiance data closely matched the values obtained with the visible imagery for the early afternoon hours, it was discovered that later in the day, as the solar zenith angle increased, numbers from the two data sources differed appreciably. In other words, "it becomes more difficult to distinguish cloud from underlying noncloud background late in the day." Later work managed to eliminate the problem by using the radiance data. Such estimates from radiance data for all hours of the afternoon and evening are considered more reliable than those using the visible imagery.

In brief, the findings derived from the four case studies indicated good agreement among the satellite, radar and raingage data. The heavy rainfall areas, as measured by raingages, were found to occur under the brightest

and highest clouds. Quantitatively, the rainfall was generally located under clouds with albedo values which measured greater than 0.44, and with tops higher than 10 km (32,800 ft), as derived from the satellite data. Conversely, there were no rain areas observed under clouds with albedos less than 0.24.

In analyzing various properties of the clouds, it was learned that the mean brightness, or "albedo," of a cloud showed realistic correlations with cloud size, except for those narrow high cells which were averaged out by the large spatial resolution of the infrared sensors. The cloud top heights were determined by using the radiance data jointly with rawinsonde data, and it was found that cloud top heights obtained from the radiance data were consistent but generally exceeded those derived from conventional radar. This would be expected because the radar is observing raindrops, and the satellite is observing ice crystals. Radiance data were found to be the best indicator (among a set of other data sources, such as visible imagery, radar data and rawinsonde data) of cloud movement in the Texas HIPLEX area.

Based on the findings that active convective regions of rainfall are brighter and colder on the satellite imagery, Griffith *et al.* (1980) developed an empirical relationship to estimate convective rainfall using satellite data. This technique, which was originally developed for and tested on Florida rainfall, was applied to Texas HIPLEX data. No attempt was made to rederive the empirical relationship. Five Texas HIPLEX case–study days were selected to test the empirical technique. And as was found in the Florida estimates, the Texas rainfall relationships generally resulted in overestimates of the heavy rainfall volume events, and underestimation of the light rainfall volume events.

3.3.2 Radar

The following subsections briefly describe meso β-scale radar echo features which have been identified by radar in and near the Texas HIPLEX area.

3.3.2.1 Radar Echo Climatology

3.3.2.1.1 General

A study, entitled *A Radar Echo Climatology for Southern HIPLEX* (Driscoll, 1978), utilized WSR-57 radar films collected by the National Weather Service at Midland, Texas. The time of year selected included the months April through September for the 1973-1976 period. This study documents radar echo characteristics of the area with respect to variation in space and time. The 10-cm radar system from which the data were gathered cannot identify

individual cells within radar echoes. Echoes were defined as single entities which were distinguishable from others. The reader is cautioned that cold fronts and squall lines may comprise a single echo.

3.3.2.1.2 Results

An annual and monthly summation of the frequency of radar echoes is given in Figure 3.16. The number of echoes by month is given within the columns. The year of minimum radar echo occurrence during the period of study is 1973, while 1975 experienced the maximum radar echo occurrence. On a monthly basis, July has the maximum number of radar echo occurrences, (75 percent of the data set), while April has the minimum number of radar echo occurrences.

Diurnal variation of radar-echo occurrence is illustrated for each of the months in Figure 3.17. Some of the more important characteristics of diurnal variations which are evident in the figure include:

— a sharp increase in echo occurrence takes place between 1200 and 1400 CDT (1700 and 1900 GMT);

— the maximum number of echo occurrences is between 1500 and 1700 CDT (2000 and 2200 GMT), followed by a gradual decrease in numbers to 2300 CDT (0400 GMT);

— echo occurrence during the period 0000 to 1300 CDT (0500 to 1800 GMT) is irregular;

— a secondary maximum is evident in July between 0200 and 0500 CDT (0700 and 1000 GMT), and a pronounced minimum occurs at 2300 CDT (0400 GMT);

— diurnal variations are most pronounced in July and August, the hottest months; and

— the time of day of maximum occurrence for all months is 1600 CDT (2100 GMT).

Radar echo films were studied until echoes either reached an 8-km (5 mi) diameter in size or attained maximum size. The 8-km diameter criterion was selected as a stopping point because this diameter appeared to be an upper limit for treatable (seedable) clouds (Bark, 1975). With regard to size, 49.8 percent of radar echoes studied did not reach an 8-km diameter; 43.2 percent of the total did grow to this size or larger. The remaining seven percent
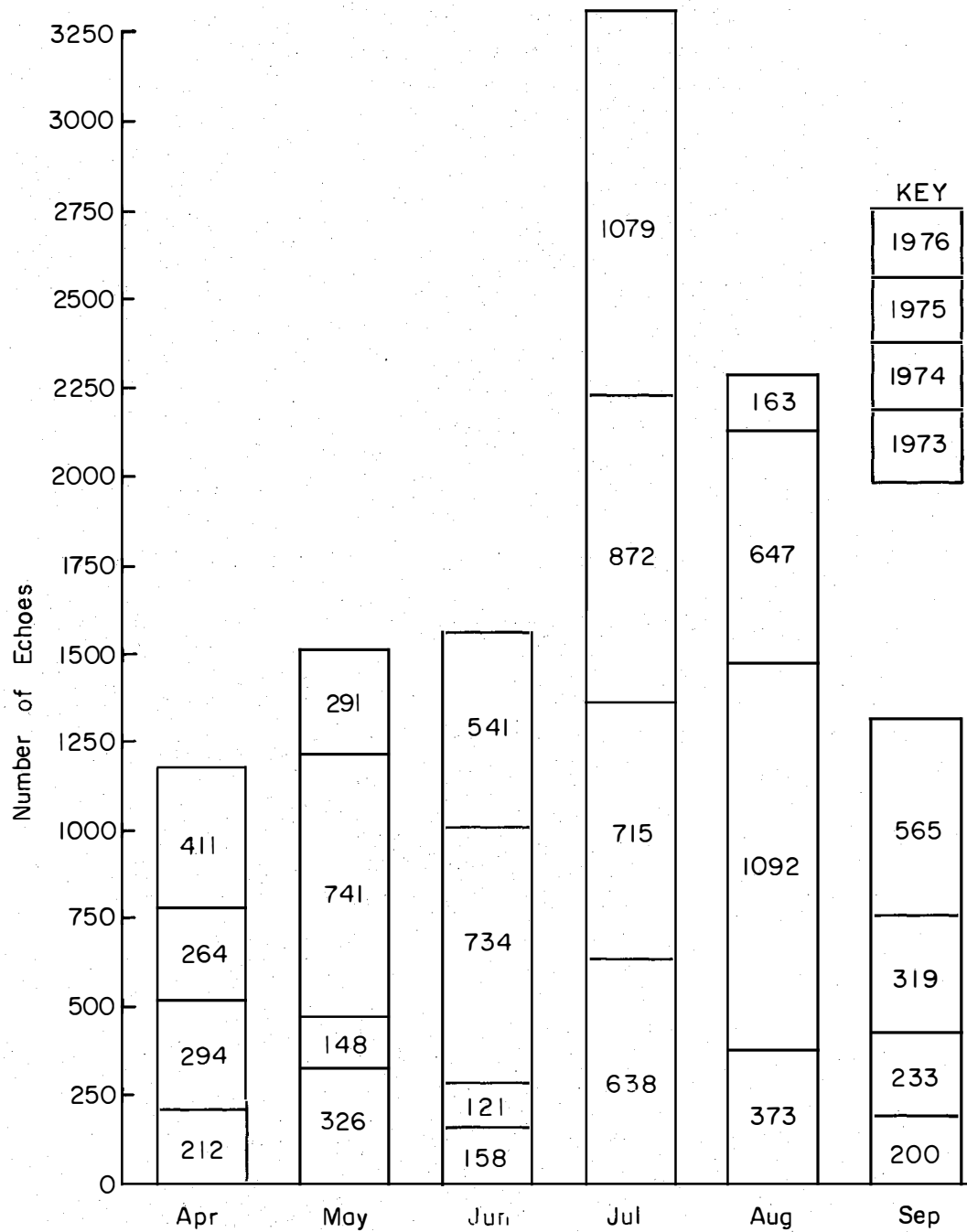
Figure 3.16. Radar echo frequency for Texas HIPLEX annual and monthly occurrence, 1973-1976.
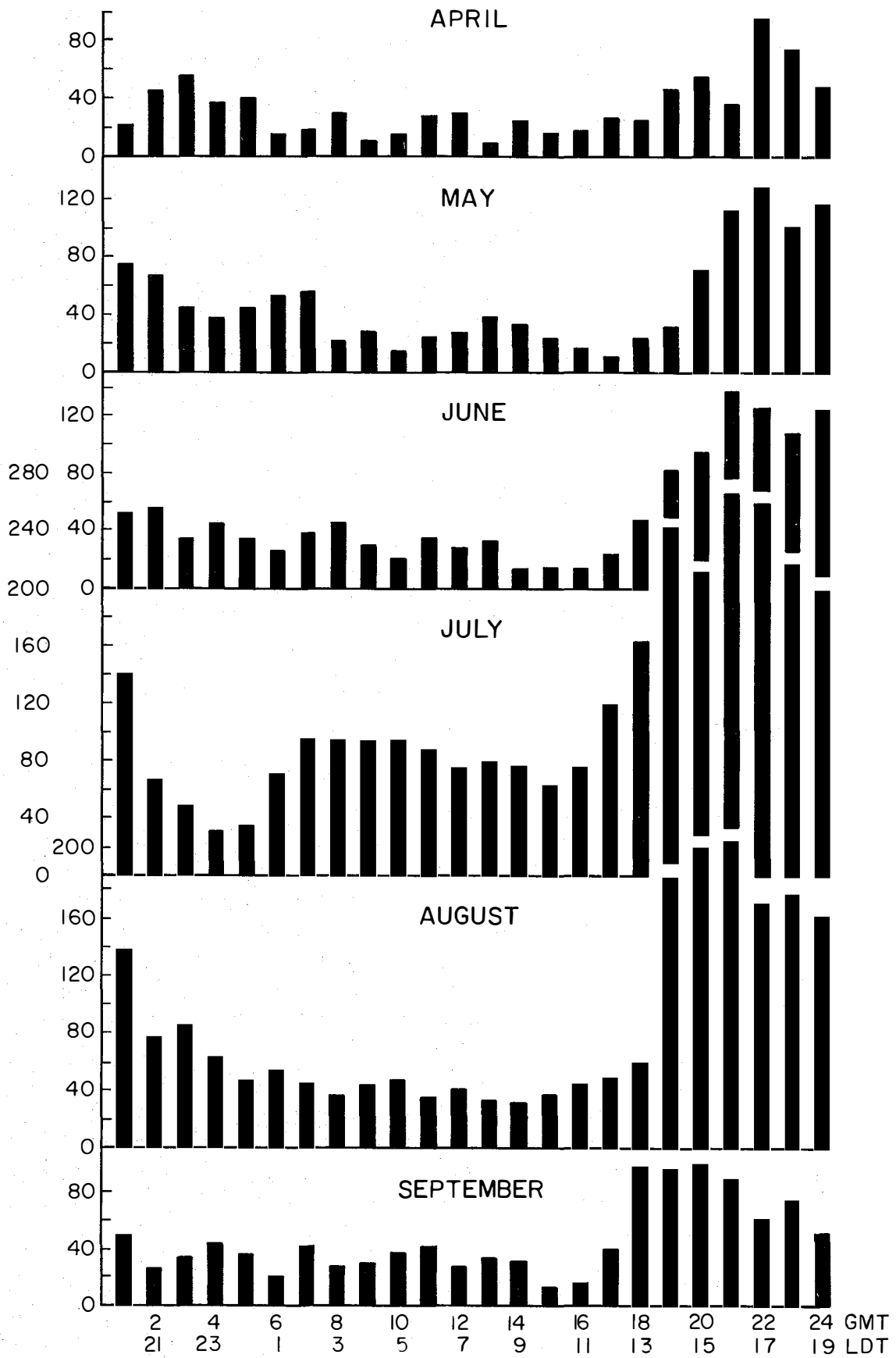
Figure 3.17. Diurnal variation of echoes by month for the 1973-1976 Texas HIPLEX seasons.

moved off the grid. Of those initial echoes observed, irrespective of size, 54.7 percent reached 8 km in diameter within 10 minutes. Figure 3.18 shows the disposition of tracked echoes for each year.

In terms of direction and speed of echo movement, it became evident that the greatest number of tracked echoes occurred in July, with the fewest in April and May. Movement was predominantly northeastward and eastward during April, May, June, and September. In July and August, the direction of echo motion was more or less evenly distributed throughout eight points of the compass. This was attributed to very light steering (850 to 700 mb) winds, and was associated with air-mass thunderstorms which occur during the hottest months.

Mean speeds of radar echoes were greatest to the northeast in all months, except in July and August when greatest speeds were eastward and southeastward, respectively. The greatest speeds occurred in April; the lowest in July and August.

Overall, the highest proportion of observed radar echoes moved in an east-northeasterly direction, except during July and August.

3.3.2.2 Radar Echo Characteristics (A Climatological Approach)

3.3.2.2.1 General

Digitized radar data were processed and examined to study the relationships between meso β-scale atmospheric processes and radar echo characteristics. The relationships at the meso α-scale have been discussed in Section 3.2.2. The meso β-scale radar characteristics will be addressed next, using climatological analyses of general characteristics and case study analyses of more specific characteristics.

The climatological approach brings together the data from a large population of radar echoes, and attempts to generalize characteristics across the population. The main weakness in the climatological approach is that detail is sacrificed for numbers.

3.3.2.2.2 Radar Echo Summary

A radar-echo summary for the Texas HIPLEX region for the years 1976-1978 was prepared by Sutherland *et al.* (1980) of North American Weather Consultants (NAWC) as a report, entitled *Analysis of Digitized M-33 Radar Data from Texas HIPLEX, 1976-1978.*

EVENT   **RECORD**

	1973	1974	1975	1976	Total
Merges	3	11	12	13	39
Moves Off Grid	2	12	9	4	28
Initial Size $\geq$ 8 km	15	11	20	6	52
No Growth, Or Growth to >8 km	142	231	236	233	842
	112	124	272	222	730
				Total Echoes =	1691
Merges	0	14	12	10	36
Moves Off Grid	0	0	1	0	1
No Growth	25	16	28	29	98
Reaches Max	29	29	86	64	208
	54	59	127	103	343
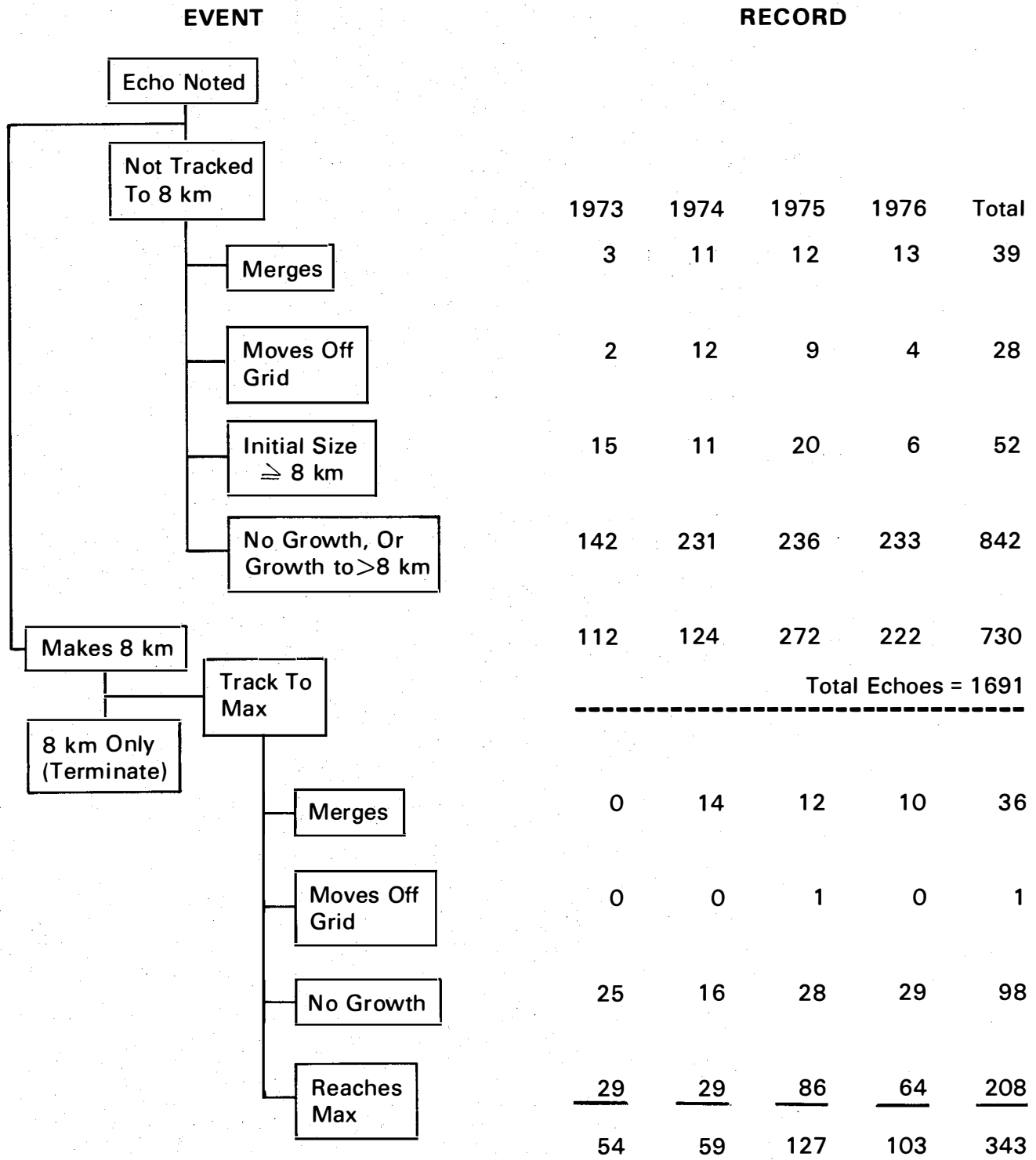
Figure 3.18. Disposition of tracked echoes

The summary provides a statistical accounting of radar-echo events from which dominant mesoscale weather occurrences may be inferred.

The data base consisted of 11,207 echoes, recorded within a 136 km (85 mi) radius of Snyder, Texas, during 33 precipitation events of 1976-1978. The selection of usable echoes included those in the reflectivity range between 10 and 70 dBz.

A statistical breakdown of the data set identified five major echo types and associated these with three surface and three upper-air conditions. The five echo types were: warm cell, cold cell, warm cluster, cold cluster, and line. The three surface conditions were pre-frontal, post frontal, and no front. The three upper-air conditions described the flow field aloft by the arrangement of pressure surfaces which included upper trough, upper ridge, and inverted trough. Analyses of the data set showed that: (1) the average number of echoes per precipitation event was 340; (2) individual cells outnumbered clusters and lines by a factor of ten; (3) periods of pre-frontal and no-front conditions each produced more echo observations than post-frontal conditions; (4) the presence of upper-level troughs caused more echoes than did ridges; (5) approximately 60 percent of all echo tops were below the -5°C level (defined as a "warm" echo) and occurred most often in post-frontal conditions; and (6) about 64 percent of all individual cells were "warm" echoes, compared to only 13 percent total for cluster and line echoes.

Median value statistics for the five major echo types and six surface conditions are listed in the left column of Table 3.5. Interpretation of the table indicates average characteristics of echoes; for example, a cold cluster of cells encompasses about 140 km^2 (54 mi^2) and has an average cloud-top height of 9 km (29,500 ft) MSL, an average cloud-top temperature of -26°C, an average maximum reflectivity of 49 dBz at about 4.3 km (14,100 ft), and exists for about 35 minutes. With respect to the Z-R (reflectivity-rainfall rate) relationship, the following equation was used to convert reflectivity values to rainfall rates:

$$R(\text{mm hr}^{-1}) = 0.025 \ (\text{antilog} \ [\text{dBz}/10])^{.62}$$

The equation was derived for the Texas HIPLEX area by Smith *et al.* (1977). The following rainfall rates correspond to the maximum reflectivity column given in Table 3.5 for the five major echo types listed: 1.4 mm hr^{-1} (.06 in hr^{-1}) for warm cells; 2.8 mm hr^{-1} (.11 in hr^{-1}) for cold cells; 7.5 mm hr^{-1} (.30 in hr^{-1}) for warm clusters; 27.3 mm hr^{-1} (1.1 in hr^{-1}) for cold clusters; and 309 mm hr^{-1} (12 in hr^{-1}) for lines. Warm cells, cold cells and warm clusters all have a relatively short duration of 10 minutes, while the cold clusters and lines tend to last longer.

Table 3.5—Median Values of Selected Echo Parameters from Texas HIPLEX, 1976-78

Type of echo	Sample size	Max area (1) (km²)	Max top hgt, (1) (km,MSL)	Echo top temp (°C)	Max reflec- tivity[1]	Hgt of max refl (km)	Dur- ation[2] (min)	Echo movement minus wind 850 mb 700 mb 500 mb direction(deg)/speed(m s⁻¹)
Warm cell[3]	6,532	4	4.3	+ 2	28	4.0	10	+17/-0.5 + 2/+0.1
Cold cell	3,565	8	7.1	-15	33	5.1	10	+20/-0.6 + 6/+0.1 - 8/-0.2
Warm cluster	138	54	5.0	- 1	40	4.2	10	+ 7/-0.3 +11/-0.4
Cold cluster	839	140	9.0	-26	49	4.3	35	+17/ 0.0 + 1/+0.6 - 3/+0.2
Line	14	10,000	15.4	-65	66	4.4	145	+45/-1.7 - 8/+1.0 +20/+0.6
Pre-frontal	4,008	6	5.0	- 2	30	4.2	10	+20/+0.1 - 1/+0.2 + 2/+0.2
Post-frontal	1,593	5	4.8	0	32	4.0	10	- 9/+0.5 -13/+0.3 +22/+0.7
No fronts	5,606	6	5.2	- 4	30	4.4	10	+25/-1.8 +18/ 0.0 -13/-0.5
Upper trough	7,204	6	5.1	- 3	30	4.3	10	+25/ 0.0 + 8/+0.3 - 4/-0.2
Upper ridge	2,916	6	5.0	- 2	31	4.1	10	- 4/-1.7 - 7/ 0.0 -10/+0.1
Inverted trough	1,087	6	5.1	- 2	32	4.3	10	+12/+0.9 - 1/+0.1 +16/+0.5

[1]Reflectivity threshold was 20 dBz
[2]Rounded to nearest 5 min.
[3]Warm echoes had maximum heights below the -5°C level

Under echo movement in Table 3.5, the average echo direction and speed relative to the 850 mb, 700 mb and 500 mb winds are provided. For example, cold cells tend to move 20 degrees to the right of the 850 mb winds, and 0.6 m s^{-1} slower than the 850 mb wind speed, i.e. +20/-0.6. At higher levels they tend to move 8 degrees to the left of the 500 mb wind and 0.2 m s^{-1} slower (-8/ -0.2). The 700-mb wind appears to be a fairly good estimate of echo movement. However, the frequency distribution revealed that about 20 percent of the echoes moved in an upwind direction, that is, the absolute value of the difference exceeded 90 degrees off the 700 mb wind.

Characteristics of echo dynamics were examined of warm and cold cells and clusters with respect to "split-off" and "merger" of fragmented echoes with the main echo. For the four echo types above (lines not included), the most common characteristic was the occurrence of split-off echoes of warm echoes. These split-off echoes dissipated twice as fast as the main echoes. Another characteristic was that cold echoes merged more often than warm echoes, particularly in the cluster type. In the 90th percentile comparison of merging echoes, cold cells outlasted warm cells by nearly three times, and cold clusters outlasted warm clusters by nearly four times. Overall, clusters endured for a longer time than cells. Other selected parameters for four echo types are given in Table 3.6.

The speed of echo motion was closely approximated by the 700 mb wind flow. The frequency distribution of echo-centroid direction indicated that only about 35 to 40 percent of the four echo types moved within 30 degrees of the environmental wind direction at 700 mb. Roughly 75 percent of the echoes had speeds within 5 m s^{-1} of the 700 mb wind.

A tabulation of line-echo statistics for the 1976-1978 M-33 radar data set is given as Table 3.7. The data were gathered from radar observations of 14 line echoes on 13 days. Of the parameters listed in the left column, area, duration, and movement exhibit large variability, whereas maximum height and maximum reflectivity vary the least. The orientation of the 14 line occurrences was: seven with NE-SW; four with E-W; one with NW-SE; and two N-S.

An analysis of the occurrence of echo types (cells, lines, and clusters) was conducted with respect to time-of-day. The results indicated that the occurrence of cells and clusters peaked during the late afternoon. Line occurrence peaked during two periods: an afternoon maximum occurred with locally developed lines; and a near-midnight maximum occurred with migrating lines (from outside the area).

Table 3.6—90th Percentile Comparisons for Selected Echo Parameters

Echo type	Maximum reflectivity (dBz)	Rainfall rate mm hr⁻¹	Rainfall rate (in hr⁻¹)	Echo top height km	Echo top height (ft)	Echo top temp (°C)	Echo duration (min)
Warm cell	38	5.7	(0.2)	5.3	(17,380)	- 2	20
Cold cell	48	23.7	(0.9)	9.6	(31,490)	-31	50
Warm cluster	49	27.3	(1.1)	5.5	(18,050)	- 4	75
Cold cluster	61	151.0	(6.0)	13.2	(43,300)	-58	145

Table 3.7—Median and Range Values for Selected Line Echo Parameters

Parameter	Median	Range
Maximum area	10,000 km² (3,856 mi²)	1,000 to 26,000 km² (386 to 10,000 mi²)
Maximum height	15.4 km (50,512 ft)	14.1 to 17.5 km (46,250 to 57,400 ft)
Echo-top temperature	-65° C	-63 to -70° C
Maximum reflectivity	66 dBz	56 to 70 dBz
Movement - 700 mb direction	-8	-121 to +141
Movement - 700 mb speed	1.0 m s⁻¹ (3.3 ft s⁻¹)	-7.8 to +8.1 m s⁻¹ (-25.6 to +26.6 ft s⁻¹)
Orientation	NE-SW	
Hour first observed	1600 CDT	0900 to 2300 CDT

A calculation of total rain volume and median rain volume was prepared for each of the five echo types, and is given in Table 3.8. The figures shown are more representative of "volume capability" of each echo rather than actual amount of rain processed. A qualitative interpretation of these figures indicates that lines account for more than two-thirds of the total rain volume, while cold clusters account for more than one-fourth the total. Warm and cold cells and warm clusters combined account for only about three percent of the Texas HIPLEX rain volume. Table 3.8 clearly illustrates the fact that cold clusters and lines are the significant rain producers in the Texas HIPLEX region.

3.3.2.2.3 Results

The climatological study generated a radar echo summary which accounted for convective activity in terms of cloud-top temperature for cells and clusters of cells. Lines were also studied. A

Table 3.8—Rain Volume Contribution by Echo Type

Echo type	Median rain volume	Mean no. of echoes per precip. event	Total rain volume by type[1]	Percent frequency
Warm cell	$1.6 \times 10^3 m^3$ (1.3 ac-ft)	197	$3.1 \times 10^5 m^3$ (256 ac-ft)	1.2
Cold cell	$3.6 \times 10^3 m^3$ (3.0 ac-ft)	109	$3.9 \times 10^5 m^3$ (327 ac-ft)	1.5
Warm cluster	$1.6 \times 10^4 m^3$ (13.0 ac-ft)	4	$6.4 \times 10^4 m^3$ (52 ac-ft)	0.2
Cold cluster	$2.6 \times 10^5 m^3$ (211.0 ac-ft)	27	$7.0 \times 10^6 m^3$ (5,700 ac-ft)	27.2
Line	$4.5 \times 10^7 m^3$ (36,500 ac-ft)	0.4	$1.8 \times 10^7 m^3$ (14,600 ac-ft)	69.9
		Sum =	$2.6 \times 10^7 m^3$ (20,900 ac-ft)	

[1]Total rain volume = (Median Rain Volume) × (Mean No. of Echoes Per Precip. Event).

"cold" cloud top was defined to be at a temperature of less than -5°C, a distinction necessary with the use of artifical ice-nucleating material. More than 11,000 echoes comprised the data set. Approximately 90 percent were cells, with warm cells numbering about twice that of cold cells. About ten percent of the echoes were clusters of cells; cold clusters outnumbered warm clusters by six to one. There were only 14 lines observed, but this type of cell development was dominant in terms of area, height, intensity and duration. Clusters were second in this regard. Estimations of precipitation volume capacity were calculated, which resulted in the ranking of lines accounting for more than two-thirds of the total rain volume, and cold clusters accounting for about one fourth the total.

3.3.2.3 Radar Echo Characteristics (A Case Study Approach)

3.3.2.3.1 General

The effects of the meso β-scale environmental conditions on convective cloud development have been well documented. The importance of conditional and convective instability, low level moisture, surface heating and meso β-scale-forcing functions have been established by Byers and Braham (1949) and by Newton (1967). The impact of dynamic mechanisms on the atmosphere and subsequent effect on convective cloud development were demonstrated by House (1959). Also, the meso β-scale triggering mechanisms, produced by mature and dissipating thunderstorms, were observed by Fujita (1963) and Matthews (1981a).

This section examines the characteristics of radar echoes observed in the Texas HIPLEX site, and their relationship to meso β-scale environmental parameters on a case study approach.

A case study approach was used in Texas HIPLEX analyses of radar data to illustrate and classify various types of meso β-scale radar echo configurations. This approach has proven useful in understanding life cycles of echo configurations, and in recognizing specific atmospheric components that are supportive of convection. Only through case study analyses can all the data be analyzed to develop a comprehensive and detailed picture of the atmospheric components that contribute to convection. However, the conclusions drawn may not be applicable to a population of radar echoes, and caution must be exercised when extrapolating findings beyond the case studies without further investigation.

3.3.2.3.2 Echo Interpretation

A study of meso β-scale echo features of the Texas HIPLEX area analyzed M-33 radar data collected during the 1976 and 1977 field seasons. A report describing the results of this study was prepared by Humbert *et al.* (1978) and is entitled *Development and Interpretation of an M-33 Radar Climatology for the Texas HIPLEX Region.*

Radar echoes were recorded on 86 days during 1976 and 1977. On 54 of these days, echoes persisted within the 140 km (87 mi) radius of the M-33 radar; 21 days had echoes in the 140 km (87 mi) to 280 km (174 mi) radial area; and 11 days had no echoes.

The study grouped radar echoes according to four meso α-scale categories, A through D. Types A and B are not associated with frontal systems, and rely on surface heating and mesoscale dynamics as the initiating convective mechanism; types C and D are associated with frontal systems, and differ only in echo orientation and subsequent affects.

Radar echo type A is characterized by mid-day development of intense surface heating along the lee side of the Rocky Mountains. A line of echoes forms along the Texas-New Mexico border and intensifies by mid-afternoon with eastward movement. Peak intensities and maximum areal coverage occur by late-afternoon. The southern extension of the line becomes oriented northeast-southwest, and moves into the Texas HIPLEX area by early evening. The line becomes stationary and either dissipates overnight, or is partially maintained into the next day.

Echo type B is airmass convective activity that is associated with deep moisture advection from the Gulf of Mexico; it is diurnal, and persistent with positive vorticity advection.

Radar echo type C is convective activity associated with cold fronts and stationary fronts. These echoes form in an east-west line, parallel with the frontal surface, and usually occur north of the Texas HIPLEX area as pre-frontal or post-frontal convection.

Type D echoes occur with advancing cold fronts that move into and through the Texas HIPLEX area, and are oriented northeast-southwest. This type is subclassified with respect to frontal, post-frontal and dissipating frontal zone echo formation.

The analysis and interpretation of echo occurrences were divided into two meso β-scale subgroups, "Isolated Systems" and "Line Systems," under meso α-scale groups A through D. A further breakdown of these two subgroups identifies the conditions of echo development which consist of "isolated cell conditions" and "echo complex conditions." The isolated cell condition was further classified with respect to environmental wind orientation. Similarly, the echo complex condition was further categorized with respect to organization of component cells making up the complex. An example of this classification scheme is indicated by the arrow-path in Figure 3.19 for Synoptic Type C, Line System Conditions, Cell Complex with Line Organization.

The "Isolated System" occurred in the data set about 50 percent of the time. All of these occurrences were not associated with the presence of surface fronts, and were classified within meso α-scale groups A and B.

The Isolated Systems exist in a combination of ways, and in various intensities, as atmospheric conditions change throughout a day. There are four distinct cloud-scale echo arrangements for the Isolated System:

— isolated cells with (and without) orientation to environmental wind shear (850-500 mb); and

— cell complexes with (and without) line organization of internal cells.

Analysis of the data set indicates that most of the Isolated Systems consisted of "isolated cells" with definite orientation to the environmental wind shear. (The reader is cautioned that wind shear was determined from the Midland sounding, and that it was
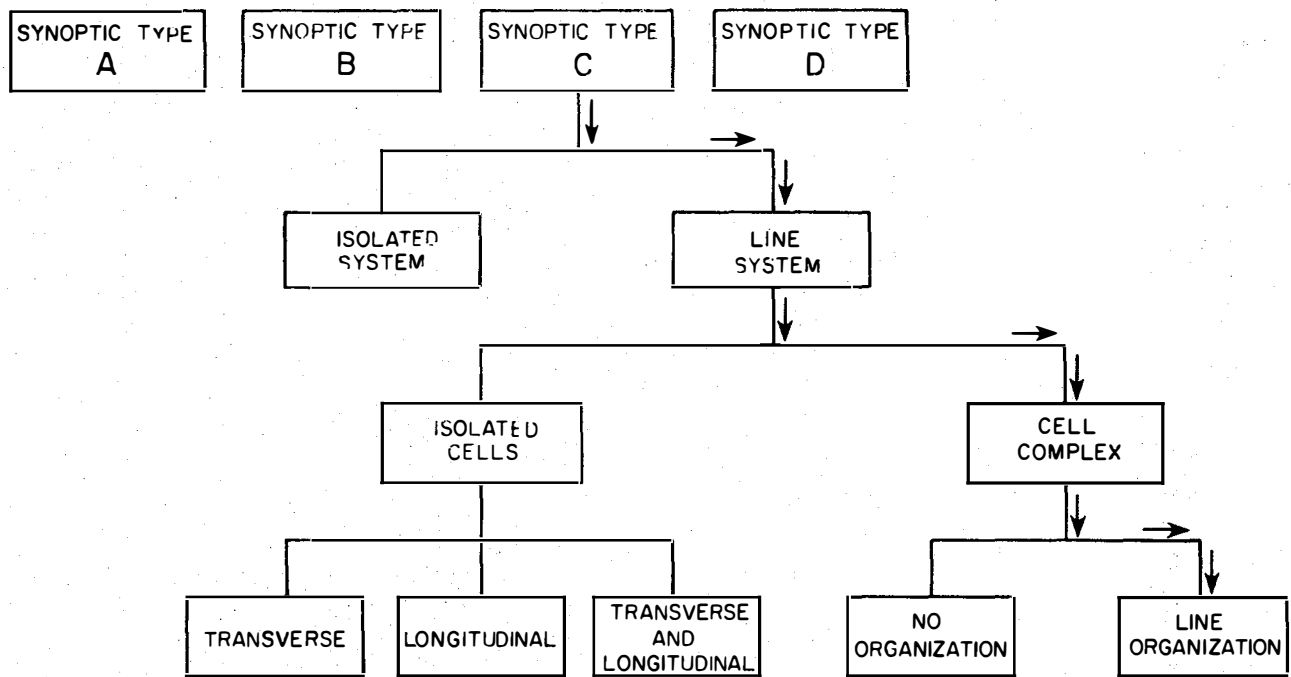
Figure 3.19. Sample mesoscale radar echo classification for Synoptic Type C, Line System Conditions, Cell Complex with Line Organization.

assumed that the sounding was representative of the atmospheric characteristics during the period of observation.)

Cell orientation to the wind shear was described as being either transverse or longitudinal. In the transverse mode, cell alignment was perpendicular to the wind shear vector; in the longitudinal mode, cell alignment was parallel to the wind shear vector. Whether the alignment was transverse or longitudinal depends on the orientation of the moisture convergence field, convective instability, and the magnitude of the wind shear vector. The subgroup of cell complex under Isolated Systems occurred on a very limited basis (an echo complex was defined as multiple cells with radar contours greater than or equal to 35 dBz, enclosed by a single 25 dBz contour). The occurrence of the cell complex with and without line organization was identifiable only temporarily in the cycle of convective systems. The occurrence of these conditions appeared to be controlled by the magnitude of wind shear speed and direction.

Line System conditions occurred about 50 percent of the time in 1976 and 1977. The Line System was supported for the most part by meso β-scale motion of fronts and upper-level troughs. This large-scale motion served as a triggering mechanism to initiate intense convective development in the Line System in either transverse or longitudinal alignment to the environmental wind field. Byers and Braham (1949) also suggested that the squall lines they observed resulted from meso β-scale atmospheric disturbances.

In all Line Systems composed of isolated cells, the cells had orientation implying that meso β-scale dynamic processes were involved in the convective development. In cases where isolated cells formed in the Line System with transverse or longitudinal orientation, and where favorable enviromental conditions prevailed, intense development resulted in the formation of a squall line. In cases where isolated cells of the Line System merged to form cell complexes which would form along a line, the internal cells of the complexes had no line organization. However, in some cases of Line Systems composed of cell complexes the line feature was so dominant that even the cells which comprised the echo complex were line-oriented.

A frequency distribution of Isolated Systems and Line Systems is presented in Table 3.9. The right column summarizes the percentage of occurrence of mesoscale events. The table demonstrates that Isolated and Line System conditions occurred an equal number of times. The dominant echo characters for each of the above were isolated cells with orientation, and cell complexes with line orientation, respectively.

Table 3.9—Mesoscale Frequency Distribution for Texas HIPLEX During the 1976 and 1977 Field Seasons

Mesoscale character	Echo character	No. days observed	Percent of total days	No. events	Percent of total events
Isolated System	Isolated cells (no orientation)	0	0	0	0
	Isolated cells (transverse and longitudinal)	6	46	7	35
	Cell complex without line organization	0	0	2	10
	Cell complex with line organization	0	0	1	5
	Sub total	6	46	10	50
Line System	Isolated cells (no orientation)	0	0	0	0
	Isolated cells (transverse and longitudinal)	1	7.7	2	10
	Cell complex without line organization	2	15.4	3	15
	Cell complex with line organization	4	30.8	5	25
	Sub total	7	54	10	50
	Total	13	100	20	100

Some other interesting mesoscale features of the 1976-1977 data set are given in Table 3.10. A tabulation of environmental averages is given for the Isolated System and Line System. The results indicate that the Line System exhibited the greater wind shear magnitude, which was more westerly (270 degrees) in direction, and had a greater change in equivalent potential temperature ($\Delta\theta_e$) between 850 and 500 mb. A further breakdown of the data indicates that isolated cells with transverse or longitudinal orientation, and complexes with line organization exhibited a more westerly wind shear. In relation to stability and organization, the data show that cell organization increases with convective instability. Note, for example, the increased magnitude of $\Delta\theta_e$ for isolated cells with orientation, a cell complex without orientation, and a cell complex with orientation.

Table 3.10—Averages of Mesoscale and Cloud Scale Variables for the 1976 and 1977 Texas HIPLEX Field Seasons

Mesoscale echo character	Cloud scale echo character	Direction (deg)[3]	Windshear[1] (m sec^{-1})	Ave. $\Delta \theta_e$[2] (°K)
Isolated System		252	5.43	8.53
Line System		271	5.93	12.83
	Isolated cells with no orientation	N/A[4]		N/A
	Isolated cells with transverse and longitudinal orientation	262	5.27	10.32
	Cell complex without line organization	233	7.23	12.80
	Cell complex with line organization	289	5.36	13.60

[1]Average windshear measured at 0000 GMT. The shear is defined as the vector difference between 500 and 850 mb winds at Midland.

[2]Average equivalent potential temperature difference between 500 and 850 mb measured at 0000 CDT.

[3]Windshear is measured from the end of the 850 to the end of the 500 mb wind vector.

[4]No data available.

3.3.2.3.3 Echo Organization

An example of meso β-scale influence on convective development is presented for squall line conditions in a report by Chen *et al.* (1979), entitled *Radar Echo Organization and Development in the Mesoscale Environment, A Case Study Approach.*

On the night of June 22-23, 1976, a squall line developed in the Texas Panhandle in association with meso α-scale disturbances at the surface and aloft. The northern section of the squall line was oriented north-south; the southern section was oriented northeast-southwest. The line was moving toward the southeast. The meso α-scale conditions characteristic of this event are reviewed in Section 3.2.2.2 of this report.

As the squall line developed, areas of high reflectivity (more than 35 dBz) were observed in the northern section of the line. The density of "echo lines" was uneven. In the northern section of the squall line, which had more echoes than the southern section, echoes were line organized in a direction parallel to the 850-500 mb wind shear vector. Echoes aligned parallel to this wind vector were

in a longitudinal mode. Along the southern end of the squall line, echoes were aligned more or less perpendicular to the 850-500 mb wind shear vector, and so were in a transverse mode.

An analysis of the surface pressure field indicated that the squall line moved with a trough, and changed orientation from northeast-southwest to west-southwest-east northeast. The northern half of the squall line moved at a greater speed in relation to its higher echo density. An analysis of the static energy field, computed from temperature and dewpoint measurements, revealed a large gradient in advance of squall line movement. A large gradient of static energy was in front of the line, which suggests its transport into the system by the low-level wind field, helping to support the system; a minimum static energy field occurred behind the squall line in the presence of a meso-high pressure area (caused by the downdraft associated with precipitation).

The combined analyses of echo pattern, pressure field, wind field, and static energy field performed during this case study revealed that a minimum static energy area follows behind a major high-reflectivity zone. This suggests that the dynamics of a near steady-state squall line may be such that the tilted updraft brings moisture and high static energy in advance of the squall line to a higher elevation and feeds it into the cloud system, leaving the precipitation in the rear side of the squall line. When the squall line moves forward (to the east), using the static energy to create kinetic energy to be used by the squall line, the residual low-energy air creates the minimum static energy zone in the high precipitation zone behind the system.

With respect to mesoscale characteristics, Chen *et al.* (1979) show the θ_e stability is an important measure of convective potential and organization, i.e. formation of nonsquall line type echoes require moist, unstable air, whereas squall line echoes can exist with less instability, even to the point of near neutral stability, although favorable environmental wind structures and moist static energy distributions are required. Squall line type echoes occur both during day and night, since echo formation, growth, and movement are controlled by environmental wind structure, while cell density is influenced by the moist static energy distribution.

A second feature of mesoscale organization of echoes is vertical shear of horizontal wind (with the shear determined between the 850 and 500 mb surfaces). Individual echoes become aligned either parallel or perpendicular to the wind shear vector. The representative environmental shear vector is best determined by the overall flow field encompassing the echoes, not the flow field between echo groups. The degree of echo organization is related to the magnitude of wind shear. The results of the study indicate that larger systems are associated with high wind shear values.

The evolution of a cloud population with respect to number and size was examined. The study identified changes from small-size echoes to large-size echoes during a brief time interval, when analysis indicated that convective potential was maximized. Merging of echoes was frequent, and very large complexes (more than 40 km [25 mi] equivalent diameter) existed longer than the smaller complexes. The study concluded that environmental static stability appeared to control echo population, and that merging of echoes changed the echo-size distribution.

3.3.2.3.4 Results

It is readily apparent from these studies that mesoscale atmospheric properties have an effect on the behavior of individual rain-shower echoes. In particular, low level moisture, the 850 mb and 500 mb wind shear vector, and the equivalent potential temperature (θ_e) lapse rate were determined to be important measures of convective potential and organization. In part, this relationship was also observed in a study by Wiggert *et al.* (1981) of radar echo data, collected as part of the Florida Area Cumulus Experiment (FACE), where it was observed that towering cumuli underwent changes in their dynamics and, perhaps, microphysical make-up as a result of the magnitude of the wind shear vector.

3.3.2.4 Skywater Radar Data Analyses

The Bureau's Skywater radar system collected 202 hours of digitized radar data on 32 days during the period May 20 to July 20, 1979, under the direction of Texas Tech University. These data were coupled with rawin-sonde mesoscale data, which were available from the seven-station network on 19 days, to study the interrelationships among mesoscale thermodynamic and kinematic properties and convection. The study is reported in total by Jurica *et al.* (1981), entitled *Invesitgations of Summer Convective Cloud Systems in the Texas High Plains.*

3.3.2.4.1 Mesoscale Thermodynamic Profiles and Intensity of Convection

Jurica *et al.* (1981) examined convective cloud systems, using Skywater radar data collected during the summer of 1979. Intensity of convection was examined by grouping echoes by maximum-top height versus maximum reflectivity. Then, a profile of atmospheric stability was made to determine the relationship between intensity and thermodynamics.

The report found that convective precipitation events in the vicinity of the study area typically had maximum echo top heights

exceeding 13 km (46,640 ft), and frequently exceeding 15 km (49,200 ft). On no days when radar data were collected were the maximum echo top heights less than 8.7 km. The deepest convection occurred on days when soundings showed high values of equivalent potential temperatures (θ_e) near the surface, a mid-tropospheric minimum θ_e, and increasing values of θ_e in the upper troposphere. Growth of convection was inhibited when there were layers with increasing θ_e with height, situated below the mid-tropospheric minimum, or with relatively low values of θ_e near the surface.

3.3.2.4.2 A Mesoscale Case Study

Satellite, radar, raingage, rawinsonde, and surface data were combined to illustrate mesoscale features of convective activity, associated with a nonsquall, weak surface frontal zone on July 17, 1979. Weak convective cells developed in a region of weak, mesoscale, low-level ascent, associated with a large-scale convergence zone at the surface. Deep convection was triggered by strong potential instability at the top of the boundary layer, which caused the development of a wide band of deep, intense convective cells with overshooting.

At 1300 CDT (1800 GMT), the Skywater radar showed a line of convective echoes developing to the east of Big Spring. The echo top height Plan Position Indicator, shown in Figure 3.20, depicts the echoes along the frontal convergence zone, observed in the automated objective analyses developed by Matthews (1983) for the Texas HIPLEX region. Note the arrow which indicates the location of the convergence zone at 101°W, 32.6°N, shown in the vertical motion and wind fields. The line of echoes developed along the axis of the 900 mb level convergence, indicated by an area of weak mesoscale lifting maxima, shown in Figure 3.2.1. This lifting triggered deep convective clouds in the strong, conditionally unstable environment.

By 1600 CDT (2100 GMT), deep convective clouds reached 16.5 km MSL in the vicinity of 101.6°W, 32.6°N (indicated by the arrow shown in Figure 3.22). Maximum radar echo reflectivities in this area were very high, reaching 50 to 60 dBz and higher. These intense, deep echoes were located in the vicinity of strong vertical motion, observed in the automated objective analyses shown in Figure 3.23. The arrow shows the core of maximum lifting at 500 mb which closely matched the most intense radar echoes from 1600 to 1700 CDT (2100 to 2200 GMT). In the dissipating stages of convection there was: a mesoscale region of horizontally uniform precipitation with a radar bright-band near the melting level; a mesoscale unsaturated downdraft beneath the melting level; and anticyclonic

Figure 3.20. Radar composit plan position indicator display at 1757 GMT on July 17, 1979. Top figure shows echo reflectivity values dBz, bottom shows maximum echo top height (km MSL). Arrows locate the convergence zone at 101°W 32.6°N, shown by corresponding arrows in Figure 3.21 in the objective analysis fields.

WIND FIELDS (KTS)
TOTAL FIELDS

300 (MB)

500 (MB)

700 (MB)

900 (MB)

VERTICAL MOTION (MMB/S)
TOTAL FIELDS

300 (MB)

500 (MB)

700 (MB)

900 (MB)

79/07/17 1800 TO 79/07/18 0300
TOTAL FIELDS

Figure 3.21. Objective analysis of wind fields at 900, 700, 500 and 300 mb levels described by 30 minute vectors from each grid point. Bold arrows co-locate points indicated by arrowheads on the radar PPI (Figure 3.20). Figure 3.21b shows the vertical motion field in -μbar/s such that positive values indicate upward vertical motion and negative values indicate downward motion as shown by arrowheads.
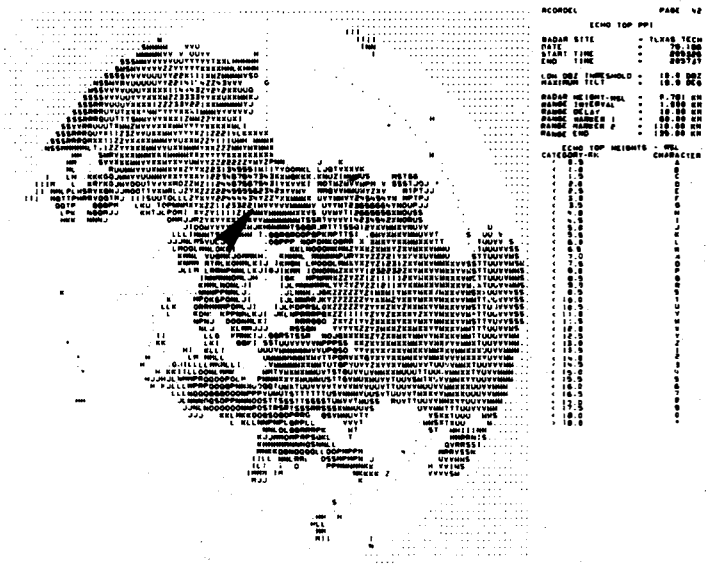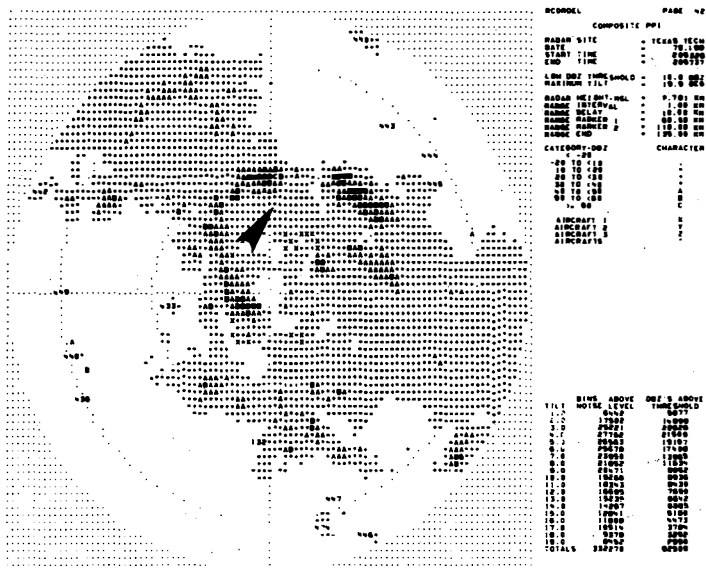
Figure 3.22. Same as Figure 3.20 at 2053 GMT. Arrowhead shows the location of maximum lifting at 101.6°W, 32.6°N, identified by objective analyses in Figure 3.23.

WIND FIELDS (KTS)
TOTAL FIELDS

300 (MB)

500 (MB)

700 (MB)

900 (MB)

VERTICAL MOTION (MMB/S)
TOTAL FIELDS

300 (MB)

500 (MB)

700 (MB)

900 (MB)

79/07/17 1800 TO 79/07/18 0300
TOTAL FIELDS
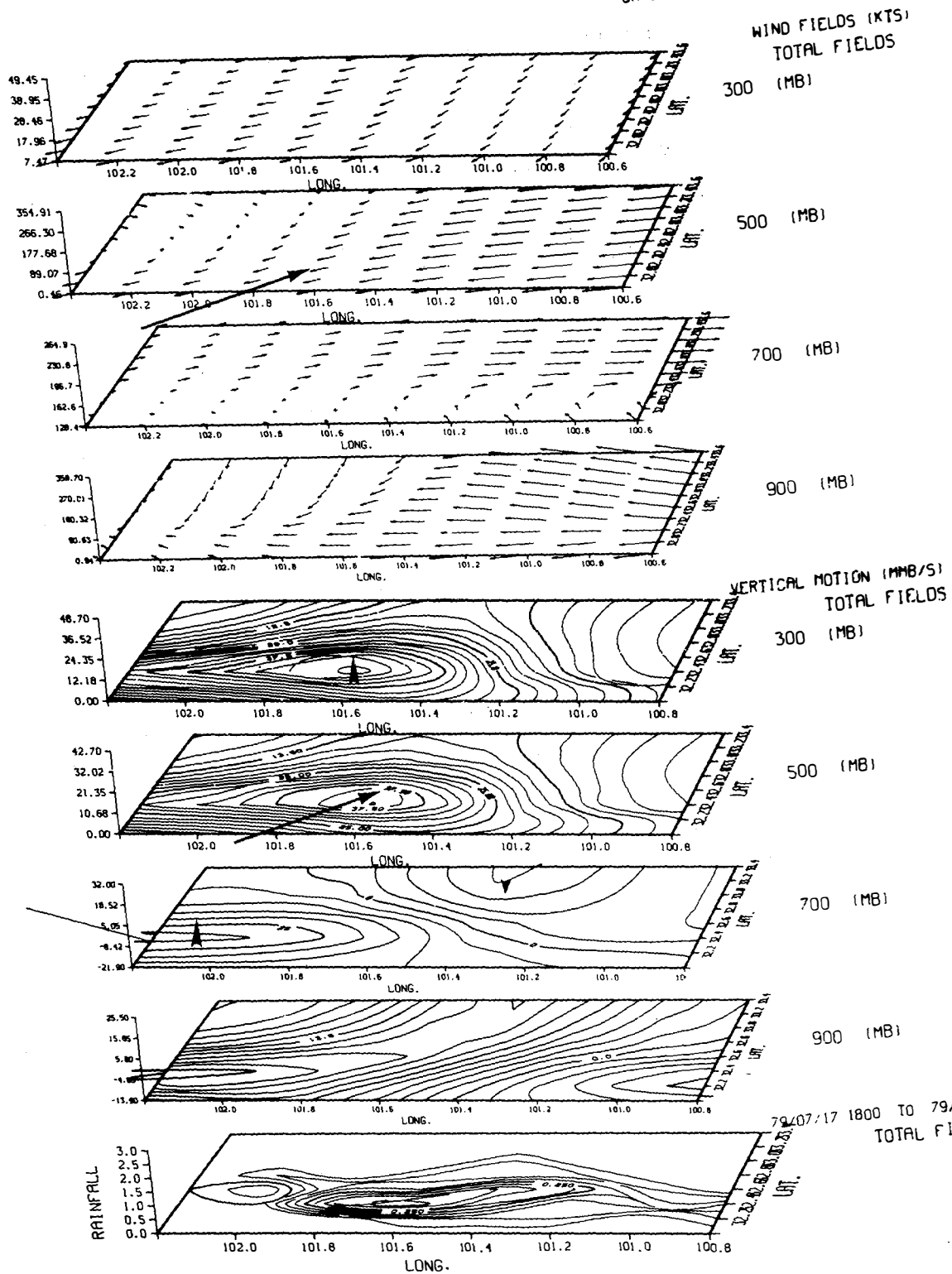
Figure 3.23. Same as Figure 3.21 for the 2100 GMT analyses. Surface rainfall contour (in) show the analysis of rain-gage data collected from 1800 GMT on July 17, 1979, to 0300 GMT on July 18, 1979. Arrows co-locate the core of maximum lifting, with radar PPI arrowheads in Figure 3.22.

flow at the 250 mb level. This unsaturated downdraft in the automated objective analyses was observed to have speeds of 20 μ bar s^{-1}.

Changes in the profiles of equivalent potential temperature (θ_e) suggested the transport of warm, moist air (high θ_e) upward from the boundary layer in convective updrafts, and transport of cool, dry air (low θ_e) downward from mid-tropospheric levels by convective-scale and mesoscale downdrafts.

Convective cells were organized along adjacent cold and warm pools of air at the surface. The presence of a warm pool during the early development stage may have enhanced low-level convergence, mesoscale ascent and subsequent convection. At the mature stage, the outflow from convective-scale downdrafts produced mesoscale cold pools at the surface, which eventually merged into a single, larger cold pool. Compressional warming in the mesoscale unsaturated downdrafts created a layer of warm air just above the cold pool (between 850 and 700 mb).

Also evident in this case study was the southward propagation of the surface frontal zone. This may have been caused by either the deposition of cold pools into the warm side of the frontal zone by convection which caused stronger thermal boundaries to form to the south, or the intensification of pressure gradients by the cold pools, imparting a southward horizontal momentum to the cold air, or both.

3.3.2.4.3 Results

The results reported by Jurica *et al*. (1981) showed that deep convection (8.7 km or greater) occurs on all days when radar echoes were observed, whether or not seeding occurred. This is not to say that all echo heights observed by radar were 8.7 km or greater, but that the maximum echo height observed on the days when radar data were collected, was 8.7 km or greater. Operationally, every effort was made to collect radar data on all days when radar detectable echoes were present. However, some radar echo days may not have been recorded due to field operations standdown. As a result, this may have introduced a slight bias toward larger echoes. On days when no echoes were observed, the atmosphere was too stable to support deep convection, and seeding on those days may produce an echo that would probably not result in significant rainfall because of the lack of atmospheric support. Therefore, one stratification criterion for cloud seeding to enhance precipitation is to operate on days when natural clouds are expected to reach a height of 8.7 km or greater.

The results of the case-study event are a first step in looking at the mesoscale interaction between individual cumulonimbus clouds. The existence of these interactions suggests a broad-scale effect may occur by enhancing the downdraft of individual cumulonimbus.

3.3.3 Convective Cloud Environment

3.3.3.1 General

Convective-type clouds form in areas where the atmosphere is unstable, sufficient moisture exists, and some type of trigger mechanism (such as a cold front) is present to provide the required vertical impetus (Byers and Braham, 1949; Newton, 1963). During the summer, these conditions often occur in localized regions, with the trigger mechanism mostly being associated with features, such as a dry line (Rhea, 1966; Schaefer, 1974).

While the localized environmental conditions are responsible for the initiation of convective-type clouds, when these clouds become relatively large in their vertical extent, the circulation system associated with them alters the local environment in which the cloud is embedded. Thus, the cloud interacts with its environment, which leads to changes not only in the wind field surrounding the cloud, but also in the thermodynamic structure of the cloud environment. These interactions influence the circulation patterns in the vicinity of the storm by affecting the flow of moist air into the storm and thus its energy source.

The very complex interactions between local convective storms and their environment will have to be well understood in order to develop a technology required for rainfall enhancement through cloud seeding. In view of the fact that such information is not available, the mesoscale research conducted during the summers of 1976 through 1980 as part of the Texas HIPLEX Program was designed to determine factors and environmental conditions responsible for the initiation, growth, maintenance, and dissipation of convective clouds.

This research is reported by Scoggins *et al.* (1978), in *Mesoscale Characteristics of the Texas HIPLEX Area During Summer 1976*; Scoggins *et al.* (1979), *Mesoscale Characteristics of the Texas HIPLEX Area During Summer 1977*; Sienkiewicz *et al.* (1980), *Mesoscale Characteristics of the Texas HIPLEX Area During Summer 1978*; Williams and Scoggins (1980), *Models of Atmospheric Water Vapor Budget for the Texas HIPLEX Area*; and Gerhard and Scoggins (1981), *Potential Flow Models of Thunderstorm-Environment Interaction*. The data used in the ambient air studies were provided by both surface and upper air measurement and recording networks.

The analyses of the mesoscale data presented in this report are based on spatial interpolation of the measured surface and upper air data over the Texas HIPLEX project area. The results should not be considered as representative of the smaller cloud scale parameters.

The surface parameters for each day and hour were stratified, using several criteria to determine relationships between each parameter and radar echo. Parameters considered were velocity divergence, moisture divergence, vertical motion 50 mb above the surface, and the vertical flux of moisture 50 mb above the surface. Contingency tables and frequency distributions were prepared for various categories of convective echoes.

The analysis of upper-level kinematics and atmospheric energetics for each sounding time were stratified and averaged according to convective or nonconvective conditions to summarize the case studies of 1977, 1978, and 1979 events. Parameters averaged included mass divergence, vertical motion, moisture divergence, horizontal and vertical flux divergence of latent heat energy, local change of latent heat energy, residual of the latent heat energy equation, diabatic heating, horizontal and vertical flux divergence of energy, local change of kinetic energy, horizontal and vertical flux divergence of potential energy, and local change of potential energy.

A study of the state of the atmosphere relative to water content in the environment surrounding convective activity was also conducted. Models were constructed to supply the water vapor transport processes relative to the presence, type, depth, and areal coverage of convective activity. The types of convection discussed are isolated cells, clusters of cells, and lines of cells. In brief, the processes of water vapor transport considered include:

(a)   net horizontal transport of water vapor;

(b)   vertical transport of water vapor;

(c)   combined net horizontal and vertical transport of water vapor;

(d)   local rate of change in the total mass of water vapor; and

(e)   residual term of the water vapor budget.

3.3.3.2   Methods of Meso β-scale Data Analysis and Parameters Evaluated

The evaluation of both the surface and sounding data varied somewhat from year-to-year primarily because of variations in data collected. However, the basic concepts remained unchanged. The methods used in mesoscale data analysis and presented here were taken from Scoggins *et al.* (1979) to illustrate the procedures. For further detail on the methods, the reader is referred to the report referenced above.

While consideration was given to errors in the computations, no attempt was made to quantify the errors. Instead, temporal and spatial continuity and consistency were considered in the interpretation of results.

3.3.3.2.1 Gridding of Data

An objective analysis scheme developed by Barnes (1964) was used to interpolate the HIPLEX surface data to an 18×18 grid, with approximately a 16-km spacing between grid points. Each grid point in the array was assigned a terrain height from a standard topographic map.

In addition to the HIPLEX mesoscale surface stations, data from the surrounding National Weather Service and Air Force station were used in the surface analyses. Only the four rawinsonde stations (Midland, Big Spring, Robert Lee, and Post) were used in the upper air analyses, but these data were not gridded. The four basic surface variables objectively analyzed onto the grid were temperature, mixing ratio, and the "u" and "v" wind components. All other surface parameters were computed from these basic fields.

3.3.3.2.2 Surface Parameters

The basic meteorological variables were objectively gridded onto the 18×18 array each hour of every day. These gridded variables were used to evaluate the parameters. Centered difference computations were performed over two grid distances and applied to the center point.

Velocity Divergence: Surface wind velocity divergence was calculated, using the expression

$$\vec{\nabla}_2 \cdot \vec{V}_2 = \frac{\partial u}{\partial x} + \frac{\partial v}{\partial y} \simeq \frac{u_2 - u_1}{2\Delta x} + \frac{v_2 - v_1}{2\Delta y} ,$$

where it is understood that all expressions refer to surface variables and have their usual meteorological meanings. The subscripts "1" and "2" reference grid points where $\Delta x = \Delta y = 16$ km.

Moisture Divergence: Surface moisture divergence was computed by use of the expression

$$\vec{\nabla}_2 \cdot q\vec{V}_2 = \frac{\partial (qu)}{\partial x} + \frac{\partial (qv)}{\partial y} \simeq \frac{q_2 u_2 - q_1 u_1}{2\Delta x} + \frac{q_2 v_2 - q_1 v_1}{2\Delta x} .$$

The subscripts have the same meaning as above, and all computed values were applied to the center point.

Vertical Motion: In computing vertical motion 50 mb above the surface, both terrain-induced vertical motion and velocity divergence of the surface wind were considered. By assuming the surface wind field as representative of the mean wind through a 50 mb deep layer above the surface, the equation of continuity in pressure coordinates

$$\vec{\nabla}_2 \cdot \vec{V}_2 = -\frac{\partial \omega}{\partial p}$$

can be integrated from the surface to the top of the 50-mb layer to give the vertical motion through the top of the layer. Thus,

$$\omega_{(P_s - 50 \text{ mb})} = \omega_{P_s} + \frac{\int_{}^{P_s}(\vec{\nabla}_2 \cdot \vec{V}_2)\,dp}{(P_s - 50 \text{ mb})},$$

where $\omega = \frac{dp}{dt}$, and P_s is the surface pressure. The magnitude of ω_{P_s} can be approximated by the terrain-induced vertical motion

$$w_T = u\left(\frac{\partial h}{\partial x}\right) + v\left(\frac{\partial h}{\partial y}\right) \simeq \frac{u(h_2 - h_1)}{2\Delta x} + \frac{v(h_2 - h_1)}{2\Delta y},$$

where h is the terrain height. For the range of surface temperatures and pressures in the Texas HIPLEX area

$$w_T (\text{cm s}^{-1}) \cong -\omega_{P_s} (\mu b \text{ s}^{-1}).$$

Therefore, the resultant vertical motion at 50 mb above the surface was calculated, using the expression

$$\omega_{(P_s - 50 \text{ mb})} = -w_T + (\vec{\nabla}_2 \cdot \vec{V}_2)\Delta p,$$

where $\Delta p = 50$ mb.

Vertical Flux of Moisture: The vertical flux of moisture is given by the product of the vertical velocity 50 mb above the ground (cm s^{-1}), the surface mixing ratio, and air density. Units are g cm^{-2}s^{-1}.

Vorticity: The vorticity of the surface wind was calculated using the expression

$$\vec{V}_2 \times \vec{V}_2 = \frac{\partial v}{\partial x} - \frac{\partial u}{\partial y} \simeq \frac{v_2 - v_1}{2\Delta x} - \frac{u_2 - u_1}{2\Delta y},$$

where subscripts have the same meaning as before.

3.3.3.2.3 Upper Air Parameters

The equations presented here were integrated vertically to obtain the energy balance of each atmospheric layer. The friction term in the total energy budget equation was not evaluated. Values of all other terms were computed as averages per unit volume through a depth of 50 mb, and horizontally covering the area bounded by the Midland-Post-Robert Lee, Texas, triangle. Terms were evaluated at the surface and at 50 mb intervals from 850 mb to 100 mb. Vertical integration was performed over 50 mb intervals, except in the lowest layer which extended from the surface (about 920 mb) to 850 mb. The trapezoidal rule was used for integration purposes.

Horizontal Velocity Divergence: For a given time period and pressure surface, the horizontal velocity divergence was computed by use of the expression

$$\vec{V}_p \cdot \vec{V}_2 = \frac{1}{A}\frac{dA}{dt} \simeq \frac{1}{\bar{A}}\frac{\Delta A}{\Delta t},$$

where A is the horizontal triangular area determined from the three rawinsonde balloon locations (Midland, Post, and Robert Lee) projected onto a constant pressure surface; $\bar{A}$ is the average area of the triangle between two pressure surfaces 50 mb apart; and ΔA is the change of triangular area that occurs as the balloons move through a pressure layer 50 mb thick in time Δt.

Horizontal Moisture and Mass Divergence: Horizontal moisture and mass divergence were determined, using the vector identity

$$\vec{\nabla}_p \cdot C\vec{V}_2 = \vec{V}_2 \cdot \vec{\nabla}_p C + C\vec{\nabla}_p \cdot \vec{V}_2 ,$$

$$\quad\quad (1) \quad\quad\quad (2) \quad\quad\quad (3)$$

where C is any scalar. For moisture and mass divergence, q (mixing ratio) and ρ (air density) replaced C. Term 2 was computed by the centered finite difference formula

$$\vec{V}_2 \cdot \vec{\nabla}_p C = u\frac{\partial C}{\partial x} + v\frac{\partial C}{\partial y} \simeq \bar{u}\frac{(C_2 - C_1)}{\Delta x} + \bar{v}\frac{(C_2 - C_1)}{\Delta y} ,$$

where $\bar{u}$ and $\bar{v}$ are the average wind components over the network along a pressure surface, and $\frac{C_2 - C_1}{\Delta x}$ and $\frac{C_2 - C_1}{\Delta y}$ are the horizontal vector components of the gradient of C in the "x" and "y" directions, respectively. Term 3 was calculated by multiplying C (an average for the pressure surface) by the horizontal velocity divergence computed previously. Since the velocity divergence represents a 50 mb layer mean value, term 2 was actually computed as a mean horizontal advection by averaging data from three 25 mb data levels constituting the 50 mb layer used in the velocity divergence calculation.

Vertical Motion: Vertical motion was computed on constant pressure surfaces, using the formula

$$(\omega_p)_k = \omega_s + \sum_{}^{k}\overline{(\vec{\nabla}_p \cdot \vec{V}_2)}_k (\Delta p),$$

where $(\omega p)_k$ is vertical velocity on a constant pressure surface k, ω_s is the vertical velocity at the ground, $\overline{(\vec{\nabla}_p \cdot \vec{V}_2)}_k$ is the 50-mb layer mean divergence below layer k, and $\Delta p = 50$ mb.

Total Energy Budget: The budget of total energy (kinetic, internal, and gravitational potential) per unit volume is given by

$$\rho\frac{dQ}{dt} = \frac{\partial}{\partial t} \rho(\frac{V^2}{2} + gz + c_v T) + \vec{\nabla}\cdot\rho\vec{V}(\frac{V^2}{2} + gz + c_p T)$$

$$+ \frac{\partial}{\partial p} \rho\omega(\frac{V^2}{2} + gz + c_p T) - \rho\vec{V}\cdot\vec{F}.$$

In this equation $\frac{v^2}{2}$ is kinetic energy, gz the gravitational potential energy, c_vT the internal energy, c_pT the enthalpy or sensible heat, $\vec{F}$ the frictional force, all per unit mass, and Q the heat added by diabatic processes. Other symbols have the standard meteorological meanings.

The above equation, written in integral form in the x, y, p, t system, is

$$\frac{1}{g} \int \frac{dQ}{dt} dV = \frac{1}{g} \int \frac{\partial}{\partial t}(\frac{v^2}{2} + gz + c_v T)\, dV$$

$$+ \frac{1}{g} \int \vec{\nabla}\cdot(\frac{v^2}{2} + gz + c_p T)\vec{V}\ dV$$

$$+ \frac{1}{g} \int \frac{\partial}{\partial p}(\frac{v^2}{2} + gz + c_p T)\,\omega\ dV$$

$$- \frac{1}{g} \int \vec{V}\cdot\vec{F}\ dV.$$

This is the form of the equation that was evaluated.

Diabatic heating can be evaluated from the first law of thermodynamics in the form

$$\frac{dQ}{dt} = c_p\frac{\partial T}{\partial t} + c_p\vec{V}\cdot\vec{\nabla}T + (c_p\frac{\partial T}{\partial p} - \alpha)\omega,$$

where $\alpha = \frac{1}{\rho}$ or the specific volume. The net effect of the various forms of diabatic heating, such as evaporation/condensation, radiation and sensible heat transfer, is obtained from this equation in integral form.

Latent Heat Energy Budget: The budget of latent heat energy is given by

$$\frac{\partial}{\partial t}(\rho Lq) + \vec{\nabla}\cdot(\rho Lq\vec{V}) + \frac{\partial}{\partial p}(\rho Lq\omega) = R,$$

where L is the latent heat of vaporization, and q is specific humidity. All other symbols have their usual meaning. The term on the right of this equation represents evaporation and/or condensation and energy processes that cannot be resolved in time and/or space by using the available input data and computational procedures. Since this term is computed as a residual, some error from the remaining terms is included as well.

- 93 -

The integral form of the latent heat energy budget in the x, y, p, t system is

$$\frac{1}{g} \int \frac{\partial}{\partial t}(Lq)\,dv + \frac{1}{g} \int \vec{V} \cdot (Lq)\vec{V}dv + \frac{1}{g} \int \frac{\partial}{\partial p}(Lq\omega) = \int R\,dV,$$

which is the form of the equation that was evaluated.

Water Budget: The equation for conservation of water substance has been derived by Haltiner (1971), and may be expressed in the form:

$$\frac{\partial (\rho_a q)}{\partial t} + \vec{V}_3 \cdot (\rho_a q\vec{V}_3) = S, \tag{1}$$

where ρ_a is the density of dry air, q is the specific humidity, $\vec{V}_3$ is the three-dimensional wind vector, and S represents sources and sinks of water vapor in mass per unit volume per unit time. Applying Gauss's divergence theorem to Eq. (1) and integrating over volume, yields:

$$\int_V \frac{\partial (\rho_a q)}{\partial t}\,dv + \int_{s'} (\rho_a q(V_3)_n)\,ds' = \int_V S\,dv, \tag{2}$$

where $(V_3)_n$ represents the normal wind components to the boundaries of the volume, and s' represents the surface of the volume. Equation (2) can be expanded to include horizontal and vertical components of water vapor transport:

$$\int_V \frac{\partial (\rho_a q)}{\partial t}\,dv + \int_s (\rho_a q V_n)\,ds + \int_A (\rho_a q w)\,dA = r. \tag{3}$$

V_n is the normal wind component to the lateral boundaries of the volume (positive in; negative out), w is the normal wind component to the horizontal boundaries of the volume (positive in; negative out), A represents the horizontal surfaces of the volume, s represents the lateral surfaces of the volume, and r represents sources and sinks of water vapor per unit time for the volume. By assuming an incom-

pressible and homogeneous atmosphere (ρ_a = constant) and using perturbation theory, Eq. (3) becomes:

$$\int\limits_{V} (\rho_a \frac{\partial \bar{q}}{\partial t})\,dv + \int\limits_{s} (\rho_a \bar{q}\,\overline{V_n})\,ds + \int\limits_{s} (\rho_a \overline{q'V_n'})\,ds +$$

$$\int\limits_{A} (\rho_a \overline{qw})\,dA + \int\limits_{A} (\rho_a \overline{q'w'})\,dA = r, \quad (4)$$

where barred quantities refer to mean values, and prime quantities to fluctuation or perturbation quantities. Equation (4) can be simplified by grouping sources and sinks of water vapor with terms containing perturbation quantities, and expressed as:

$$\int\limits_{V} (\rho_a \frac{\partial \bar{q}}{\partial t})\,dv + \int\limits_{s} (\rho_a \bar{q}\,\overline{V_n})\,ds + \int\limits_{A} (\rho_a \overline{qw})\,dA = R,$$

$$\qquad (1) \qquad\qquad (2) \qquad\qquad (3) \qquad (4) \qquad (5)$$

where R represents the residual term of the water budget. Equation (5) represents the water budget at any particular time, expressed as mass per unit time. The terms in the equation have the following interpretation: (1) the local rate-of-change or the net gain or loss of water vapor within the volume; (2) the transport of water vapor through lateral boundaries; (3) transport of water vapor through horizontal boundaries; and (4) the sources and sinks of water vapor (evaporation, condensation and some water vapor which eventually may be lost through precipitation, and the turbulent flux of water vapor or translation or cloud liquid water through the boundaries). Because of the sign convention used with $\overline{V_n}$ and $\overline{w}$ in the calculations, terms (2) and (3) will be negative (convergence) when there is a net gain of water vapor, and positive (divergence) for a net loss of water vapor in the volume.

3.3.3.3 Results

In most cases, both surface and upper air conditions were altered significantly by convective activity. In some cases, pronounced changes in variables, such as moisture divergence at all levels, including the surface and vertical motion aloft, were associated with the occurrence and extent of convective activity.

Various surface and upper air analyses were performed and have been published for each of the first three years (1976-1977-1978). Similar results were obtained for each year and included in the reports referenced previously. Results for 1977 are emphasized below, but apply generally to the other years as well. In 1979 and 1980 the number of rawinsonde stations increased from four to seven, making it possible to perform spatial analyses. The results for these two years are not yet available in published form, and are not summarized in this report.

Surface: Maximum values of velocity and moisture convergence (negative divergence), positive vertical motion ($-\omega$) 50 mb above the surface, and upward flux of moisture ($-q\,\omega$) 50 mb above the surface, observed anywhere in the Texas HIPLEX mesonet, were obtained from the computer charts each hour between 1000 and 2200 CDT (1500 and 0300 GMT). The data were grouped for echoes and no echoes. During 1977, there were 122 observation times when echoes were present, and 96 when they were not present. Percentage frequency distributions were prepared for each variable. The value of a variable at the cross-over point (where the distributions cross) represents the value that best distinguishes between the occurrence or nonoccurrence of a radar echo. These values are: velocity divergence, $-10^{-4}s^{-1}$; moisture divergence, $-10^{-6}g\;cm^{-1}s^{-1}$; vertical motion 50 mb above the surface (ω), $-5\;\mu bars\;s^{-1}$; and vertical flux of moisture 50 mb above the surface (ωq), $-5 \times 10^{-5}\;g\;cm^{-2}s^{-1}$. When the magnitudes of these variables are smaller than the cross-over values, there is a higher percentage of no echoes than when the values are exceeded. Also, for each variable the extreme magnitudes are larger when echoes are present than when they are absent.

To aid further in the interpretation of the frequency distributions, contingency tables were prepared, using the cross-over values as criteria for distinguishing between echoes and no echoes. These tables confirm in a different way what the distributions showed. When values of all variables exceed the cross-over values, there usually is more than a 2:1 probability that echoes will be observed. The ratios for values below the cross-over values vary between approximately 2:1 and 3:1 in favor of no echoes. It should be remembered that the values of the variables chosen at a given time are not necessarily associated with a specific echo, if one was observed.

To gain some idea of how the cross-over values are related to echoes of various types, the echoes were classified as follows.

Lines: Cells organized into a line which exhibits movement.

Clusters: Organized group of 3 or more cells, determined by closed contours of radar codes 1(tops < 6.1 km [20,000 ft]), 2(tops 6.1 km [20,000 ft] ≤ 9.1 km [30,000 ft]), or 3(tops > 9.1 km [30,000 ft]) or any combination of these codes.

Unorganized (A): One or more individual cells the tops of which are under 10 km (32,800 ft) and none of which are organized into a line or cluster, as defined above. This includes cells that are not entirely on the grid.

Unorganized (B): Same as above except tops exceed 10 km (32,800 ft). Echo(es) approaching or receding from area: Edge of echo(es) on edge of grid area, and there is no cell present in the gridded area. This does not include cases in which there is a complete echo in the grid area at the same time.

No echoes: No echoes observed anywhere in grid area.

The number of occurrences when the magnitudes of the variables were less than or greater than the cross-over values, are shown in Table 3.11 for each echo classification and when no echoes were present. In all cases, there is a greater probability for echoes when the cross-over values are exceeded than when they are not, but the delineation is defined better for lines and clusters than for the other categories.

Upper Air: In 1977, there were 70 time periods that contained the necessary data for kinematic calculations aloft. These time periods were classified as either convective or nonconvective, depending upon whether thunderstorms were present over the network bounded by the Midland, Post, Robert Lee, Texas, triangle. If a radar echo in excess of 6.1 km (20,000 ft) was observed ± 1 hour within a sounding time, the period was termed convective. All other cases were termed nonconvective, except when balloons were suspected of entering thunderstorms. These cases were considered as not representative of the mesoscale environment in which thunderstorms were present, and were excluded from averages presented here. Using this classification, there were 15 time periods with and 55 time periods without convective activity. Results were calculated for 50 mb intervals from 850 to 100 mb, and profiles prepared.

The primary difference between the convective and nonconvective profiles of horizontal mass divergence is the occurrence in low levels of strong mass convergence in the convective profiles. Mass convergence was present in both profiles in mid levels, but mass divergence was computed above 600 mb with convective activity, whereas near zero values occurred in upper levels when convective activity was absent.

Vertical velocity profiles were clearly different during times with and without convection. Upward vertical velocities, capable of releasing potential instability, were observed at all levels in the convective profile, while subsidence was present at all levels in the nonconvective profile, possibly suppressing thunderstorm formation. Ulanski and Garstang (1978) found similar convergence patterns associated with convective precipitation in Florida.

Table 3.11—Occurrences of Echoes as Function of Echo Characteristics and Cross-Over Values For Velocity and Moisture Divergence, Vertical Motion 50 mb Above the Surface, and Vertical Flux of Moisture 50 mb Above the Surface.

Echo classification	Divergence (s^{-1})		Moisture divergence ($g\ kg^{-1}s^{-1}$)		Vert. moist. flux ($g\ cm^{-2}s^{-1}$)		Vertical motion ($\mu bars\ s^{-1}$)	
	$>-10^{-4}$	$<-10^{-4}$	$>-10^{-3}$	$<-10^{-3}$	$>-5\times10^{-5}$	$<-5\times10^{-5}$	>-5	<-5
Lines	9	16	4	21	3	22	8	21
Clusters	4	12	2	14	1	15	5	14
Unorganized (A)	15	17	12	20	10	22	16	20
Unorganized (B)	12	16	10	18	7	21	11	18
Receding or approaching	8	13	5	16	3	18	8	16
No echoes	73	23	67	29	57	39	63	29

Horizontal moisture convergence in low levels was large in the convective profile, and large moisture divergence was present in the nonconvective curve as water vapor was supplied horizontally during activity times, and removed horizontally during periods without activity. This same pattern is found in the horizontal flux divergence profiles of latent heat energy where net inflow in low levels supplies latent heat for storm development and removes it horizontally when convection fails to form.

Vertical flux divergence of latent heat energy occurred in low levels, and flux convergence was computed aloft for the convective case. This corresponds to a net vertical transport within the upward vertical velocity field of latent heat energy and water vapor from low levels to mid levels, where cooling and condensation produce convective cloud formation and the release of latent heat. The reverse vertical pattern of convergence/divergence was computed for the nonconvective profile. This indicates that a net downward transport of latent heat energy within the downward vertical velocity field occurs between mid- and low-levels, which does not promote condensation and cloud formation since adiabatic warming probably lowers relative humidities in mid-levels.

Local changes in latent heat energy are small and positive in the nonconvective profile, indicating that evaporation or turbulent fluxes of latent heat may be important when activity is absent. Negative values in low- and mid-levels during times when activity was present probably reflect the losses of water vapor that occur during condensation.

The residual profiles from the latent heat budget equation show losses of latent heat energy in the convective profile that are large in the middle troposphere, and gains of energy at mid-levels in the nonconvective profile. This distribution is consistent with condensation and environmental heating when activity is present, and evaporation and environmental cooling from losses of sensible heat when activity is not present.

The profiles of diabatic heating support this interpretation, since the general shape and sign of the latent heat budget profiles closely resemble the diabatic heating profiles below 300 mb. Sensible heating in the convective profile is strongly related to condensation (within an upward vertical velocity field) and cooling in the nonconvective profile, and relates well with evaporation (within a downward vertical velocity field). However, both the diabatic heating and cooling are somewhat smaller than would result if the latent heat residual profiles were completely responsible for these diabatic effects. Both net radiation and turbulent flux divergence of water vapor and heat may be responsible for the differences.

The nonconvective profiles for both the horizontal and vertical flux divergence of kinetic energy are near zero at all levels, except above 300 mb when net horizontal inflow of kinetic energy occurs. The convective profiles show net horizontal inflow in low levels and outflow at mid- and upper-levels, with vertical flux divergence of kinetic energy in low- and mid-levels

and flux convergence aloft. During convective activity, kinetic energy flows inward in low levels, and flows upward to the high troposphere where it is horizontally exported. As a result, local changes of kinetic energy are small and near zero at all levels during nonconvective periods, and small but slightly negative in the upper-troposphere during times of convection.

Horizontal flux convergence of sensible heat energy in low levels and flux divergence in mid- and upper-layers appear in the average convective profile. In contrast, net horizontal outflow of sensible heat in low levels and net inflow in mid-levels were computed for the nonconvective profile. The pattern contributes to creating increasing low level temperatures and decreasing upper-level temperatures in the convective profile, and conversely, for the nonconvective profile. The static stability is therefore possibly decreased in convective areas and increased in no activity areas, consistent with storm formation and suppression.

Vertical flux divergence of sensible heat in low levels and flux convergence in upper levels in the convective profile are associated with the net vertical transport of sensible heat, accomplished by thunderstorms and resulting from upward environmental vertical velocities. The reverse vertical convergence/divergence pattern appears in the nonconvective profile, with sensible heat experiencing a net downward transport from mid-to-lower levels in a sinking vertical velocity field. Local changes of sensible heat are generally small at most levels in the nonconvective profile, except near the ground where radiational heating probably creates large positive values when skies are particularly cloud free, and summer solar heating is large. However, local changes of sensible heat energy are large and positive in low levels in the convective profile, indicating the possible destabilization of the atmosphere during times of convective activity.

The horizontal and vertical flux divergence profiles of potential energy for convective and nonconvective areas are generally similar in sign and shape, except in low levels where horizontal flux convergence and vertical flux divergence of potential energy are found in convective areas. Net horizontal outflow and net vertical inflow of potential energy in low levels are computed in the nonconvective areas. Net horizontal outflow of potential energy is very large in upper levels when activity is present.

Local changes in geopotential energy are small and negative in low levels, and small and positive in the upper troposphere in the nonconvective profile. However, large negative values are found at all levels, especially in the lower and upper troposphere during times of convective activity. This pattern points to the falling geopotential heights that are observed during times of thunderstorms.

In summary, substantial differences occur in energy budget terms and kinematic parameters when averages over times of convection are compared with averages over times of no convection. Low-level net horizontal inflow, net upward transport, and upper-level net horizontal outflow of

internal, kinetic, and latent energy are found during times of convection. By contrast, upper- or mid-level net horizontal inflow, net downward transport, and lower-level net outflow of internal, kinetic, and latent energy are found when convective activity is absent.

Water (Moisture) Budget: Because of the importance of moisture in the formation, maintenance and decay of convective storms (House, 1959; Fankhauser, 1969; Ulanski and Garstang, 1978), the analysis of the water (moisture) budget will be considered separately from the upper air parameters discussed above. Of course, it is recognized that all upper air processes are interrelated. The results presented here are based on analyses for the three years 1976, 1977 and 1978.

At all levels of the atmosphere, changes in moisture divergence between convectively active and convectively nonactive periods are not large. While both active and nonactive periods feature moisture convergence in the lower levels, moisture convergence is more pronounced and extended higher into the atmosphere to near 3.5 km (11,480 ft) on convectively active days, as opposed to near 2.8 km (9,184 ft) for nonactive periods. Also, moisture divergence is much more pronounced from 3.5 km (11,480 ft) to 6.7 km (21,976 ft) on active days than on nonactive days.

Pronounced vertical changes in moisture divergence from the surface through 7.5 km (24,500 ft) on convectively active days, coupled with the fact that moisture divergence varies little above 3.5 km (11,480 ft) on convectively nonactive days, indicate that while the atmosphere is quite active kinematically during convectively active periods, relatively little kinematic interaction takes place on nonactive days.

Of particular note are the relatively minor fluctuations in vertical motion from convectively nonactive periods to convectively active periods. Upward vertical motion was observed through all layers on convectively active days, but the same motion was observed below 15.7 km (51,496 ft) on convectively nonactive days as well. However, upward vertical motion was slightly larger throughout most layers on the active days, and was significantly greater above 7.5 km (24,600 ft) than during the convectively nonactive periods.

During each year analyzed (1976, 1977 and 1978), moisture convergence occurred deeper in the lower levels, while divergence was much more pronounced at mid-levels during convective periods. Also, it was shown that the vertical changes in moisture divergence above 3.5 km (11,480 ft), which proved to be small on nonconvective days, were highly variant during convective periods. Finally, the hypothesis regarding a significant increase in vertical motion in the upper levels on convective days was confirmed.

Even though the number of days considered during each of the three seasons was smaller than desired, it may be concluded preliminarily that

the horizontal moisture convergence below 3 km (less than 10,000 feet), and the vertical transport of moisture from the lower to the mid- and high levels of the atmosphere, are the principal energy sources for convective activity in the Texas HIPLEX region. Therefore, one seeding criterion for selecting a seeding condition may be the presence of low level moisture.

Table 3.12 shows a comparison of various convective activities to each water budget term. The horizontal and vertical water vapor terms (terms 2 and 3 in Equation 5) represent moisture divergence , negative terms indicate an increase in water vapor, i.e. convergence, resulting from flow through respective horizontal or vertical surfaces. The horizontal surface is the Post, Robert Lee, and Midland triangular area. The vertical surfaces are the 50 mb increment walls of the triangle.

Table 3.12—Inter- and Intra-Comparisons of Terms Summed Using Each 50-mb Layer, From 850 mb to 300 mb, Over the Post, Robert Lee, and Midland Triangular Area in the Water Vapor Budget Models

| Model | Stratification | Water vapor budget terms ($\times 10^8$g s^{-1}) | | | |
		Net horizontal transport	Net vertical transport	Local rate-of change	Residual
Presence	Nonconvective	- 3.02	2.38	5.05	4.41
	Convective	-26.70	- 9.57	-0.57	-36.84
Type	Lines of cell	-17.31	-19.24	2.17	-34.38
	Clusters of cells	-52.54	- 9.53	-0.37	-62.44
	Isolated cells	- 1.16	- 1.88	-4.36	- 7.40
Depth	Cell tops less than 6.1 km	-21.60	4.95	-2.45	-19.10
	Cell tops between 6.1 and 9.1 km	-32.40	-14.50	0.35	-46.55
	Cell tops greater 9.1 km	-30.70	-31.20	2.16	-59.74
Areal Coverage	Less than 50%	3.72	- 1.09	-1.87	.76
	Greater than or equal to 50%	-62.27	-21.04	0.94	-82.37

For each model and intra-model stratification, a strong net gain of water vapor transported by the horizontal components of the wind was

observed, with the exception of days when no convection was observed, days when isolated cells were observed, and days when areal coverage was less than 50 percent. The greatest horizontal transport of water vapor occurred on days when the areal coverage was greater than or equal to 50 percent, on days when cell tops were greater than 6.1 km (20,008 ft), and on days when convective clusters were observed, suggesting the need for increased water vapor flux to support increased convection.

Looking only at the vertical components of the wind, the largest values of net vertical transport of water vapor were observed on convective days with tops greater than 9.1 km (29,848 ft), and on days when the areal coverage was greater than or equal to 50 percent. This suggests the need of mid- and low-level moisture for large-scale cumulus development.

An intercomparison of net horizontal and vertical water vapor transport indicates that less water vapor was transported vertically than horizontally, except for the taller convective entities. This observation supports the concept that the height of a convective cell is the result of the amount of water vapor transported vertically from the low levels. During most cases, the net horizontal transport of water vapor was found to be 2 to 3 times greater than the vertical transport.

The local rate-of-change term quantifies the net gain or loss of water vapor within the volume. The net gain of water vapor on days with lines of cells, cell tops greater than 6.1 km (20,000 ft), and areal coverage greater than or equal to 50 percent, was attributed to water vapor "storage" which was needed to maintain developed wide-spread convection.

The residual term is a source (positive term) or sink (negative term) of water vapor resulting from evaporation or condensation of cloud droplets or precipitation drops. The greatest negative values of the residual term are observed for cases with an areal coverage greater than or equal to 50 percent, cell tops greater than 9.1 km (29,848 ft), and when clusters are observed. This appears reasonable because one would expect the greatest amount of condensation and rainfall to occur from widespread and deep convection.

Generally speaking, a strong positive relationship is shown between the occurrence of water-vapor transport above about 3.5 km (11,480 ft) and the presence of convection. Similarly, its absence corresponds with non-convective situations. Water vapor transport varies among the types of activity, however, being most pronounced and organized with lines of convection, less so with clusters, and rather disorganized in association with isolated cells.

Both depth and areal extent of convective activity correspond well with water vapor transport. Both the amount of low-level transport near the surface and the degree of vertical transport aloft correlate well with increasing depth of convection. Too, horizontal outflow in the upper air is

shown to compliment the low-level inflow and upward motion. The greatest amount of water vapor is processed by increased depth and coverage of activity, with the type and organization of the convection of lesser importance.

The analyses indicate that the net horizontal transport of water vapor is by far the most significant factor in providing moisture to support convection. Also, the water vapor transport, an important energy source for convective development, occurs near the surface, and the net horizontal transport term appears to be the dominant energy transport term.

Ulanski and Garstang (1979) relate moisture convergence fields with convective rainfall over Florida. Observations recorded from a surface meteorological meso β-scale network document the importance of the cloud-subcloud layer interactions in understanding better the variability of natural rainfall from convective cloud systems. They concluded that surface moisture convergence, observed up to 90 minutes before the rainfall event, is one of the most crucial factors in determining the total amount of rainfall produced by a given convective system. Both the area and magnitude of low level moisture convergence are proportional to measured rainfall amounts. An examination of Table 3.12 also shows a strong relationship between strong horizontal moisture convergence (negative terms) and large negative residual terms (which indicates precipitation).

Initial mesoscale analyses have been completed for each day on which significant (radar echoes) convective activity occurred during the field programs of 1976, 1977 and 1978. However, there remains much analysis to be done. For example, mesoscale models for various classifications of convective activity have not been developed, and interactions between mesoscale processes, precipitation, and cloud physics have not been addressed in a suitable manner. During the five years covered by this summary report, the primary emphasis was placed on field programs, rather than analysis of data. While achievements were made within the constraints of resources and equipment, much remains to be done in the analysis area. Relationships between mesoscale processes and rainfall, as well as many other topics, will be addressed when funds and time permit.

Comments: It is important to assess the value of experimentation at the mesoscale to the overall HIPLEX effort for Texas. While significant steps must be taken to acquire a knowledge of cloud microphysics, the importance of mesoscale convective interactions and their relationship to the near-cloud environment must be comprehended prior to developing a sophisticated and effective precipitation-augmentation seeding hypothesis. Furthermore, these studies have shown the necessity of acquiring atmospheric data on a scale much smaller than that commonly available for determining specific patterns of temperature and moisture with sufficient accuracy and detail to test a working microphysical or dynamic seeding hypothesis.

3.4 Microscale

3.4.1 Radar Structure

An examination of the internal structure of convective clouds which form in the Texas HIPLEX region was made by Haragan *et al.* (1980) in the report, entitled *Determination of Cloud and Precipitation Characteristics From Satellite, Radar and Raingage Analysis*. The particular system selected for the case study was a non-squall mesoscale convective system associated with a cold front. This system was less intense and less organized than a squall-line system, and was more representative of systems that produce the major summer precipitation events in this semi-arid region of Texas.

A mesoscale precipitating anvil cloud located within the Texas HIPLEX area was selected for the case study. This system existed in the HIPLEX region for about eight hours during the afternoon on July 8, 1977. The convective system was situated behind a southeastward-moving cold front. The wind field at the surface was southeasterly ahead of the front, and northeasterly behind the front. A southwesterly wind field prevailed in the upper-air behind the convective system.

The cloud structure of the selected precipitating anvil is illustrated in Figure 3.24. This represents a side view of the anvil's internal structure which is contoured by varying degrees of radar echo intensities (25, 30, 35 dBz) of precipitation cloud particles. The orientation of the extended anvil top is towards the north.

The figure illustrates low-level precipitation observed by radar at 1604 CDT (2104 GMT), about midway through the system's life cycle. The anvil of precipitation particles aloft extends to the rear of the precipitation feature located at ground level. A horizontal bright band of high reflectivity (35 dBz) is located below the 0°C isotherm (at 3.7 km [12,100 ft], above the 16-mile marker). The thermodynamic structure of the anvil cloud, suggested by atmospheric analysis charts, indicated mesoscale subsidence below 600 mb with a divergent wind field at the surface, convergence at the 700 mb level, and divergence near 250 mb. These thermodynamic characteristics are in agreement with Scoggins *et al.*, 1978 and 1979.

These cloud scale dynamic features are similar to those reported by Houze (1977) and Leary (1979), implying that methods currently developed to compute vertical transports of mass and heat in tropical cloud clusters using digitized radar data may be applicable to intense convective systems which develop within the Texas HIPLEX area.

3.4.2 Cloud Physics

Acquiring an understanding of the natural precipitation mechanism predominant in convective clouds over the southern High Plains is an essential step prior to developing and testing any precipitation-augmentation hypotheses. Two microphysical studies of Texas HIPLEX convective clouds were performed to better
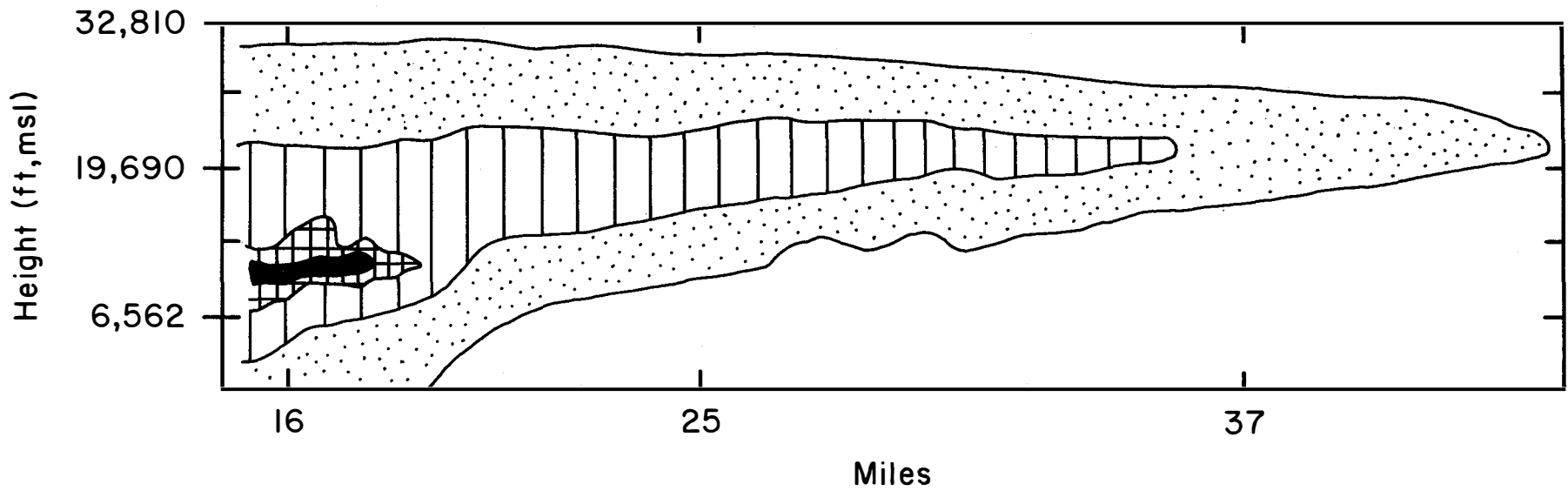
Figure 3.24. Cloud structure of a precipitating anvil illustrated by analysis of digitized M-33 radar data, July 8, 1977, 1604 hours local time.

understand the natural precipitation processes and the effects cloud seeding may have on these processes.

One study was performed at Texas A&M University in 1979-1980. This study centered on data collected by two Texas HIPLEX research aircraft during the 1979 Texas HIPLEX field season (May 21 - July 20). Data pertaining to the thermodynamic, kinematic, and microphysical aspects of growing cumulus clouds were collected on magnetic tape. Subsequently, the raw data were processed using appropriate computer programs. Those processed data are the basis for the analysis performed by Long (1980) in the report, entitled *Preliminary Cloud Microphysics Studies for Texas HIPLEX 1979*.

The second study was performed by Takeuchi (1980) of Meteorology Research, Inc. The analyses were primarily concerned with data collected during the 1978 and 1979 Texas HIPLEX field seasons.

The aircraft and cloud physics data equipment used in both studies are described in Section 2.5. The reader should be aware of the cloud selection process. While the initial selection of the sample clouds was very subjective, following the initial pass made by the p-Navaho at the -10°C level, a much more quantitative assessment of the clouds' characteristics was made, based on rules developed at the beginning of the field program to provide guidelines for cloud selection. A list of criteria that each sample cloud must meet is shown in Table 3.13.

Table 3.13—Cloud Selection Criteria for 1979 Texas HIPLEX Missions

1. Cloud top no colder than about -10°C.

2. No precipitation size particles.

3. Peak ice particle concentration no higher than $10 \, \ell^{-1}$ at -10°C.

4. Cloud liquid water content of at least $1 \, g \, m^{-3}$ somewhere on the initial pass.

5. Updrafts of at least $2.5 \, m \, s^{-1}$ ($500 \, ft \, min^{-1}$).

Sampling by the MRI aircraft consisted of cloud penetrations at the -5°C to -8°C levels, while the District p-Navaho aircraft made cloud penetrations at the -10°C level. Sampling would continue throughout most of the cloud's life cycle or until cloud conditions became too severe.

3.4.2.1 The Microphysical Process

An excellent review of the cloud microphysical processes, likely to occur in Texas HIPLEX convective clouds, was provided in Long (1980). Because of the qualitative nature of the discussion and the fact that it may

be of value to anyone not familiar with cloud microphysical studies, it is repeated below:

"The microphysical processes are laid out in Figure 3.25. The diagram is similar to one developed by Braham and Squires (1974); however, the present diagram differs in two respects. First, it includes recently acquired knowledge of cloud microphysical processes. Second, it focuses only on those processes likely to occur in the Big Spring, Texas, area in the summertime. Represented in Figure 3.25 are the Bergeron-Findeisen (ice) process, the warm-rain (coalescence) process, and the more recently discovered process of ice multiplication. The items in upper case and/or underlined represent water substance in various forms, condensation nuclei, or ice nuclei. The items in lower case are processes whereby water substance is changed from one form to another. For example, if graupel melts it becomes cold rain. The arrows show the direction of a transformation or else show where particles of a given type come into a process.

"The transformation of water substance to rain by the ice process is represented on this diagram by three different routes. Water vapor and condensation nuclei with either a continental or maritime particle size spectrum enter a cloud through its base, and by nucleation and condensation are transformed into a narrow or a broad spectrum of cloud droplets. As the droplets rise upward through the cloud they may eventually reach temperatures cold enough for a number of contact and/or immersion ice nuclei to be activated. The nuclei lead to heterogeneous freezing of some of the droplets. The frozen droplets then increase in size by diffusional growth from vapor. Simultaneously, other ice nuclei may act as deposition nuclei which help ice crystals to develop directly from the vapor. These ice crystals will increase in size by diffusional growth from the vapor.

"Regardless which of the three processes for producing ice particles is dominant, some particles develop in a cloud when the temperature becomes cold enough for ice nuclei to be activated. This may not happen at a temperature as cold as -10°C, but often happens once the cloud top has reached a temperature of -15°C, and almost always happens by -20°C. Once frozen droplets and/or ice crystals have diffusionally grown to sufficient sizes they may then collect some of the original cloud droplets by riming. Riming will eventually lead to the development of graupel. Graupel can grow further by riming. Once graupel falls below the 0°C level it will melt and become rain. It is called "cold" rain because it originates through the ice phase.

"The ice process was rather widely accepted for many years as the only mechanism by which precipitation could be produced. The alternative process of coalescence was believed to be too slow to be

CONTINENTAL
CONDENSATION NUCLEI
LESS WATER VAPOR

ICE NUCLEI
WATER VAPOR

MARITIME
CONDENSATION NUCLEI
MORE WATER VAPOR

nucleation
condensation

nucleation
deposition

nucleation
condensation

NARROW CLOUD SPECTRA

ICE CRYSTALS

BROAD CLOUD SPECTRA

slow broadening
by coalescence

heterogeneous
freezing

heterogeneous
freezing

rapid broadening
by coalescence

FROZEN
DROPLETS

diffusional
growth

FROZEN
DROPLETS

FROZEN
DROPS

continued
coalescence

riming

continued
coalescence

GRAUPEL

SECONDARY
ICE PARTICLES

riming

WARM RAIN

melting

WARM RAIN

COLD RAIN

Figure 3.25. Flow diagram of the major types of cloud and precipi-
tation elements and of the physical processes
through which they originate, grow, and interact.

effective. The calculation made of the rate at which coalescence leads to precipitation were predicted, however, on a rather narrow cloud spectrum. The route to precipitation shown in the left side of Figure 3.25 was assumed, and "warm" rain was indeed unlikely to occur.

"It is now accepted that warm rain can, in fact, occur. The primary requisite is that there be a broad spectrum of cloud droplets. This spectrum most commonly exists if the distribution of condensation nuclei is "maritime", but a droplet spectrum with a fair number of large droplets may also develop from a more "continental" nucleus spectrum if there is a high water-vapor concentration. It is to allow for this latter possibility that the words "more water vapor" and "less water vapor" have been included near the top of Figure 3.25. Regardless how an initially broad spectrum of cloud droplets is produced, the important point is that from such a spectrum coalescence by itself can produce rain.

"It is important to note that if there is a broad cloud droplet spectrum the frozen droplets that develop from heterogeneous freezing will tend to be larger than if there is a narrow spectrum. Less diffusional growth will be required of these larger droplets before they can grow by riming. The implication is that the Bergeron-Findeisen or ice process may be accelerated if the cloud droplet spectrum is broader and more maritime in character.

"In recent years it has become apparent that some clouds, particularly those with broader cloud spectra, contain what are called *secondary* ice particles (see Figure 3.25). These are called secondary particles because their concentrations, of $1\ell^{-1}$ or greater at temperatures of -3°C to -8°C where they are prevalent, are about 1,000 times greater than the average concentration of ice nuclei active at these warm temperatures. The particles apparently are produced by some process other than primary ice nucleation. Considerable effort has been expended in defining the conditions under which secondary ice particles are produced. The evidence suggests the particles are produced when droplets larger than 25 μm diameter in concentrations greater than 10 cm^{-3} collide with graupel particles already present at temperatures of -3°C to -8°C. Although secondary particles are small initially, they can grow diffusionally from the vapor (see Figure 3.25) and then by riming and lead to more graupel particles. Some of the secondary particles may contact and cause to freeze some of those drops already present in the cloud of sizes large enough immediately to become rimers. Calculations have shown this latter process of graupel reproduction is faster than the process involving diffusional growth of the secondary particles. In either case there is a positive feedback process whereby graupel are rapidly reproduced or "multiplied" in a cloud. Ice multiplication

may accelerate the development of significant concentrations of graupel, and it may accelerate the production of rain.

"As stated, a minimum concentration of droplets larger than 25 μm must be present for ice multiplication to occur. Such a concentration will more likely exist if there is a broad cloud droplet spectrum. It is for this reason that the possibility of secondary ice particles is included only in the right side of Figure 3.25.

"The first task of the cloud microphysics studies is to establish which of the several precipitation processes shown in Figure 3.25 and just described operated in convective clouds in the Texas HIPLEX study region. Is the ice process necessary for precipitation in significant amounts, or will the warm rain process suffice? If the ice process turns out to be necessary, are broad spectra of frozen droplets, developed in part by coalescence, often present to accelerate the ice process? Does ice multiplication occur frequently, and what is its effect on the production of rain?

"Any study of precipitation processes that is based on field work, fundamentally, is a study of the end products of the precipitation processes, namely, the cloud and precipitation particles themselves. From knowledge gained about the particles, inferences about the processes are drawn. Precipitation processes act to increase the overall size of condensed particles of water substance and the number of such particles. The precipitation processes may involve either liquid or solid particles, and the solid particles may have a structure (e.g., shape in the case of ice crystals and density in the case of graupel) that is important for the rate at which precipitation is produced. It was the intention of the TAMU cloud microphysics studies to examine the size, number (or concentration), phase, and structure of condensed particles within a cloud.

"Cloud microphysics studies have two basic limitations, even though these studies can provide information on dominant precipitation mechanisms and can lead to precipitation augmentation hypotheses that are capable of being tested. First, cloud microphysics studies are based on a limited sample of data. Ideally, the studies should be based on data on every particle in the cloud, and data should be available at all times. This ideal data sample is not available in practice and probably never will be. Instead, particle information is available only along a few filamentary paths through the cloud, usually spaced several minutes apart in time and usually not successively placed in the same part of the cloud. Data are also limited on particle structure, and the 3-dimensional aspects of particle shape are also of limited quality.

"A second basic limitation of cloud microphysics studies is the lack of emphasis they usually place on the dynamic environment within

the cloud in which the microphysics data are collected. (Information on the larger, mesoscale environment has been and is being collected in Texas HIPLEX and has important uses.) Information on the motions within a cloud is needed to establish, among other things, the dynamic support the cloud gives to particles while they grow and the expected lifetime of the cloud as turbulent entity. Information on motions could aid in determining whether those natural microphysical processes, which may have been established to be the only ones of potential importance for precipitation, in fact, proceed at a rate fast enough for precipitation likely to occur.

"Despite the two basic limitations of cloud microphysics studies just discussed, these studies can still provide much of the fundamental information needed on dominant precipitation processes.

"Cloud microphysics (particle) data are more useful for deducing precipitation processes if they are collected at certain times during the life of a cloud and at certain positions within a cloud. General data collection guidelines have been established for Texas HIPLEX as follows. Data should be collected early in the life of a cloud, when only droplets are present and before precipitation has begun to form, and data should be collected as particles pass through the transient stage between cloud droplet sizes (diameter in 10's of micrometers) and precipitation sizes (diameter in 1,000's of micrometers); and finally data should be collected when preciptation has developed. Data should be collected aloft within a cloud, at levels colder than 0°C but warmer than about -15°C. In the Texas HIPLEX those clouds are of marginal interest which never rise above the 0°C level. The types of data to be collected at each stage in the life of the cloud are now described in more detail. Examples are given of the deductions to be made from the data.

"Data collected early in the lifetime of a cloud, before precipitation has begun to form, include the liquid water content and concentration of cloud droplets, and the distribution (spectrum) of droplet diameters. The cloud droplet size distribution is useful in assessing the importance of the warm rain (coalescence) process in a particular cloud in 1) producing droplets which may eventually act as precipitation embryos, in 2) accelerating the ice process, as described earlier, and in 3) providing the droplets necessary for the ice multiplication process. It is noted that the rate at which large droplets are being produced by the coalescence process is better estimated if droplet size distributions are available both from aloft within a cloud and from cloud base. A parameter also of importance early in the lifetime of the cloud is the amount of spatial distribution of liquid water in cloud droplets. Cloud liquid water content is especially important from an operational point of view because it serves as the source of condensed water from which precipitation ulti-

mately has to form. An operational decision to study a cloud further will be based in part on the liquid water in cloud droplets."

The primary objective of both studies was to better understand the important precipitation mechanism of the Texas HIPLEX convective clouds. The precipitation mechanisms investigated included the warm rain or coalescence process, the ice phase process, ice multiplication, and recycling of large precipitation-size particles.

By studying the end products of precipitation processes—which are the precipitation particles themselves—an understanding of other processes that produced the particles may be realized. The intention of both studies was to study the precipitation particles by examining the size, concentration, phase, and structure of condensed particles within the sampled clouds.

These analyses must only be considered as preliminary, due to the limited number of cloud samples and the limited time and manpower available for analyses. Other limitations include the relatively small sampling cross section when compared to the size of cloud. The assumption which must be made is that the microphysical processes measured in the sampling cross section are representative of the microphysical processes throughout the cloud. A second limitation of these studies is that they do not include the effects of the mesoscale processes outside the cloud. However, in spite of the limitations imposed on these studies, the findings are of value in helping to establish the Texas HIPLEX seeding hypothesis.

3.4.2.2 Results

In the Long (1980) study, the findings were based on clouds examined during the 1979 field season. The sampled clouds were either isolated growing clouds or convective clusters. Table 3.14 lists the clouds sampled. Aircraft sampling penetrations generally occurred near -5°C through most of the cloud's life cycle.

Table 3.15 summarizes the clouds sampled by tabulating the answers to two questions: Did ice develop in the sampled cloud? Did precipitation develop in the sampled cloud? Texas HIPLEX Mission 6 sampled three clouds, and each of the other missions sampled one cloud.

Preliminary, albeit qualitative, results from the Long study address the question of the necessity for ice development in the West Texas convective precipitation process, and the importance of ice multiplication in these types of clouds. Briefly, results suggest that the ice process is associated with significant amounts of precipitation, although precipitation is indicated to result from the warm rain (coalescence) process as well. Significant amounts of water, in quantities several orders of magnitude greater than water produced by the warm rain process, are indicated to have

precipitated from clouds which underwent the ice process. Furthermore, clouds undergoing the ice process were both of longer duration and larger spatial extent than warm rain process clouds. These results support the findings of Smith *et al.* (1974) on convective clouds in the San Angelo, Texas, area.

Table 3.14—Types of Clouds Selected in 1979 HIPLEX Missions

HIPLEX	Date	Type of cloud treated
1	4 June (1)*	Growing turret, associated with a convective complex
2	4 June (2)	Isolated growing cumulus congestus
3	25 June	Turret growing from altocumulus
4	3 July (1)	One turret in a cluster of short-lived turrets
5	3 July (2)	Isolated growing cumulus congestus
6	5 July (1)	Growing turret, associated with a convective complex
7	5 July (2)	Turret growing from altocumulus
8	8 July	Growing turret, associated with a convective complex
9	15 July	Isolated growing cumulus congestus

* Parenthetical number denotes whether the mission is the first (1) or second (2) on this date.

Takeuchi (1980) analyzed cloud microphysics data, collected during the 1978 and 1979 Texas HIPLEX field seasons. One of the objectives of the analysis effort was to determine the dominant precipitation mechanisms of growing isolated convective cells or turrets of convective clusters. The procedure to accomplish this objective was to analyze time history plots of vertical velocity, liquid water content, ice particle concentrations, reflectivity values and turbulence recordings. These data were measured from nine clouds during the 1978 field season, and from three clouds during the 1979 season. Plots of the clouds' particle mass density (Q_D) versus the cloud particle diameters, ranging from about 3 μm to 4500 μm and measured within the clouds updraft regions, were plotted as a function of time and were also studied. This spectrum is referred to by Takeuchi (1980) as the G-function.

The G-function identifies the diameter ranges of the cloud particles which account for the greatest portion of a cloud's rising particle mass relative to the total mass of the cloud. Two additional and oppositely skewed axes relative to the Q_D axis are included to provide size distribution information related to number density (N_D) and to radar reflectivity factor (Z_D). The analyses revealed a bi-modal distribution (Figure 3.26 for t=0) of the rising particles in the updraft regions. This signature is characteristic of the coalescence process and implies that the warm rain process initiates pre-

Table 3.15—Development of and Total Precipitation for Clouds Sampled and Treated in 1979 HIPLEX Missions

HIPLEX mission number	Date	Did ice develop?	Did precipitation develop?	Total precipitation (kton)
1	4 June (1)	No	Yes	0.7
2	4 June (2)	No, small amount was present initially but decreased	No, not in time of observations	0
3	25 June	N/A*	N/A*	N/A*
4	3 July (1)	??	Yes	0.8
5	3 July (2)	Yes	Yes, and increased with time	210
6	5 July (1)	N/A*	N/A*	N/A*
7	5 July (2)	Yes, but ice was present initially	Yes, and increased with time	1,100
8	8 July (1)	Yes, and ice also increased in spatial extent, but ice was present initially	Yes, but precipitation was present initially	3,000
9	15 July	No	Yes	25

*Only P-Navaho data collected; data not available for analysis.
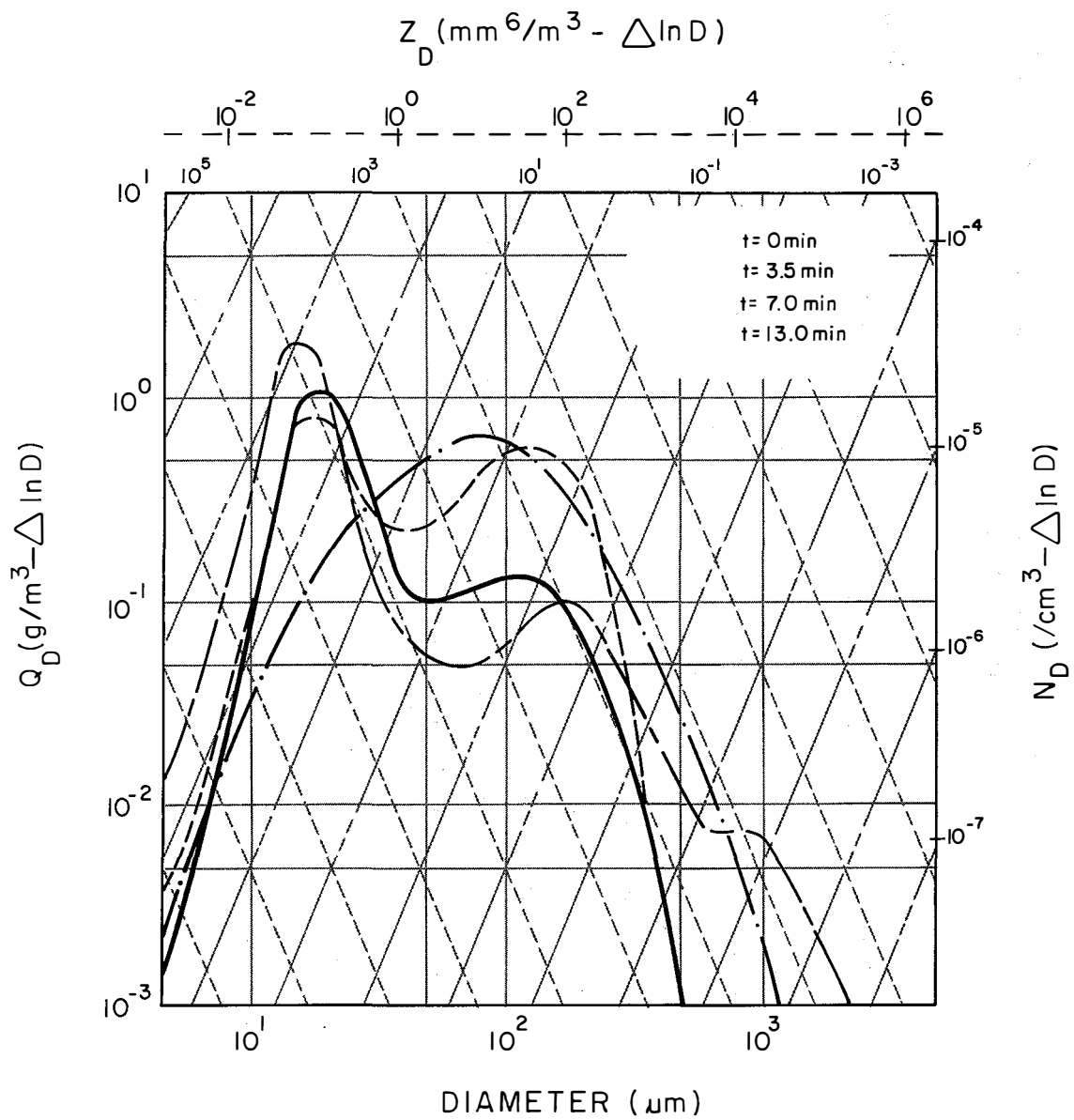
Figure 3.26. The evolution of the G function of rising particles in an isolated small cloud of 20 July 1978.

cipitation in Texas HIPLEX convective clouds, at least during the earlier stages of cloud development. These characteristics were also evident in the San Angelo, Texas, summertime convective clouds (Smith *et al.*, 1974).

Concerning the ice processes, the ice multiplication process was evidenced in regions observed to have extensive ice phase precipitation development in the form of graupel. The observed graupel was believed to be the result of freezing rain drops and not a result of the Bergeron process, suggesting that the ice multiplication process may be active. Also, supercooled cloud droplets were observed with diameters greater than 24 μm, and in concentrations of about 10 cm^{-3}, again suggestive of the Mossop (1978) ice multiplication process. The ice-phase process appeared to dominate most clouds during the mature and late cloud stages. Ice particle concentrations were reported to be between 10 to 100 ℓ^{-1}. Major precipitation development appeared to be associated with graupel formation during the mid and later stages of the clouds' life cycle.

Recycling of up to 50 percent of the total number density of the precipitation size particles (solid and/or liquid) was observed in the updrafts of the larger clouds, rendering them more efficient in producing rainfall. Often in the larger clouds the G-function was tri-modal (Figure 3.27), indicating the presence of large rising particles (1 to 3 mm) which increases the productivity of the coalescence process.

Takeuchi concludes that:

> "Due primarily to the relatively efficient precipitation growth process of the larger clouds, it is implied that unless seeding can result in significant dynamic effects, a greater potential for ice-phase seeding lies in the treatment of the smaller clouds at a time prior to major precipitation development. Also, ice-phase seeding to initiate early precipitation development appears less favorable than in the Miles City clouds due to the presence of the active coalescence process during the early stages of cloud development. Hence, ice-phase seeding to cause dynamic changes to the smaller clouds is also inferred.

> "Table 3.16 presents some average properties of the updraft (>2 m s^{-1}) regions observed at about the -5 to -8°C cloud levels of the data set for use in evaluating seeding potential. Aside from the updraft properties observed during the initial cloud penetrations, the table presents estimates of the duration of the seeding window as determined by the shorter of the time periods to either cloud dissipation (LWC $\leq$ 0.2 g m^{-3}) or cloud glaciation (IPC $\geq$ 10 ℓ^{-1}). Based on the adequate ($\sim$1 g m^{-3}) LWC and the low (< $\sim$1 ℓ^{-1}) IPC found during the early stages of cloud development and on the sufficient times shown for subsequent precipitation development, it is indicated that the ice-phase growth process can be significantly altered by seed-
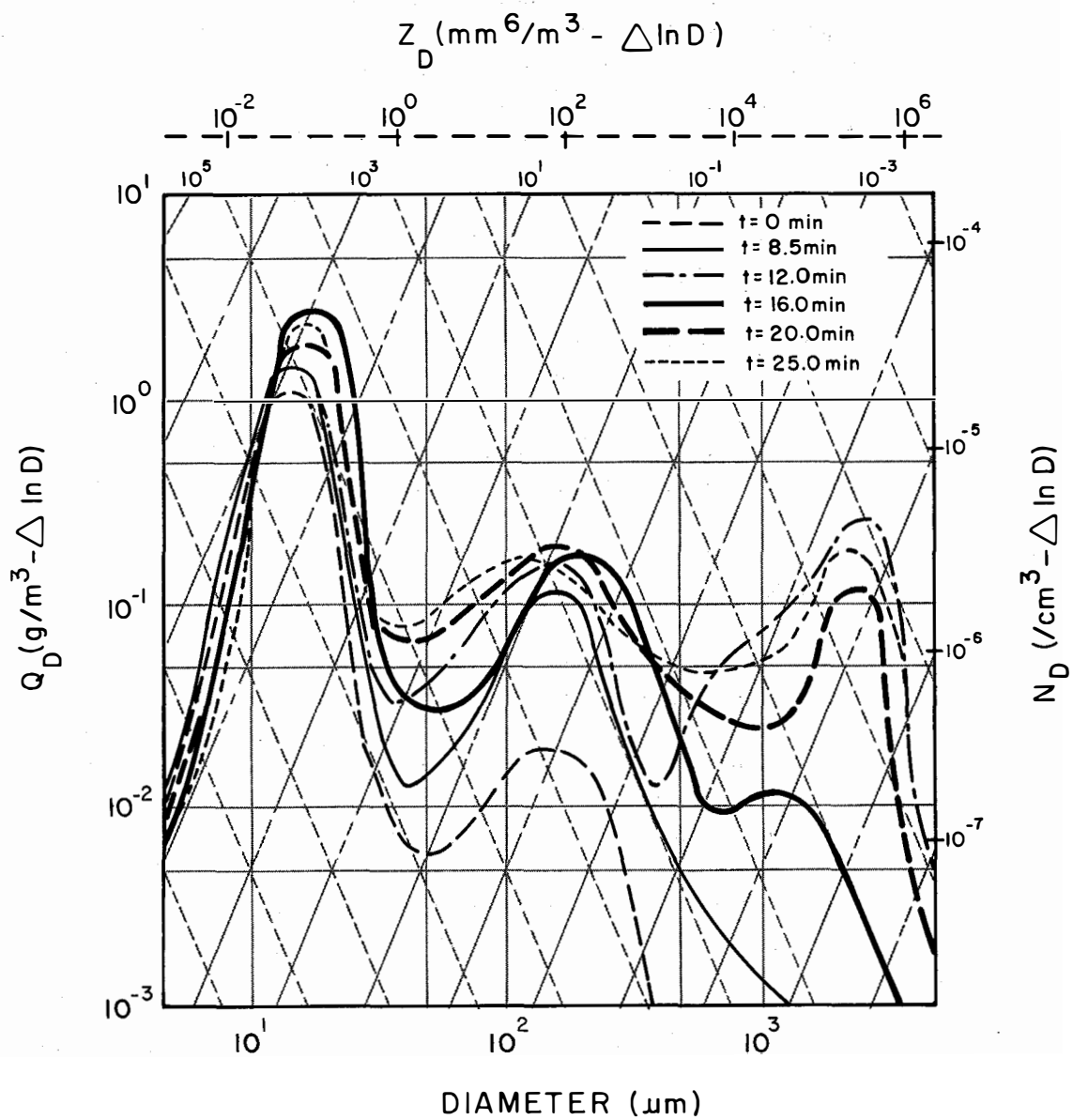
Figure 3.27. The evolution of the G function of rising particles in the large cloud complex of 3 July 1978.

ing. It is also noted that due to the relatively short seeding window, on–top seeding, as opposed to cloud-base seeding, is indicated to perhaps lead to more definitive results."

Table 3.16—First Pass Cloud Statistics in Updrafts - 12 Clouds, Texas

	Mean	Standard deviation
Updraft distance	2.0 km (6,560 ft)	0.7 km (2,296 ft)
Fraction of cloud	0.48	0.22
Updraft velocity	6.0 m s^{-1} (19.7 ft s^{-1})	3.0 m s^{-1} (9.9 ft s^{-1})
Liquid water content	1.1 g m^{-3}	0.3 g m^{-3}
Ice particle concentration	0.7 ℓ^{-1}	1.3 ℓ^{-1}
Embryo concentration	5.0 ℓ^{-1}	4.8 ℓ^{-1}
Big droplet (d$\geq$24 μm) concentration	14 cm^{-3}	14 cm^{-3}
Seeding window	13 min	6 min

3.4.3 A Massive-Seeded Case Study

Humbert *et al.*, 1979, reports that on July 3, 1978, a Texas HIPLEX isolated growing cumulus was seeded at the -10°C level with 960 g of silver iodide. Seeding was performed by injecting 30 g flares into the cloud top at a rate of 1 flare per second (Riggio and Alexander, 1978).

Time-height radar data showed multiple surges of maximum reflectivity and echo-top heights. These multiple surges could indicate that the cloud was going through cycles of precipitation development consistent with the Byers and Braham (1949) multicelled thunderstorm model.

The coalescence process initiated the precipitation development, and the ice process was just beginning to dominate when the cloud was seeded. Large droplets (d$\geq$750 μm) were present at the seeding level, and liquid water was relatively large, reaching a maximum value of 2 g m^{-3} . The cloud was seeded shortly after the second surge. It was noted that the third surge and the most intense surge recorded had a secondary surge associated with it. The timing of the secondary surge coincided with the arrival of seeded air parcels at cloud top. The secondary surge, which was observed in the upper portion of the cloud after seeding, is consistent with a dynamic seeding effect. The study concludes that hygroscopic seeding of the cloud would have been ineffective due to the 1 to 10 per liter concentrations of natural recycled large droplets. However, the presence of large numbers of supercooled droplets, along with the lack of ice in the updrafts, suggests ice-phase seeding as having the greatest potential to effect the precipitation process.

After the cloud was seeded, a shift in the mass mode of the precipitation spectrum to smaller sizes was observed. It can be argued that these types of results are nonbeneficial to the precipitation process because it would reduce the effects of the coalescence process. Conversely, such results may be beneficial by increasing cloud efficiency. Houghton (1968) hypothesized that natural scavenging of cloud drops by precipitation particles is incomplete in convective clouds. Therefore, precipitation may be increased by introducing additional precipitation particles early in the cloud's lifetime to increase the effectiveness of the scavenging process.

3.5 Forecast Development

In support of the Texas HIPLEX field program, atmospheric and cloud parameters were measured at intervals during each operational day of the field season by a network of surface weather stations, rawinsonde units, cloud physics aircraft, radar, and satellite. Funding shortages limited the number of days on which operations were fully implemented. Therefore, during the late morning of each day of the summer field studies, the Project Director declared the day either operational or nonoperational. This decision was based on weather forecasts issued from early morning data. Associated with an incorrect decision was a cost factor, resulting either from gearing up operations when no potentially shower-producing clouds developed or from a failure to operate when such clouds did develop, thereby extending the duration of the field studies. Since National Weather Service (NWS) forecast products were not designed for use in fine-scale research programs, localized forecast procedures were developed to aid the Project Director in making the decision about operational status.

3.5.1 Forecast Decision Tree

After the two field programs of 1976 and 1977, it was determined that the implementation of a logical, stepwise, objective forecast methodology was required to assess as precisely as possible the aniticipated meteorological conditions for each day during the field season in support of operations. In response to this need, data derived from each day of the 1976 and 1977 field seasons were compiled and analyzed statistically to devise the Texas HIPLEX Forecast Decision Tree (FDT). The FDT is described by Alexander and Riggio (1978) in the report, entitled *A Texas HIPLEX Forecast Decision Tree.*

The FDT is designed to prestratify each forecast day into a classification system called the Convective Index (CI). The CI is a modified version of the Hartzell Single Stratification Scale (Hartzell, 1977), and consists of nine categories of convective activity ranging from "1" for clear or cirrus clouds, to "9" for wide-spread precipitation with embedded cumulonimbus. The CI is shown in Table 3.17. Radar data and surface weather observations from the 1976 and 1977 field seasons were used to arrive at a post-stratified CI for each day during those seasons. Various meteoro-

logical paratmeters from each of the forecast days were then cross-correlated with the post-stratified CI to determine predictor variables.

A first-generation FDT was developed which featured the presence of a recognizable synoptic or sub-synoptic forcing mechanism (such as a front, trough, dryline or upper air disturbance) as the principal and dominant determinant of convectively active and nonactive days. Secondarily, air-mass temperature/moisture analysis was used to determine relative precipitation intensity on forcing days, and the likelihood of deep convection on nonforcing days.

3.5.1.1 Initial Stratification and Findings

The FTD study revealed that in most cases the presence of a forcing function is required for convective activity.

The temperature/moisture analysis was based on upper air data extracted from the morning (1200 GMT) Midland National Weather Service sounding. The temperature value (N_{AT}) is a measure of the relative warmth of the airmass from near the surface through 500 mb, as compared to the mean 1976-1977 field season values for Midland. The moisture (N_{PW}) value is a measure of the cumulative precipitable water from near the surface through 500 mb. Both values were normalized and made dimensionless for ease of interpretation.

Table 3.17—Class Definitions of the Convective Index*

Class no.	Definition
1	Clear or cirrus and nonprecipitating mid-level altocumulus or altostratus
2	Mid-level clouds with virga or RW-; no low-level clouds
3	Nonprecipitating, low-level convective clouds (i.e., stratocumulus to small congestus)
4	Towering cumulus with virga, but no rain reaching ground
5	Towering cumulus with light rainshowers which developed within the operational area either randomly or in lines; no cumulonimbus observed
6	Similar to 5, with cumulonimbus and thunderstorms which developed within operational area in addition to towering cumulus
7	Mesoscale cumulonimbus system which developed W-SW of operation area due to upslope and/or dry line-sfc trough, and moved across operational area as line of thunderstorms or rainshowers

*Modified for West Texas HIPLEX Operational Area from Hartzell, 1977.

Table 3.17—Class Definitions of the Convective Index—Continued

Class no.	Definition
8	Mesoscale cumulonimbus system developed along synoptic feature (i.e., front or short wave aloft), and moved across operational area as line of thunderstorms or rainshowers
9	Widespread precipitation from overcast nimbostratus with embedded cumulonimbus

A grid was then established, using these data. The grid featured temperature as the ordinate and moisture as the abscissa. The results for each forecast day were plotted as points on the grid, annotated by that day's post-stratified CI.

The temperature/moisture grid scheme was given in quadrants, each quadrant describing a definite type of airmass. The grid is shown in Figure 3.28. The 1976-1977 statistics for nonforcing days indicated that Quadrants I and IV corresponded to convective activity, while Quadrants II and III corresponded to convectively inactive days. However, of the 77 convectively active days with forcing, 46 fell into Quadrants I and IV, while 31 were in Quadrants II and III. Those convectively active forcing days which fell into Quadrants I and IV, produced heavier precipitation than did the Quadrants II and III cases. This means that, while the effect of forcing almost exclusively outweighed the significance of the temperature-moisture relationship, on nonforcing days temperature-moisture relationship identified convectively active days quite well.

A number of additional variables were examined for possible use as predictors to delineate further individual values of the CI. Among those which proved to be of value were the 12-hour forecasted vorticity advection, the presence of a capping temperature inversion, and the presence of southeasterly windflow from the surface through 500 mb. The classification of individual days based on these characteristics resulted in further stratifying each day beyond either convectively active or inactive; hence, the further refining of the CI.

Some predictors were included in the FDT as definitions of individual CI's necessitated. For example, the class 7 cumulonimbus mesosystem commonly arises due to a steep 850 to 500 mb temperature lapse rate, coupled with the presence of a dryline or surface trough, and convergent low-level flow from the southeast into the operational area. When these criteria are met, the class-7 activity is quite likely. Thus, this was abbre-
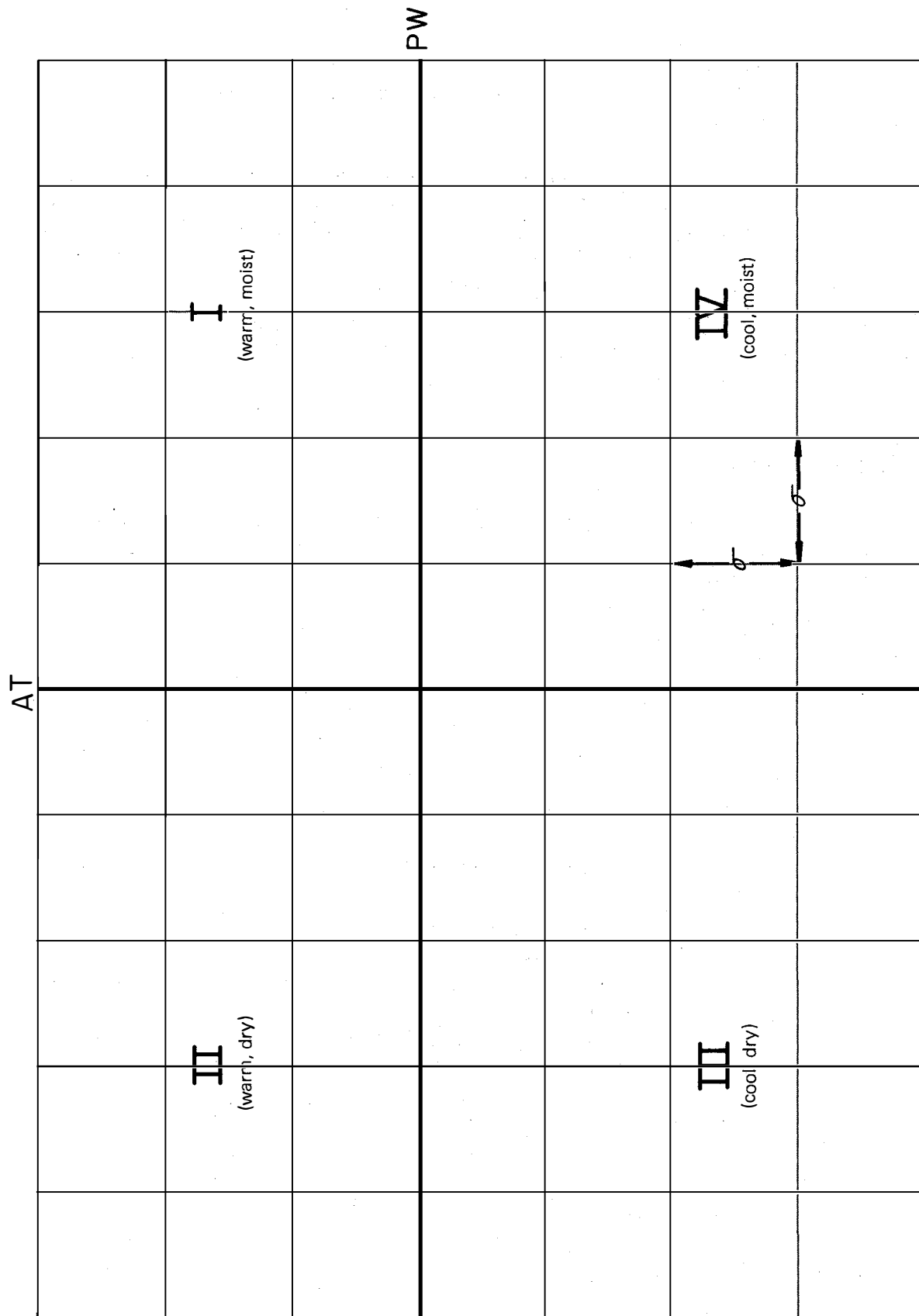
Figure 3.28. Quadrant Location of Convective Index

- 123 -

viated as "conditions right for cumulonimbus mesosystem," rather than to list each of the stipulations. Similarly, the class 9 conditions were abbreviated.

Finally, other constraints were added to delineate convective activity during nonforcing situations. A class-2 day is defined as occurring when the minimum cloud base is greater than 3.7 km (12,000 feet) above ground level (AGL). If the morning sounding indicated that the cloud base would be in excess of 3.7 km (12,000 feet) AGL, and all other criteria were met, a class-2 day would result. Also, because subsidence (downward motion) in the upper air inhibits deep convection, its presence was included as a delineator between showers (CI of 5) and fair-weather cumulus (CI of 3).

3.5.1.2 Refinement

The first generation FDT was used in 1978 with considerable success, but it was known that further improvement was needed. First, the term "subsidence" had to be quantified. Secondly, it was necessary to quantify any changes in the upper-air profile during the convective period because it would indicate if the airmass could continue to support afternoon convection.

If the sounding indicated that a parcel could be lifted to 500 mb and remain positively buoyant throughout its assent, it could be assumed that there existed much potential for deep convection. However, it was deduced that if, based on the 12-hour, 500-mb temperature forecast, the effect of subsidence would induce sufficient warming aloft to render the airmass negatively buoyant, very little deep convection would occur. This was quantified by adding the 12-hour temperature changes at 500 mb ($\Delta T_{500 \text{ mb}}$) to the Lifted Index (LI), and setting this sum equal to zero, or $\Delta T_{500 mb} (12 \text{ h}) + \text{LI} = 0$, where LI is the 100 mb lifted index. For example, if the change in the 500-mb temperature (ΔT) was +3 °C from 0700 to 1900 CDT (1200 to 0000 GMT), and the 0700 CDT (1200 GMT) LI was -2.5, then +3 + (-2.5) = + 0.5, and the airmass was stable and therefore negatively buoyant, the convection would be repressed. Similarly, if $\Delta T = -2$, and the LI = +1.5, then 2+ 1.5 = -0.5, and the airmass is unstable and therefore positively buoyant, the convection would be enhanced.

Prior to the 1979 Texas HIPLEX field program, the FDT was structured as a computer program. This program performed well, and provided a permanent record of all input and output, as well as a prestratification of the forecast period and a written description of the anticipated weather.

3.5.1.3 Performance

Since its development prior to the 1978 Texas HIPLEX field program, the FDT served as an important part of the forecasting effort. Forecast

performance, shown in Table 3.18, steadily improved through the 1978-1980 period, as refinements were incorporated into the FDT program.

Table 3.18—Texas HIPLEX Forecast Decision Tree Performance, 1978 - 1980

Mo./year	No. fcsts.	A. Forecasting Convective Activity				B. Prestratification Accuracy		
		Hit	Miss	%	% for yr.	Hit	Miss	% for yr.
(1978)								
May	14	11	3	78.6				
June	30	25	5	83.3				
July	31	28	3	90.3	85.3	49*	24	67.1
(1979)								
May	11	11	0	100.0				
June	27	24	3	88.9				
July	21	18	3	85.7	89.8	41	18	69.5
(1980)								
May	13	9	4	6.0				
June	28	28	0	100.0				
July	25	24	1	96.0	92.4	45	21	68.2

*Two of the 75 forecast days in 1978 were not prestratified due to computer failure.

The FDT performed particularly well throughout each season in forecasting the occurrence of convective activity without regard to individual CI's. Forecasting support for the 1978 Texas HIPLEX Program began on May 15, and terminated July 31. Statistically, the performance of the FDT exhibited a gradual month-by-month improvement in forecasting the occurrence of convective activity, verifying 78.6 percent for May, improving to 83.3 percent in June, and 90.3 percent in July. The improved forecasts were attributed to familiarization with the FDT and refinements which were implemented during early June, as well as to more persistent nonoperational days in July than in May.

The 1979 field season marked the first routine use of the computerized FDT as a standard forecasting tool for the Texas HIPLEX Program. During the 1979 season (May 21 through July 20), a total of 59 forecasts were

made for HIPLEX purposes, using the FDT model to prestratify each day by CI. Of the 59 forecasts issued, 53 were verified as correct, and 6 were incorrect (89.8 percent correct) in forecasting the occurrence of convective activity.

During the 1980 field season, the FDT was used as an integral component of the forecasting methodology to prestratify and generally organize the forecasting effort at the Big Spring Meteorological Facility. Results of the forecasting procedure were quite promising with a verification percentage of 92.4.

While the gradual improvement in forecasting the occurrence of convection may be practically attributed to refinements in the FDT, it is important to understand that the FDT is not completely objective; it is, in fact, a highly subjective tool in its most critical area—forcing. More than one of the branch points rely on the subjective expertise of the forecaster, rather than on the implementation of an objective numerical weather prediction.

While the term "subsidence" has been made objective, assessment of the forcing variable relies on the forecaster's ability to recognize the presence and determine the movement of some type of forcing mechanism. Much of the gradual improvement in the forecasting is therefore attributable to the experience gained by the forecaster.

The principal purpose of the FDT was to prestratify each forecast period by CI in order to fine-tune the operational forecast. A measure of accuracy of the FDT during the 1978 through 1980 field seasons to forecast the individual CI's was calculated. During the 1978 field season, 67.1 percent of all prestratifications were correct. The 1979 season was marked by an improvement to 69.5 percent, and the FDT prestratified 1980, forecasted correctly on 68.2 percent of the occasions.

3.5.1.4 Conclusions

It has been shown that the FDT was a valuable tool in providing a general operational forecast for the Texas HIPLEX Program. However, further work is required to produce a totally objective method of forecasting the anticipated convective types on a day-to-day basis. Given the large time and areal resolution of the FDT input data relative to the small time frame and target area of the Texas HIPLEX Program, significant improvements of the FDT are not expected. It is concluded that only when mesoscale input data are collected and processed in near real time, can significant forecasting improvements be expected.

3.5.2 Rainshower/Thunderstorm Forecasting Model

The Texas Department of Water Resources' staff developed a site-specific, multivariate statistical forecast procedure, using discriminant analysis to predict thunderstorm and/or rainshower occurrence. Meteorological parameters available in the early morning were utilized as predictors for the occurrence of rain-generating storms later in the day. Individual forecast models were developed for each of the months of June and July to reduce the deleterious effects that seasonal influences on distributions of meteorological parameters might have on the models.

The numerical forecast model was structured to allow the on-site forecaster to have ready access to it on a daily basis. The forecaster supplied certain morning weather measurements, and the model then determined the probability of rainshower/thunderstorm occurrence for that day. Probabilities were given for seven different prior conditions, i.e. previous day weather phenomena and the existence of a front or trough in the Texas HIPLEX project area. Arbitrary risk factors of missing an operational forecast were also computed.

The accuracy of the model for forecasting the occurrence of rainshower/thunderstorms within the Texas HIPLEX operational area was estimated to be 62 percent. Additional details of the model may be found in a paper by Riggio and Topham (1979), entitled *Using Discriminant Analysis to Predict Rainshower Occurrence in the High Plains Area.*

3.5.3. Severe Weather Studies

Texas HIPLEX cloud-seeding experiments were performed with the constraint that under those circumstances in which any portion of the project site was covered by the issuance of a severe weather watch or warning (by the National Weather Service), operations within that area would either be terminated or not scheduled. A census of the number of "severe storm days" in the Texas HIPLEX project area was made in 1978, to provide project planners with an estimate of the probability that a "candidate" cloud-seeding day would be marred by the issuance of a severe weather watch or warning.

The survey examined data over a 4-year period (1974-1977), and found that whenever a severe weather watch is issued for a segment of the project site, "there is a good likelihood that local storms of severe proportions will not be observed." Table 3.19 lists watches issued and verification results.

The results of the survey suggest that instead of terminating experiments at the time of issuance of a severe weather watch, conditions in the region be monitored by HIPLEX radar, concurrently with airborne observations, until a severe weather warning is received. With respect to severe weather warnings, the census found that such warnings were most frequent in June, with the majority (4 out of 5)

valid from mid-afternoon through the early evening hours.* The extreme western sector of the project area was most often affected by warnings, both in June and July.

Table 3.19—Severe Local-Storm Watches Issued for Portions of the Study Area for June-July 1974-1977

Type of watch	Period of effectiveness		Counties affected	Verification reports
	Date	Time		
TORNADO & SEVERE THUNDERSTORM	June 3, 1974	4:30-9:30 pm	all of the project area	tornado observed at 10:10 pm 10 mi NE Sweetwater
	June 3-4, 1974	9:30 pm-1:30 am	Terry, Lynn, and Garza	no reports of severe storms filed
	June 8, 1974	2-8 pm	Fisher and Nolan	no reports of severe storms filed
	June 7, 1975	5-11 pm	Lynn, Garza, Terry, Scurry, and Fisher	no reports of severe storms filed
	June 8, 1975	2-8 pm	Coke & Nolan	no reports of severe storms filed
	June 9, 1975	7-11 pm	most of the project area	hail as large as 1¾" and strong winds occurred in Dawson and Borden Counties in the evening
	June 22, 1975	6-11 pm	most of the project area	hail up to 1¾" and wind gust to 50 mph occurred in Lynn County in early stages in the early evening.
	June 23-24, 1976	9 pm-3 am	Scurry, Garza, Fisher, Nolan and Mitchell	winds of 60 mph caused $100K in damages in Snyder (Scurry Co.); high thunderstorm winds caused $45K in damages to homes 8 E Big Spring (Howard County)
SEVERE THUNDERSTORM	June 11, 1974	4:30-9 pm	Garza	no reports of severe storms filed
	June 8, 1975	2-8 pm	Coke	no reports of severe storms filed
	June 9, 1975	2-8 pm	Nolan, Scurry, and Fisher	hail up to 1¾" and strong winds occurred in Dawson and Borden Counties
	June 30, 1976	5-11 pm	southeastern half of project area	no reports of severe storms filed
	June 13, 1977	5:30-11 pm	Lynn and Garza	no reports of severe storms filed
FLASH FLOOD	June 9-10, 1975	eve/night	Scurry, Fisher, Mitchell & Nolan	less than ½" of rain fell in the affected region

*Criteria that must be satisfied to justify the issuance of a severe weather warning are surface winds of 50 knots or stronger and/or surface hail with a diameter of ¾ inch or larger.

Type of watch	Period of effectiveness		Counties affected	Verification reports
	Date	Time		
FLASH FLOOD	July 17-18, 1975	5:30 am- next day	Coke and Sterling	3-4" rains fell in Coke County
	July 20-21, 1975	9:25 pm- early am	northeastern half of project area	2-7" rains were common in the region affected
	July 25, 1975	2 pm- next am	Garza, Scurry, Nolan & Mitchell	½" or less fell in most of the region covered
	July 11, 1976	4 pm-next day	Borden, Dawson, and Scurry	1-2" rains occurred in the affected region
	July 8, 1977	6 pm-9 pm	most area of the project	¼-½" rains fell in most of the region

The investigation went one step further and considered the frequency of actual severe weather events during June and July. It revealed that phenomena such as hail, tornadoes, and damaging winds were rather scarce during the first three years of HIPLEX experiments (1975-1977). Of the events reported, most occurred in June.

3.6 Economic Studies

The goal of the HIPLEX Program is in part a better understanding of the feasibility of rain augmentation. Therefore, the Texas Department of Water Resources performed a three-part economic analysis of the potential effects of an additional amount of precipitation from cloud seeding on irrigated and nonirrigated farming communities in the Big Spring-Snyder area of West Texas. The details of these studies can be found in Department reports, entitled *The Economic Effects of Weather Modification Activities: Part I-Crop Production; Part II-Range Production and Interindustry Analyses; and Part III-Irrigated and Dryland Agriculture with Estimates of Production, Employment, and Income Effects on the Area Economy,* by Allaway *et al.* (1975), Lippke (1976), and Kengla *et al.* (1979), respectively.

The estimates of the effects of an increase of precipitation on crops and rangeland were developed by using multiple linear regression techniques. The dependent variable was crop yield in the Part I study, and range-forage production in the Part II study. The independent variables were precipitation, temperature, and technology in the Part I study, and precipitation and previous range forage conditions in the Part II study. Holding the nonprecipitation related independent variables constant at their means, precipitation amounts were altered to observe the estimated effects on the dependent variable.

In the Part III study, a projected 10-percent increase in annual growing season precipitation for each county was calculated, and multiplied by each county's average annual

irrigated acreage in the years 1971-1975, to determine the extent to which the additional rainfall could be expected to replace ground-water pumpage in each county.

The Department's economic studies revealed that the additional rainfall could have the following net economic effects on the Big Spring-Snyder West Texas region:

1. A reduction in ground-water pump irrigation requirements of 28.16 million m³ (22,800 acre-feet) per year, which would reduce irrigation costs by approximately $547,159 in 1977 dollars, and would expand regional income of persons by $370,598;

2. The additional rainfall in the study area would expand dryland crop and livestock production, as well as farm income, by approximately $1.6 million, which would eventually expand regional output by approximately $3.9 million, and regional income by over $1.9 million; and

3. The net effect of the additional rainfall in the dryland and irrigation crop sectors of the Big Spring-Snyder regional economy would be to create an overall expansion in regional output of approximately $3.86 million, and a similar expansion of regional income of $2.30 million.

4. Preliminary Findings and Conclusions

4.1 General

The first objective of the HIPLEX Program is to increase the understanding of natural cloud and precipitation processes in convective cloud entities. Knowledge of these processes is a necessary prerequisite for developing a statistical design of a cloud-seeding experiment, capable of testing our ability to alter these processes.

Indeed, the HIPLEX Program has provided the State of Texas with the opportunity to increase its knowledge of West Texas convective clouds. Specifically, basic knowledge was acquired about the mesoscale systems which control the development of convective systems, and their integrated effect on the precipitation mechanisms responsible for the formation of precipitation.

The preliminary findings of the Texas HIPLEX Program are presented in terms of West Texas convective cloud behavior, precipitation and principal effects of seeding. Due to the nature and requirements of the different studies, some of the findings are based on a climatological approach, while others are based on a case study approach. Specific findings are listed in the Appendix.

4.2 Convective Cloud Behavior

The Texas HIPLEX Program has shown that the natural variability of convective clouds is a result of integrated meteorological processes observed at the meso α-, meso β-, and meso γ-scales.

The meso α-scale parameters provide information concerning general convective cloud characteristics. Its been learned that the dominant summertime synoptic pattern for the West Texas region is one with no front at the surface, and with a pressure ridge aloft. This pattern does not support shower-producing clouds. However, when a 500 mb trough is observed west of the Texas HIPLEX region, and/or a surface front is also west of the region or in the project area, then conditions are extremely favorable for shower-producing clouds to develop. Low-level convergence of moist air is important to the initiation and development of isolated, cluster and line-type convective clouds. Summertime radar echo occurrence is most frequent during the period between 1500 CDT (2000 GMT) and 1800 CDT (2300 GMT). The convective clouds generally travel in the direction of the 700 mb winds, which are predominantly flowing in a northeastward and eastward direction.

The drawback of using only meso α-scale parameters to describe the natural behavior of convective clouds is that the scale is not sensitive enough to account for the small-scale parameters which have a substantial effect on the natural variability of the convective clouds. The Texas HIPLEX analyses heretofore have illustrated the need for better

understanding of the meso β- and meso γ-scale parameters to distinguish better the behavior of convective clouds.

Simple numerical cloud model results, reported by Matthews (1981b), have indicated that useful opportunities for dynamic seeding may exist in the Texas HIPLEX area. In fact, the Texas HIPLEX area had the highest frequency of dynamic seeding potential for all cloud types, when compared to the Miles City, Montana, and Goodland, Kansas, sites. Also, Matthews (1981a) concluded that Kansas HIPLEX clouds, triggered by thunderstorm outflow, had potential for increased growth due to seeding for dynamic effects. And seeding techniques, which enhance the mesoscale thunderstorm outflow and intensity of lifting along the mesoscale front, may initiate clouds with additional potential for seeding. Consistent with Matthews' modeling results, the July 3, 1978, case study, reported by Humbert et al. (1979), of a massively seeded convective cloud appeared to respond in a dynamic fashion. The prospects for artifically stimulating "new growth" and additional rainfall from mesoscale convective clusters by seeding for dynamic effects may be a viable option in the Texas HIPLEX area.

Other studies of mesoscale numerical models have suggested that seeding for dynamic effects of mesoscale systems can strengthen the dynamics of the mesoscale system, and subsequently can enhance rainfall through new growth by strengthening downdrafts and their associated mesohigh outflow (Fritsch and Chappell, 1981, Tripoli and Cotton, 1980, and Matthews, 1981a). A detailed case study of a Texas HIPLEX convective complex (Jurica et al., 1981) has established the existence of a mesolow and mesohigh at the surface, with well defined boundaries and thermodynamic characteristics. An important consequence of the existence of a mesolow and a mesohigh is evidence of interaction between individual cumulonimbus clouds when they are organized into a mesoscale precipitation feature.

Simpson (1980) developed a hypothesis which links downdrafts from dynamically seeded cloud towers with new growth areas, subsequent cloud system expansion and enhanced rainfall. Inasmuch as the potential for seeding for dynamic effects may exist in Texas HIPLEX convective systems, and well defined mesohighs can be identified, the Simpson hypothesis, which addresses mesoscale convective systems, may find application in the Texas HIPLEX program.

Also, meso β-scale Texas HIPLEX analyses have identified relationships between the development and organization of convective clouds; the transport of low-level moisture; convective stability, as measured by potential temperature; and the magnitude of the 850-500 mb wind shear vector. These findings are consistent with numerical model results by Matthews and Silverman (1980), Chen and Orville (1980), and Tripoli and Cotton (1980). Matthews and Silverman reported that days with organized convection were more stable and required mesoscale lifting to initiate convection. Chen and Orville reported that to better understand cloud scale convection, some knowledge of the mesoscale convergence field is required. Tripoli and Cotton reported that ". . . the opportunities are greater for obtaining significant enhancement of convective rainfall by 'dynamic seeding' under conditions during which moderate intensity, low-level wind shear and mesoscale convergence are present." It is reasonable to suggest that the three mesoscale

parameters appear to be excellent candidates as covariates for the Texas HIPLEX cloud-seeding experiment, and warrant further investigation.

Tripoli and Cotton state that "...the ultimate potential of weather modification must lie with the ability to modulate mesoscale convective systems." The preliminary findings of the Texas HIPLEX Program support this statement and provide the data to develop mesoscale hypotheses.

4.3 Precipitation

The ultimate goal of the Texas HIPLEX Program is to increase summertime rainfall to benefit the people of West Texas. Consequently, the precipitation studies will play a key role in the development of the convective cloud-seeding experiment design. Therefore, it is necessary to understand the natural variability exhibited by precipitation in the Texas HIPLEX area.

From the perspective of the meso α-scale it has been learned that for the five-month summertime period, May through September, there exists a daily precipitation maximum in mid-May, decreasing to a minimum in late June, with secondary maxima centered on July 4 and July 22, and secondary minima on July 14 and the first week of August. An increase in daily precipitation is then observed from early August to a broad maximum in late August and early September. Upper-air troughs are responsible for about 72 percent of the precipitation, followed by frontal activity at 20 percent, and airmass at 7.7 percent.

A closer and more detailed look at the meso β- and meso γ-scale characteristics of precipitation events has revealed some interesting findings relative to cloud seeding.

(1) Precipitation events in the Texas HIPLEX region can be stratified into distinct categories of convective activity, based upon radar reflectivity patterns.

(2) Advection of the rainfall pattern through the raingage network appears to dominate the temporal distribution of rain volumes in the network.

(3) Significant differences exist among the several convective categories with respect to the volume of rain produced and the duration of the event.

(4) Most of the summer precipitation is produced by a few large storms.

Approximately 90 percent of all radar echoes observed were isolated cells. Convective clusters made up about 10 percent, and less than 1 percent of the radar echoes were lines. Concerning the amount of the rain produced by cells, clusters and lines, it was found that 2.8 percent of the total rainfall produced over the 1976-1978 period came from cells, while 27.2 percent came from clusters, and 70.0 percent came from lines. Results were similar over the 1978-1980 period, with 0.1 percent of the total rainfall coming from cells, 31.8 percent from clusters (small and large), and 67.9 percent from larger systems. Thus, it seems clear that a few events produce a large percentage of the area's rainfall.

A closer look at the cluster category has revealed that 34 percent of the precipitating echoes over the raingage network were small clusters. Thus, there are a significant

number of events in which small clusters are present for treatment. In addition, it was found that in some cases small clusters do not rain.

From an applied research point of view one would like the experimental unit to account for a substantial portion of the area's rainfall. Unfortunately, this is not the case with small clusters; they produced only 4.3 percent of the total rainfall from 1978 through 1980. Producing a 20-percent increase in rainfall from small clusters would lead to an apparently insignificant percentage increase in total rainfall. Over the 3-year period,1978-1980, this would have amounted to an increase of only 4.57 mm (0.18 in). Even a 100 percent increase would not yield much more rain in the area. However, if small clusters could be induced to develop further into large clusters or if large clusters could be induced to rain more, a substantial increase in the area's rainfall could result, since large clusters accounted for 27.5 percent of the total rainfall from 1978 through 1980. Understanding the complicated interactions related to causing large clusters to develop further into lines is beyond the state of the art. It therefore seems advisable to identify clusters as the experimental unit, and to direct further investigations toward discerning the feasibility of inducing small clusters to intensify into large clusters, for example, by initiating new growth along mesoscale frontal boundaries or by merging with other small clusters, or augmenting the rainfall from large clusters.

4.4 Principal Effects of Seeding

Texas HIPLEX studies have indicated that precipitation is initiated in West Texas convective clouds by the warm-rain processes. However, the ice process appears to dominate throughout much of the subsequent development, and operates in clouds with significant precipitation. The findings have indicated that during the mature and later stages, the ice particle concentrations are between 10 to $100 \ell^{-1}$, and may be a result, in part, of ice multiplication. Because of the existence of adequate liquid water during the early stages of cloud development, and of the rapid development of high ice particle concentrations in the later stages of natural clouds, it is reasoned that seeding hypotheses should test either hygroscopic seeding, seeding for dynamic effects early in the lifetime of the clouds, or static ice phase seeding in the smaller clouds at a time prior to major precipitation development.

4.5 Conclusions

From the outset, the Texas HIPLEX Program has been an applied research program, and as such its goal is to develop a technology to maximize increased rainfall from West Texas summertime-cumulus clouds. Working within this conceptual framework, initial analyses have been performed to identify an experimental unit, seeding hypotheses, covariates and response variables.

It is tentatively concluded that of the five types of convective clouds observed in West Texas (which includes lines, cold clusters, warm clusters, cold cells and warm cells)

cold clusters appear to be the most favorable candidates for the experimental unit. Operationally, cold clusters have a workable life span of 35 minutes, as opposed to only 10 minutes for warm and cold cells. Also, frequent radar observations of merging cold echoes, particularly clusters, and mesoscale analyses have suggested an interaction between individual convective clouds within the mesocale system. This enhances the feasibility of affecting the system by seeding cluster turret(s). In order to maximize opportunities to collect additional cloud microphysics data, cold cells should be considered as an alternate experimental unit.

It is tentatively concluded that seeding for dynamic effects may have a substantial impact on clusters, and that, *if environmental thermodynamic data and microscale cloud measurements warrant seeding for dynamic effects,* seeding clusters for dynamic effects should be included in the seeding experiment. Seeding for microphysical effects by light to moderate static ice phase seeding should also be considered and addressed. The ISWS design document carefully reviewed all the current state-of-the-art cloud seeding hypotheses (Ackerman *et al.,* 1976). The ISWS recommended two hypotheses for the HIPLEX Program: 1) light to moderate ice phase seeding, and 2) massive seeding for dynamic results. Hygroscopic seeding was rejected due to logistical problems and anticipated small economic benefits. In line with the reasons presented by the ISWS design document, a hygroscopic seeding hypothesis for the Texas HIPLEX experiment is rejected. Also, due to the relatively short seeding window, on-top seeding is recommended, as opposed to cloud base seeding.

The Texas HIPLEX Program demonstrates the need for near-real time data collection and analyses to successfully conduct most weather modification programs, whether they are experimental or operational in nature. The comprehensive and near-real time mesoscale data collection and analytic capabilities developed for the Texas HIPLEX Program, particularly during the 1979 and 1980 field seasons, demonstrated the rather rapid and substantial local changes of atmospheric energetics and kinematics over a 12-hour period on convectively active days. It is apparent that a morning, 1200 GMT, upper-air atmospheric profile should not be considered as representative of the afternoon atmospheric profile when convective precipitation is expected to develop. Visual comparisons of Texas HIPLEX mesoscale upper-air data taken only three hours apart show important differences in appearance. Important differences in the atmospheric profiles were also observed among the upper-air profiles taken at stations approximately 65 km (40 mi) apart at identical times. Consequently, to truly understand the characteristics of the atmosphere affecting convective precipitation development, the upper-air profiles need to measure and interpret mesoscale characteristics at near-real time (i.e. two hours after launch). Also, to know whether a cloud system is a favorable candidate for seeding, it is necessary to have near-real time information available for the project manager. It is apparent that any future Texas HIPLEX field activity should evolve around the collection and analyses of near-real time data. These data are to include primarily mesoscale, radar, and cloud microphysical information.

The following section elaborates on the tentative experimental units, seeding hypotheses, response variables, and future work.

5. Recommendations

5.1 General

The major objective for the future Texas HIPLEX Program is to formulate a single-cloud experimental design to include the best possible working hypotheses or conceptual model which express and explain the precipitation processes which occur within summer-time shower-producing clouds of West Texas. These hypotheses are to be expressed in terms of the environmental factors of the West Texas area, and should include microphysical and mesoscale variables, data, and information, which are necessary steps toward the conduct of the experimental cloud-seeding phases of the project.

This Section presents tentative Texas HIPLEX seeding hypotheses, response variables, and the definition of the experimental units, as currently perceived and based upon findings from weather modification research, primarily the Texas HIPLEX project. Past studies have provided useful insight into the initial formulation of seeding hypotheses which appear to be most appropriate for the Texas HIPLEX project area. The tentative seeding hypotheses are presented in this report to provide a preliminary guide for subsequent analytical efforts, and to help identify manpower, equipment, and information gaps in planning future research.

Future Texas HIPLEX research will be directed at developing an experimental design document by verifying and/or modifying each link of the tentative seeding hypotheses, by critical review of analyses of data already collected, and possibly by additional physical measurements and analyses of certain parameters which are needed to fill information gaps.

5.2 Classification of Shower-Producing Clouds

Utilization of the tentative Texas HIPLEX seeding hypotheses requires that the shower-producing clouds common to West Texas be classified as either cells, clusters, or lines. Because radar information can be recorded and can provide an acceptable, real-time perspective of cloud characteristics, the classification system will be based on radar-echo measurement. The classification system will follow Sutherland *et al.* (1980), and is as follows:

— *Cell:* An individual echo with, at most, two reflectivity peaks throughout its expected treatment and measurement period;

— *Cluster:* An echo containing three or more reflectivity peaks usually within a common echo boundary throughout its expected treatment and measurement period.

The distinction between isolated convective cells and convective clusters is more clearly demonstrated by radar examples. Figures 5.1 and 5.2 show a schematic of the cell and cluster, respectively. Radar, satellite, and raingage examples from the 1979 Texas HIPLEX field season are presented which, respectively, depict a systematically increasing meso-scale of organization from isolated cells (Figure 5.3) to small clusters (Figure 5.4), and on to large convective clusters (Figure 5.5) and nested convective clusters (Figure 5.6). It is worth noting that mesoscale processes have been classified into several categories (Orlanski, 1975). In this accepted classification scheme, isolated cells are placed in the meso γ-scale, small clusters are placed in the meso α-scale, and large clusters are placed in the meso β-scale. The distinction between small and large convective clusters has been arbitrarily set at a size near 100 km (62 mi). The distinciton is important when one considers the practical aspects of aircraft sampling and the measurement of response variables. The need for this distinction will be discussed in the Section, entitled "Experimental Unit."

5.3 Experimental Unit

The experimental unit is the entity upon which the experiment is to be performed. The sampling unit is the entity from which the seeding effect is measured. In the Texas HIPLEX Program it is envisioned that the experimental unit and the sampling unit will be the same convective entity, thus all subsequent discussion will be in terms of the experimental unit. A major concern of identifying and defining the experimental unit is the problem of documenting the effects from other surrounding convective activity. However, it has been shown (Jurica *et al.*, 1981) that an analysis of mesoscale data can identify and document conditions when interactions among convective entities are occurring.

The Texas HIPLEX Program has identified two convective entity candidates for the experimental unit—the isolated convective cell and the convective cluster. Because of the relatively frequent occurrences of isolated convective cells, when compared to convective clusters (Sutherland *et al.*, 1980), it is highly likely that opportunities for isolated cell investigation will be numerous. Therefore, isolated convective cells should be studied when opportunities exist because the cells provide valuable information needed to define more precisely the precipitation mechanism in the Texas HIPLEX area. Additionally, they are relatively simple to understand and observe for any microphysical seeding effect.

Previous studies in the Texas HIPLEX Program concentrated mostly on the isolated convective cell. However, in spite of their frequency of occurrence, only a small portion (3 percent) of summer rainfall in the southern High Plains is produced from isolated convective cells (Sutherland *et al.*, 1980, and Jurica *et al.*, 1981). Consequently, any positive seeding effect from isolated cells may not significantly increase area rainfall, provided the cells retain the isolated cell classification for the duration of their life cycles. Also, since the mean diameter for isolated cells is approximately 3 km (1.9 mi) (Sutherland *et al.*, 1980), and since the density of the Texas HIPLEX raingage network is about one gage per 10 km (6.2 mi), it would be extremely difficult to establish the natural variability of rain on the ground and then ascertain any effects resulting from seeding.

a) Aircraft side view

10 km

b) Overhead plan view

10

10

10

30

30 dBz

c) Radar PPI view

Figure 5.1 Isolated convective cells (pre-cluster stage)
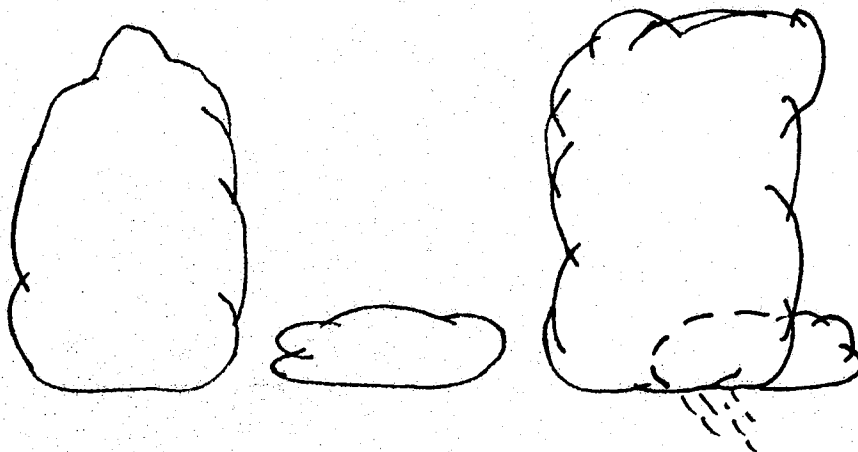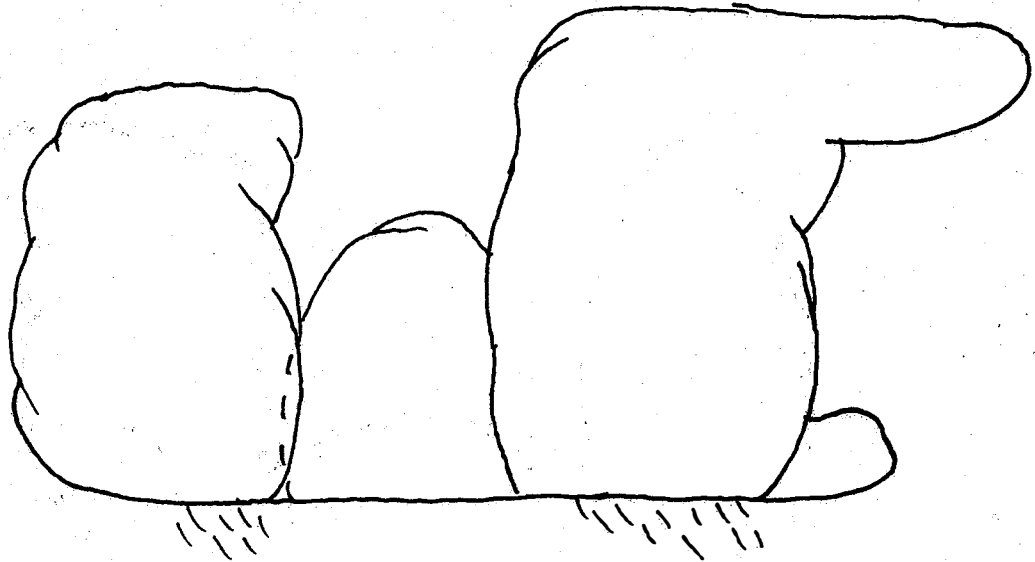
a) Aircraft side view

10 km
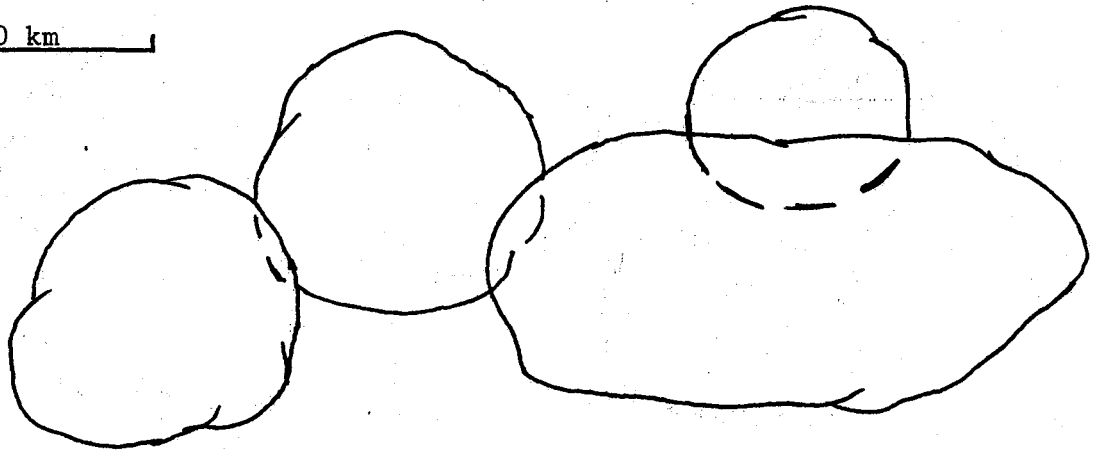
b) Overhead plan view
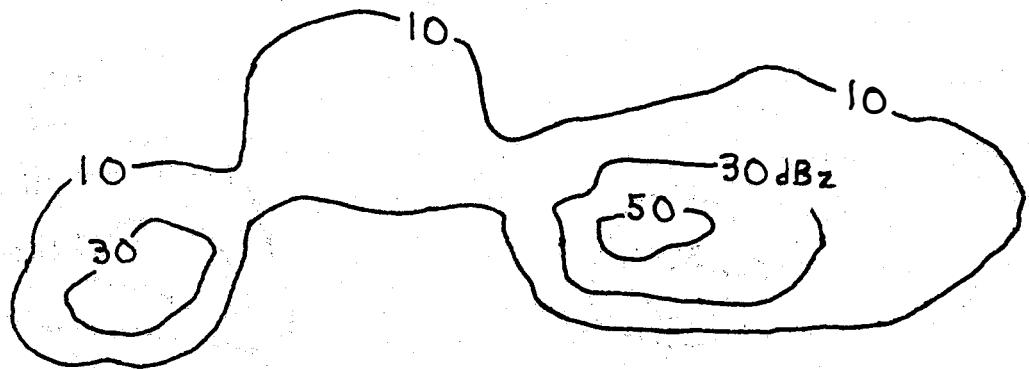
c) Radar PPI view

Figure 5.2 Several views of the Texas HIPLEX experimental unit, the convective cell cluster
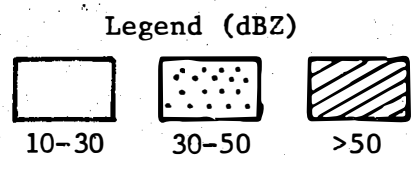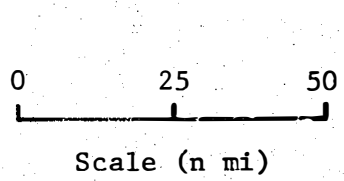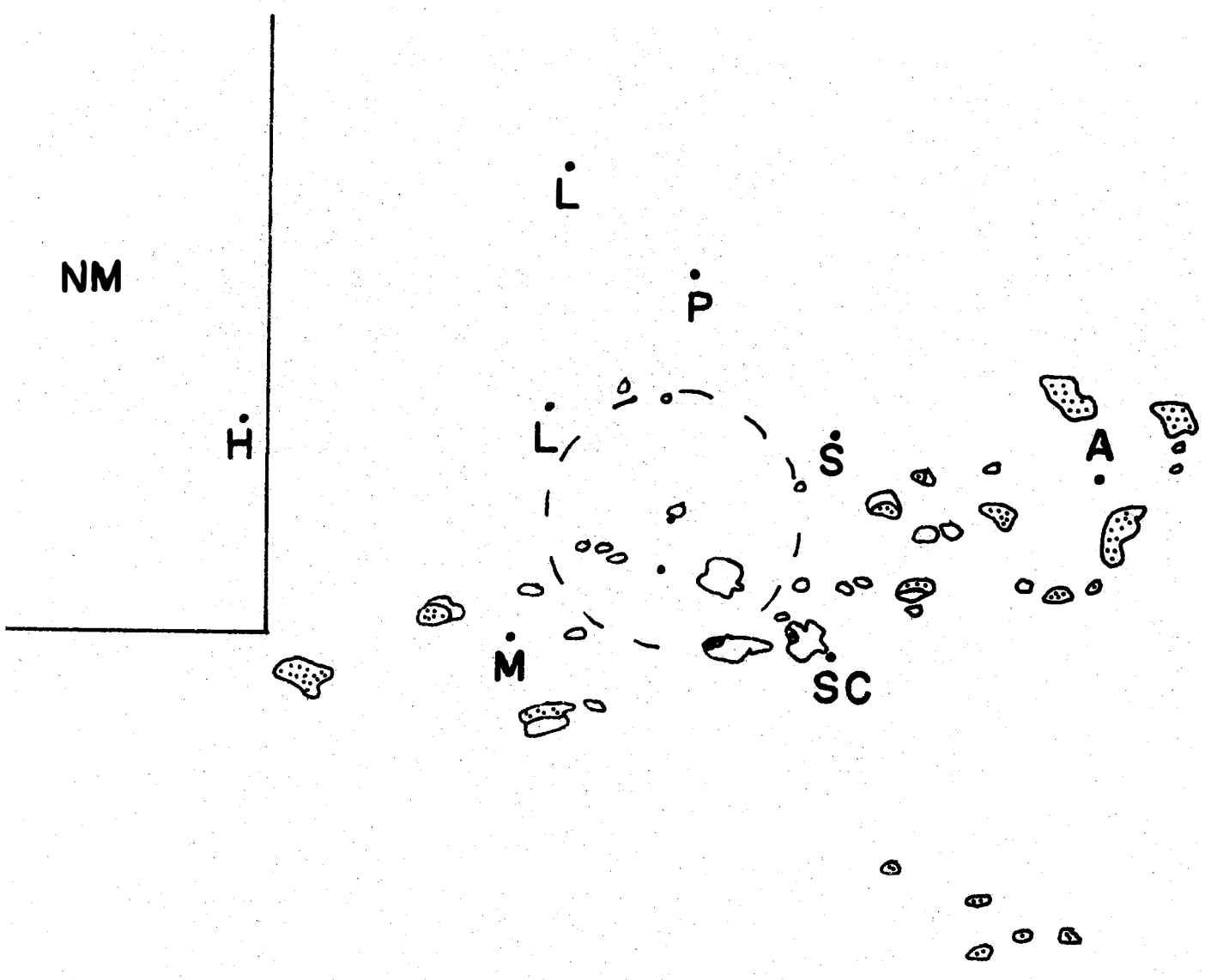
Figure 5.3 An example of convective cells taken on 6 July 1979,
at 19:40:04 GMT (tilt angle 1.0°)
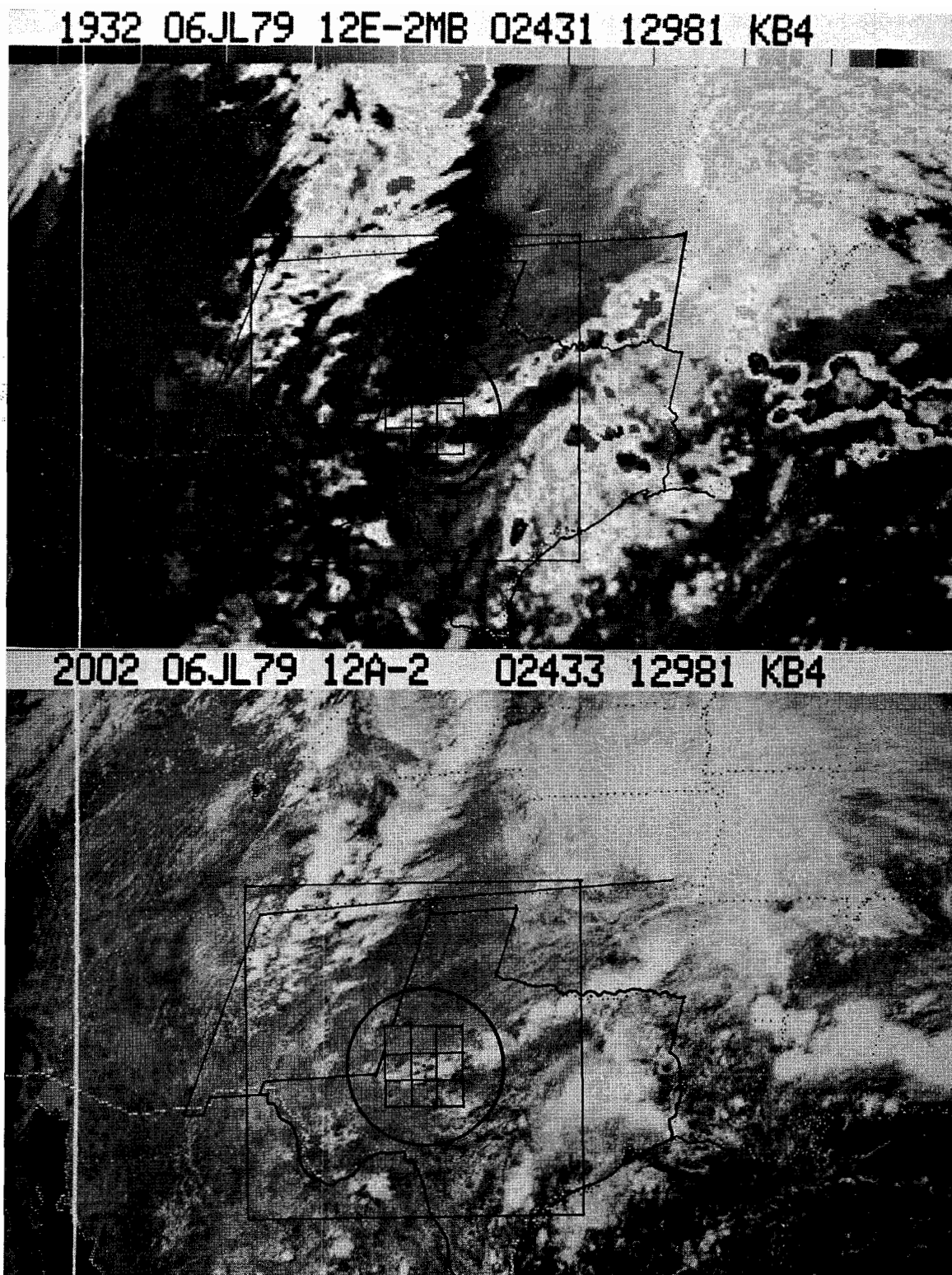
Figure 5.3a Satellite imagery on 6 July 1979, showing the convective cells depicted by radar in Figure 5.3; the solid circle corresponds to the total radar coverage in Figure 5.3

NO

RAINFALL

RECORDED

Figure 5.3b   Rainfall observed during 1915-1930 GMT on 6 July 1979, produced by the convective cells depicted by radar in Figure 5.3
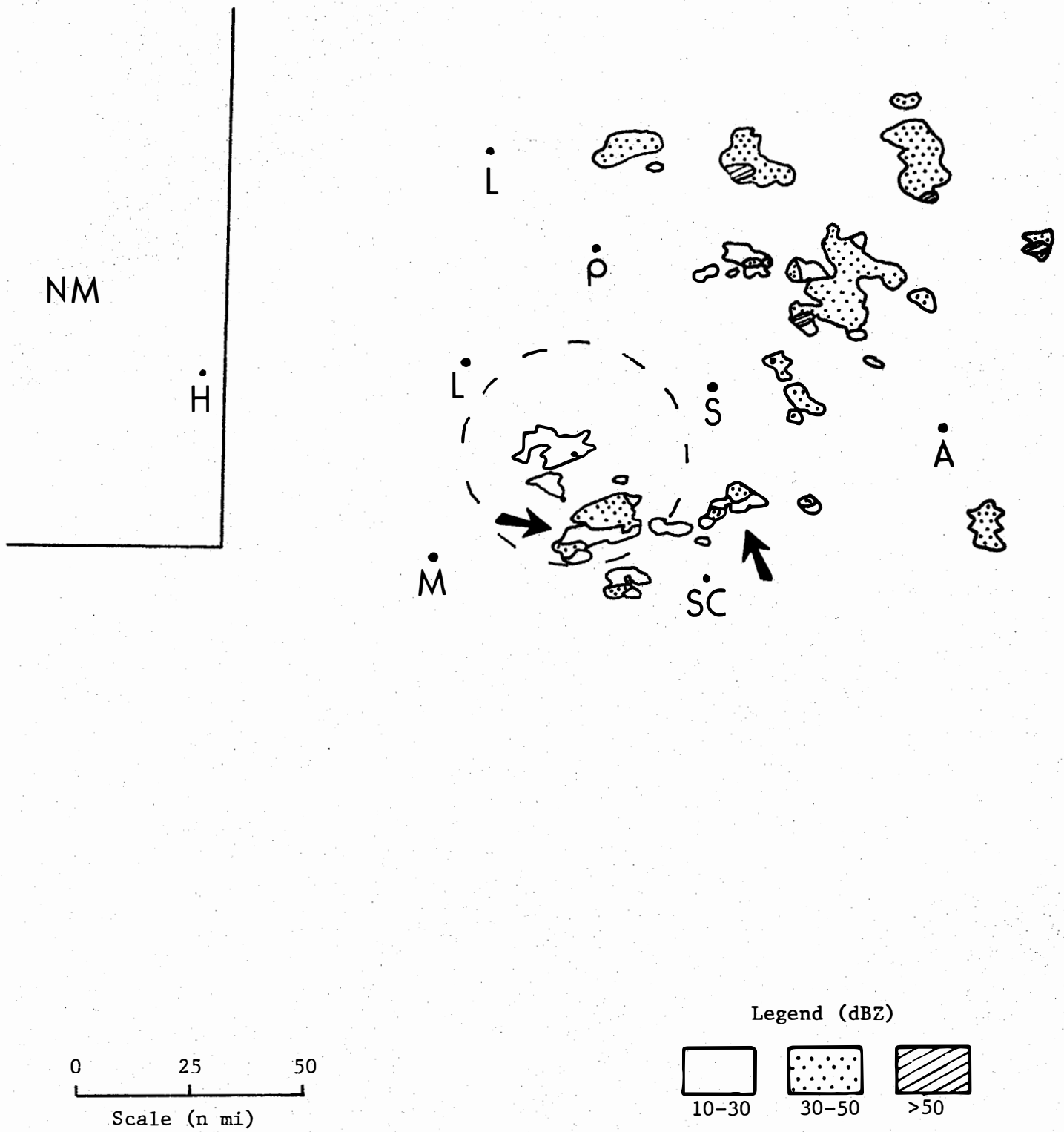
Figure 5.4   An example of small convective clusters taken on 25 June 1979, at 19:15:40 GMT (tilt angle 1.0°)

1902 25JN79 12A-1 02204 11954 KA4
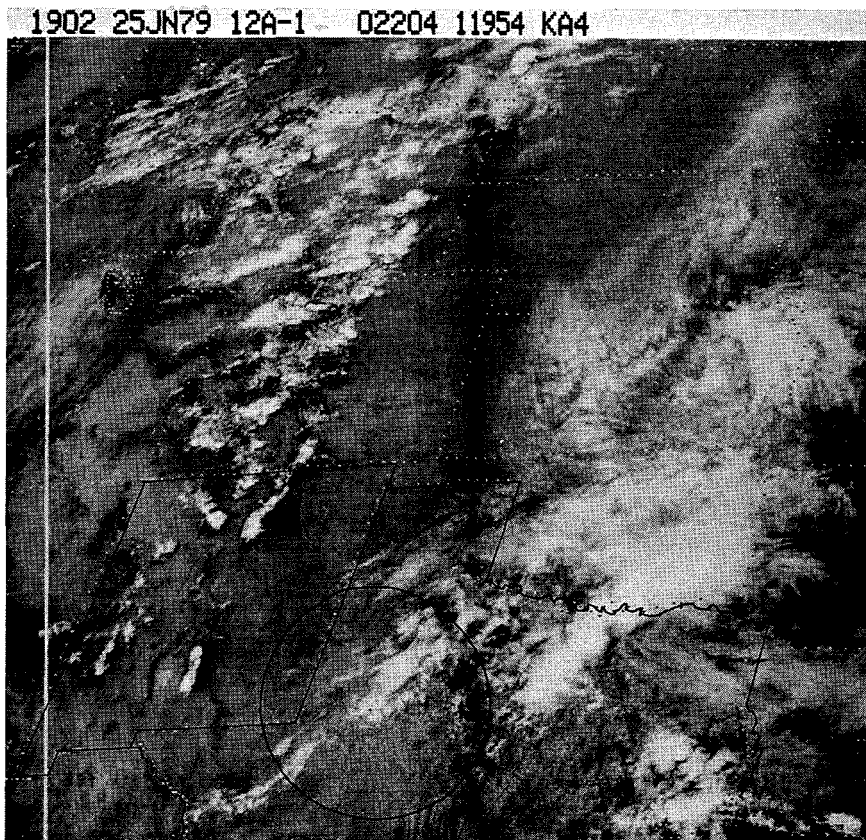
Figure 5.4a Satellite imagery on 25 June 1979, showing the small convective clusters depicted by radar in Figure 5.4; the solid circle corresponds to the total radar coverage in Figure 5.4
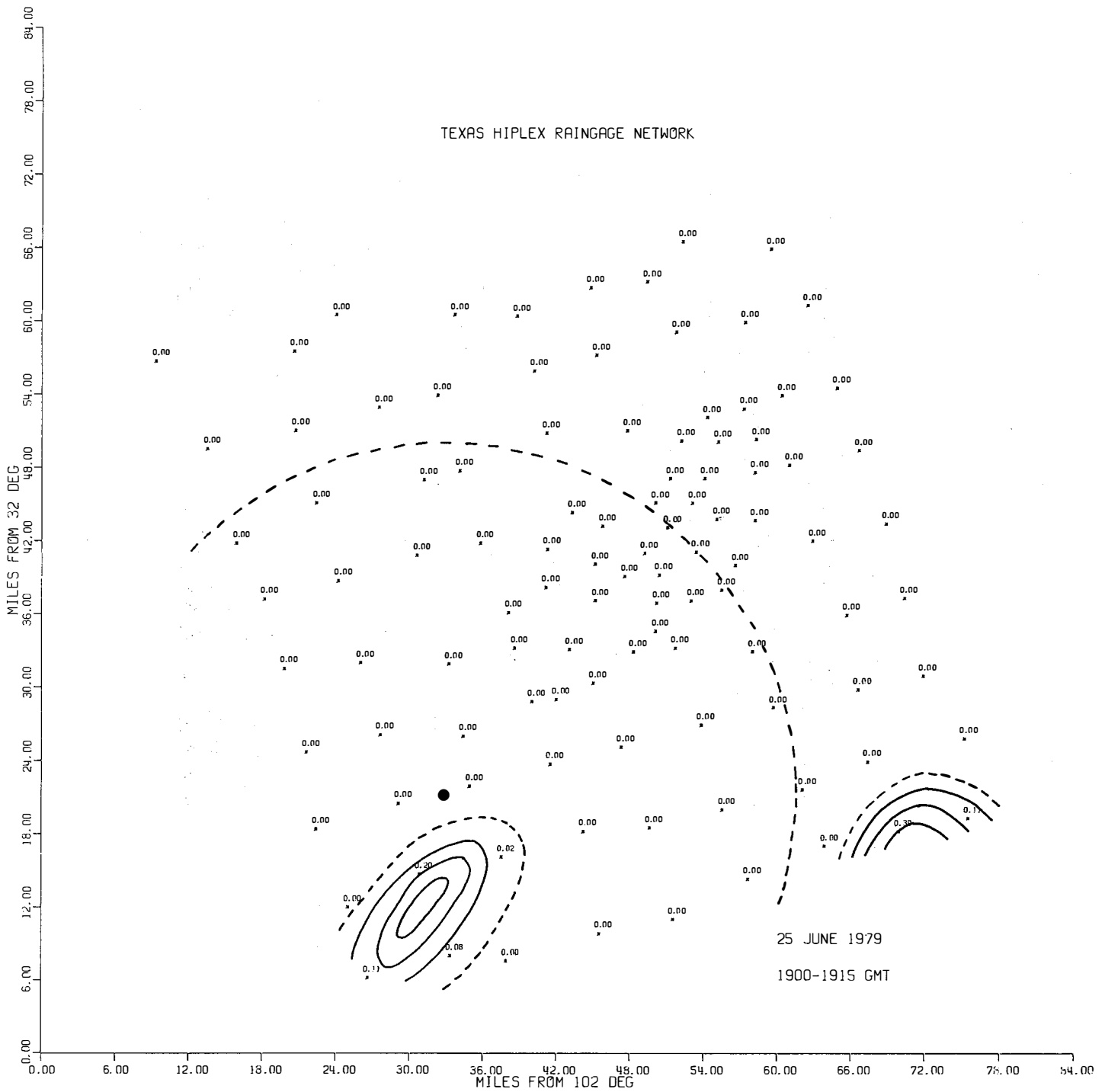
Figure 5.4b Rainfall observed during 1900-1915 GMT on 25 June 1979, produced by the small convective clusters depicted by radar in Figure 5.4; the dashed circle is at a 25 n. mi. distance from the radar and corresponds to the dashed circle in Figure 5.4
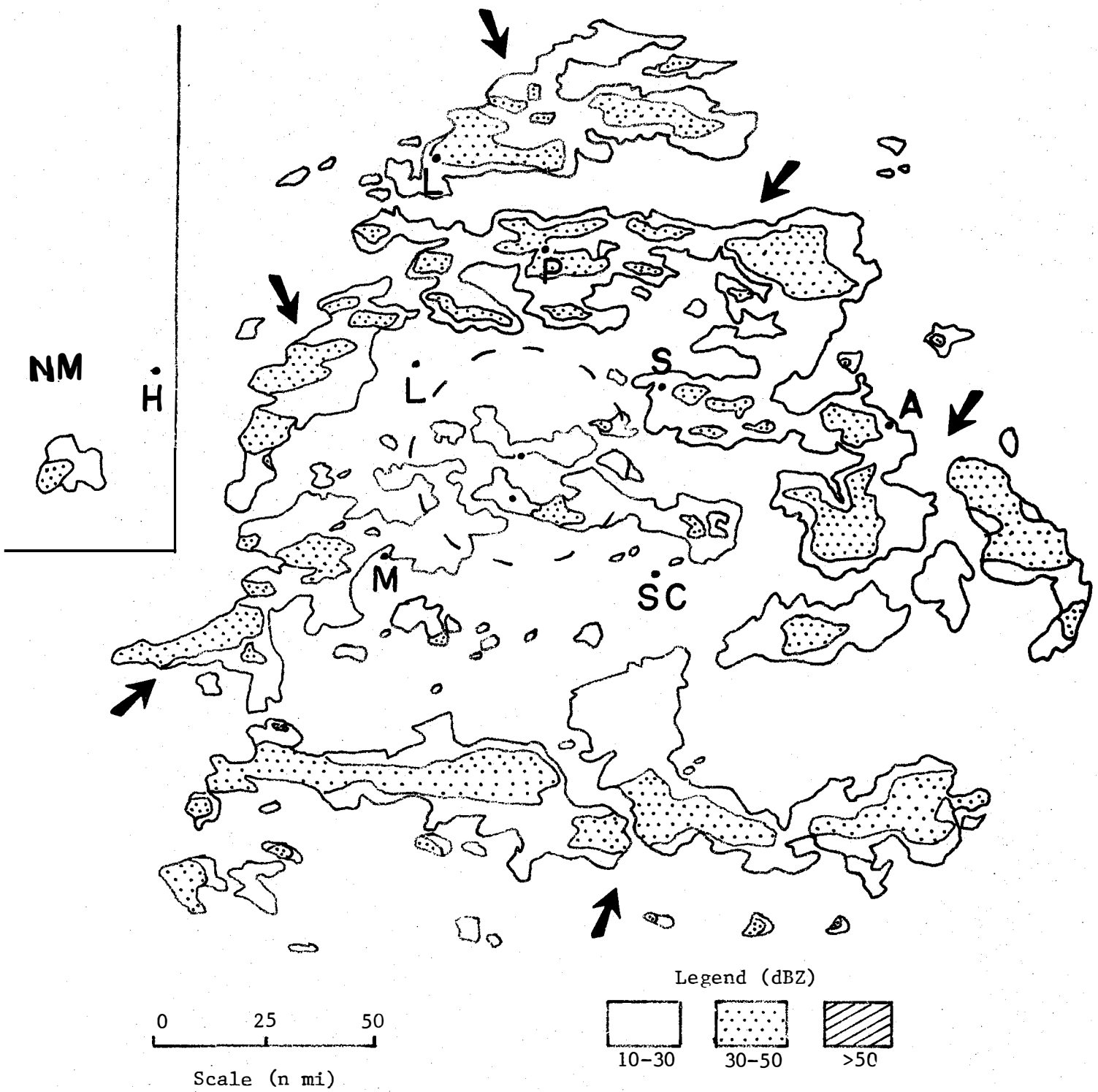
Figure 5.5   An example of large convective clusters taken on 18 July 1979, at 23:23:54 GMT (tilt angle 1.0°)
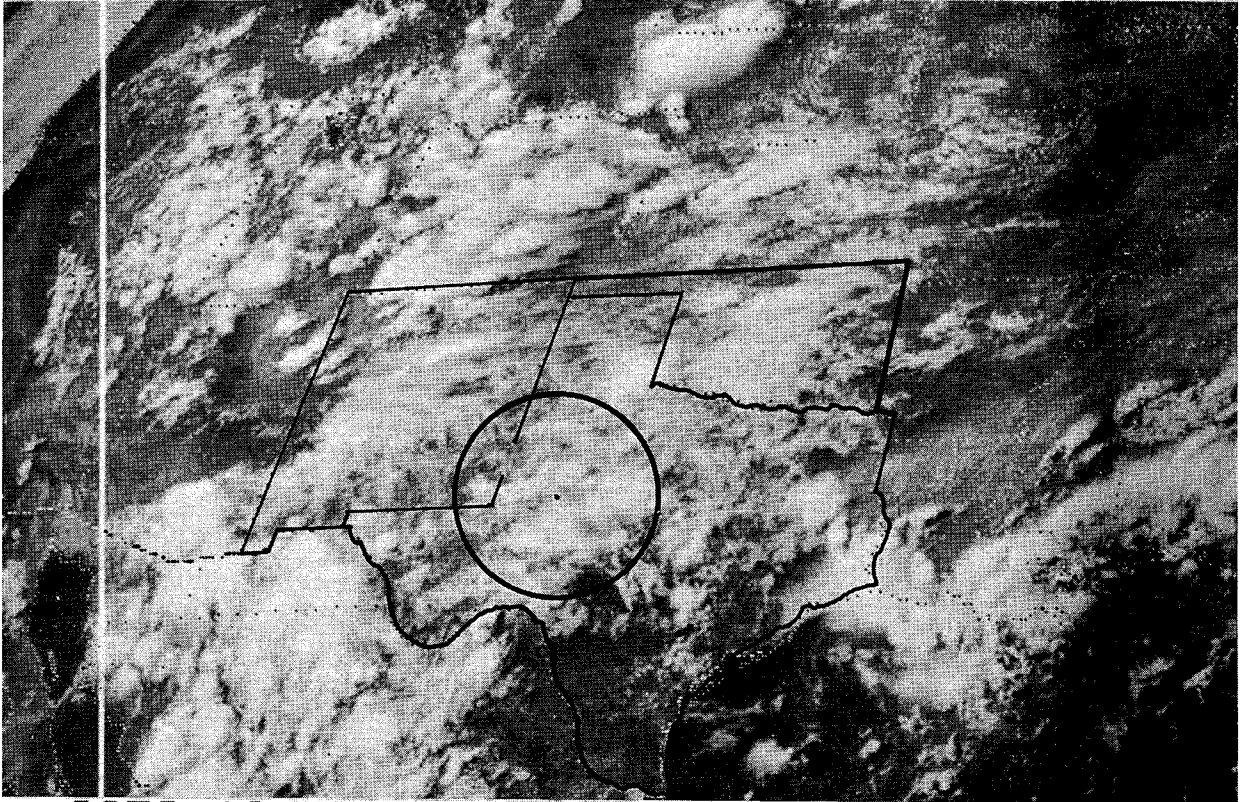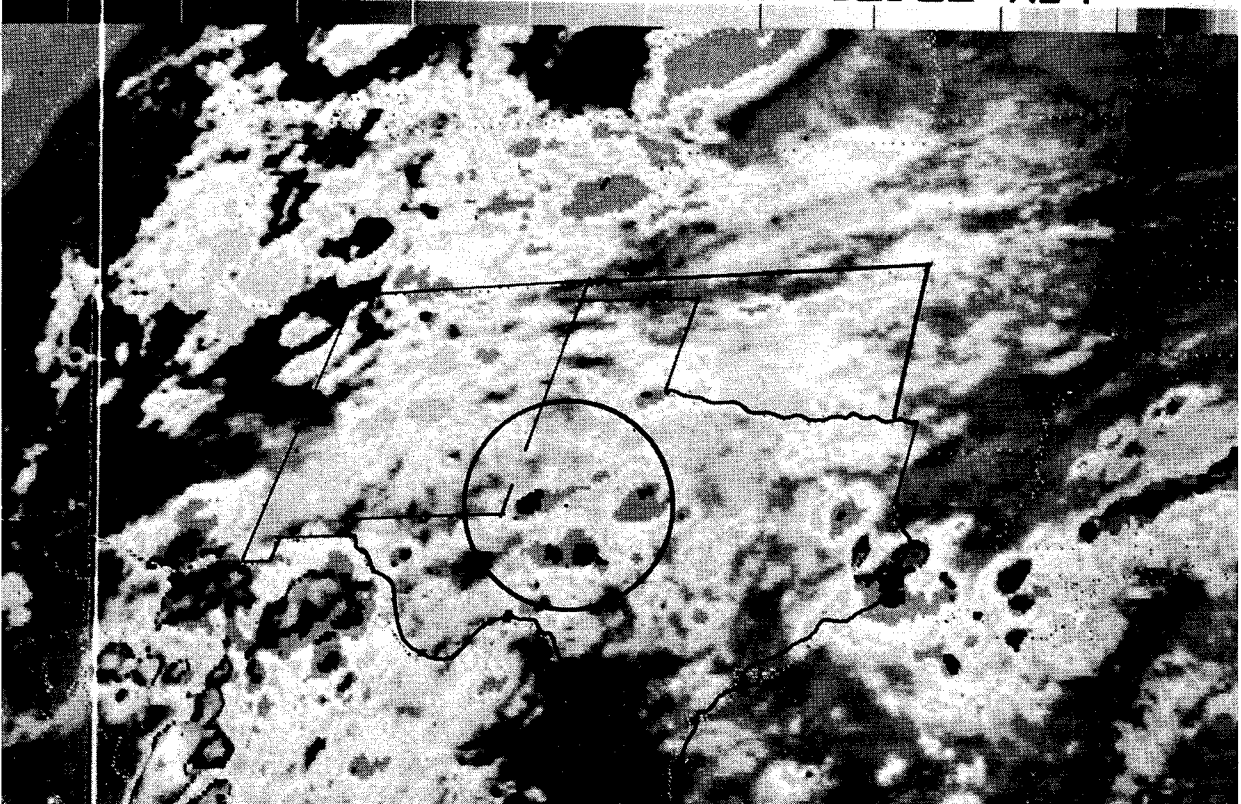
Figure 5.5a Satellite imagery on 18 July 1979, showing the large convective clusters depicted by radar in Figure 5.5; the solid circle corresponds to the total radar coverage in Figure 5.5
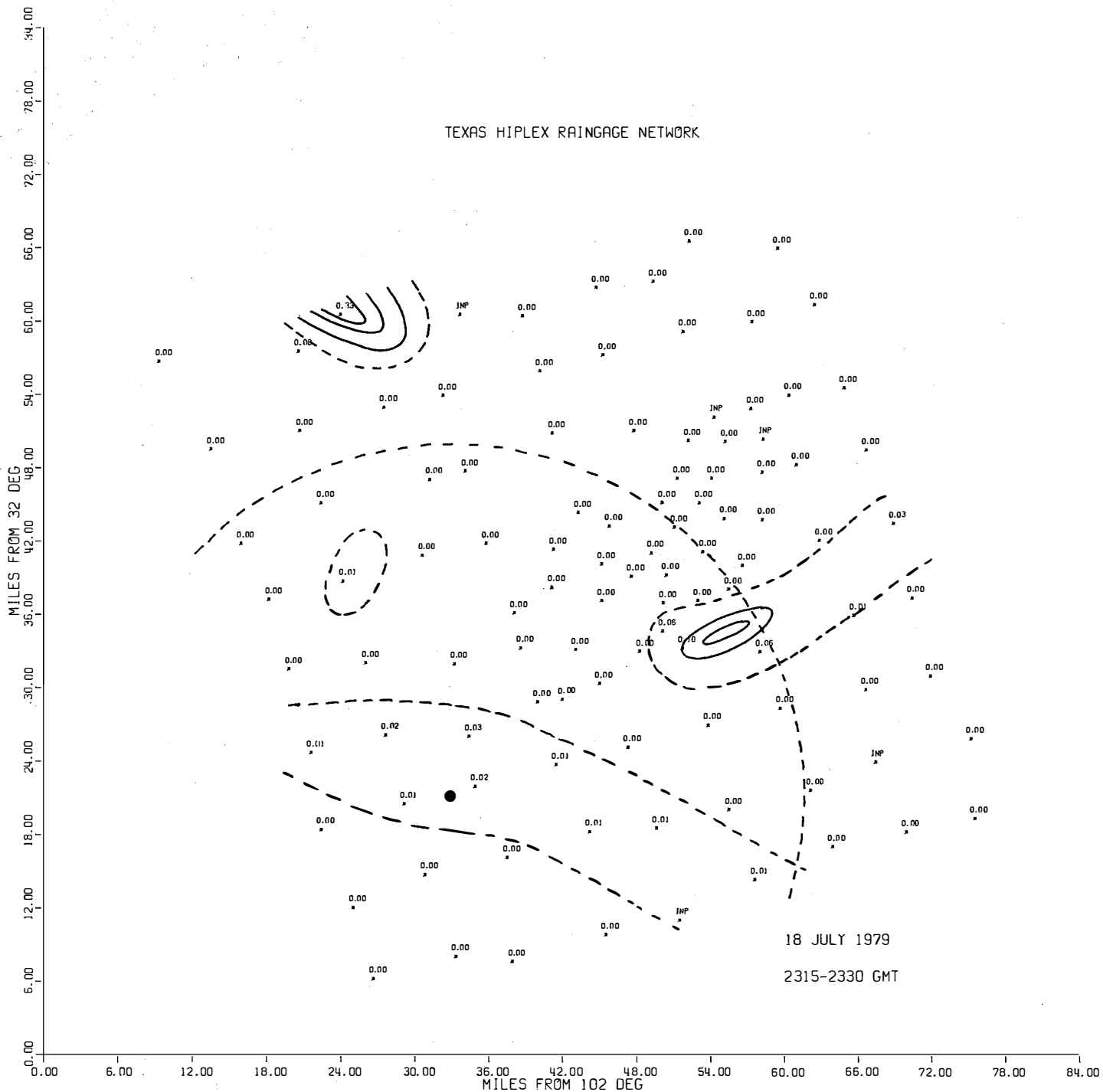
Figure 5.5b   Rainfall observed during 2315-2330 GMT on 18 July 1979, produced by the large convective clusters depicted by radar in Figure 5.5; the dashed circle is at a 25 n. mi. distance from the radar and corresponds to the dashed circle in Figure 5.5
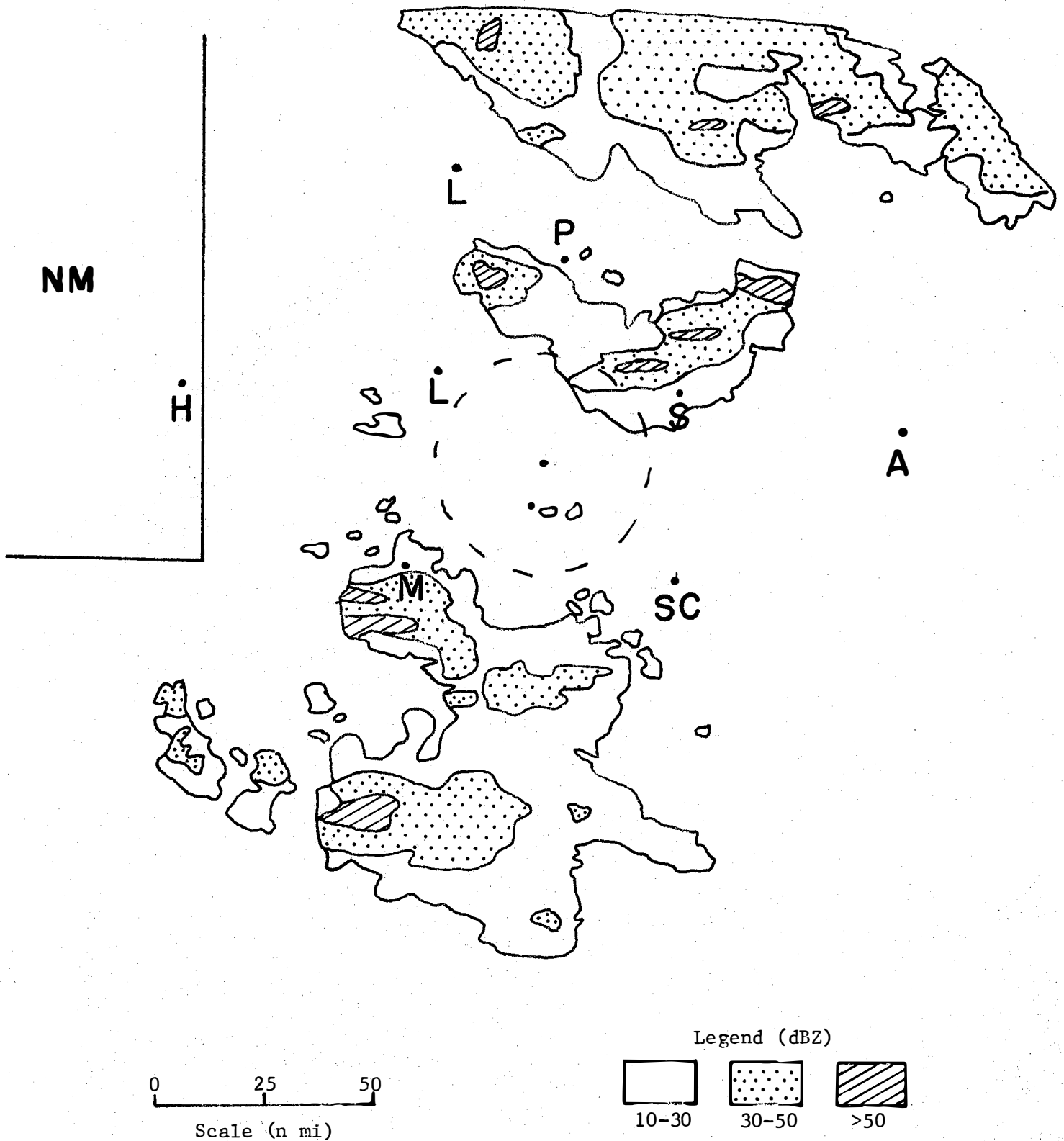
Figure 5.6 An example of nested convective clusters taken on 10 July 1979, at 01:04:31 GMT (tilt angle 1.0°)
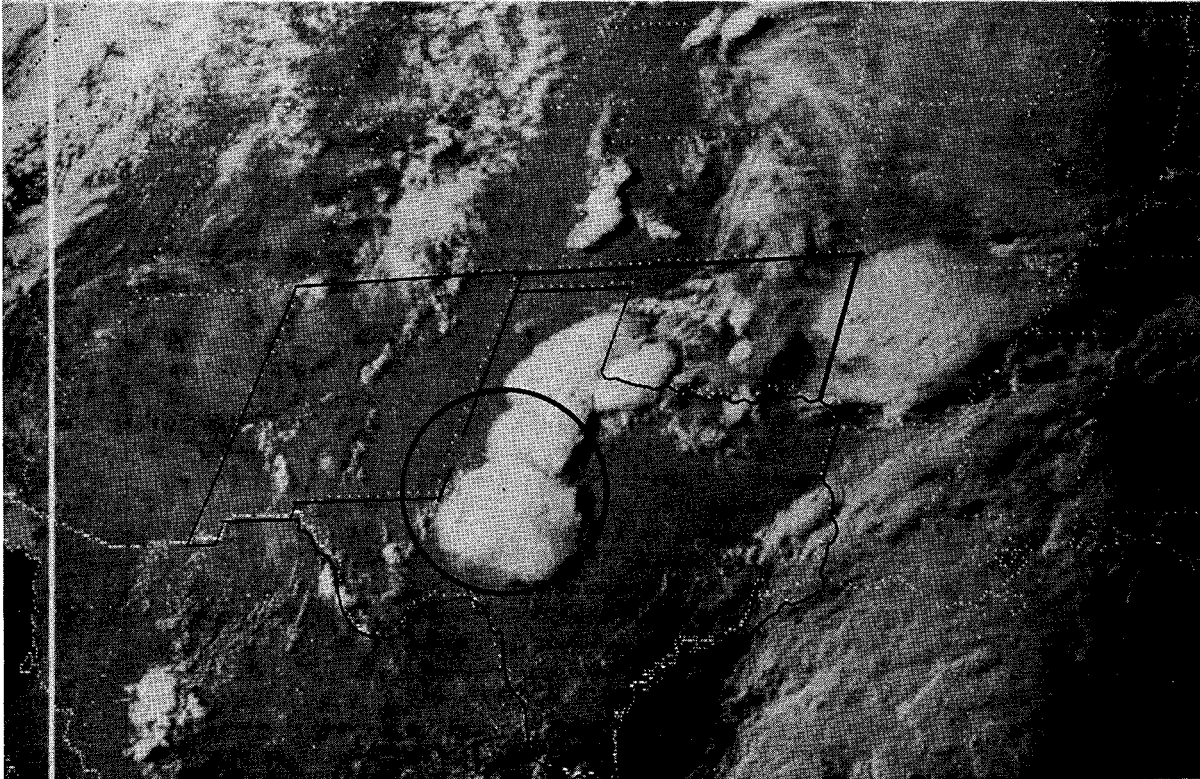
Figure 5.6a Satellite imagery on 10 July 1979, showing the nested convective clusters depicted by radar in Figure 5.6; the solid circle corresponds to the total radar coverage in Figure 5.6
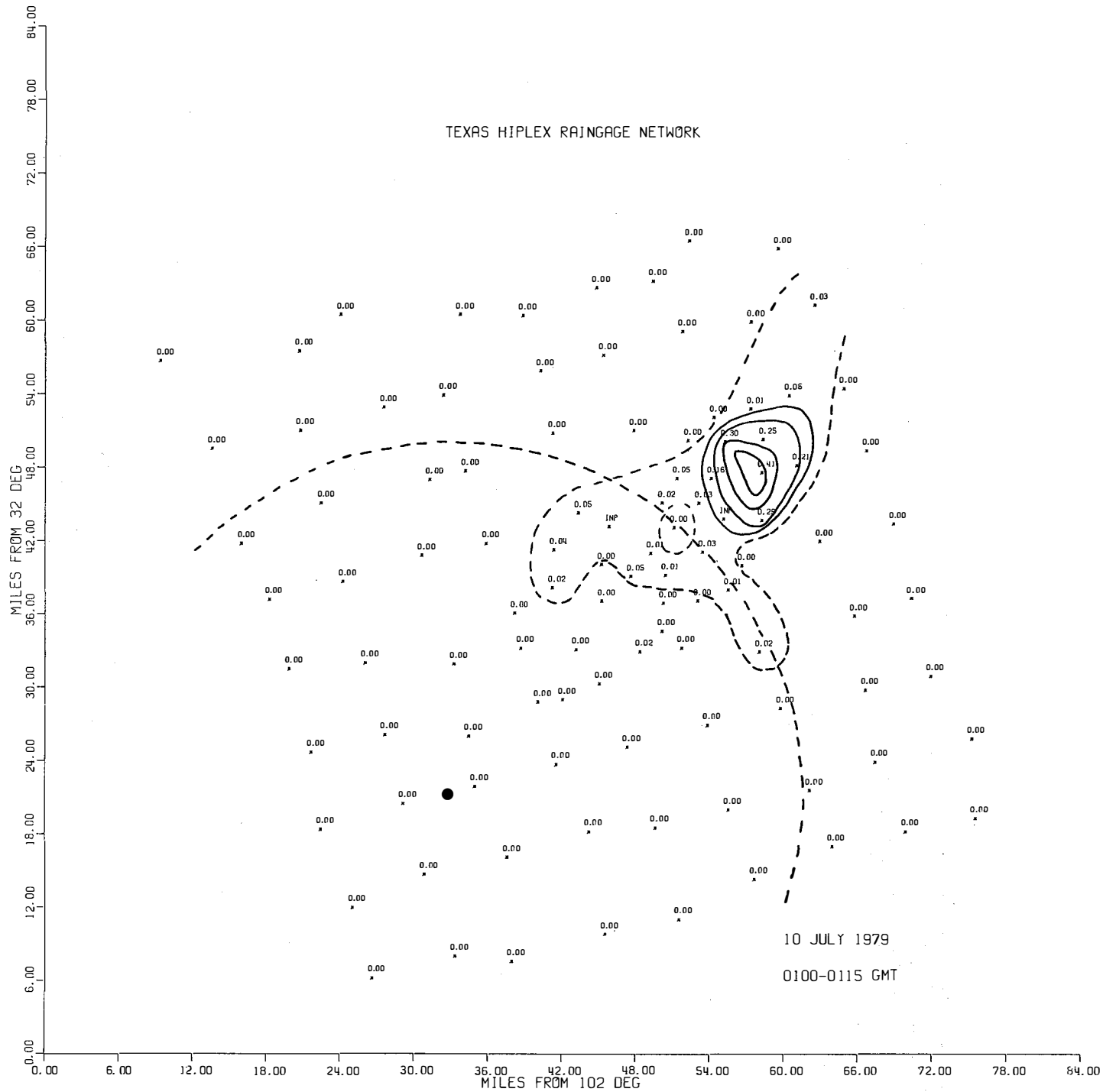
Figure 5.6b   Rainfall observed during 0100-0115 GMT on 10 July 1979, produced by the nested convective clusters depicted by radar in Figure 5.6; the dashed circle is at a 25 n. mi. distance from the radar and corresponds to the dashed circle in Figure 5.6

When convective cells exist in an organized state as a convective cluster, which is admittedly infrequent, a greater portion of summer rainfall (27 percent) has been observed (Sutherland *et al.*, 1980, and Jurica *et al.*, 1981). Therefore, it is conceivable that a positive 10-20 percent seeding effect on cluster rainfall may substantially increase rainfall over the area. The natural variability of rain-on-the-ground could also be documented more easily than with isolated cells (Haragan, 1978), and the seeding effect may be observed more precisely in the rainfall patterns on the ground (Jurica *et al.*, 1981).

There are additional reasons why the study of the convective cluster is worthy of consideration:

— The turrets associated with convective complexes are relatively accessible by aircraft for treatment and sampling;

— The microphysical properties of the turrets can be easily documented;

— New growth areas can be visually verified;

— Past field observations of the microphysical makeup of turrets show that they closely resemble the properties of cells, thereby allowing for ease of technology transfer;

— The environment-cluster system has a longer lifetime than isolated cells, thereby reducing the problem of arriving on station in time for operational treatment;

— The study of clusters in Texas will broaden overall HIPLEX research, and conceivably allow for technology transfer between Montana isolated cell studies and Texas cluster studies;

— Mesoscale and radar data are currently available to address the complexities of the large systems; and

— The study of convective clusters is more closely akin to applied research, as viewed by potential users of the technology.

Further classification of the convective cluster as the experimental unit is necessary. As presented in the previous section, the scale of the cluster, as we have defined it, ranges from small clusters to large clusters, and then to nested clusters. Examples were presented in Figures 5.4, 5.5, and 5.6. Based on the reasons stated in Section 4.5 and on the practical and safety aspects associated with the aircraft limits, the experimental unit shall be "small" clusters (Figure 5.4), as opposed to the larger clusters (Figures 5.5 and 5.6).

The convective line is defined as an organization of echoes along a common axis, and generally enclosed by a common echo boundary. The line which is responsible for 70 percent of the area's summer rainfall is far too complex to select as an experimental unit. It should be pointed out, however, that both the isolated convective cell and the convective line seem to present great opportunities for study. The previous and ongoing investigations of isolated convective cells are leading to an understanding of certain aspects of precipitation processes in the Texas HIPLEX area. Although the convective line appears far too complex to be the target of modification in the near future for Texas HIPLEX, every

effort should be made to study this producer of most of the southern High Plain summer rain at some future time.

The Bureau of Reclamation and the National Center for Atmospheric Research recognized that there was a place for longer and more comprehensive projects in which major emphasis would be placed on understanding the more complex systems. As a result, the *Cooperative Convective Precipitation Experiment* (CCOPE) was adopted*. During the summer of 1981, comprehensive and well coordinated observations were recorded and documented. Hopefully, the results of analyses of convective lines observed during the 1981 CCOPE field season will provide information relevant to the Texas HIPLEX area.

5.4 Tentative Seeding Hypotheses

The primary hypothesis of the Texas HIPLEX Program is that seeding of summertime convective clouds will augment rain on the ground. However, the number of interrelated processes which take place in the precipitation process from the time the cloud is treated to the time rain reaches the ground is quite large. Consequently, a better understanding of these processes is also necessary in order to perform experiments and measure responses. Furthermore, understanding of the physical processes involved is critical to the development of the technology before technology transfer to other areas can be considered. The tentative seeding hypotheses of the Texas HIPLEX Program, the first two of which address the events in the precipitation process, are listed and should provide the focal point of future analysis.

The first two seeding hypotheses which follow are an adaptation of ideas presented for the Florida Area Cumulus Experiment (FACE) most recently by Simpson (1980) and Woodley *et al.* (1981).

5.4.1 Seeding for Dynamic Effects of an Isolated Convective Cell

The tentative hypothesis for dynamic effect seeding of an isolated convective cell is similar to the heavy seeding hypothesis incorporated into previous Texas HIPLEX activity (Texas Department of Water Resources, 1980). The isolated cell is taken to be a cumulus mediocris, cumulus congestus, or towering cumulus, growing through the -5 to -10°C region in an environment not conducive to convective cluster development.

For the reasons cited previously, the isolated convective cell has been selected as a possible experimental unit for the proposed single cloud experiment. Methods of seeding for dynamic effects appear to have the potential for affecting the depth of the isolated convective cell (Matthews, 1981b), and thereby increase the amount of rainfall generated from cloud base. The processes comprising the sequence of events are:

(a) heavy AgI seeding within the updraft region at the -5 to -10°C level of a convective cell leads to freezing of much of the available cloud liquid water;

---

*CCOPE—Preliminary Experiment Design, sponsored by the Bureau of Reclamation and the National Center for Atmospheric Research, March, 1980.

(b)   the latent heat release by freezing of liquid water and by condensation and deposition of water vapor produces positive buoyancy and leads to intensification of the updraft;

(c)   the intensified updraft causes greater inflow of environmental air into lower cloud levels, increasing the water mass ingested by the cell;

(d)   the intensified updraft carries a greater mass of precipitation to higher levels in the cell;

(e)   the greater mass of precipitation descends and produces an enhanced downdraft which penetrates more vigorously into the lower-cloud and sub-cloud layers; and

(f)   more precipitation is carried to the ground within the more protected and favorable environment of the enhanced downdraft (Simpson, 1980).

5.4.2   Seeding for Dynamic Effects of a Convective Cluster

Methods of seeding for dynamic effects appear to present an opportunity to increase the size and lifetime of the cluster and thereby increase rainfall (Matthews, 1981a, and Jurica *et al.,* 1981). Investigation of seeding hypotheses of other rainfall enhancement experiments points to a striking similarity between aspects of the Florida Area Cumulus Experiment (FACE) and Texas HIPLEX conditions. The early stages of FACE entailed a series of experiments on single convective clouds, and specifically sought to increase rainfall through seeding for dynamic effects. During the single cloud experiments it was found that most convective rain fell from large cumulus complexes, consisting of merged convective cells (Simpson and Woodley, 1971). Subsequent interest has been concentrated on the application of seeding for dynamic effects of convective cloud complexes in order to promote organization and growth on the mesoscale.

Simpson (1980) suggests that the ability of gust fronts to enhance summertime convective clouds depends upon the kinematic structure of the environment relative to the cloud. Linkage of the two may involve such parameters as vertical shear and horizontal convergence. Chen *et al.* (1978) and Jurica *et al.* (1981) observed similar characteristics in Texas HIPLEX clouds.

The processes hypothesized by Simpson that comprise the sequence of events leading to enhanced rainfall from seeding for dynamic effects of convective clusters are:

(a)   heavy AgI seeding within the updraft region of the -5 to -10°C level of a convective turret leads to freezing of much of the available cloud-liquid water;

(b)   the latent heat released by freezing of liquid water and by condensation and deposition of water vapor produces positive buoyancy, and leads to intensification of the updraft;

(c) the intensified updraft causes greater inflow of environmental air into lower cloud levels, increasing the water mass ingested by the cell;

(d) the intensified updraft carries a greater mass of precipitation to higher levels in the cell;

(e) the greater mass of precipitation descends and produces an enhanced downdraft which penetrates more vigorously into the lower-cloud and sub-cloud layers;

(f) the enhanced downdraft produces convergence at the boundary of the downdraft region at low levels within the convective cluster, forcing stronger updrafts within other nearby cluster cells, enhancing the growth of these cells, and extending the duration of the cluster;

(g) the enhanced downdraft produces low-level convergence at the boundary of the cluster, and induces development of new cells which become part of the cluster and increase the horizontal size of the cluster;

(h) either f or g, or both f and g can occur, resulting in a longer-lived cluster, a larger cluster, or both;

(i) the longer-lived cluster produces more rain by ingesting and processing greater volumes of cloud water, and by extending the duration of precipitation processes;

(j) the larger cluster produces more rain by allowing the precipitation processes to take place in a more protected and, therefore, more favorable environment; and

(k) either i or j, or both i and j can occur.

5.4.3 Seeding for Microphysical Effects

The findings of the Texas HIPLEX Program have not ruled out the seeding for microphysical effects hypothesis for a Texas cloud seeding experiment. A principal area of uncertainty in the Texas HIPLEX Program is in the microphysical rain-making process. Additional microphysical studies need to be conducted and linked with mesoscale observations to determine the natural precipitation efficiencies of West Texas convective clouds. If the precipitation efficiencies are found to be small, then microphysical seeding to increase the clouds natural efficiency may be a viable option for the Texas cloud seeding experiment.

5.5 Response Variables

Following is a tentative list of response variables identified from consideration of seeding hypotheses, physical reasoning, and measurement capacity. The list will be revised and prioritized as the research progresses. The proposed measurement instruments are shown in parentheses.

— Development of detached or new cells away from the cluster along the gust front. (Radar and Cloud Base Aircraft)

— Change in precipitation patterns. (Raingages and Radar)

— Storm rainfall variations with time. (Raingages and Radar)

— Appearance of precipitation-size particles at the treatment level within the downdraft and later near cloud base. (Penetration & Cloud Base Aircraft)

— Change of horizontal area within a specifed dBz value for clusters and/or cells. (Radar)

— Changes in reflectivity levels. (Radar)

— Change in ice concentration at treatment level. (Penetration Aircraft)

— Change in growth rates of cells or turrets containing liquid water. (Radar)

— Changes in liquid water content of turret. (Penetration Aircraft)

— Changes in outflow from below the base of the treated storm. (Rawinsonde, Surface Weather Network and Cloud Base Aircraft)

— Increased horizontal moisture convergence below the level of seeding. (Rawinsonde and Surface Weather Network).

5.6 Future Work

To bring the exploratory portion of the Texas HIPLEX Program to a meaningful and satisfactory conclusion, it is necessary to complete the experimental design document. The design document will be considered the master plan for conducting the experimental phase, which is the second phase of the multi-phase Texas HIPLEX Program. The design document, when completed, will identify the experimental unit, statistical hypothesis, experimental unit declaration criteria, experimental procedure, seeding technique, and statistical evaluation method.

The Texas HIPLEX experimental design document cannot be completed unless a number of lingering uncertainties are resolved. The tasks listed below need to be addressed to resolve those uncertainties.

5.6.1. Meso β-scale Tasks

A successful rainfall enhancement experiment depends upon both a plausible seeding hypothesis to test, and seeding criteria to define carefully those conditions which must be present for the seeding hypothesis to apply. The Texas HIPLEX Program has demonstrated that the seeding criteria should include information at the three mesoscale levels, i.e., meso α-, meso β- and meso γ-scale. The Texas HIPLEX Program has produced one of the most accurate and comprehensive environmental mesoscale data bases in the nation. The mesoscale stratification criteria, covariates, and response variables, identified by previous case study

analyses need to be reexamined, quantified and confirmed. Therefore, the following mesoscale tasks need to be completed.

(a)   *Descriptive models.* Descriptive mesoscale models need to be developed and interpreted in terms of dynamic, thermodynamic and kinematic processes to better define and confirm: the initiation mechanisms for convective activity; the cloud—environment interactions; and the impact of seeding for dynamic effects on convective cluster development and the environment.

(b)   *Interpret model results.* The Texas HIPLEX seeding for dynamic effect hypothesis stratification, criteria covariates, and response variables need to be reexamined and confirmed or modified in terms of the descriptive model results.

(c)   *Refine the cluster-seeding hypotheses through detection of rainfall.* Evidence from gage-monitoring of surface rain events has clearly established that organized convective complexes (small, large and nested clusters) are the primary precipitation producers in West Texas during the warm season (Haragan *et al.,* 1981). Spatial limitations on the extent of the surface network require long periods of record to insure adequate sampling of all classes of events.

The raingage network operated by the Colorado River Municipal Water District (CRMWD) has produced a long, continuous record of rainfall over a limited area. When dealing with a limited area, it is imperative to acquire as long a time record as possible to counter-balance the effect of the limited space scale. Thus, the raingage network needs to be operated in order to maintain this very valuable record, since it offers scientific benefits which extend beyond the scope of the Texas HIPLEX Program.

(d)   *Conduct physical evaluation studies of the structure and evolution of clusters.* Monitoring surface rainfall patterns with 15-minute temporal resolution provides a means of tracking storm systems and their changes in space and time (Haragan, 1978). Structure of the cloud cluster is indicated by the evolution of rainfall intensity, spatial changes in rainfall patterns, total-volume rainfall, and storm speed and direction. This information, coupled with the meso β-scale analysis and the cloud microphysical analysis, is needed to establish seeding criteria.

(e)   *Establish response variables in terms of rainfall natural variability.* The natural variability of West Texas rainfall is large on all time scales. Variability is high for both the distribution of rainfall events and the amount of rain received per event (Haragan, 1979). For a particular day, clusters which develop in a similar environment in response to the same dynamic or thermodynamic trigger may produce vastly different rainfall patterns at the ground (Haragan *et al.,* 1981). By establishing the natural variability of rainfall produced by convective cell clusters, response variables will be established which take into account the expected variability. Also, the expected length of the experimental period required to reach statistical significance based on rainfall amounts can be better estimated.

(f)   *Establish the natural behavior and variability of the convective complex.* This task is needed to assess the impact of seeding of a convective complex on the

meso γ-scale features including downdrafts, mesohighs, gust fronts, and subsequently rainfall amounts.

5.6.2 Microscale Tasks

Although certain meso β-scale parameters are expected to help define the "suitability" of a convective cell or cluster for treatment, the microscale state of the convective cell or cluster selected for treatment is of equal importance. The micro-scale tasks which need to be accomplished are listed below.

(a) *Establish and quantify seeding criteria in terms of microscale properties.* Due to the scarcity of cloud microphysical data, it is necessary to collect and analyze additional data needed to quantify general microphysical properties in both convective cells and clusters. This information needs to be used with meso-scale observations to determine the natural efficiency of the precipitation process and to quantify expected microphysical seeding effects.

In addition, microphysical seeding criteria for convective cells and clusters will be established and linked with meso β-scale criteria. The microphysical seeding criteria will include establishing the "seeding window," the seeding altitude, material and amounts, and the cloud selection criteria.

(b) *Develop the seeding hypotheses through documenting the behavior of hydrometeors.* The immediate evidence of a response to seeding for dynamic effects of a cell is the appearance, within the updraft, of glaciated conditions accompanied by an enhanced updraft. In-cloud sampling can document the evolution of hydrometeors and the direct response at the -5°C to -10°C level. However, a critical link in the chain of events leading to the hypothesized increase in cluster rainfall is the appearance of precipitation particles low in the enhanced downdraft region, and the presence of increased vertical motions away from the enhanced downdraft. Therefore, a cloud base aircraft equipped with instrumentation capable of reliable vertical velocity and precipitation particle measurements is needed to help verify steps e and f of the tentative seeding hypotheses.

5.6.3 Supportive Tasks

(a) *Establish experimental procedures and evaluation techniques.* Local climatological studies of the Texas HIPLEX summertime shower-producing clouds by Haragan *et al.* (1978) and Sutherland *et al.* (1980) suggest that rain on the ground from isolated convective cells is much too difficult to measure with the existing Texas HIPLEX recording raingage network. The variability present in ground-truth measurements is so great that it would require an extremely large data base and/or many more years of data gathering before statistically significant seeding effects can be detected. Also, the greater rain-producing, and possibly less variable, clusters occur much less frequently than isolated con-

vective cells, thereby requiring many more years of data gathering before statistically significant seeding effects can be detected. Therefore, it is proposed to develop a design document for a physical experiment to define and better understand the physical aspects of the seeding hypothesis concomitant with developing a statistical cloud seeding experiment.

(b) *Continue a critical link in Federal/State cooperation through local citizen support.* Two distinctive aspects of the Texas HIPLEX Program have been financial support and staff participation by the State of Texas, together with the strong support of the citizenry in the area of the field experiments. The raingage network operated by the CRMWD has for years given visible evidence of the concern and efforts to increase the water available for agricultural and municipal water needs of the area. The importance of State and local support to a program of this nature cannot be overemphasized and must be maintained.

(c) *Continue Socio-economic Studies.* The success of the Texas HIPLEX Program will not be measured by the scientific findings of fact but by how the public perceives those findings. Therefore, it is important that sociological and economic studies continue concomitant with the technical studies.

ACKNOWLEDGEMENTS

REFERENCES

Ackerman, B., G. L. Achtemeier, H. Appleman, S. A. Changnon, F. A. Huff, G. M. Morgan, P. T. Schickedanz, and R. G. Semonin, 1971: Design of the High Plains experiment with specific focus on Phase 2 single cloud experimentation. Bureau of Reclamation Contract No. 14-06-0-7191, 231 pp.

Alexander, W. O., and R. F. Riggio, 1978: A Texas HIPLEX forecast decision tree. TDWR LP-74, Texas Department of Water Resources, Austin, Texas, 50 pp.

_____, 1980: Texas HIPLEX 1979 Field Operations Summary. TDWR LP-112, Texas Department of Water Resources, Austin, Texas 397 pp.

_____, 1981: Texas HIPLEX 1979 Field Operations Summary. TDWR LP-138, Texas Department of Water Resources, Austin, Texas, 418 pp.

Allaway, W., L. Lippke, R. F. Riggio, and C. Tuck, 1975: The economic effects of weather modification activities. Part I: Crop production in the Big-Spring Snyder area. TDWR WR-1, Texas Department of Water Resources, Austin, Texas, 50 pp.

Anthes, A., and T. Warner, 1978: Development of hydrodynamic models suitable for air pollution and other mesometeorological studies. *Mon. Wea. Rev., 106,* 1054-1078.

Bark, L. Dean (1975), A survey of the radar echo population over the western Kansas High Plains, Vol. 1, Dept. of Physics, Kansas Agricultural Experiment Station, Kansas State University, Manhattan, Kansas.

Barnes, S. L., 1964: A technique for maximizing detail in numerical weather map analysis. *J. Appl. Meteor., 3,* 396-409.

Blackadar, A., 1979: High-resolution models of the planetary boundary layer. *Adv. Envir. Sc. Eng., 1,* 50-85.

Bleck, R., 1978: On the use of hybrid vertical coordinates in numerical weather prediction models. *Mon. Wea. Rev., 106,* 1233-1244.

Braham, R. R., Jr., and Squires, 1974: Cloud Physics 1974. *Bull. Amer. Meteor. Soc., 55,* 543-556.

Byers, H. R., and R. R. Braham, 1949: *The Thunderstorm.* U. S. Government Printing Office, Washington, D. C., 287 pp.

Carbone, R. E., P. LeVieu, and R. Schaff, 1976: M-33 radar modification at Snyder, Texas. MRI 76 FR-1445. Bureau of Reclamation Contract No. 14-06-D-7657, Meteorology Research, Inc. Altadena, California, 30 pp.

Chen, C. H. and H. D. Orville, 1980: Effects of mesoscale convergence on cloud convection. *J. Appl. Meteor., 19,* 256-274.

Chen, P. C., M. E. Humbert, and T. B. Smith, 1979: Radar echo organization and development in the mesoscale environment — a case study approach. MRI 78 FR-1580 Tech. Rep., Bureau of Reclamation Contract No. 14-06-D-7587, Meteorology Research, Inc., Altadena, Calif., 89 pp. Also published as: TDWR LP-97 Texas Department of Water Resources, Austin, Texas.

Das, P., 1970: On the concentration of precipitation particles in convective storms. *J. Atmos. Sci., 27,* 330-332.

Driscoll, D. M., 1978: A radar-echo climatology for Southern HIPLEX, TDWR LP-64, Texas Department of Water Resources, Austin, Texas, 89 pp.

_____, 1980: Investigations of the Radar-Echo Climatology of Southern HIPLEX, TDWR LP-121, Texas Department of Water Resources, Austin, Texas, 130 pp.

Eaves, C. D., 1952: Charles William Post. *The Handbook of Texas, Volume 2,* 397.

Eskridge, R. E., and P. Das, 1976: Effect of precipitation-driven downdraft on rotating-wind field: A possible trigger mechanism for tornadoes. *J. Atmos. Sci., 33,* 70-84.

Fankhauser, J. C., 1969: Convective processes resolved by a mesoscale rawinsonde network, *J. Appl. Meteor., 17,* 415-425.

Friend, A. L., D. Djuric, and K. C. Brundidge, 1976: Numerical weather prediction using a combination of isentropic and sigma coordinates. *Annalen der Meteorologie (Neue Folge), 11,* 9-12.

_____, 1977: A combination of isentropic and sigma coordinates in numerical weather prediction. *Contrib. Phys. Atmos., 50,* 290-295. Also published in: Amer. Meteor. Soc., *Third Conference on Numerical Prediction,* Omaha, 388-396.

Fritsch, J. M., and C. F. Chappell, 1981: Preliminary numerical tests of the modification of mesoscale convective systems. *J. Appl. Meteor., 20,* 910-921.

Fujita, T., 1963: Analytical mesometeorology: A review. *Meteor. Monogr.,* No. 27, Amer. Meteor. Soc., 77-125.

Gerhard, M. L., and J. R. Scoggins, 1981: Potential Flow Models of Thunderstorm-Environment Interaction. TDWR LP-170, Texas Department of Water Resources, Austin, Texas, 75 pp.

Girdzus, J. P., 1979: 1979 Weather Modification Program Rain Enhancement, Colorado River Municipal Water District, Big Spring, Texas, 32 pp.

Girdzus, J. P., 1980: 1980 Weather Modification Program Rain Enhancement, Colorado River Municipal Water District, Big Spring, Texas, 32 pp.

Griffith, C. G., W. L. Woodley, and J. A. Augustine, 1980: The estimation of convective summertime rainfall in the United States High Plains from thermal infrared geostationary satellite data-Volume 1. Final Report, Water and Power Resources Services, Denver, Colorado, 49 pp.

Haltiner, G. J., 1971: *Numerical Weather Prediction,* New York, Wiley, 317 pp.

Haragan, D. R., 1978: Precipitation climatography for the HIPLEX southern region. TDWR LP-63, Texas Department of Water Resources, Austin, Texas, 64 pp.

Haragan, D. R., G. M. Jurica, and C. A. Leary, 1980: Determination of cloud and precipitation characteristics from satellite, radar, and raingage analysis. TDWR LP-127 Texas Department of Water Resources, Austin, Texas, 70 pp.

Hartzell, C. L., 1977, Development of objective forecasting techniques for the Montana HIPLEX project area. Western Scientific Services, Inc., Fort Collins, Colorado, 50 pp.

Hearings before the Committee on Commerce, U.S. Senate, 89th Congress, 1966. U.S. Government Printing Office, Washington, D. C.

Henderson, T. J., and Changnon, S. A., Jr., 1972: 3rd AMS Conf. Weather Modification, Rapid City, South Dakota, 260-264 (preprints).

Houghton, H. G., 1968: On precipitation mechanisms and their artificial modification. *J. Appl. Meteor., 7,* 851-859.

House, D. C., 1959: The mechanics of instability line formation, *J. Meteor., 16,* 108-127.

Houze, R. A., Jr., 1977: Structure and dynamics of a tropical squall-line system. *Mon. Wea. Rev., 105,* 1540-1567.

Houze, R. A., Jr., C. P. Cheng, C. A. Leary, and J. F. Gammage, 1980: Cloud mass and heat fluxes over tropical oceans: Diagnosis from radar and synoptic data. *J. Atmos. Sci., 37,* 754-773.

Hsie, E. Y., R. D. Farley, and H. D. Orville, 1980: Numerical simulation of ice-phase convective cloud seeding. *J. Appl. Meteor., 19,* 950-977.

Huff, F. A., 1967: Time distribution of rainfall in heavy storms. *Water Resources Research, 3,* 1007-1019.

Humbert, M. E., S. M. Howard, P. C. Chen, and T. B. Smith, 1978: Development and interpretation of a M-33 radar climatology for the Texas HIPLEX region. MRI 78 FR-1581 Tech. Rep., Meteorology Research, Inc., 37 pp.

Humbert, M. E., G. J. Mulvey, T. B. Smith, D. M. Takeuchi, and P. C. Chen, 1979: Observed cloud characteristics and their influence on Texas HIPLEX Program plan. Paper presented at the

AMS Seventh Conference on Inadvertent and Planned Weather Modification, October 8-12, 1979, Banff, Alberta, Canada.

Jurica, G. M., and S. Y. Chi, 1979: Determination of cloud properties from bispectral satellite measurements. TDWR LP-92, Texas Department of Water Resources, Austin, Texas, 101 pp.

Jurica, G. M., and Meteorology Research, Inc., 1979: Texas HIPLEX 1978 Satellite and Radar Data Summary. TDWR LP-84, Texas Department of Water Resources, Austin, Texas.

Jurica, G. M., D. R. Haragan, and C. A. Leary, 1981: Investigations of summer convective cloud systems in the Texas High Plains. TDWR LP-174, Texas Department of Water Resources, Austin, Texas, 205 pp.

Kengla, M., R. Morey, J. Hull, and H. W. Grubb, 1979: The economic effects of weather modification activities. Part III: Irrigated and dryland agriculture with estimates of production, and income effects on the area economy. TDWR LP-21, Texas Department of Water Resources, Austin, Texas, 59 pp.

Leary, C. A., 1979: Behavior of the wind field in the vicinity of a cloud cluster in the intertropical convergence zone. *J. Atmos. Sci., 36,* 631-639.

Leary, C. A., and R. A. Houze, Jr., 1980: The contributions of mesoscale motions to the mass and heat fluxes of an intense tropical convective system. *J. Atmos. Sci., 37,* 784-796.

Lippke, L. A., 1976: The economic effects of weather modification activities. Part II: Range production and interindustry analysis. TDWR WR2, Texas Department of Water Resources, Austin, Texas, 83 pp.

Long, A. B., 1980: Preliminary cloud microphysics studies for Texas HIPLEX 1979. TDWR LP-124, Texas Department of Water Resources, Austin, Texas, 75 pp.

Longley, R. W., 1974: Spatial variation of precipitation over the Canadian prairies. *Mon. Wea. Rev., 102,* 307-312.

Matthews, D. A., 1980: Summary of clouds and mesoscale forcing observed from synchronous meteorological satellites during the High Plains Cooperative Program 1976-1977. Technical Report Bureau of Reclamation, Denver, Colorado.

_____, 1981a: Observations of a cloud arc triggered by thunderstorm outflow *Mon Wea. Rev., 109,* 2140-2157.

_____, 1981b: Natural variability of thermodynamic features affecting convective cloud growth and dynamic seeding: A comparative summary of three high plain sites from 1975 to 1977. *J. App. Meteor., 20,* 971-996.

_____, 1983: Analysis and classification of mesoscale triggering effects on convective clouds and precipitation. Technical Report, Bureau of Reclamation, Denver, Colorado.

Matthews, D. A., and B. A. Silverman, 1980: Sensitivity of convective cloud growth to mesoscale lifting: A numerical analysis of mesoscale convective triggering. *Mon. Wea. Rev., 108,* 1056-1064.

Mellor, G. L., and T. Yamada, 1974: A hierarchy of turbulence closure models for planetary boundary layers. *J. Atmos. Sci., 31,* 1791-1806.

Miller, T. L., and K. C. Young, 1979: A numerical simulation of ice crystal growth from the vapor phase. *J. Atmos. Sci., 36,* 458-469.

Mossop, S. C., 1978: Some factors governing ice particle multiplication in cumulus clouds. *J. Atmos. Sci., 35,* 2033-2037.

Mulvey, G. J., and M. Young, 1980: Processing of the M-33 Snyder, Texas radar data. MRI 79 FR-1723 Final Report TWDB Contract No. 14-80038, Texas Department of Water Resources, Austin, Texas, 207 pp.

Newton, C. W., 1967: Severe Convective Storms, *Advances in Geophysics,* Vol. 12, Academic Press, 257-303.

Nickerson, E. C. 1979: On the numerical simulation of airflow and clouds over mountainous terrain. *Contrib. Atmos. Phys., 52,* 161-177.

Orlanski, I., 1975; A rational subdivision of scales for atmospheric processes. *Bull. Amer. Meteor. Soc., 56,* 527-530.

Orville, H. D., and F. J. Copp, 1977: Numerical simulation of the life history of a hailstorm. *J. Atmos. Sci., 34,* 1597-1618.

Perkey, D. J., 1976: A description and preliminary results from a fine-mesh model for forecasting quantitative precipitation. *Mon. Wea. Rev., 104,* 1513-1526.

Pielke, R., 1974: A three-dimensional numerical model of the sea breezes over South Florida. *Mon. Wea. Rev., 102,* 115-139.

Pielke, R., and Y. Mahrer, 1978: Verification and analysis of the University of Virginia three-dimensional mesoscale model prediction over South Florida for 1 July 1973. *Mon. Wea. Rev., 106,* 1568-1589.

Powers, E., 1890: War and the Weather, E. Powers (Revised Edition) Delavan, Wisconsin.

Reynolds, D. W., and E. A. Smith, 1979: Detailed analysis of composited digital radar and satellite data, *Bull. Amer. Meteor. Soc., 60,* 1024-1037.

Reynolds, P. G., M. L. Gerhard, G. S. Wilson, and J. R. Scoggins, 1979: Texas HIPLEX mesoscale experiment—Summer 1978 data tabulations. TDWR LP-80, Texas Department of Water Resources, Austin, Texas, 584 pp.

Rhea, O., 1966: A study of thunderstorm formation along dry lines, *J. Appl. Meteor. 5,* 58-63.

Riggio, R. F., and W. O. Alexander, 1978: Texas HIPLEX 1978 Field Operations Summary. TDWR LP-73, Texas Department of Water Resources, Austin, Texas, 281 pp.

Riggio, R. F., and K. Topham, 1979: Using discriminant analysis to predict the rainshower occurrence in the High Plains area. Paper presented at the Sixth Conference on Probability and Statistics in Atmospheric Sciences.

Schaefer, J., 1974: Motion and morphology of the dry line, *J. Atmos. Sci., 31,* 956-964.

Schickedanz, P. T., 1974: Evaluation of rainfall data in the vicinity of the Texas hail suppression program. Atmospherics, Inc., Fresno, California, 27 pp.

_____, 1975: Evaluation of hail suppression. NHRE Symposium/Workshop on Hail: Preprint Vol. 1, NCAR Boulder, Colorado, 24 pp.

Schroeder, M. J., and E. Klazura, 1978: Computer processing of digital radar data gathered during HIPLEX. *J. Appl. Meteor., 17,* 498-507.

Scoggins, J. R., 1977: Texas HIPLEX mesoscale experiment—Summer 1977 data tabulations. TDWR L-10, Texas Department of Water Resources, Austin, Texas 565 pp.

Scoggins, J. R., J. F. Griffiths, H. O. Hartley, R. D. Lacewell, and G. W. Bomar, 1975: An evaluation of weather modification activities in the Texas High Plains. TDWR LP-193, Texas Department of Water Resources, Austin, Texas, 91 pp.

Scoggins, J. R., H. E. Fuelberg, S. F. Williams, and M. E. Humbert, 1978: Mesoscale characteristics of the Texas HIPLEX area during summer 1976. TDWR LP-65, Texas Department of Water Resources, Austin, Texas, 343 pp.

Scoggins, J. R., and G. S. Wilson, 1976: Texas HIPLEX mesoscale experiment—Summer 1976 data tabulations. TWDB 76-12, Texas Department of Water Resources, Austin, Texas, 545 pp.

Scoggins, J. R., G. S. Wilson, and S. F. Williams, 1979: Mesocale characteristics of the Texas HIPLEX area during summer 1977. TDWR LP-99, Texas Department of Water Resources, Austin, Texas, 433 pp.

Sienkiewicz, M. E., J. R. Scoggins, S. F. Williams, and M. L. Gerhard, 1980: Mesoscale characteristics of the Texas HIPLEX area during the summer 1978. TDWR LP-123, Texas Department of Water Resources, Austin, Texas, 609 pp.

Simpson, J., 1980: Downdrafts as linkages in dynamic cumulus seeding effects. *J. Appl. Meteor., 19,* 477-487.

Simpson, J., and W. H. Woodley, 1975: Florida area cumulus experiment 1970-1973 rainfall results. *J. Appl. Meteor., 14,* 734-744.

Smith, T. B., R. L. Peace, and S. M. Howard, 1977: Radar evaluation of Big Spring Weather Modification Program. TDWR LP-5, Texas Department of Water Resources, Austin, Texas.

Smith, T. B., D. M. Takeuchi, and C. W. Chien, 1974: San Angelo Cumulus Project. Final Report MRI 74 FR-1244., Bureau of Reclamation Contract No. 14-06-D-7132, Meteorology Research, Inc., Altadena, California, 100 pp. Also prepared for the Texas Water Development Board, Austin, Texas.

Sutherland, J. L., H. R. Swart and D. A. Griffith, 1980: Analysis of digitized M-33 radar data from Texas HIPLEX 1976-1978. TDWR LP-135, Texas Department of Water Resources, Austin, Texas, 54 pp.

Takeuchi, D. M., 1980: Microphysics observations of convective clouds in the Texas HIPLEX area. MRI 80 RM-1765, Bureau of Reclamation Contract No. 14-06-D-7699, Meterology Research, Altadena, California, 66 pp.

_____, 1981: MRI airborne research studies in support of HIPLEX. MRI 81 FR-1799, Bureau of Reclamation Contract No. 14-06-D-7699, Meteorology Research, Inc., Altadena, California, 110 pp.

Texas Department of Water Resources, 1980: HIPLEX 1980 operations plan, Big Spring, Texas. TDWR LP-125, Texas Department of Water Resources, Austin, Texas, 47 pp.

Tripoli, G. J., and W. R. Cotton, 1980: A numerical investigation of several factors contributing to the observed variable intensity of deep convection over South Florida. *J. Appl. Meteor., 19,* 1037-1061.

Ulanski, S. L., and M. Garstang, 1978: The role of divergence and vorticity in the life cycle of convective rainfall, Part I. Observation and analysis, *J. Atmos. Sci., 35,* 1047-1062.

Wiggert, V., G., J. Lockett, and S. S. Ostlund, 1981: Radar rainshower growth histories and variations with wind speed, echo motion, location and merger status. *Mon. Wea. Rev., 109,* 1467-1494.

Wilhelmson, R. B., and J. B. Klemp, 1978: A numerical study of storm splitting that leads to long-lived storms. *J. Atmos. Sci., 35,* 1974-1986.

Williams, S. F., M. L. Gerhard, and J. R. Scoggins, 1980; Texas HIPLEX mesoscale experiment summer 1979 data tabulations. TWDB LP-118, Texas Department of Water Resources, Austin, Texas, 734 pp.

Williams, S. F., and J. R. Scoggins, 1980: Models of atmospheric water vapor budget for the Texas HIPLEX area. TDWR LP-117, Texas Department of Water Resources, Austin, Texas, 51 pp.

Woodley, W. L., J. Jordan, J. Simpson, R. Biondini, and J. Flueck, 1981: Rainfall results of the Florida Area Cumulus Experiment, 1970-1976 (Unpublished manuscript).

APPENDIX

The preliminary findings are presented in terms of the Texas HIPLEX cumulus behavior, cumulus convection, precipitation, and principle effects of seeding. Some of these findings are based on many years of data, some on only a few years, and others on case studies. Because the significance of the findings is, in part, dependent upon the length of record, the period of data collection is shown alongside each finding. Also included are the preliminary findings of economic studies.

Cumulus Behavior

1944-1970   In May, the major storm track is oriented southwest to northeast, while in June the storm track shifts to a northwest to southeast orientation.

1972-1977   Cumulus cloud maximum normally occurs at 1400 CDT, while cumulonimbus maximum normally develops at 1800 CDT, resulting in a four-hour lag time between the two occurrences.

1972-1977   The convection efficiency index (Cb freq./Cu freq.) for Midland, Texas, during: May-72 percent, June-69 percent, July-60 percent, and August-50 percent.

1973-1976   During the 1973-1976 four-year period the frequency of radar echoes increased to a maximum in July, then decreased to September.

1973-1976   Summer radar echo occurrence is most frequent during 1500 to 1700 CDT.

1973-1976   A sharp increase in radar echo activity tends to occur during July.

1973-1976   There are ten radar echoes/day or less on 66 percent of the days, and greater than 50 radar echoes/day on 7.3 percent of the days.

1973-1976   Irrespective of the size of the initial radar echo, 54.7 percent reached 8 km within ten minutes, 32.6 percent attained this size within 11 to 30 minutes, while the remaining percentage (12.7) took longer than 30 minutes.

1973-1976   Mean growth rates for radar echoes reaching maximum size of 50-100 km² was 4.5 km²/min, and for radar echoes reaching a maximum size greater than 3,000 km² it was 66.5 km²/min.

1973-1976   The vector motion of radar echoes in April, May, June, and September is predominantly northeastward and eastward. In July and August directions and speeds tend to be spread more evenly over the eight compass points.

Case Studies Echo movement is closely associated with lower level (700 mb to 850 mb) winds.

1972-1977 A better distinction among the convective season days with respect to convective activity will most likely be attained only when mesocale (as opposed to synoptic-scale) atmospheric circulation parameters are utilized, i.e. no matter how detailed the synoptic analysis, there is no way of inferring temperature and moisture from map patterns with the accuracy that is needed.

Case Studies West Texas summertime clouds which organize into lines exhibit a multiple surge behavior, where each surge is a new precipitation development cycle. The sequencing, time window, and preferred cloud spacing must also be considered in the development of an evaluation plan.

1976-1978 Echo occurrence had a maximum in the late afternoon, but only lines had another maximum near midnight.

1976-1978 Winds at the 700-mb level tended to be closest to echo movement.

1976-1978 Approximately 90 percent of all the echoes observed were cells. Cells tend to develop in a locally drier environment than occurred with clusters or lines, and they tended to last 10 minutes on the average.

1976-1978 Clusters made up about 10 percent of the echo population. They tended to last approximately 35 minutes, and developed in a moister air mass at all levels.

1976-1978 Cold echoes tended to merge more than warm echoes, especially cold clusters as compared to warm clusters.

1976-1978 In order to produce meaningful increases in total precipitation, research efforts may need to be directed toward the echo types that produce the most precipitation (clusters and lines).

> Precipitation Contribution
> 70 percent for lines
> 27 percent for cold clusters
> 1.5 percent for cold cells
> 1.3 percent for warm cells
> 0.2 percent for warm clusters

1976-1977 The dominant synoptic pattern for the Texas HIPLEX region is one with no front at the surface and a pressure ridge aloft.

1976-1977 A 500-mb trough, located to the west of the Texas HIPLEX region, increased the chances for echoes on "no front" days (air mass) and usually had echoes on "frontal" days.

1976-1977 Days with fronts produced high percentage frequencies of echoes.

1976-1977   Echoes occurred on about half of "post frontal" days.

1976-1977   Convection was found to have been sustained when cell alignment was parallel to the 850-500 mb vertical wind shear vector, and to diminish when alignment was perpendicular to the wind shear vector.

Cumulus Convection

1976   Surface velocity divergence, surface moisture divergence, vertical motion 50 mb above the surface, and vertical flux of moisture 50 mb above the surface are important for the initiation of convective activity, as well as being a major source of latent heat energy for the convective activity.

1976   The magnitude of moisture convergence and the depth of the layer of convergence are greater during times of convection.

1976   Horizontal inflow of latent heat energy in the lower troposphere is much greater during convection than during times of nonconvection.

1976   Low-level horizontal inflow, upward transport, and upper level horizontal outflow of internal, kinetic, and latent energy are enhanced during times of convection.

1976   Strong horizontal inflow of latent energy in the lower atmosphere is nearly balanced by latent heat release during times of convection, and is very important in the formation and maintenance of convective activity.

1977   Upper- or mid-level net horizontal inflow, net downward transport, and lower-level net outflow of internal, kinetic, and latent energy are found when convective activity is absent.

1977   The greatest differences of net horizontal and vertical transport of water vapor between convective and nonconvective conditions occur in layers above approximately 700 mb. For convective conditions, the largest increases occur between 600 and 450 mb with appreciable amounts of water vapor present.

1978   Particularly strong energy sources for convective activity occur near the surface and at approximately 450 mb.

1978   Maximum water vapor transport occurs in two layers, near the surface and approximately 450 mb, and corresponds to layers of maximum flux convergence of the total energy budget which indicates important convective energy sources.

1978   Comparisons of individual water vapor budget terms have shown the net horizontal transport term to be the dominant term during convective activity.

Case Studies	In most cases, echo formation is associated with the presence of a surface front/trough and upper air trough.
Case Studies	Nonsquall-line type echoes required a moist, unstable environment; while the squall-line type echoes required less instability.
Case Studies	The magnitude of the 850-500 mb shear vector was related to the echo organization scale. High shear was connected with a large system.
Case Studies	The environmental static stability controls the echo population.
1976-1977	A strong net gain of water vapor exists in all layers above cloud base for cases of convective activity, whereas a net loss in these same layers occurs for cases of nonconvection. In sub-cloud layers similar net gains in water vapor exist for *both* cases.
1976-1977	Cases for clusters of convective cells show a larger combined net horizontal and vertical transport of water vapor than for lines of cells, leading to larger precipitation amounts. Water vapor transport and accumulation of water vapor in cases of isolated cells are noticeably smaller than for lines and clusters of cells. Soundings near lines are relatively more stable than soundings near cells.
Case Study	Echo formation, growth, and movement of the squall line was controlled by the environmental wind structure (vertical profile and horizontal distribution), as well as the moist static energy distribution.
Case Study	The orientation of echoes was sensitive to the vertical shear of the horizontal winds between 850 and 500 mb.
Case Study	The echo movement was closely associated with lower level (700 or 850 mb) winds.

Precipitation

1944-1970	For the five-month period, May through September, there exists a daily precipitation maximum in mid-May, decreasing to a minimum in late June, with a secondary maximum centered on July 4 and July 22, and a relative minimum on July 14 and during the first week of August. The daily precipitation increases from the early August minimum to a broad maximum in late August and early September.
1944-1970	Monthly precipitation pattern for July is much less organized than either May or June.
1972-1977	Upper-air waves were responsible for 72 percent of the precipitation, followed by frontal activity (19 percent), air mass (7 percent), and the dry line (1 percent).

Principle Effects of Seeding

Case Studies Based on information on whether ice and precipitation developed in each cloud, and from estimates of the precipitation from each cloud, a preliminary conclusion is that the ice process is necessary for significant precipitation to occur.

Case Studies Although the warm rain process is indicated to be active in the initiation of precipitation, the ice phase process appears to dominate throughout much of the subsequent development of precipitation in Texas HIPLEX convective clouds.

Case Studies In most cases, during the mature and later cloud stages ice phase precipitation development is associated with high ice particle concentrations of between 10 and 100/ℓ. Hence, seeding during these cloud stages would not be as effective as during the early active growth stages of cloud development.

Case Studies The evaluation of the G-function (mass density vs cloud particle diameters, ranging from about 3 m to 4500 m) for isolated cumulus congestus clouds and convective complexes indicates that for a time prior to ice phase and/or precipitation initiation, the rising particles in the updraft regions are characterized by a bimodal distribution, a signature for the coalescence process.

Case Studies The suggested ice multiplication process is also evidenced in cloud regions where ice phase precipitation development is extensive. The presence of supercooled cloud droplets having diameters of greater than about 24 m, and occurring in concentrations of about 10/cm^3, fulfills the requirement of the Mossop-Hollet ice multiplication process.

Case Studies It is implied that unless seeding can result in significant dynamic effects to the larger clouds, a greater potential for ice phase seeding lies in the smaller clouds or at times prior to major precipitation development.

Agri-Economic Impact

The greatest crop response to increases in rainfall occurs when the precipitation is received before the crop is planted or during its growing season. For the two major crops, cotton and grain sorghum, these two periods include the months of January, February, and March, and June, July and August, respectively. During these periods, significant increases in crop production could result from increased average precipitation.

Substantial increases in regional crop revenue could result from an increase in mean monthly precipitation of 10 percent in the late winter and summer months.

Based on 1967 prices, crop revenue in the study area could increase by approximately $323,600 if normal March precipitation could be increased by 10 percent.

Rainfall during the spring months is very important to determining the condition of the range during the rest of the year. A 10-percent increase in rainfall in May, for example, would increase forage yield by 29.2 million pounds (13.3 million kg) over the region, resulting in a value of as much as $235,900 in income to the area livestock producers.

The range condition of the previous year has a significant impact on the current range condition. A carryover of healthy range plants through the winter months is very important in establishing a good stand of plants in the following spring.

A 10-percent increase in rainfall in April would have the largest effect on total income to area livestock producers. This 0.16 inch (0.41 cm) increase could result in an income increase of as much as $299,100.

A 10-percent increase in April-October rainfall annually in the study area is equivalent to ground water furrow irrigation requirements of $15.5 \times 10^6 m^3$ (150,565 acre-inches), and sprinkler irrigation of $12.7 \times 10^6 m^3$ (123,346 acre-inches), or a total of $28.2 \times 10^6 m^3$ (22,826 acre-feet).

Reduced irrigation requirements would reduce furrow irrigation costs (in 1977 dollars) by $283,061 annually, and sprinkler irrigation costs by $291,098 annually for a total reduction in costs of $574,159, based on 1977 input prices.